Utility of the *Calliphora vicina* (Diptera: Calliphoridae) Pupal Stage for Providing Temporal Information for Death Investigations

Katherine Elizabeth Brown

The thesis is submitted in partial fulfilment of the requirements for the award of the degree of Doctor of Philosophy of the University of Portsmouth

August 2012

School of Biological Sciences
King Henry Building
Portsmouth
PO1 2DY

Declaration

Whilst registered as a candidate for the above degree, I have not been registered for any other research award. The results and conclusions embodied in this thesis are the work of the named candidate and have not been submitted for any other academic award.

Abstract

Blowflies (Diptera: Calliphoridae) are primary colonisers of cadavers; the ages of the eldest immature stages can be used to estimate minimum post-mortem interval (PMI). These estimates are obtained using calliphorid larvae, for which there are established and reliable preservation protocols and age estimation methods. The opposite is true for pupae; non-standardised crime-scene collection and preservation methods are employed, resulting in poorly preserved specimens for age estimation, which is often conducted using limited and inadequate research data. This has hindered the use of this sedentary, long-lasting stage of the blowfly lifecycle in PMI estimation. A multidisciplinary approach to age estimation of *Calliphora vicina* pupae was explored, including development of standard preservation protocols, with the aim of improving PMI estimation.

Initial work involved the development of standardised egg collection protocols for the purpose of minimising variation in lifecycle length and precocious egg occurrence. This enabled quantification of pupal age error, which was subsequently applied to developmental timelines. Multiple preservation protocols were then trialled on pupae with the aim of retaining native morphological form and nucleic acid integrity for species identification and proposed age estimation methods. Optimal preservation methods for each analysis were suggested and the following universal preservative protocol proposed: pupae are pierced, hot-water-killed, and stored in 80% ethanol at -20°C.

Three methods of pupal age estimation were developed using changes in external morphology, histology and temporal gene expression. The external morphological development of 23 features was recorded from 1494 pupae. These data was used to create a Pupal Age Estimator tool, comprising a manual age-range correlation method and a regression equation for age estimation. Blind sample analysis indicated that age could be estimated to within 23 hours at 22°C, approaching the observed natural variation range. Internal morphological development of 42 pupae sampled at 24-hourly intervals was examined using histology and optical coherence tomography (OCT). Six additional features were identified as suitable age markers, however full analysis was limited by the inherent tissue loss due to sectioning and the low resolution of OCT. Finally, temporal gene expression levels of 42 pupae (selected at 24-hourly intervals) were quantified using qRT-PCR. Expression ratios were calculated between three developmentally expressed genes (Ecr, LSP-2 and Trp) and two housekeeping genes (EF1α and RP49). Regression analysis of these data indicated age estimation was possible to approximately 23 hours at 22°C.

It can therefore be considered that the reliability and precision of PMI estimation using the *C. vicina* pupal stage is much improved from that possible at present. Pupal age estimation is critically dependent on appropriate preservation, now facilitated by the proposed standard protocols and by combining all age estimation methods presented here, a multidisciplinary approach can estimate *C. vicina* pupal age to within 23 hours at 22°C.

Table of Contents

List of tables

List of figures

List of equations

Abbreviations

4d	Four days after puparium formation
7d	Seven days after puparium formation
Ab	Abdominal macrochetae
ADD	Accumulated degree days
ADH	Accumulated degree hours
AE	Adult eclosion
ANOVA	Analysis of variance
Ap	Appendage
APF	After puparium formation
awp	after the white pupa
B1	Blind sample analysis trial 1
B2	Blind sample analysis trial 2
bp	base pair
Br	Brain
Bs	Orbital/frontal bristles
cDNA	Complimentary DNA
CHCs	Cuticular hydrocarbons
COI	Cytochrome oxidase I
COII	Cytochrome oxidase II
CT	Computed tomography
$\mathbf{C_T}$	Cycle threshold
°C	Degrees Celsius
$\mathbf{\Delta C_T}$	Delta C_T
ddPCR	Differential display PCR
DEG	Developmentally expressed gene
$\mathbf{dH_2O}$	Distilled water
$\mathbf{ddH_2O}$	Double distilled (molecular biology grade) water
DNA	Deoxyribonucleic acid
dNTP	Deoxyribonucleotide triphosphate
DPX	Slide mounting medium
dsDNA	Double-stranded DNA
Dv	Development of muscle
Ecr	Ecdysone receptor
Ed	Eye imaginal disc
EDTA	Ethylenediaminetetraacetic acid
EF1α	Elongation factor 1-alpha

EIA	Enzyme-linked immunoassay
EtOH	Ethanol
Ey	Compound eye
F	Female
F1	First generation of adults from wild type
F2	Second generation of adults from wild type
Fb	Fat body
GAPDH	Glyceraldehyde 3-phosphate dehydrogenase
Gc	Gastric caecae
gDNA	Genomic DNA
GFP	Green fluorescent protein
H_2O	Water
Hg	Hindgut
HKG	Housekeeping gene
HWK	Hot-water-killing
Id	Imaginal disc
ISSR	Inter-simple sequence repeats
Is	Intersegmental muscle
ITS	Internal transcribed spacer
K	Potassium
La	Labellum
Lb	Labrum
LDT	Lower developmental threshold
Lg	Lamina ganglionaris
Lgu	Larval gut
Lg1	Prothoracic leg
Lg2	Mesothoracic leg
Lg3	Metathoracic leg
Lm	Longitudinal muscle
Lo	Lobula
Lp	Lobular plate
LS	Longitudinal section
LSP2	Larval serum protein 2
M	Male
Mb	Mushroom body
MCB	Multiple comparison with best
Me	Medulla
Mg	Midgut

$MgCl_2$	Magnesium chloride
Mp	Malpighian tubules
MRI	Magnetic resonance imaging
MRM	Magnetic resonance microscopy
mtDNA	Mitochondrial DNA
N/A	Not applicable
Na	Sodium
NH_4OH	Ammonia
NMR	Nuclear magnetic resonance
OCT	Optical computed tomography
Oe	Oesophagus
On	Optical neurones
Onv	Ocellar nerves
PAS	Periodic acid schiff
PCR	Polymerase chain reaction
PIA	Period of insect activity
PMI	Post mortem interval
Pr	Protocerebrum
PTA	Phosphotungstic acid
Pu	Puparium
qPCR	Quantitative PCR
qRT-PCR	Quantitative reverse-transcriptase PCR
Re	Retinal cells
RFLP	Restriction fragment length polymorphism
Rh	Rhabdomeres
RNA	Ribonucleic acid
rRNA	Ribosomal RNA
RP49	Ribosomal protein 49
RPL32	Ribosomal protein L32
rpm	**R**evolutions per minute
RT-PCR	Reverse-transcriptase PCR
SB1	Semi-blind analysis trial 1
SB2	Semi-blind analysis trial 2
S.D.	Standard deviation
SEM	Scanning electron microscopy
Sg	Salivary glands
SS	Sagittal section
T1	Trial one pupae (collected for development of age estimation methods)

T2	Trial two pupae (collected for development of age estimation methods)
Ta	Tarsi
Tb	Thoracic bristles
TBE	Tris-borate-EDTA
T_{CS}	Control colony of the starved trial
T_{FF}	Fully fed trial
T_{FS}	Fully fed and disturbed cohort of the starved trial
Tg	Thoracic ganglion
Tm	Transverse muscle
% TPS	Percentage of development through the pupal stage
Tr	Trachea
Trp	Transient receptor potential
T_S	Starved trial
TS	Transverse section
U	Unit
UV	Ultraviolet
VOCs	Volatile organic compounds
Wg	Wing
wpp	white prepupal (stage)
WP	White pupa

Acknowledgments

First and foremost I must thank my Director of Studies, mentor and life-long friend Michelle Harvey. You have provided endless support, advice, direction and contacts throughout my undergraduate and postgraduate studies, for which I am truly thankful. Your enthusiasm and passion for entomology is immensely inspiring and contagious. Thank you for giving me the freedom to explore my research topic and funding for international conferences. I am indebted to you for all of the thesis and paper writing help you have given me, as well as for the opportunities to teach and demonstrate undergraduate classes; without this support I would not be where I am today and looking forward to my career ahead. You will always be someone I can turn to as a trust-worthy and caring friend, wherever we are in the world...until we meet again.

I would like to thank Alan Thorne, my second Director of Studies, for all your thorough and critical comments on my thesis and papers and our lengthy discussions at meetings. Your advice was invaluable, and you always knew someone who could help in the unlikely event it was not yourself. Despite how busy you were you always made time to help, and I really appreciate it, thank you.

I must also thank the whole of the Biophysics department at the University of Portsmouth, especially Colin Sharpe and Garry Scarlett for proof-reading chapters, and Fiona Myers, Frank Schubert, Garry Scarlett and Suzannah Page for helping me through the minefield of RNA and gene expression. Thanks go to Phil Warren and Martin Villet (Rhodes University, South Africa) for histological advice.

This work would not have been possible without funding from the School of Biological Sciences. In addition, thanks to the Royal Entomological Society, British Society for Developmental Biology and the University of Portsmouth for travel grants, allowing me to disseminate my work and meet the leaders in the field.

Thank you to my mum, dad and grandparents for excusing my absence at family events, providing meals and company when I am too drained to think anymore and the financial support over the past 7, especially 4 years. I am forever in your debt but eternally grateful that you allowed me to follow my dream. Finally, my husband, Jason; you are my soul mate and my life. I can’t thank you enough for all you have done for me. You have put up with too much over the past few years; too little money, too many nights spent working instead of spending time together, too many social events missed or disrupted due to sampling at ‘silly-o-clock’ in the morning. I will make it up to you, I promise. Thank you also for all your photos of my insects and keeping me company at conferences – I will turn you into an entomologist one day!

Dissemination

Publications

- Davies, K., & Harvey, M. (2012). Internal morphological analysis for age estimation of blow fly pupae (Diptera: Calliphoridae) in post-mortem interval estimation. *Journal of Forensic Sciences*, *x*(x).
- Davies, K., & Harvey, M. (2012). Precocious Egg Development in *Calliphora vicina* (Diptera: Calliphoridae): Implications for Developmental Studies and Post-Mortem Interval Estimation. *Medical and veterinary entomology*, *x*(x).
- Brown, K., Thorne, A., & Harvey, M. (2012). Preservation of *Calliphora vicina* (Diptera: Calliphoridae) Pupae for use in Post Mortem Interval Estimation. *Forensic Science International. x*(x).
- (In Preparation) Brown, K., Thorne, A., & Harvey, M. (2012). External morphological development of *Calliphora vicina* (Diptera: Calliphoridae) pupae: a new tool for age and PMI estimation. *International Journal of Legal Medicine.*

Oral presentations

A Multidisciplinary Approach to Age Estimation of Calliphora vicina (Diptera: Calliphoridae) Pupae for Post-Mortem Interval Calculation

- North American Forensic Entomology Association annual meeting at Texas A&M University, in Texas, USA in July 2011
- European Association of Forensic Entomology annual meeting at Nicolaus Copernicus University in Torun, Poland in April 2012
- The Forensic Science Society Inaugural Postgraduate Research Symposium at Warwick University, in Coventry, England in November 2012 (accepted)
- Presented by Dr Michelle Harvey on my behalf at the Australian and New Zealand Forensic Science Society International Symposium, Tasmania, Australia in September 2012

The Implications of Precocious Egg Development in Calliphora vicina (Diptera: Calliphoridae) for Developmental Studies and Post-Mortem Interval Estimation

- Presented at the Royal Entomological Society annual meeting at the University of Greenwich in Kent, England in September 2011

Poster

Preservation of Blowfly Pupae for Age and Post-Mortem Interval Estimation

Presented at European Association of Forensic Entomology annual meeting at the University of Murcia, Murcia, Spain in September 2010.

Dedication

I would like to dedicate this work to
my husband, Jason,
my parents, Richard and Claire
and my grandparents.

Without their endless love, moral and financial support throughout my student years,
I would not be where I am today.

Chapter 1 - Introduction

Forensic entomology, by definition, is the use of insects and arthropods as evidence in legal investigations. This thesis explores the use of the pupal stage of *Calliphora vicina* Robineau-desvoidy (Diptera: Calliphoridae) for estimating post-mortem interval (PMI), based on morphological and molecular methods.

1.1 Forensic entomology

Applications in forensic entomology are divided into three main areas; urban, stored product and medico-legal entomology. Urban and stored product entomology frequently involves termite and cockroach infestations, and insects found in foodstuffs respectively, along with their associated economic costs and legal implications (Amorim & Ribeiro, 2001; Byrd & Castner, 2009; Gagliano-Candela & Aventaggiato, 2001). Medico-legal entomology encompasses cases of human and animal neglect or abuse, but most commonly involves estimating post-mortem interval (PMI) in criminal investigations (Amendt *et al.,* 2007). PMI estimates obtained using insect assemblages and age estimates must be robust enough to withstand cross-examination in court, hence must be underpinned with thorough, well-grounded research.

PMI estimation involves the amalgamation of multiple areas of entomological research, including species identification using morphological and molecular methods in the different lifecycle stages (Byrd & Castner 2009; Harvey *et al.,* 2008; Erzinclioglu 1996), drug or chemical-affected growth of insects (Goff & Lord 1994), decomposition and succession studies (Campobasso *et al.,* 2001; Payne 1965), and lifecycle data (Anderson 2000; Donovan *et al.,* 2006). Estimates obtained can be accurate to within a few days or hours, but this depends on the condition of the cadaver (as described in decomposition studies), insect sampling strategy, species present and their developmental stage (Pai *et al.,* 2007; VanLaerhoven 2008).

1.2 Utility of insects as evidence

The most common insects to visit a cadaver are flies and beetles. Forensically important dipteran families include the Muscidae, Sarcophagidae, Piophilidae and Phoridae, however the blowflies (Calliphoridae) are most frequently the primary colonisers of cadavers, making them the most useful indicators of PMI.

1.2.1 *Forensically important Calliphoridae*

Over 1000 calliphorid species have been identified, and are commonly known as the blue- and green-bottle flies. Members include the forensically important genera *Calliphora* and *Lucilia*, which are globally distributed and frequent cadavers for feeding and oviposition.

Two common primary colonising species belonging to these genera are *Lucilia sericata* and *Calliphora vicina*. *Lucilia sericata* has a lower temperature limit below which development does not occur (lower developmental threshold; LDT) of 9°C (Marchenko, 2001), limiting its activity to warmer, sunny climes such as Africa and Australia or summer in the UK and northern Europe. *Calliphora vicina* has a lower development threshold of 1°C (Donovan *et al.,* 2006); hence thrives throughout the northern hemisphere (Fig. 1.1). More recently however, *C. vicina* has been considered as a globally invasive and cosmopolitan primary coloniser (Byrd & Castner, 2009), therefore *C. vicina* was chosen as the species for this study.

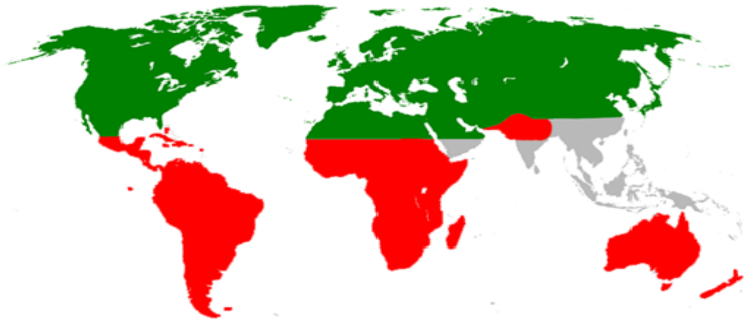

Figure 1.1 Distribution of *Calliphora vicina.* Traditionally a holarctic species inhabiting the northern hemisphere (green shading), *C. vicina* has invaded areas of the southern hemisphere (red shading), making it a fly of global forensic importance.

1.2.2 *Calliphora vicina lifecycle*

The lifecycle of *C. vicina* (Fig. 1.2) resembles that of most Calliphoridae species, with familial differences only in ovi- or larviposition, developmental times and pupation sites. After location of a suitable oviposition site using chemosensory stimuli, *C. vicina* lays eggs in batches of between 100-300 (Smith, 1986 and Zumpt, 1965 in Delhaes *et al.,* 2001; personal observation), many of which desiccate if not laid in a sheltered, humid location such as the nose, mouth, ears and genitalia of a cadaver.

Upon hatching larvae feed on tissue, growing through three instars separated by larval ecdyses. The greatest increase in size occurs during the third instar when larvae feed together as a ‘maggot mass’, which can be ~20°C above ambient temperatures (Anderson & VanLaerhoven 1996). Larvae circulate from inside the cadaver to the surface to maintain an optimal temperature range for larval development.

After reaching their maximum size larvae enter the post-feeding stage where they wander away from the cadaver in search of a dry, sheltered environment for pupation. In contrast to *C. vicina*, some species such as *Protophormia terraenovae* pupate on the cadaver as well as the immediate surroundings (Gaudry, *et al.,* 2006). The pupal or metamorphosis stage is a quiescent point within the lifecycle that requires protection from extreme environmental changes for development of the adult fly. To achieve this, post-feeding larvae bury into the ground prior to formation of the protective puparium. Pupal cases are chitinous and resistant to rainfall and humidity fluctuations; they can remain at the scene for millennia (Huchet, 2010).

Once development is complete, pupae emerge as adult flies. Ovary maturation takes roughly six days (Davies 2006) and after this time these adults may revisit, mate at and lay eggs on the same cadaver should enough larval food source (i.e. tissue) remain. The presence of empty puparia at the scene indicates a complete lifecycle of the respective species has occurred, which can be used to estimate minimum PMI.

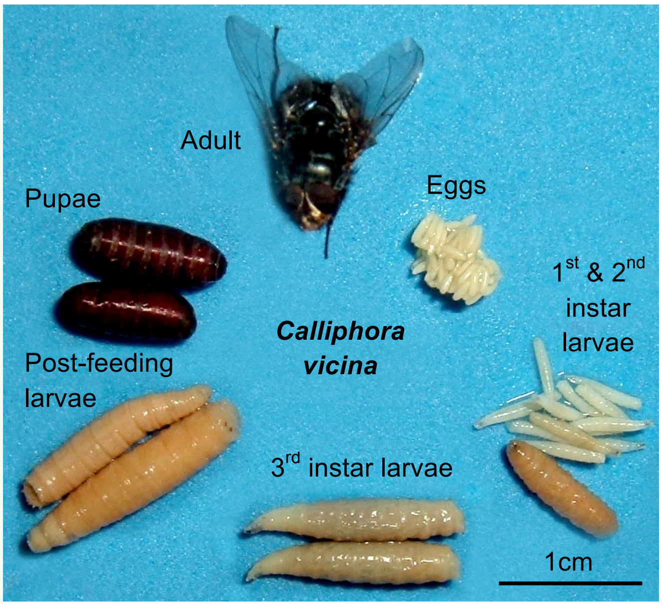

Figure 1.2 Lifecycle of *Calliphora vicina.* The lifecycle of the Calliphoridae comprises similar stages as other holometabolous insects. Adults lay eggs on the cadaver, which once hatched feed on the tissues. Once growth is complete, the larvae enter the metamorphic pupal stage. After adult development is complete, the imago hatches to the adult fly.

Prior to PMI estimation, insect identification must first be conducted as each species have different developmental rates. It is well established that the same species from different geographical locations also have different LDTs and upper developmental thresholds (UDTs), cold-tolerances and developmental times (Saunders & Hayward 1998; VanLaerhoven 2008). As such, local data should be used where available when calculating PMI from age estimates.

1.3 Species identification

Insects collected from the crime scene for identification and age estimation are split into two cohorts; preserved and reared under controlled conditions. This allows rapid PMI estimation from preserved immature stages. Then following eclosion, identification is confirmed using adult morphology and age estimates are obtained for corroboration. Two methods are used for species identification; comparison of morphological characteristics and DNA sequence analysis.

1.3.1 Morphology – based identification

Most Calliphoridae are identified using morphological examination of external features (Table 1.1) allowing retention of voucher (original) specimens. Closely related species that occupy similar locations such as *C. vicina* and *Calliphora vomitoria* (Hwang & Turner 2005; Aak 2011) are easily identified using adult jowl and bristle colour (Fig. 1.3) and basicosta colour, or larval intersegmental spine pattern (Fig 1.4).

Table 1.1. Morphological characteristics used for identification of Calliphoridae spp. Examples of the anatomical structures examined when determining species of calliphorids, using both light and scanning electron microscopy and accompanying keys where available.

Lifecycle stage	Morphology used	Authors
Adult	Jowl, bristle and basicosta colour	Erzinclioglu (1996); Whitworth (2006)
	Thoracic bristle pattern	
	Wing venation	
Eggs	Plastron, micropyle and chorion ultrastructure	Davies (1948); Mendonça *et al.*, (2008); Sukontason, Bunchu, *et al.*, (2007); Sukontason *et al.*, (2008); Sukontason *et al.*, (2004); Hinton (1963)
Larvae and Puparia	Number and structure of papillae	Holloway (1991); Sukontason *et al.*, (2005); Sukontason, Kanchai, *et al.*, (2006); Sukontason, Narongchai, *et al.*, (2006); Siriwattanarungsee *et al.*, (2005); Whitworth (2003); Amorim & Ribeiro (2001)
	Posterior spiracle and peritreme structure	
	Form of intersegmental spines	

Many closely related species and earlier instar (smaller) larvae require the use of scanning electron microscopy (SEM) for species identification (Fig. 1.5), which enables higher resolution analysis than light microscopy but requires more costly equipment, time and complex sample preparation (Table 1.2).

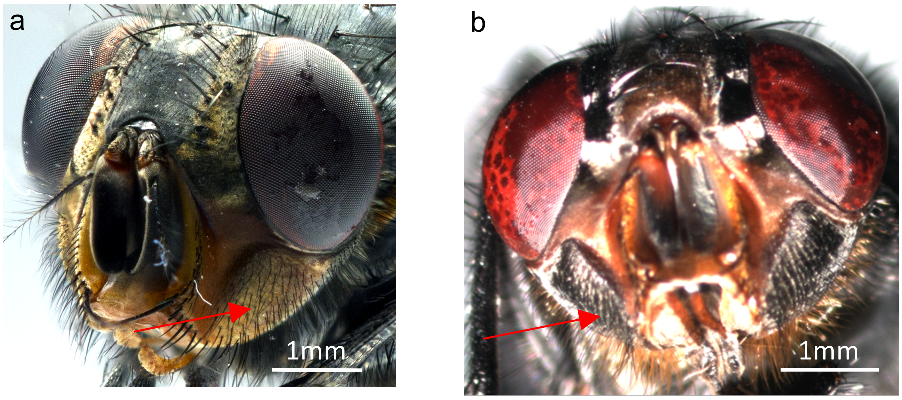

Figure 1.3 Differentiation of *C. vicina* and *C. vomitoria.* *C. vicina* (a) has black vibrissae on pale brown jowls; *C. vomitoria* (b) has orange vibrissae on black jowls (arrows). Differences are visible with or without microscopy. Images courtesy of Jason Brown Photography.

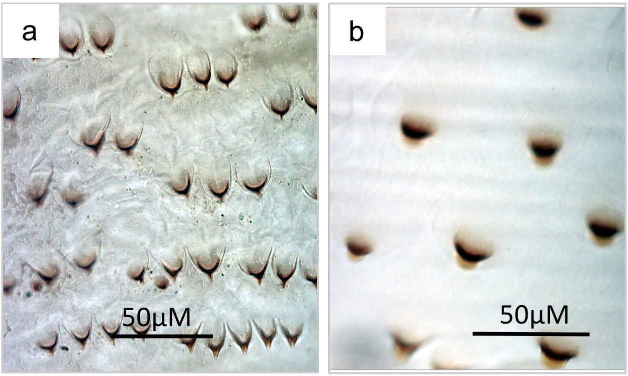

Figure 1.4 Morphological differences of the intersegmental spines in *C. vicina* and *C. vomitoria* larvae. *C. vicina* spines (a) are pointed in structure and are clustered into groups of three. *C. vomitoria* spines (b) are more rounded and are arranged singularly.

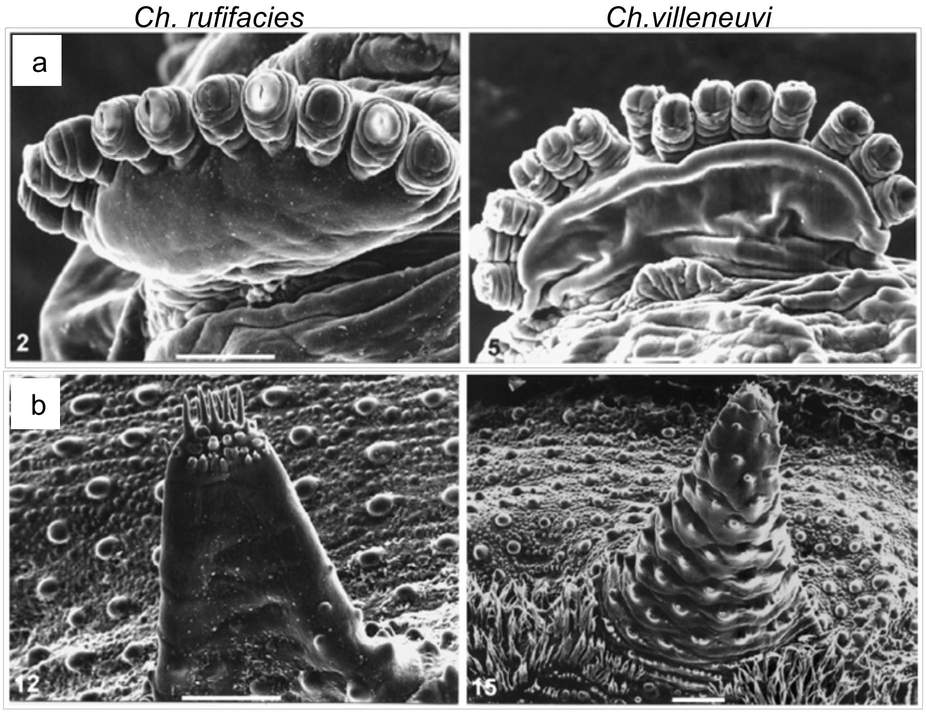

Figure 1.5 Identification of closely related species by scanning electron microscopy. Distinguishing between *Chrysomya rufifacies* and *Chrysomya villeneuvi* is only possible using SEM, by comparison of features including (a) the number of papillae on anterior spiracles, (b) the structure of the inner dorsal tubercles. Scale bar = 50µM (Sukontason, *et al.*, 2006).

Table 1.2. Microscopy methods. Species identification using morphology may require both light and scanning electron microscopy, which are summarised in this table.

Method	Advantages	Disadvantages
Light microscopy	Rapid	Light may not penetrate material (e.g. puparia)
	Inexpensive equipment	
	Minimal preparation procedures	Low resolution - Cannot view intricate details of some closely related species
	Permits later analyses such as DNA/SEM	
Scanning Electron Microscopy	High resolution - useful for closely related species and highly detailed features	Expensive equipment
		Time consuming preparation and analysis of samples
		May not permit later DNA analysis

Whilst some species and lifecycle stages are able to be identified using morphology alone using the wealth of morphological data, others require individual or multiple regions of their genome to be analysed.

1.3.2 DNA-based identification

Identification using DNA polymorphisms can be more efficient than using morphological characteristics, as it is relatively low-cost, it can be performed on all lifecycle stages and conclusions are objective. Identification of geographical origin of specimens is also possible (Harvey *et al.,* 2008), providing additional case information. DNA-based identification is also important when presented with fragmented puparia or degraded samples (Mazzanti *et al.,* 2010) for which an accurate morphological identification may not be possible.

The Cytochrome Oxidase I (COI) gene of the mitochondrial genome (mtDNA) (Fig. 1.6) is the region of DNA primarily utilised for species identification in all organisms for many reasons. The dipteran COI gene is 1536bp in size (Oliveira *et al.,* 2007) and due to the high copy and number relative conservation of mtDNA it is rapidly amplified from small samples using multiple sets of universal primers (Simon *et al.,* 1994). Sequencing of the COI and other regions of both mtDNA and genomic DNA (Table 1.3) highlights sequence polymorphisms unique to each organism, permitting identification of even closely related, morphologically and genetically similar (cryptic) species (Harvey *et al.,* 2008; Wells *et al.,* 2007).

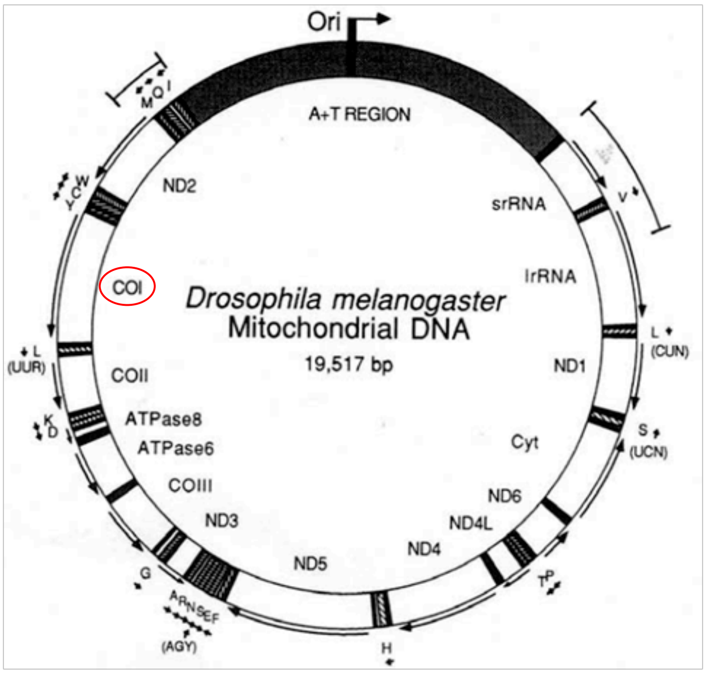

Figure. 1.6 Mitochondrial DNA Map of *Drosophila melanogaster* The mitochondrial DNA of *Drosophila melanogaster* includes respiratory pathway genes, due to its close proximity to ATP generating apparatuses. The Cytochrome Oxidase I gene is highlighted in red (Lewis *et al.*, 1995).

Table 1.3. Methods of DNA-based identification. Many methods of DNA-based identification are possible, with three main types used for the Calliphoridae highlighted below. COI = cytochrome oxidase I gene, COII = cytochrome oxidase II gene, gDNA = genomic DNA, ITS = internal transcribed spacer, rRNA = ribosomal RNA genes

Methods of Analysis	Regions	Summary	Authors
Sequencing	COI	Barcoding region - used to identify many organisms	Harvey, Mansell, *et al.*, (2003); Harvey, Dadour *et al.*, (2003); Harvey (2006); Harvey *et al.*, (2008); Wells *et al.*, (2007); Park *et al.*, (2009)
		Well developed technique with large database and multiple primers available	
		May not provide enough variation to identify some species	
	Control (A+T)	High mutation rate permits identification of intra-species populations	Lessinger & Azeredo-Espin (2000); Oliveira *et al.*, (2007); Duarte *et al.*, (2008)
		Difficult to amplify due to AT richness	
	rRNA genes	Alternative region - provides additional information.	(Stevens *et al.*, 2002; Stevens 2003)
PCR-RFLP	COI, COII, ITS1 & ITS2	Utilises sequence polymorphisms at restriction sites with PCR fragments to differentiate between species	Ratcliffe & Webb (2003); Schroeder (2003); Nelson *et al.*, (2008)
		Does not (always) require sequencing - rapid method	
		Minimal database size at present	
ISSR	Whole genome	Comparison of PCR fragment sizes produced using multiple primers	He *et al.*, (2007); Su *et al.*, (2008)
		Shows population-level variation	
		Band patterns often difficult to distinguish	

Other methods such as PCR-RFLP (restriction fragment length polymorphism) and ISSR (inter-simple sequence repeats) analysis (Schroeder 2003; Ratcliffe & Webb 2003; He *et al.,* 2007) enable preliminary species identification without sequencing, by the comparison of restriction fragment or PCR product sizes respectively.

Sequencing of longer regions (e.g. 1167 bp compared to 278 bp) reveals greater numbers of species-specific polymorphisms and use of multiple regions and methods permits accurate species identifications to be made (Harvey *et al.,* 2008; Wells *et al.,* 2007; Stevens 2003), after which insect age and then PMI estimation can commence.

1.4 Post-mortem interval estimation

The main methods used for PMI estimation are analysis of total insect assemblage and age of the eldest insects present at the crime scene. The choice of method depends on the state of decomposition (Campobasso *et al.,* 2001).

1.4.1 Decomposition and insect succession

Immediately after death (the fresh stage), the cadaver displays changes termed rigor-, livor- and algor- mortis, which can be used to estimate PMI with a high degree of accuracy for the first 12-72 hours. After this time, entomological evidence becomes the most accurate technique for PMI estimation (Payne 1965; Catts & Haskell 1990). Decomposition then progresses through the bloat, decay and dry stages (Payne 1965). The stages are not discrete but describe the state of the cadaver caused by environmental and entomological action within a continuous process, taking between weeks and years, until all matter has fully decomposed (Campobasso *et al.,* 2001).

The rate of decay is dependent on environmental factors such as temperature, humidity, rainfall, sun exposure, seasonality, altitude and habitat differences as well as covering, confinement or burning of the body (Campobasso *et al.,* 2001; Davies 1990; Davies 2002; Sharanowski *et al.,* 2008). These factors affect PMI estimation as they may delay or advance insect colonisation time and rates of tissue consumption and succession.

In the majority of cases of decomposition, the fresh stage attracts the Calliphoridae, Sarcophagidae and Muscidae (Fig. 1.7a) within minutes of a cadaver being made accessible, due to chemosensory detection of the chemicals produced by bacterial fermentation within the body (Amendt *et al.,* 2007; Reed 1958). The Silphidae (carrion beetles) (Fig. 1.7b), Piophilidae and Sepsidae (Diptera) colonise the cadaver shortly after. The primary coloniser larvae loosen cadaver tissue making the environment suitable for the Staphylinidae and Histeridae (Coleoptera), which consume the primary coloniser larvae as well as decaying tissue. Finally the Dermestidae (Fig. 1.7c) and other beetle families feed on the fully decomposed and dried cadaver. Little insect activity remains at the skeletal stage. Adventive insects such as the Lepidoptera visit the cadaver throughout decomposition and do not indicate PMI.

Figure 1.7 Carrion colonisers. *Musca domestica* (a) is a common representative of the Muscidae, colonising the cadaver within hours of death. The first of the beetles to visit the cadaver are the Silphidae (b) or Carrion beetles. All of the initial colonisers lay eggs on the cadaver, which hatch into larvae that feed on the tissues. Silphidae larvae also feed on dipteran larvae. The Dermestidae (c) frequent the cadaver later on, when the tissues are drier. (a) obtained from http://www.cdc.gov/nceh/publications/books/housing/figure_cha04.htm, (b) obtained from http://www.zin.ru/ANIMALIA/COLEOPTERA/eng/all_fams.htm, (c) obtained from http://www.zin.ru/animalia/Coleoptera/eng/derfrikm.htm.

The assemblage of insects collected from the crime scene is compared to locally obtained research data where possible (Fig. 1.8). Insect succession data are most often used in latter decay stages once the first flies have completed a lifecycle, to estimate the number of weeks, months or years passed (Schoenly 1992).

1.4.2 Insect lifecycles

In the early stages of decomposition, before the initial colonisers have developed to adults, the age of the oldest insects present at the crime scene are used to estimate PMI.

Insects are poikilotherms; warmer temperatures promote faster development, as the amount of heat required to reach each stage is accumulated in a shorter period of time. Insect age is therefore expressed in accumulated degree hours (ADH) or accumulated degree days (ADD), which is the product of the time and temperature for temperatures between the LDT and UDT. The ADH required to reach each stage is species-specific (Table 1.4), indicating the importance in correct species identification when using lifecycle data to estimate PMI, shown in detail in Appendix I.

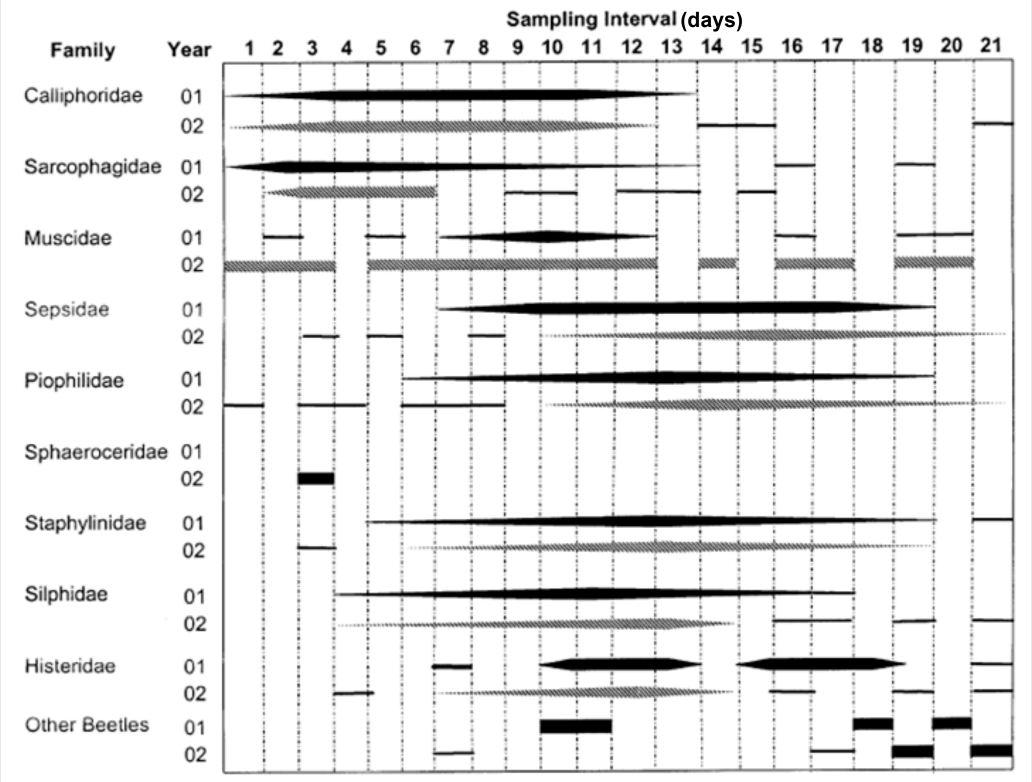

Figure 1.8 Insect succession in southwest Virginia. The abundance of insect families present on cadavers over a period of 21 days in spring in southwest Virginia. Wider bars indicate higher abundance. Diptera tend to appear at least three days before the first Coleoptera (Tabor *et al.*, 2005).

Table 1.4 Variation in ADH required to reach key developmental stages for common Calliphoridae. The average ADH was calculated from min/max developmental times at 23°C for three species (Anderson 2000), using LDTs of 1, 9 and 7.8°C for *C. vicina*, *L. sericata* and *P. regina* respectively (Donovan *et al.*, 2006; Marchenko 2001).

Stage	ADH required to reach stage		
	Calliphora vicina	*Lucilia sericata*	*Phormia regina*
1st Instar	556	301	334
2nd Instar	1067	630	1245
3rd Instar	1782	1078	2050
Prepupa	3509	2132	3078
Pupal	5300	3696	3692
Adult	10489	7651	6111

To estimate the age of insects from a crime scene, accurate environmental data must be obtained. Temperatures of the inside of the cadaver are measured and also of larval feeding masses. At 3rd instar, internal mass temperatures may be 20°C higher than ambient temperatures (Anderson & VanLaerhoven 1996; Sharanowski *et al.,* 2008), however mortality can occur above ~37°C (Slone & Gruner 2007) and cycling of larvae within the larval mass usually limits developmental temperature to around this figure. Ambient temperatures are collected using a probe placed at the crime scene after cadaver recovery. The temperatures obtained are used to estimate temperatures prior to cadaver recovery (which enable back-calculation of PMI) using regression analysis of crime scene and weather station data.

The ages of all insects collected are estimated in ADH (Chapter 1.5) and the eldest are assumed to indicate the point at which first colonisation occurred; the period of insect activity (PIA) (see Appendix 1). The minimum PMI is longer than the PIA, to account for the additional time required for detection of and oviposition on the cadaver. Oriented flight and oviposition rarely occur at night so the PMI should be lengthened accordingly. Variables such as wind speed and direction, rainfall, humidity, location and covering of the cadaver can affect PMI (Amendt *et al.,* 2007), thus obtaining accurate environmental information is essential. The data obtained from the crime scene is then interpreted accordingly, based on locally obtained research, to give a PMI estimate. Whilst the method of PMI estimation using ADH is essentially the same for all developmental stages, age estimation methods used for the different stages vary.

1.5 Age estimation of the Calliphoridae

Calculating the age of each stage of the lifecycle poses different problems. For a comprehensive PMI estimate, age is estimated for all samples collected from the crime scene.

1.5.1 Collection of insects from the scene

Representative numbers of insects are collected from multiple sites on the cadaver and the surrounding environment and the physical locations of all samples recorded. Larval growth can be affected by chemicals including drugs and toxins (see Introna, Campobasso, & Goff (2001) for a review) concentrated at different bodily locations or in tissues. Unusually large larvae collected from the nasal passages for example may indicate feeding on tissue containing cocaine residue and can reduce the PMI estimate by up to 21 hours (Kharbouche *et al.,* 2008).

Half the samples collected are transported and reared to adults under temperature-controlled conditions, and half are preserved following published standards and guidelines as shown in Table 1.5 (Amendt *et al.,* 2007). Preservation of half the samples is critical to avoid the possibility of data loss by failure of immature-stage rearing. Hot-water killing of larvae ensures maximum elongation (prevents curvature) facilitating consistent length measurement, and also prevents putrefaction (Adams &

Hall 2003) that may result from slow penetration of ethanol (used as an alternative killing-agent). In contrast, preservation of pupae is not described; all samples should be sent alive.

Table 1.5 Preservation methods for insect samples. Standards and guidelines dictate how insect stages should be collected and transported from the scene, prepared and preserved (Amendt *et al.*, 2007).

Stage	Collection conditions	Preservation method
Adults	Kept alive in ventilated containers	Frozen at -20°C; preserve in 70-95% ethanol
Eggs	Kept alive on moist tissue	In 70-95% ethanol
Larvae	Kept alive in ventilated containers	Hot-water-kill in >80^{o}C water for >30 seconds; preserve in 70-95% ethanol
Pupae	Kept alive in dry conditions	None suggested
Puparia	Non-living samples	Dry or in 70-95% ethanol

1.5.2 Age estimation of adults

Adults collected from the scene are typically used only for analysis of insect assemblage and not normally used for age estimation since their origin is uncertain. An age estimate may be obtained within one hour of eclosion, since this period is required for wing expansion (Fig. 1.9) and cuticular hardening (Cottrell 1962a & 1962b) though this period is affected by pupal burial depth, which is not readily determined. Larvae collected alive from the scene are also reared to adults for species identification and their eclosion time used to estimate PMI.

Figure 1.9 A recently emerged *Musca domestica* adult. At less than 1 hour old, the head remains enlarged between the eyes, where the ptilinum previously protruded, the wings remain shrivelled and deflated, and the abdomen is relatively small. Image from of Warwick Sloss / naturepl.com

1.5.3 Age estimation of eggs

With each female fly laying hundreds of eggs (Smith, 1986 and Zumpt, 1965 in Delhaes *et al.,* 2001; present study) the number of eggs present on a cadaver during the initial stages of decomposition may be many thousands. Despite this, cadavers are not usually found within the short period of time (approx. 24 hours at 22°C) prior to egg hatching and any PMI estimates obtained using eggs are usually used in corroboration with an estimate based on pathological data (Anderson 2004). Since no studies of calliphorid embryogenesis have been conducted, egg age can only be estimated using *Drosophila melanogaster* staging (Bownes 1975). Typically, eggs are reared to hatching point and back-calculation of PMI based on developmental data is performed (Bourel *et al.,* 2003).

Tarone *et al.,* (2007) examined changes in three temporally expressed genes over the *Lucilia sericata* embryonic period, mapping the expression levels of egg clusters to age in hours. Using expression data from all genes the age of unknown egg masses could be predicted to within two hours of their actual age, 91% of the time. Even though this technique requires considerable time and expertise, as well as correctly preserved and intact samples, this is a significant improvement on using morphological data from *D. melanogaster* and represents a promising advancement in the field.

1.5.4 Age estimation of larvae

60% of cadavers are found within a month of death (Gaudry *et al.,* 2001) and are therefore likely to have larvae associated to them. The number of slits in the posterior spiracles, which can be seen with low magnification, indicate the larval instar (Figure 1.10a & b) and the absence of food in the crop indicates larvae have reached the post-feeding stage (Figure 1.10c) (Amendt *et al.,* 2007). Larval length and width are directly proportional to larval age in ADH (Day & Wallman 2006). Thus, provided

Figure 1.10 Larval ageing using morphological characteristics. A crude analysis of age can be conducted by comparison of posterior spiracles with second instar (a) and third instar (b), after which (c) the presence of food in the crop (black arrow) indicates feeding, or disappearance (red arrow) which indicates food digestion at the wandering stage. Images a & b are *Lucilia sericata*; image c was obtained from http://entomology.unl.edu/images/blowflies

developmental temperatures can be estimated and reference data are available, larval size can be used to estimate time since death to within a few hours. Charts such as isomegalen/isomorphen diagrams, growth curves and tables of developmental data are used to convert length to age (Anderson 2000; Donovan *et al.,* 2006; Grassberger & Reiter 2001; Marchenko 2001; Richards *et al.,* 2008). Larvae must be rapidly killed with hot water and preserved correctly for accurate age estimation, with no curvature, shrinkage or putrefaction, which could prevent assessment of size and morphology (Adams & Hall 2003).

1.5.5 Age estimation of puparia

The presence of puparia at the scene indicates that at least one complete lifecycle of that species has occurred, which may provide information for PMI estimation. Puparia are also useful when found associated with burials in older or ancient cases. Some species are specific to particular geographical regions, environments or seasons and so their presence may indicate the approximate month and location of death, mummification or burial (Gilbert & Bass, 1967). DNA extraction from puparia and subsequent COI sequence analysis has been used to determine species (Mazzanti *et al.,* 2010), should the puparia be too weathered or fragmented for morphological characteristics to be analysed.

Puparia contain cuticular hydrocarbons, which reduce in chain length over time; their composition can indicate the age of a 2-3 day old pupa but is otherwise inaccurate (Zhu *et al.,* 2007). Total hydrocarbon composition has been shown to vary in ageing adults and over the lifecycle, which may also prove to be useful for estimating age and PMI (Trabalon *et al.,* 1988; Trabalon *et al.,* 1992; Roux *et al.,* 2008). The utility of hydrocarbons for age estimation will be discussed in detail later (Chapter 7).

1.5.6 Age estimation of pupae

Pupae were reported present and collected in 11/21 cases selected at random from the literature (Amendt *et al.,* 2000; Benecke 1998; Benecke *et al.,* 2004; Bonacci *et al.,* 2009; Delhaes *et al.,* 2001; Disney & Manlove 2005; Archer *et al.,* 2006; Introna *et al.,* 1998; Turchetto *et al.,* 2001). In contrast, in one study comprising 30 cases (Sukontason *et al.,* 2007) the presence or absence of pupae at the crime scene were not mentioned, indicating the considerable variation in practice in the use of this stage.

When collected, pupae are normally reared to the adult stage and the PMI back-calculated from eclosion. This requires controlled rearing conditions and assumes the pupae have not died within the puparium, been parasitised or entered diapause, preventing emergence or affecting their lifecycle length (Myskowiak & Doums, 2002). Age estimation of pupae can take considerable time in context of a criminal investigation; emergence takes up to ~11 days for *C.vicina* pupae at 22°C.

Two age estimation techniques are currently used for preserved pupae (despite the absence of published standard protocols for preservation). These provide PMI estimates to a resolution of days-weeks at best. The first is puparium colouration (Fig. 1.11). At pupariation, sclerotisation of the puparium changes its colour from white to brown over a period of 12-24 hours at 22^{o}C (Greenberg & Kunich 2002). Pupae with pale puparia are likely to be less than 550 ADH from the start of pupation. However since full tanning does not always occur (Fig. 1.11) this may be unreliable and may underestimate their age. An additional problem is that there are no studies of the colouration rates of different species or their final colour intensities after preservation for short- or long-term periods.

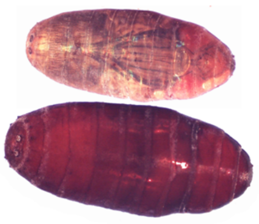

Figure 1.11 Natural differences in puparium colouration. These *C. vicina* pupae are the same age (despite variation in size), yet the top one has developed past the point at which its puparium should be fully tanned, hence showing the inaccuracy of the technique for ageing.

The pupal stage is a quiescent period in which, unlike larvae, no size changes are observed. Instead, perceived stage of development through metamorphosis is used to estimate pupal age. However, pupae are typically classified only as relatively ‘young’ or ‘old’, resulting in a PMI estimate with a window of approximately one week, backed by limited research (Gaudry *et al.,* 2001; Greenberg & Kunich 2002).

Molecular approaches to pupal age estimation using gene expression patterns are currently under investigation. Variation in temporal expression of *C. vicina* genes has been identified but to date only a limited correlation between expression level and age, suitable for PMI estimation, has been made (Ames *et al.,* 2006; Zehner *et al.,* 2009; Tarone & Foran 2011). This will be discussed in further detail in Chapter 1.6.2 and 7.

In summary, PMI is estimated with the greatest accuracy using larval stages. However, should pupae be found associated with a cadaver, and not considered as contaminants (Archer *et al.,* 2006), then estimating PMI from these, as the oldest stage present, is essential. Currently, pupal ageing methodologies are inaccurate and unreliable, even utilising pupae reared to eclosion, and this suggests an important area for further research in the field.

1.6 Improving PMI estimates from pupae

Pupae are immobile and remain associated to the scene for over 50% of the *C. vicina* lifecycle (approx. 10 days at 22°C). As a result, PMI estimates using pupae are relatively wide. This is partly due to the paucity of research into developmental morphology studies in this period.

1.6.1 Morphological development

Early ideas on the evolution of insect holometaboly (complete metamorphosis) from primitive forms of metamorphosis (ametaboly and hemimetaboly) were put forward in the early 20th Century, with new concepts based on changes in endocrinology being presented more recently (Berlese (1913) & Poyarkoff (1941) in Truman & Riddiford (1999)). Initial metamorphosis research was conducted on the complete development of individual organs, systems and physiology in a very limited number of species (Snodgrass 1930; Wigglesworth 1954; Wigglesworth 1965). Most studies were carried out on model organisms and those of medical importance such as *Drosophila* and *Anopheles* species respectively.

Development of, or the final, adult anatomy has since been studied by multiple authors, on many different dipteran species and is summarised in Table 1.6. The absence of *C. vicina* data suitable for age estimation is evident; for morphological comparison, the wealth of Drosophilidae data can be used. *Drosophila melanogaster* rhodopsins (Rh3 and Rh6 photoreceptors) display 80% amino acid sequence homology to *C. vicina* (Schmitt *et al.,* 2005), and their most recent common ancestor was 100 million years ago (Hennig (1981) in Codd *et al.,* 2007), indicating a fairly close relationship. Where available, studies of the Muscidae and Sarcophagidae, which are more closely related to the Calliphoridae, should also be used for comparison.

Calyptrate leg and wing formation during pupation have been documented, however hand-drawn appendage images (Fig. 1.12) lack detail and the absence of developmental temperature information limits utility for age estimation purposes (Ranade 1977). SEM and histology images of eye formation (Fig. 1.13) are correlated to stage in metamorphosis and may help to estimate age and PMI but with a large window of error (Finell & Jarvilehto 1983).

Table 1.6 Studies of morphology and development of specific anatomical features in Diptera. *Calliphora vicina* is the main Calypterate and forensically important species studied. The table does not include complete metamorphosis studies, which tend to describe multiple features in lesser detail.

Morphology	Species	Authors
Compound eyes	*Calliphora vicina*	Finell & Jarvilehto (1983); Jarvilehto & Finell (1983); Wunderer & Smola (1982)
Compound eyes	*Drosophila* spp.	Hausman (1949); Krafka (1924)
Labellar taste hairs	*Calliphora vicina*	De Kramer & Van Der Molen (1984)
Proboscis	*Calliphora vicina*	Graham-Smith (1930)
Ptilinum	*Calliphora vicina*	Laing (1935)
Head and mouthparts	Diptera	Peterson (1916)
Neurosecretory system	*Calliphora vicina*	Thomsen (1969)
Eye neurones	*Musca domestica*	Frohlich & Meinertzhagen (1982)
Neurones	*Drosophila* spp.	Tissot & Stocker (2000)
Brain	Diptera	Shiga (2003)
Salivary glands	*Calliphora vicina*	Berridge *et al.*, (1976); Levy & Bautz (1985)
Leg sensory organs	*Phormia regina*	Lakes & Pollack (1990)
Leg disc	*Drosophila* spp.	Condic *et al.*, (1991); Fortier *et al.*, (2006); Reed *et al.*, (1975)
Leg muscles and tendons	*Drosophila* spp.	Soler *et al.*, (2004)
Legs and wings	*Musca domestica*	Ranade (1977)
Leg and wing disc	*Drosophila* spp.	Taylor & Adler (2008)
Wing disc	*Drosophila* spp.	Aegerter-Wilmsen *et al.*, (2007)
Wing muscle	*Drosophila* spp.	Lehmacher *et al.*, (2009)
Trachea	*Drosophila melanogaster*	Whitten (1957)
Abdominal muscle	*Calliphora vicina*	Crossley (1965); Crossley (1972)
Reproductive organs	*Calliphora vicina*	Graham-Smith (1938)
Ovarioles	*Musca domestica*	Kulshrestha (1970)
Imaginal discs	*Calliphora vicina*	Sprey (1970)
Imaginal discs	*Drosophila* spp.	Chen (1929)
Cuticle	*Sarcophaga falculata*	Dennell (1947)
Cuticle	*Drosophila* spp.	Fristrom *et al.*, (1982); Madhavan & Madhavan (1980)

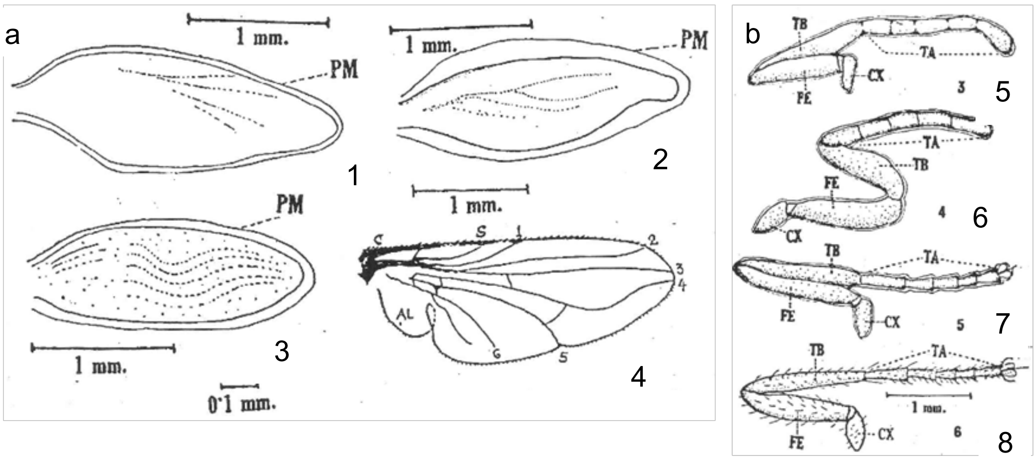

Figure 1.12 *Musca domestica* pupal wing and leg development. a: Wing development shown at 24 hours (1), 48 hours (2), 72 hours (3) and 96 hours (4), with the peripodal membrane (PM) indicated. b: Leg development shown at 24 hours (5), 48 hours (6), 72 hours (7) and 96 hours (8), with the tarsi (TA), tibia (TB), femur (FE) and coxa (CX) indicated (Ranade, 1977).

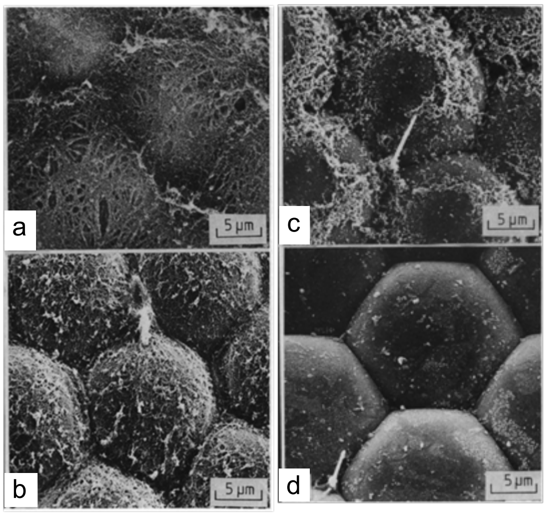

Figure 1.13 The developing ommatidia of the compound eye of *Calliphora erythrocephala (vicina).* The images show the changes in morphology over time of the external structure of the corneas of the compound eye. a: juvenile pupa, b: histogenic pupa, c: premature pupa, d: mature pupa (Finell & Jarvilehto, 1983).

More recent studies use more advanced techniques. Taylor & Adler (2008) document leg development in *Drosophila* spp. using fluorescent staining and secondary antibodies with confocal microscopy (Fig. 1.14). Whilst this is clearly a useful technique for morphological study for small translucent drosophilid pupae, the method requires genetically modified fly stocks expressing green fluorescent protein (GFP)-tagged proteins. This is unsuitable for age and PMI estimation of larger, opaque wild type calliphorid pupae collected from the crime scene.

The only accounts of *C. vicina* pupal development are given by Perez (1910) and Lowne (1985). Lowne focuses on larval histolysis, with limited data on imaginal disc and adult morphological development; Perez provides hand-drawn images and descriptions, but they are difficult to follow. Both studies have limited utility for age and PMI estimation. Accounts of *D. melanogaster* metamorphosis (Robertson 1936; Bainbridge & Bownes 1981), despite it not being a forensically important species, provide the most detailed descriptions for comparison to *C. vicina* although times and morphological differences between species will be present.

Despite the lack of developmental data demonstrated here (which will be discussed further in Chapter 5), it is claimed that calliphorid pupal age can be estimated using morphology to within 10% of pupal development (Gaudry *et al.,* 2001), which equates to ~1.1 days at 22°C for *C. vicina*. Gaudry *et al.* (2001) presents no data, nor indicates which data it uses to substantiate its claim; it is assumed the estimate is based on a qualitative and subjective assessment of relative developmental stage of the pupa. More reliable and robust pupal age estimation methods must be sought. Two possible molecular analyses for age estimation that have been studied in Diptera are steroidogenesis, and temporal gene expression.

Figure 1.14 Fluorescent staining of a *Drosophila* leg. The series of images show the growth of a *Drosophila* leg from the 3rd instar stage, through white pre-pupal stage (wpp), and 2, 4, 6 and 30 hours after the white pupa (awp). Fluorescent secondary antibody staining highlights the *omd* domain (GFP – green), and red fluorescent phalloidin staining highlights the actin cytoskeleton (Taylor and Adler, 2008).

1.6.2 Molecular methods

Circulating levels of ecdysteroids (hormones) vary significantly throughout the moult cycle and metamorphosis. Quantification by Enzyme-linked immunoassay (EIA) of 20-hydroxyecdysone in the pupal stage has the potential to provide a method of age estimation, as shown in *Protophormia terranovae*. Pupae were collected every 6 hours and comparisons were made between fresh pupae and those preserved at -20°C then dried at room temperature for 5 weeks (a relatively long time for legal investigations). Fresh pupae (Fig 1.15) showed a distinct pattern of titre levels, the peak corresponding to pupation. Dried pupae produced a more erratic pattern and inter-individual variation was higher. Using fresh pupae it is therefore possible to determine whether a pupa is aged between 2-3 days (at 22°C) (Gaudry *et al.,* 2006), but no indication of age older or younger than this is possible, as levels are similar, for example a fresh weight of 375 fmol/mg was recorded at ~4, 41 and 79 hours (Fig. 1.15).

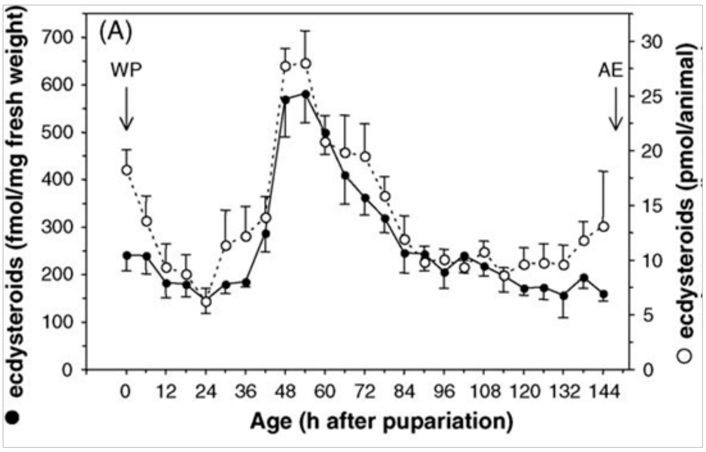

Figure 1.15 Ecdysteroid titre in fresh *Protophormia terranovae* pupae. Age of pupae (in hours after pupation, at 24^{o}C) is correlated to ecdysteroid mass per mg of pupa and per animal. WP = white pupa, AE = adult eclosion (Gaudry *et al.*, 2006).

During metamorphosis, gene expression levels change dramatically as tissues are histolysed and new proteins synthesised. This has been studied extensively in *Drosophila* spp. (Arbeitman *et al.,* 2002; Lebo *et al.,* 2009; White *et al.,* 1999); variations in expression levels are shown throughout embryogenesis, though few studies have focussed on the pupal stage. *Drosophila* data could be used to predict which genes may be most suitable for examination in *C.vicina*, but to date limited studies have been made. For assessment of temporal gene expression, robust housekeeping genes must be used for comparison as an internal control for RNA quantity (Zehner *et al.,* 2009; Zehner *et al.,* 2006). The absence of *C. vicina* sequence data has led to attempts to identify candidate genes by differential display PCR (ddPCR). This method is highly time-consuming for the level of age resolution required for accurate PMI estimation. Studies will be discussed in more detail in Chapter 7, however Ames *et al.,* (2006) demonstrate that gene expression can be correlated to calliphorid pupal age, allowing quantitative analysis of accurate age and subsequent PMI estimation, highlighting the potential of this methodology. A pre-requisite for the correlation of morphological or molecular changes to age, is the collection of pupae of a known age.

1.6.3 Oviposition behaviour and natural lifecycle length variation

There are three important issues that can lead to errors in collection of known-age samples, which need to be addressed. These are a) the definition of a starting time point, b) the occurrence and development of precocious eggs and c) the variation in pupal stage length.

The age of pupae may be logically measured from one of two starting points; oviposition or pupariation. Variation in start time will ultimately result in variation in the age correlated to specifc developmental events, therefore causing errors in PMI estimation of crime scene samples using research data. Previous studies into calliphorid pupal development give age relative to pupation (which occurs over ~24 hours (Fraenkel & Bhaskaran 1973)), however the variation in the definition of and difficulties in observation of this point results in inconsistencies in age estimation (Robertson 1936; Bainbridge & Bownes 1981; Finell & Jarvilehto 1983; Robertson 2005; Sivasubramanian & Biagi 1983). Oviposition is a far more definable point and is more easily controlled and represents a more robust start point for measuring pupal age.

Egg collection within a defined time frame is therefore a necessary pre-requisite to ensure the ages of samples are accurately known. Precocious eggs result from premature fertilisation of a single egg, held within the genital chamber or ovipositor of the adult fly resulting in advanced development of such eggs relative to the rest of the batch. In some cases embryogenesis can be completed prior to oviposition, and a larva would then be laid. If this larva were used to estimate PMI then the estimate would be overestimated by one day at 22°C. The phenomenon is known to occur in the calliphorids (Erzinclioglu 1996; Lowne 1895; Wells & King 2001), but levels of occurrence of these significantly older samples in developmental studies and at crime scenes has not been widely studied. General oviposition behaviour in *Calliphora vicina* is largely unknown, though some studies have been carried out in *Lucilia* spp. (Hobson 1937; Barton Browne 1958). Information such as meat receptivity and laying times required by flies need to be documented to establish a minimum collection timeframe and develop suitable egg collection protocols.

All immature calliphorids collected within a single cohort will develop at slightly different rates due to natural variation (Finell & Jarvilehto 1983). This increases with lifecycle progression, thus later stages will have larger associated variation. Development of particular features will therefore occur over an age range. To date only limited data are available that document variation in the length of the lifecycle and pupal stage.

Overall, there are significant gaps in our fundamental knowledge of *C. vicina* oviposition behaviour and morphological development in the pupal stage, and since this underpins all developmental data required for accurate age and PMI estimation, further research in these areas is required.

1.6.4 Summary

The pupal stage may be considered as a so far untapped resource for PMI estimation due to the length of time spent within it, its persistence at the scene, and the large developmental changes occurring during metamorphosis. General *C. vicina* behaviour and pupal development are understudied, despite its status as a species of global forensic importance, resulting in underutilisation of the pupal stage in PMI estimation.

With improved knowledge of the oviposition behaviour and natural lifecycle variation of this species, it may be possible to improve the accuracy of age estimates from the pupal and other lifecycle stages, resulting in more robust PMI estimates. The development of pupal preservation protocols, in conjunction with documentation of detailed morphological and molecular developmental data, should enable more widespread collection and analysis of the stage, allowing their increased and better use in forensic investigation involving PMI estimation.

1.7 Aims of the thesis

The purpose of this study is to improve the age assessment of *C. vicina* pupae for use in PMI estimation. The specific aims of this study are divided into four broad sections:

a) To establish protocols for the collection of eggs with accurately calculated age and minimised precocious development, and to document natural variation in *C. vicina* lifecycle length.

b) To establish optimal preservation methods suitable for lab and/or field use for individual pupal age estimation techniques, and to test whether a general pupal preservation method can be found that is suitable for a multidisciplinary age estimation approach.

c) To test whether development of morphological features at the macro- or microscopic level can be used to estimate pupal age, and establish the associated morphological variation.

d) To test whether temporal gene expression patterns can be used to estimate pupal age. This will entail identification of appropriate housekeeping and candidate developmentally expressed genes.

Chapter 2 – Methods

2.1 Trapping and colony establishment

Trapping of wild *C.vicina* for colony establishment was carried out at two locations: Portsmouth, UK (50° 47′ 51.08″ N, 1° 5′ 46.87″ W) and Waterlooville, (50° 54′ 26.02″ N, -1° 1′ 16.29″ W), depending on the experiment.

Ox or pigs liver-baited fly traps were constructed using plastic or glass bottles (Fig. 2.1). They were placed in shaded locations amongst vegetation to minimise disturbance and increase the numbers of *C. vicina* adults caught and eggs recovered.

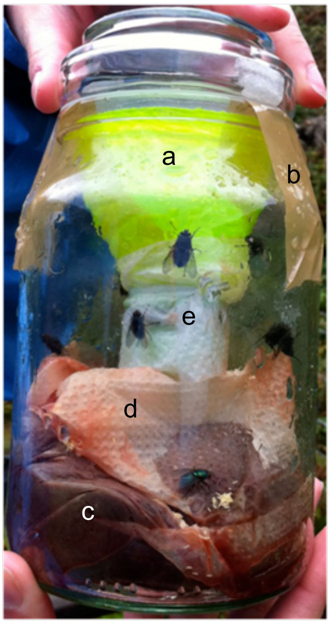

Figure 2.1 Trap used for wild adult and egg collection. The top of a plastic bottle (a) was cut off, inverted and taped to the glass jar (b) or plastic bottle, after adding liver (c) on paper towel (d), to absorb excess liquid. Flies entered through the funnel (e), which limited escape after laying eggs on the paper/liver.

Colonies were established and maintained in controlled growth rooms. The temperature was set at 22°C, humidity levels were between 40-60% and a 16:8 hour light:dark regime was imposed to regulate photoperiodism.

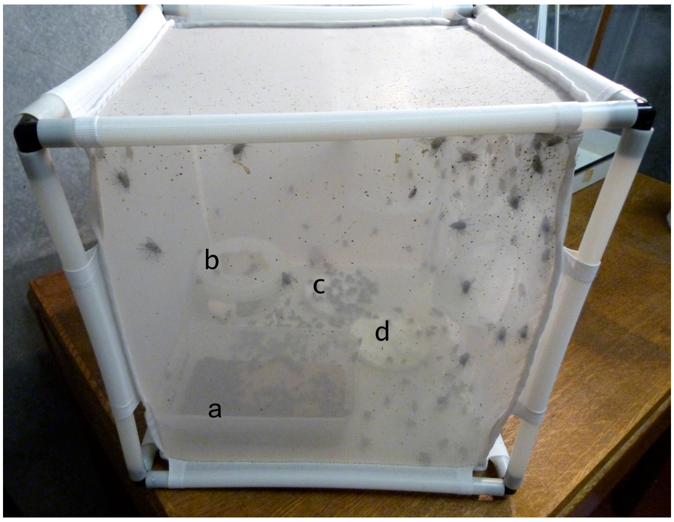

Figure 2.2 BugDorm set up at adult emergence. Pupae were placed in a plastic container prior to emergence (a). Water was provided in a plastic tub with a felt wick (b). Sugar (c) and milk powder (d) were provided in Petri dishes.

Following collection, adults were identified using a standard key (Erzinclioglu 1996), and transferred to BugDorms (http://bugdorm.megaview.com.tw) (Fig. 2.2). Colonies were supplied with water and granular sucrose (in a Petri dish) at all times, and also milk powder (also in a Petri dish) when not presented with meat for oviposition (including during meat starvation).

Eggs collected from the wild were reared on liver in plastic containers at 22°C (Fig. 2.3). The meat/paper towel was sprayed daily with water to retain humidity. Fresh liver was supplied to larvae as required until the post-feeding stage. Prior to emergence (at ~10 days at 22°C), pupae were sieved from the sand transferred to a sand bed in smaller containers which were placed in a BugDorm (Fig. 2.2). Disturbance was kept to a minimum throughout development.

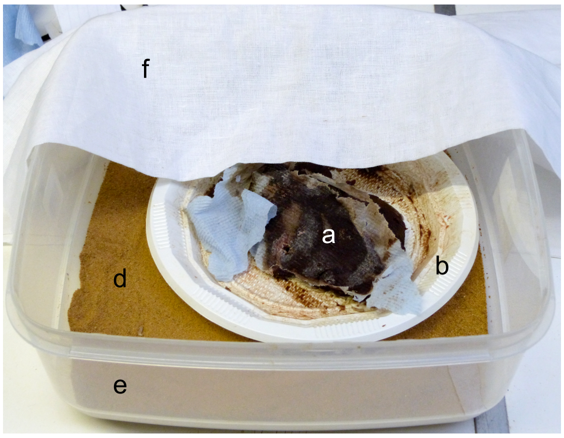

Figure 2.3 Collection and rearing of wild eggs. Liver and tissue carrying the eggs (a) in the trap were transferred to a plastic plate (b), which was placed on a bed of sand (d) in a plastic container (e). The container was covered with a double layer of muslin (f), to prevent larvae escaping and parasitic wasps entering.

2.2 Colony maintenance

Adult *C. vicina* require a meat feed for ovary maturation (Pappas & Fraenkel 1977). To achieve this, ~150 g liver was placed in the BugDorm from at least 3 days after the first flies emerged. Meat was allowed to equilibrate to room temperature overnight in a sealed container in the growth room, unless stated otherwise. In the BugDorm, meat was placed on moistened paper towel, in small plastic containers, and sprayed daily to retain humidity. After ~5 days, eggs were laid on the meat, which indicated that ovary development was complete in at least some individuals. A period of meat starvation was then introduced (adapted from Hobson, 1937b), which a) permits adequate time for ovary development in all females, b) assists predictable laying on re-introduction of meat and c) imitates wild situations where oviposition sources may only be located days or weeks after eclosion.

When eggs were required for larval or pupal sampling, or for starting new adult colonies, fresh liver (organic pigs liver for sample collection) replaced the milk powder in the BugDorm. Eggs were collected at set oviposition intervals, or overnight, depending on the experiment (as described below). Unless otherwise stated, 100-150 g liver was initially presented for 30 minutes and eggs laid discarded. The liver was then presented for 30 minutes. Eggs laid in this period were retained for rearing (as suggested by Sonnenblick in Demerec (1950)) and as previously described (Fig. 2.3).

2.3 Temperature monitoring

During sampling periods, the temperature of the growth room and each of the colonies was monitored at 15-minute intervals using iButtons (Thermochron, http://www.maxim-ic.com) or probes (Thermatag, http://us.digitron.co.uk). iButtons were tied inside nitrile glove tips to prevent water damage. Sensors were moved to the centre of the larval mass as they formed and moved around the meat.

2.4 Rearing, collection and preservation of immature Diptera

Eggs were handled carefully using a water-moistened scalpel, spoon, paintbrush or forceps depending on numbers. They were preserved by placement in 80% ethanol, and stored in this solution at 4°C. Larvae were collected for histological analysis, and preserved by hot-water-killing and storage in 80% ethanol at 4°C. Details of the different rearing, sampling and preservation strategies for pupae are described for each experiment accordingly.

2.5 Calculation of pupal ages

2.5.1 ADH age

Temperature data in °C obtained from iButtons or probes every 15 minutes was multiplied by 0.25 to obtain the ADH accumulated during that time, starting from the mid-point of the oviposition interval (Table 2.1). The ADH values were then added together throughout the larval and pupal stages to calculate sample ages in ADH, taking into account larval mass temperatures. An LDT temperature correction of 0°C was applied (as this is non-lethal), to allow the possibility of geographically different *C. vicina* LDTs (Donovan *et al.,* 2006; Davies & Ratcliffe 1994; Marchenko 2001; Saunders & Hayward 1998) to be incorporated into the data set.

Table 2.1. Calculation of ages in ADH. ADH calculation shown starting from the mid-point of oviposition, applying an LDT of 0°C. The first 15 minutes development is shown at 21.95°C, giving an age of 5.49 ADH at this point. This method takes account for rises and falls in temperature as shown.

Temperature °C	Time interval (hours)	Age ADH	Calculation
21.95	0.00	-	-
21.95	0.25	5.49	= 0.25 x 21.95
22.00	0.25	10.99	= 0.25 x 22.00 + 5.49
30.00	0.25	18.49	= 0.25 x 30.00 + 10.99
18.55	0.25	23.13	= 0.25 x 18.55 + 18.49

2.5.2 Percentage development through lifecycle or pupal stage

Pupal ages were also calculated as percentages of the maximum total lifecycle (laying to eclosion) and through the pupal stage (% TPS). The minimum and maximum pupal ages observed in this study were 3911 ADH and 11358 ADH respectively, thus ages were calculated as follows:

$$Lifecycle\,\% = \frac{\mathrm{ADH}}{11358}\,x\,100$$

$$Pupal\ stage\,\% = \frac{\mathrm{ADH}}{7447}\,x\,100$$

Where ‘ADH’ is the age at which the pupa was calculated as, or the age at which a specific feature was noted. 7477 ADH was the maximum length of the pupal stage (11358 ADH – 3911 ADH).

2.6 Microscopy and imaging

All immature stages and slides thereof were observed initially using Mazurek Zoom Microtec HM-3 and Nikon Eclipse E800 microscopes at 7 – 20x and 40 – 100x magnification respectively. Images were taken using a Zeiss SteREO Lumar.V12 microscope and accompanying Axiovision software unless stated otherwise. Post-processing was carried out using Adobe Photoshop to adjust shadows and highlights. Measurements of pupae (to monitor the effects of preservation) were carried out using a standard ruler to the nearest 0.5 mm.

Living *C. vicina* pupae 4 days and 10 days post-puparium formation were analysed by optical coherence tomography (OCT). Pierced and hot-water-killed pupae were also examined. Pupae were individually placed on the motorised stage of the OCT microscope (Michelson Diagnostics), and scanned at different orientations and lateral resolutions, up to 30 frames per second (Table 2.2).

Scans were saved as .tiff files, and viewed in Voxx (http://www.nephrology.iupui.edu/imaging/voxx) and Image J (http://rsbweb.nih.gov/ij), in three dimensions and as 2D stacks respectively.

Table 2.2. Analysis of pupae using OCT. Live and fixed 4 and 10-day old pupae, were analysed with their dorsal, ventral or lateral surfaces upwards. The lateral scanning resolution was either 8 or 12 µm.

Pupa #	Age (days)	Condition	Orientation	Resolution
1	4	Alive	Dorsal	12 µm
2	4	Fixed	Ventral	8 µm
3	10	Fixed	Dorsal	12 µm
4	10	Alive	Ventral	12 µm
5	10	Alive	Lateral	12 µm
6	10	Fixed	Lateral	12 µm

2.7 Observation of oviposition behaviour

Following protein starvation for one week, 10 females were selected, cooled to 4°C and individually identified by painting their thoraces with acrylic paint. Cubed organic pigs' liver was provided for oviposition. Oviposition behavior and periods of activity were recorded for individual flies by a webcam in real time for 5 hours 54 minutes (Fig. 2.4).

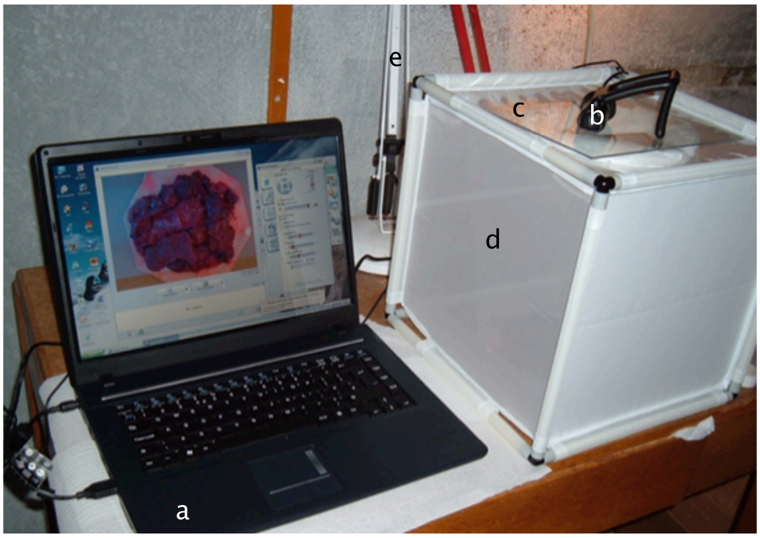

Figure 2.4 Set up for observation of oviposition behaviour. Laptop (a), with webcam (b) placed on glass (c) over the opening hole of a standard BugDorm (d). Within the BugDorm was a thin, flat metal plate, covered in blood-soaked tissue with 150 g cubed liver placed on top. The light (e) was positioned slightly to the right of the meat.

2.8 Analysis of precocious egg occurrence

2.8.1 Influence of protein starve and permitted oviposition periods

Flies were allowed to oviposit under constant lighting conditions, on liver for periods of 15 or 30 minutes, after 1, 2 or 3-week protein starves (Table 2.3). Fresh meat was then immediately placed in with the colony again, and oviposition allowed to continue for the same period and then repeated a final time. Upon removal of the meat each time, eggs and larvae were counted and the percentages of precocious eggs (noted as larvae) of total egg number were calculated.

Table 2.3. Colony set up for the examination of the effect of protein starve and oviposition period times. All females were F1 generation. Colonies 1 & 3 and 2 & 4 are direct repeats Colonies 5 and 6 are single trials.

Colony Number	Starvation Time (weeks)	Oviposition Period (minutes)
1	1	15
2	1	30
3	1	15
4	1	30
5	2	30
6	3	30

2.8.2 Timing of egg-hatching throughout embryonic development

Three mature colonies comprising 50 males and 50 females were established from a single colony. Liver was presented for 60 minutes (smaller colony sizes required longer to lay eggs) every 8 hours to collect eggs from each colony. Hatching was monitored throughout embryogenesis (Table 2.4). This method resulted in three repeats for each observation time interval, and removed any bias caused by either a) repeat collections from the same colony or b) collection throughout the night during un-natural laying hours. The percentage of precocious egg occurrence was calculated and ages were calculated in ADH.

Table 2.4. Oviposition sampling and monitoring schedule. Embryogenesis and hatching were monitored over the entire stage (26 hours) using eggs collected from three colonies every 8 hours. For example, collection 1 was observed during 0-10 hours from colony 2, 9-18 hours from colony 3 and 17-26 hours from colony 1.

Colony	Collection number	Collection time	Observation time
1	1	16:00	17-26 hours
	2	00:00	9-18 hours
	3	08:00	0-10 hours
2	1	08:00	0-10 hours
	2	04:00	17-26 hours
	3	00:00	9-18 hours
3	1	00:00	9-18 hours
	2	08:00	0-10 hours
	3	16:00	17-26 hours

2.8.3 Assessment of precocious eggs occurrence in wild-caught adults

Glass jars containing meat covered with dry tissue (to prevent egg laying) were placed in shaded locations in Waterlooville, UK over two days in June 2010 to attract *C. vicina* female adults. Traps were continuously monitored, and flies were removed and preserved in 80% ethanol before oviposition could occur. Their abdomens were then dissected and ovary development examined, with their size in relation to the abdomen ranked as small or large (Fig. 2.5). In addition, the presence of eggs and larvae in the genital chamber or ovipositor beyond the spermatheca were noted.

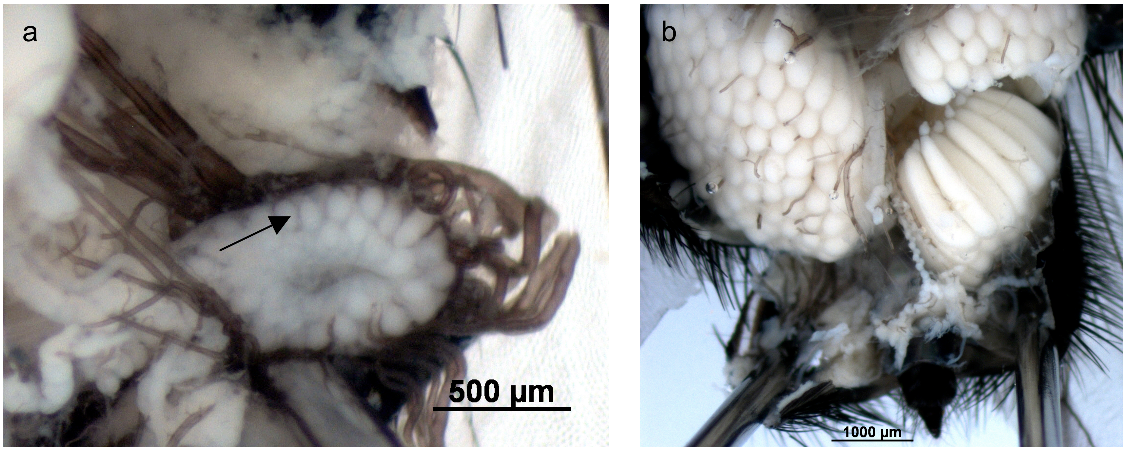

Figure 2.5. Ovary development. Early in adult development, the ovaries are small (a) and contain immature oocytes (arrow). Fully developed ovaries (b) comprise mature oocytes and occupy most of the abdomen. The fly is termed gravid once ovaries have reached this large size.

2.9 Examination of variation in pupal stage length

2.9.1 Larvae reared on an unlimited food supply

Two ‘fully fed’ trials were conducted ($T_{FF}1$ & $T_{FF}2$). Control colonies were established from the eggs collected in each trial to monitor the effects of disturbance (including sieving) of larvae and pupae. In $T_{FF}1$, wandering larvae were sieved daily and pupae (1407 in total) were collected in vials and covered with sand. Collection of pupae ceased after all remaining post-feeding larvae had either died or pupated. At eclosion adults were counted and sexed daily, ceasing once >95% adults had emerged. In $T_{FF}2$, a small cohort of eggs was selected from the total laid, to reduce the effect of maggot mass temperatures on developmental rates and to facilitate sexing upon emergence. Developmental temperatures were measured every 6 hours using both an iButton and an infrared thermometer directed 5 cm above the mass. Pupae (71 in total) were collected daily as in trial one. Eclosion of adults was monitored as in $T_{FF}1$. Pupal stage and lifecycle lengths were then calculated for all pupae ($T_{FF}1$ & $T_{FF}2$) in days, and also in ADH for $T_{FF}2$, using temperatures from throughout the lifecycle.

2.9.2 Starved larvae

Two ‘starve’ trials were conducted (T_S1 & T_S2). Larvae were given meat *ad libitum* until the third instar stage, 3-4 days after oviposition at 22°C. The larvae in each trial were then split into three cohorts: a control ($T_{CS}1$ & $T_{CS}2$ - fully fed and undisturbed), a ‘fully-fed and disturbed’ cohort ($T_{FS}1$ & $T_{FS}2$ – treated similarly to $T_{FF}1$ & $T_{FF}2$) and a ‘starved’ cohort, with either a) 16 larvae and 16 g meat (after 3rd instar) in T_S1 or b) 73 larvae with no meat in T_S2. All pupae were sampled as previously described, using sieving to select pupae from the substrate. Developmental temperatures and eclosion were monitored for all colonies, and analysis of results was conducted as before.

2.10 External morphological analysis

Two collection trials were conducted (denoted T1 and T2 respectively), in order to a) obtain large sample numbers of the same age for multiple analyses (see also Chapters 6 & 7) and b) repeat the analysis with an increased dataset. Subtle differences in collection protocols were present in T1 and T2.

2.10.1 T1: Collection protocol used for morphological and molecular analysis

Eggs were collected from a wild colony overnight, reared under standard conditions and three F1 colonies were established and matured. After 7-day protein starves, eggs were collected from all 3 colonies at 30-minute oviposition intervals on to organic pigs liver. The second batch collected was retained for analysis. A small batch of the F2 eggs (<300) from each F1 colony was pooled as a control, monitoring lifecycle length and the effect of disturbance (by collection – see below). Remaining F2 eggs were reared as individual colonies for sampling, and developmental temperatures were recorded.

Upon formation of the white puparium, 27 pupae were collected and pooled from all three F2 colonies every six hours, using sterile forceps. Pupae were brought to the surface of the sand by gentle shuffling of the containers. Optimal preservation methods had not been established at this point; as such 10 pupae were preserved by piercing three times (once through each tagma) and placement in Kahles solution (see Appendix II) at 4°C for external morphological analysis. The remaining pupae were preserved for histological and gene expression analyses (Chapters 6 and 7 respectively). Temperature data obtained was averaged for each sample set as pupae were pooled (overall mean = 23.2°C, S.D. = 0.17°C), and these data used to calculate age in ADH.

2.10.2 T2: Morphological analysis (repeat)

Eggs (F1) were collected and split into six cohorts; an undisturbed control, a control monitoring pupal stage length (see Chapter 3), and four sampling cohorts (to minimise larval mass effects on temperature). Developmental temperatures were monitored as before.

After pupation, five pupae were collected from each container every six hours and preserved in corresponding separate vials. The optimal preservation method for external morphological analysis was utilised: pupae were pierced three times, hot-water-killed, preserved in 80% ethanol and stored at -20°C. All pupae were collected from two of the four containers before sampling was complete (at adult emergence) so extra pupae from the other containers were collected to complete the total set of 20 pupae.

2.10.3 Analysis of external morphological characteristics

Pupal cases were removed within two weeks of preservation, and pupae remained in preservative for a maximum of two months prior to analysis in 70% ethanol. Changes in morphological characteristics/features over time were categorised (Table 2.5). Observations included colour, form and size changes. Due to complexity, eye colour was categorised using a Pantone colour chart (Table 2.6), which was obtained from Adobe Photoshop CS5 and printed on a Canon colour laser printer.

2.10.4 Age estimation and validation

Age estimates were calculated based on observed age ranges of developmental categories of features (Table 2.5), and using statistical regression analysis in Minitab to construct an age estimation equation.

Validation of methods was carried out initially using two separate semi-blind analyses (SB1 and SB2) of pupae taken from both trial test sets (T1 and T2). 15 (SB1) and 20 (SB2) pupae were selected from both T1 and T2 by another researcher, who recorded the actual age of the samples. Age estimation was carried out on these individual SB1 and SB2 pupae, and finally compared with actual ages.

In the blind-sampling trial (B1), eggs were collected from an F3 colony after a 9-day protein starve with a 60 minute oviposition interval. Eggs collected were divided into two cohorts for rearing; an undisturbed control and a test set. 15 pupae were collected at 10 known points throughout the pupal stage by another researcher, and preserved using optimal methods. In the second (repeat) trial (B2), a wild colony was used for egg collection, and 10 pupae were collected at each sampling point. Upon completion of analysis, predicted ages were compared to the collection dates and actual ADH ages.

Table 2.5. Morphological features examined and categories selected. The following features were examined on all pupae, and development observed for each feature categorised as shown.

Compound eye colour	Brown
	Red
	Pink
	Pale Pink
	Cream
	Absent
Orbital/frontal bristles	Black
	Brown
	White
	Absent
Thoracic Bristles	Black
	Brown
	1/2 brown
	White
	Developing
	Absent
Abdomen Macrochatae	Black
	Brown
	White
	Absent
Abdomen Microchatae	Black
	Brown
	Developing brown
	White
	Absent
Antennae colour	Black
	Brown
	1/2 Brown
	White
	Absent
Arista colour	Black
	Brown
	White
	Bald
	Absent
Labella colour	Brown
	White
	Absent
Oral lobe setae	Brown
	Absent
Palp colour	Pale brown
	Brown or Black hairs
	Developing/White
	Absent
Labrum colour	Brown
	Pale brown
	White
	Absent
Jowl bristles	Black
	Brown
	White
	Absent

Wing Colour	Dark silver
	Silver
	Pale silver
	White
	Absent
Wing Folding	All folded
	Partially folded
	All unfolded
	Fat veins
	Tissue mass (no veins)
	Absent
Leg Bristle Colour	Thick black
	Fine black
	White
	Absent
Leg length	Full
	Short
	Very short
	Absent
Abdominal segments	Adult
	Pupal
	Larval
Leg width	Fine
	Inflated
	Absent or short
Antennae shape	Full length
	Elongated
	Round
	Round and wide
	Round and lateral
	Absent
Labella shape	Complete
	Oral hair growth
	Double end lobed
	End lobed
	Double lobed
	Slightly lobed
	Square
	Absent
Labrum shape	Complete
	Full length
	Pointed
	Elongated
	Arrow
	Absent
Palp shape	Full length
	Long or clubbed
	Slightly elongated
	Round
	Absent
Cephalopharyngeal skeleton	Everted
	Membrane-enclosed
	Loosened
	Attached

Table 2.6. Eye colour chart. The following Pantone colour chart (sourced from Adobe Photoshop CS5 was used to assess compound eye colour, then assign it a category. The chart was read from the y-axis then the x-axis, e.g. 51.36.

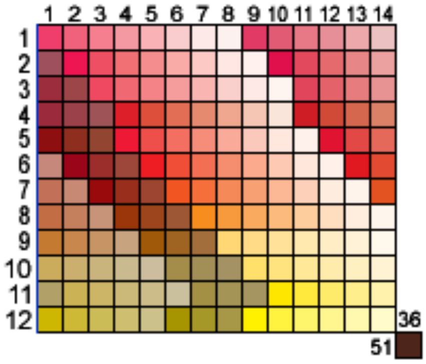

Eye Colour	Shades								
Brown	51.36								
Red	3.3	3.4	4.3	5.2	6.2	6.4	8.6	9.7	
Pink	2.4	2.5	3.5	4.6	5.7	5.8	6.9	7.10	8.9
Pale pink	7.11	7.12	7.13	8.12	8.13	8.14	9.14	10.14	
Cream	12.14								

2.11 Histological analysis

2.11.1 Clearing and embedding

Pupae were transferred from preservative solution into cassettes (Simport Plastics) and cleared overnight using a method adapted from Bodenstein in Demerec (1950), in a Citadel 2000 (Thermo Shandon) tissue processor at room temperature (Fig. 2.6). Briefly, pupae were washed in water before being transferred through an increasing concentration series of ethanols to a xylene substitute, Histosolve (Thermo Shandon),

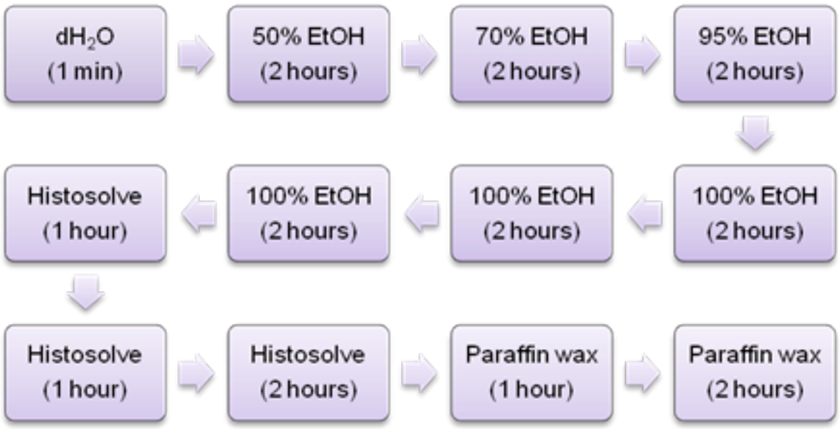

Figure 2.6. Summary of the clearing process. Preserved pupae were cleared in a Citadel 2000 tissue processor over night according to the protocol above. EtOH = ethanol. Pupae remained stationary in each solution for the stated time. Molten paraffin wax was at 57°C; all other solutions were at room temperature.

each step taking 1-2 hours. After clearing, they are transferred into molten paraffin wax (57°C) in two successive stages to remove all Histosolve. After the final wax step in the tissue processor, pupae were then embedded in fresh molten paraffin wax at 57°C in metal moulds.

2.11.2 Sectioning and staining

Once embedded, pupae were sectioned using a Leica Manual Rotary Microtome. 10 µm sections were taken in longitudinal (dorsal-ventral), sagittal (lateral-medial) and transverse planes. Sections were transferred to a warm (37°C) water bath containing 0.5% gelatin (where stated), and mounted onto glass slides. Excess water was absorbed from slides using paper towel, then they were left to dry vertically overnight at 37°C. Sections were put through a series of solutions (400 mL) for staining (Fig. 2.7). They were dewaxed in xylene and rehydrated through a decreasing ethanol series to water, before staining with Harris' haematoxylin (Mercury-free: BDH). Destaining was conducted by washing in Scots water (400mL tap water + 2 drops of 1M NH_4OH) and dipping the slides gently in and out of acid alcohol (1% v/v HCl in 70% v/v ethanol) 2-3 times. Slides were then stained with 1% w/v aqueous eosin yellowish (BDH) before sections were dehydrated through an increasing ethanol series, to xylene. Sections were mounted using DPX.

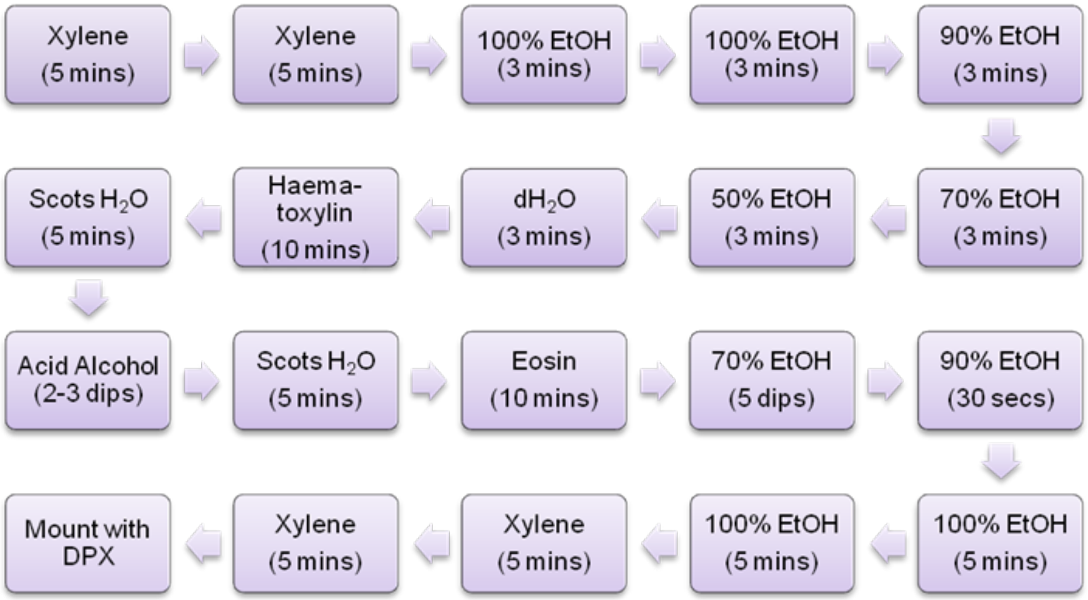

Figure 2.7. Summary of the staining process. All slides were put through the staining process as outlined. All solutions were placed in glass containers. 'Dips' indicates slides were lowered and raised slowly in and out of solution for the specified number of times. 400mL of each solution was used. Scots H_2O comprised 400 mL tap water + 2 drops of 1 M NH_4OH. Acid alcohol was 1% HCl in 70% ethanol. Eosin solution was 1% aqueous.

2.11.3 Examination of internal morphology

Eggs were collected and reared as previously described for external morphological examination (T1). Larvae (when present) and pupae (10 in total per 24-hourly interval) were pierced three times, hot-water-killed, and preserved in 80% ethanol at 4°C.

After one week in preservative, three pupae (from each sample) were bisected (Lowne 1895) between the thorax and abdomen, and cleared overnight through an ethanol series and histosolve to paraffin wax. Pupal halves were separately embedded in fresh paraffin wax for sectioning.

Embedded pupae were sectioned to expose the pupal surface, and then left face-down on melting ice to soften the tissue for sectioning. Pupae were sectioned in longitudinal, sagittal and transverse planes. To faciliate adhesion to slides, sections (take every 250-300 µM) were transferred to 0.5% w/v gelatin in a 37°C water bath prior to mounting on glass slides. Slides were dried prior to staining, mounting and viewing under compound and stereomicroscopes.

2.12 Analysis of DNA

2.12.1 DNA extraction

Pupae (with puparia intact) were separately ground under liquid nitrogen in a 1.5 mL microcentrifuge tube with a sterile micro-pestle. DNA was extracted using the Macherey Nagel Nucleospin Tissue kit, according to manufacturer's instructions. Cell lysis was performed overnight, with an additional 0.1 mg (2 µL of 50 mg/mL) proteinase K added per pupa (in 205 µL lysis buffer & standard proteinase K mix). Extractions lacking pupal tissue (DNA) were also performed and run similarly throughout.

2.12.2 PCR

Amplification of a 1270 bp fragment of the cytochrome oxidase I (COI) gene was carried out using a Veriti 96-well Thermal Cycler (Applied Biosystems), on 100 ng template DNA in a 25 µL PCR reaction. Reaction and cycling conditions and primers were taken from Harvey *et al.,* (2008) and are shown in Tables 2.7, 2.8 and 2.9 respectively.

Table 2.7. COI gene PCR reaction conditions. A 1167bp COI gene fragment was amplified using reaction conditions from Harvey *et al.*, (2008).

Reagent	Concen-tration	Manufacturer
PCR buffer	1x	Genecraft
$MgCl_2$	1.5 mM	Genecraft
dNTPs	0.2 mM	Genecraft
Forward primer	0.5 mM	Eurogentec
Reverse primer	0.5 mM	Eurogentec
Taq polymerase	0.5 Units	Genecraft or Thermo Sci.

Table 2.8. COI gene PCR cycling conditions. A 1167bp COI gene fragment was amplified using a standard set of cycling conditions (Harvey *et al.,* 2008). The reaction was carried out on a Veriti 96-well Thermal Cycler (Applied Biosystems).

Stage	Number of cycles	Time (s)	Temp. (°C)
1	1	90	94
2	36	22	94
		30	48
		80	72
3	1	60	72

Table 2.9. COI gene primers for PCR. A 1167bp COI gene fragment was amplified using standard primers (Harvey *et al.,* 2008). Their sequences are given here orientated 5' – 3'.

Primer name	Direction	Sequence
C1-J-1718	Forward	GGAGGATTTGGAAATTGATTAGTTCC
TL2-N-3014	Reverse	TCCATTGCACTAATCTGCCATATTA

2.12.3 Gel electrophoresis

DNA and RNA extracts and PCR products were visualised on a 1.5 - 2% agarose TBE gel containing 20-75 µg ethidium bromide in 40 mL and 150 mL gels respectively, visualised in a Gel Doc UV transilluminator (BioRad). Various DNA markers were used as appropriate (Table 2.10). Electrophoresis was carried out at 180-200V for 10-15 minutes (40 mL gel) or ~30 minutes (150 mL gel).

Table 2.10. DNA markers for gel electrophoresis. Different DNA markers were used for identification of PCR products and assessment of DNA and RNA extract integrity.

Marker name	Band range	Manufacturer	Uses
Low range plus exACTGene DNA ladder	0.1-2 kbp	Fisher Scientific	Actin, arylphorin and COI gene PCR products and RNA extract analysis
1 kb DNA ladder	0.25-10 kbp	Genecraft	RNA extract analysis

2.12.4 Sequencing

DNA extracts were amplified using high-fidelity Extensor *Taq* polymerase (Thermo Scientific) according to manufacturers instructions. This was to minimise base incorporation errors due to *Taq* polymerase. The resulting PCR product was purified directly using a Macherey Nagel Nucleospin Extract kit. Sequence analysis was carried out by GATC (Germany). The resulting forward and reverse sequences were compared using FinchTV v4.1 (http://www.geospiza.com/Products/finchtv.shtml). A variety of COI gene sequences of similar size (1167bp) from global Diptera species were selected from *NCBI (*www.ncbi.nlm.nih.gov) and aligned with sequences obtained in this study using BioEdit v7.0.5 (www.mbio.ncsu.edu/BioEdit/bioedit.html), and a neighbour-joining analysis using the Tamura-Nei model and bootstrapping (n=500) was performed using Mega 4 (Tamura *et al.,* 2007).

2.13 Analysis of temporal gene expression

2.13.1 Collection and preparation of pupae for developmental analysis

Five pupae were collected every 6 hours (External morphological analysis; T1) using sterile forceps and were stored in sterile 1.5 mL microcentrifuge tubes at -80°C. RNA was extracted from three pupae separately, collected at 24-hourly intervals.

2.13.2 RNA extraction

To extract intact gDNA-free RNA, the Macherey Nagel Nucleospin RNA II kit was used. Fresh or preserved (as detailed in chapters 4 and 7) whole pupae (including puparia) were completely homogenised in a mini bead-beater with 50 mg 0.5mm zirconia-silica beads (Biospec, USA) in 350 µL lysis buffer and 3.5 µL β-mercaptoethanol for 45 seconds. The homogenate was briefly centrifuged (~3-second pulse) before incubation with 100 mg proteinase K for 10 minutes at 55°C (where stated). The standard protocol was then followed after the filtration step. RNA was eluted in 100 µL molecular biology-grade water (Sigma), and stored at -80°C. Extractions without pupal RNA were also performed and run similarly throughout, to assess contamination. Extracts were run on an agarose gel to check for high integrity (presence of rRNA bands (Bagnall & Kotze, 2010)).

2.13.3 DNase I digestion

In addition to the on-column digestion, 50 µL was treated afterwards with DNase I to remove all traces of DNA. 12 µL DNase I incubation buffer (400 mM Tris-HCl, 100 mM NaCl, 60 mM $MgCl_2$, 10 mM $CaCl_2$; pH 7.9; Roche), 2 µL RNase-free DNase I (20 units; Roche) and 1.5 µL Protector RNase Inhibitor (60 units; Roche) were added to 50 µL RNA (35-150 µg), and incubated for 30 minutes at 37°C. An extra 1 µL DNase I

(10 units) was added prior to another 30 minute incubation at 37°C. 335 µL ddH_2O was added and a standard phenol:chloroform extraction and ethanol precipitation (Chapter 2.9.3) was carried out. RNA was precipitated in absolute ethanol at -70°C for at least 1.5 hours. RNA was collected by centrifugation (18,000g, 20 minutes, 4°C), washed with 70% ethanol at 4°C and was finally resuspended in 50 µL dH_2O (Sigma).

2.13.4 Phenol:chloroform extraction

After DNase I digestion, RNA was purified using phenol:chloroform extraction. RNA (~400 µL) was added to 600 µL phenol in a 1.5 mL microcentrifuge tube. This was vortexed for 10 seconds and centrifuged at 13,000 x g for 5 minutes at room temperature. The aqueous phase was added to 600 µL phenol:chloroform:isoamyl alcohol (25:24:1) and vortexed and centrifuged as before. This was repeated with another 600 µL phenol:chloroform:isoamyl alcohol (25:24:1) and then 600 µL chloroform. The aqueous layer was mixed with 1 mL 100% ethanol by inversion of the microcentrifuge tube, and RNA was precipitated at -80°C for a minimum of 1.5 hours or overnight. The RNA was then centrifuged at 4°C for 15 minutes, the pellet was washed with 1 mL 70% ethanol (-20°C) and the RNA centrifuged at 4°C for 5 minutes. Finally, the pellet was resuspended in 50 µL dH_2O (Sigma). RNA was stored at -80°C.

2.13.5 Reverse transcription

The concentration of RNA was crudely estimated using a Nanodrop 1000 (Thermo Scientific) spectrophotometer, by measuring the absorbance at 260 nm (1 absorbance unit = 40 µg/mL RNA). Reverse transcription of 1-2.5 µg total RNA was carried out in a 20 µL reaction volume using Genescript (Genecraft, Germany) and the accompanying manufacturers' protocol. Control reactions without enzyme and without template RNA were also carried out to test (using PCR) for residual DNA and for contaminating RNA introduced at this stage. cDNA was stored in 100 µL dH_2O (Sigma) at -20°C.

2.13.6 Cleaning cDNA using sephadex

Random hexamers and nucleotides were separated from cDNA by gel filtration using Sephadex G-50 resin (Sigma) (Fig. 2.8). cDNA was concentrated by ethanol precipitation (as previously described) and resuspended in 50 µL ddH_2O. cDNA concentrations were estimated using a Nanodrop 1000 by measurement of the absorbance at 260 nm (1 absorbance unit = 50 µg/mL).

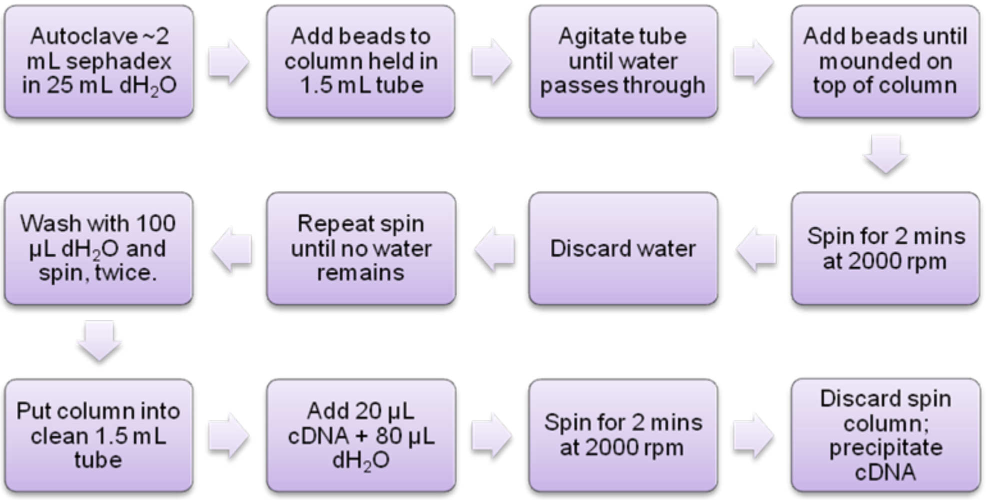

Figure 2.8. Cleaning of cDNA using Sephadex columns. Sephadex G-50 was added to blank chromatography columns, cleaned, spun down and used to remove random hexamers and nucleotides from cDNA.

2.13.7 Standard PCR

A known concentration of cDNA, no-template and no-reverse transcriptase controls were amplified by PCR using actin (85bp amplicon) and arylphorin receptor (133bp amplicon) primers from Ames, Turner, & Daniel (2006) (Table 2.11). PCR reagent concentrations are outlined in Table 2.2, cycling conditions are outlined in Table 2.12. Products were analysed on a 2% agarose TBE gel to determine the presence of specific gene products from cDNA and the absence (no PCR products visible) of contamination from the RNA extraction and reverse-transcription stages.

Table 2.11. Primer sequences for actin and arylphorin receptor genes. Amplification of actin (85bp) and arylphorin receptor (133bp) gene fragments was conducted to examine the suitability of cDNA for quantitative PCR. Primer sequences were taken from Ames *et al.*, (2006).

Gene	Direction	Sequence
Actin	Forward	TCAAGTCATCACCATCGGTAA
	Reverse	ACCGCAAGATTCCATACCCAA
Arylphorin receptor	Forward	CAGACAATGCAGGGTATAAGAG
	Reverse	GGGGCATATAGACCTGATGTAA

Table 2.12. Actin and arylphorin receptor gene PCR cycling conditions. The actin and arylphorin receptor gene amplification conditions were as indicated in the table. The reactions were carried out on a Veriti 96-well Thermal Cycler (Applied Biosystems).

Stage	Number of cycles	Time (s)	Temp. (°C)
1	35	60	94
		60	55
		60	72

2.13.8 Gene selection and primer design

Housekeeping genes were selected based on existing expression data. Nucleotide sequences from other insects (Table A4) were selected from NCBI (www.ncbi.nlm.nih.gov) and aligned using Clustal W in BioEdit (www.mbio.ncsu.edu). Exons were identified using Ensembl (www.ensembl.org) and intron-spanning primers were designed in regions of high homology using Primer-BLAST (www.ncbi.nlm.nih.gov). Primers with the highest levels of conservation, including a 3' end base match to all sequences were selected for amplification of mixed-age pupal cDNA (described below). Primers for RP49 (Table 2.13) amplified a 249 bp product, which was sequenced using both forward and reverse primers and compared to existing sequences of the RP49 (RpL32) gene. New *C. vicina* specific primers were then designed for semi-quantitative PCR (Table 2.14) to allow evaluation of expression level throughout the pupal stage.

Table 2.13. Housekeeping genes selected for analysis. Three HKGs were identified from previous research (Chapter 7.4.2.1) as being potentially suitable for this work. General gene structure information obtained from Flybase (www.flybase.org), Interactive fly (www.sdbonline.org) and Ensembl (www.ensembl.org) is shown in Appendix IV. Sequences were obtained from and RP49 primers designed using NCBI (www.ncbi.nlm.nih.gov).

Gene	Primer	Sequence	Amplicon (bp)
EF1α	Forward	GGYTGGCACGGTGAYAACATGTTGGA	563
	Reverse	ACGACGATCGACCTTCTCCTTGATTTC	
GAPDH	Forward	ATYAAYGGMTTTGGHCGMATYGGYCG	944
	Reverse	RTADCCRAACTCRTTRTCRTACCA	
RP49 (RpL32)	Forward	CACCAGTCGGATCGATATGC	249
	Reverse	TGGGCGATCTCGCCGCAGTA	

The initial primers, based on conserved regions (sequence not shown), failed to amplify fragments of the GAPDH and EF1α genes (data not shown). Protein sequence homology was therefore utilised to design new primer sets; amino acid sequences were obtained from NCBI, aligned using BioEdit and stretches of 8-10 conserved amino acids were selected and converted to nucleotide sequences. These ~30bp sequences were aligned to multiple insect nucleotide sequences for each gene, and primers were designed with minimal degeneracy and a 3' end base match across all species (Table 2.13). This method of primer design risks amplification of sequences not crossing an intron boundary, therefore gDNA contamination was eliminated using two rigorous DNase I digestion steps (as explained previously). The degenerate primers were used to amplify GAPDH and EF1α in *C. vicina*, and the resulting PCR products were sequenced. Sequences were aligned to other dipteran nucleotide data and used to design *C. vicina* primers, permitting semi-quantitative analysis (Table 2.14a) (described below). For fully quantitative analysis Taqman primer and probe sets were designed for RP49 and EF1α using Primer Express (http://www.appliedbiosystems.com), as their expression levels appeared more consistent than GAPDH (Table 2.14b-c).

Table 2.14. Semi-quantitative and quantitative PCR primers and probes for HKGs. (a): Semi-quantitative PCR primers were designed from the *C. vicina* sequences obtained using initial/degenerate primers (Table 2.13). (b) and (c): Upon assessment of developmental gene expression levels qPCR primers and probes were designed using Primer Express for RP49 and EF1α. Only the reverse primer for RP49 was different to the semi-qPCR primer.

a

Gene	Semi-qPCR Primer	Sequence	Amplicon (bp)	[Mg^{2+}] mM	Annealing temp. °C	PCR cycles
EF1α	Forward	GCACAGTACCCGTCGGTCGT	139	1.5	55	26
	Reverse	TCACCGGGAACAGCTTCAACG				
GAPDH	Forward	ATGCCACCACTGCCACCCAA	155	1.5	55	26
	Reverse	ACAGCCTTGGCAGCACCAGT				
RP49 (RPL32)	Forward	CACCAGTCGGATCGATATGC	143	2.5	40	26
	Reverse	AGCATGTGACGGGTACGCTTGT				

b

Gene	qPCR Primer	Sequence
EF1α	Forward	GCACAGTACCCGTCGGTCGT
	Reverse	TCACCGGGAACAGCTTCAACG
RP49 (RPL32)	Forward	CACCAGTCGGATCGATATGC
	Reverse	CGACGTACTCTGTTGTCAATACCT

c

Gene	Taqman Probe
EF1α	CGGTACCGTTGTTGTCTTCGCTCCCGCT
RP49 (RPL32)	AGTTGTCGCACAAATGGCGTAAACCA

Developmentally expressed gene (DEG) primer design was based on existing *C. vicina* sequences available on NCBI (Figure 2.9 and Table A5 in Appendix IV). Primers (Table 2.15) were tested as previously described. PCR products of the expected size were obtained from all primer sets (Table 2.15a). Gene expression was analysed semi-quantitatively (described below), and Ecr, LSP-2 and Trp were selected for developmental gene expression analysis of *C. vicina* pupae. qPCR probes were designed using Primer Express for existing Ecr, LSP-2 and Trp primers (Table 2.15b).

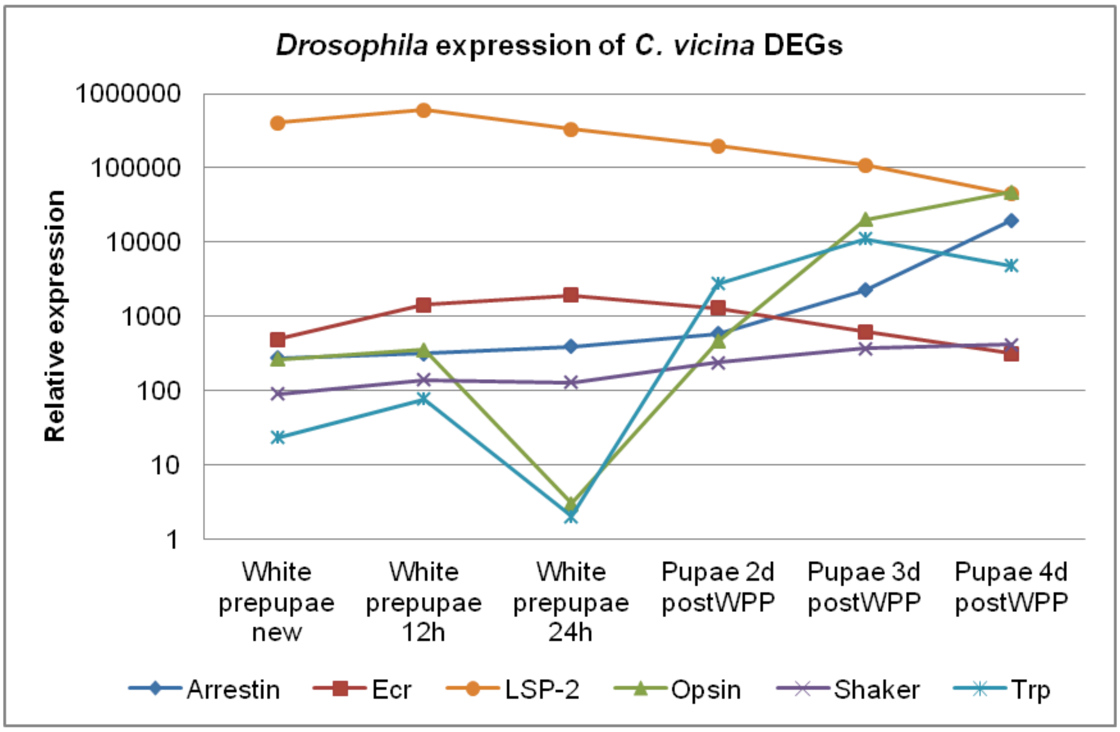

Figure 2.9. *Drosophila* pupal expression levels of candidate DEGs. Genes were selected from available *C. vicina* sequences on NCBI. *Drosophila* expression levels are shown, obtained from www.flybase.org. Prepupae indicates pre-head eversion; postWPP indicates after white pupal stage.

2.13.9 Primer testing and sequencing

All primers were tested by amplification of mixed pupal age cDNA. 20 µL PCR reactions contained 1x PCR buffer (Genecraft), 0.2 mM dNTPs, 0.5 mM each primer and 1U Taq polymerase (Genecraft). [Mg^{2+}] and annealing temperatures are given in Table 2.14. Cycling conditions were as follows: 94°C for 1 minute, followed by 35 cycles of 94°C for 1 minute, 40-60°C for 1 minute, 72°C for 1 minute, and a final extension of 72°C for 5 minutes.

Sequences of RP49, GAPDH and EF1α PCR products were obtained (GATC - http://www.gatc-biotech.com). All sequences were identified as derived from their respective genes in related Diptera, using NCBI Blast.

Table 2.15. Primer and probe sequences and semi-qPCR conditions for candidate *C. vicina* DEGs. (a) Genes were selected from available *C. vicina* sequences on NCBI (Table A5) and primers designed using Primer-BLAST. Genes in bold were selected for qPCR analysis. The PCR cycle numbers for observation of the exponential amplification phase were determined. (b) Taqman probes were designed for the three selected DEGs and their corresponding primers using Primer Express

a

Gene	Primer	Sequence	Amplicon (bp)	[Mg^{2+}] mM	Annealing temp. °C	PCR cycles
Arrestin 1	Forward	GAGCAGCGAGGGCTGTCCTTTG	103	2.5	60	36
	Reverse	AACCGCTATGCCGGCACGA				
Ecdysone receptor (Ecr)	Forward	TCGTCACTGGACTCGCCCGT	121	1.5	60	30
	Reverse	ATGAGGTGCAGCCCTGCAGC				
Larval serum protein (LSP-2)	Forward	AGCGATCGCACCACCTACTTGG	113	3	60	28
	Reverse	ATGCGTTGGGGTACACCGCA				
Opsin	Forward	GGTTACACCCGACATGGCCCATT	140	3	60	34
	Reverse	AAATCACCACACCGTTGCCGC				
Shaker	Forward	AGAGGAGATGCAGAGCCAAAACTTC	149	3	60	34
	Reverse	TTCCTGGCGTTGATTCGACACC				
Transient receptor potential (Trp)	Forward	ACGTGTTGACGGAGACAGAGAAAAC	143	3	60	34
	Reverse	GGCCGAACGATTCATGGGATCA				

b

Gene	Taqman Probe
Ecr	CAACGATTCAGCCTCCTACAATACAAACAGTCATCAGCAC
LSP-2	TGGATGCCACCAATAGTGACTACAAATTCCCTCTCAATC
Trp	TTTATATTGGCTTGTGAGCGCGGTGACATAGC

2.13.10 Semi-quantitative PCR

Temporal expression levels for all genes were examined using semi-quantitative PCR. Prior to this, PCR reactions with increasing cycle numbers were carried out in order to identify the exponential phase (approximate threshold value) for each gene. Optimal salt concentrations, annealing temperatures and cycle number are given in Tables 2.14 and 2.15. 1 µg cDNA was amplified using the following cycling conditions: 94°C for 1 minute, 60°C for 1 minute, 72°C for 1 minute, for the corresponding number of cycles. From this the following genes were selected for temporal expression analysis: EF1α, RP49, Ecr, LSP-2 and Trp.

2.13.11 qPCR

Quantitative real-time PCR of the two housekeeping genes (HKGs) and three developmentally expressed genes (DEGs) was carried out using custom Taqman probes (Tables 2.14c and 2.15b) on an Applied Biosystems 7900 HT qPCR system. 100 ng cDNA was amplified in 10 µL qPCR reactions comprising 1x Maxima Probe qPCR standard master mix (Fermentas), 0.9 µM each primer and 0.2 µM probe (Table 2.14b and 2.15a). Cycling conditions were as standard for the qPCR system (Table 2.16). Fam/Tamra fluorescence was automatically recorded in the annealing/extension phase at 60°C.

Table 2.16. qPCR cycling conditions for all genes. All HKGs and DEGs were amplified by qPCR using the standard cycling conditions for Applied Biosystems 7900 HT system.

Stage	Number of cycles	Time (s)	Temp. (°C)
1	1	120	50
2	1	600	95
3	40	15	95
		60	60

Relative gene expression level was calculated as a ratio using the ΔC_T method (Tarone & Foran 2011; Antonov *et al.,* 2005). This is simplified from the $\Delta\Delta C_T$ method (Livak & Schmittgen, 2001) which gives an expression ratio between the test and a comparison sample, such as a larva or mixed age pupal sample in this case. This method is not useful for age estimation, as the comparison sample does not exist at the crime scene. Instead, the expression ratios must be calculated from a single-aged sample. ΔC_T was calculated by subtracting the mean combined and individual HKG C_T from the mean C_T for all for the DEGs at each age. These were converted to relative expression levels (by $1/2^{DEG(CT) - HKG(CT)}$) for age estimation using both combined and individual HKG data. Subtraction of the exponents (C_T values) is the equivalent of division of the HKG and DEG levels to give the expression ratio.

2.14 Analysis of pupal preservation methods

2.14.1 Collection of pupal samples

Eggs were collected using organic pigs liver and reared as previously described. Thirty 4d pupae and thirty 7d pupae were randomly selected from the batch and preserved in each solution (Appendix II, Table A2) at each temperature (Table 2.17). Live samples were collected and analysed immediately. Where appropriate, pupae were pierced three times (see Table 2.17), once through each body segment, and

Number	Pierce	Solution 1	Temp 1	Time	Solution 2	Temp 2	Time	Solution 3	Temp 3	Primary Use	References
1	Yes	HWK	>80°C	>30s	80% ethanol	4°C	-	-	-	External morphology	(Adams & Hall 2003; Amendt *et al.*, 2007; Tantawi & Greenberg 1993)
2	Yes	HWK	>80°C	>30s	80% ethanol	-20°C	-	-	-		
3	Yes	Kahle's	4°C	½ day	70% ethanol	4°C	-	-	-	External and internal morphology	(Day & Wallman 2008; Linville *et al.*, 2004; Madhavan & Madhavan 1980)
4	Yes	Kahle's	-20°C	½ day	70% ethanol	-20°C	-	-	-		
5	Yes	Bouin's	4°C	4 hrs	70% ethanol	4°C	-	-	-	Histology	(Cox *et al.*, 2006; Quicke *et al.*, 1998)
6	Yes	Bouin's	-20°C	4 hrs	70% ethanol	-20°C	-	-	-		
7	Yes	Bouin's	4°C	4 hrs	Carnoy's	4°C	2 hours	70% ethanol	4°C	Histology	(Brazil & Brazil 2000)
8	Yes	Bouin's	-20°C	4 hrs	Carnoy's	-20°C	2 hours	70% ethanol	-20°C		
9	Yes	Modified methacarn	4°C	4 days	70% ethanol	4°C	-	-	-	DNA analysis	(Buesa 2008; Cox *et al.*, 2006; Tsai 2006)
10	Yes	Modified methacarn	-20°C	4 days	70% ethanol	-20°C	-	-	-		
11	Yes	Propylene glycol	4°C	1 week	95% ethanol	4°C	-	-	-	DNA analysis	(Vink *et al.*, 2005; Holler *et al.*, 2006)
12	Yes	Propylene glycol	-20°C	1 week	95% ethanol	-20°C	-	-	-		
13	Yes	Isopropanol	4°C	1 week	95% ethanol	4°C	-	-	-	DNA analysis	(Day & J. E. Wallman 2008; Einarsson *et al.*, 2002; Post *et al.*, 1993)
14	Yes	Isopropanol	-20°C	1 week	95% ethanol	-20°C	-	-	-		
15	Yes	RNAlater	4°C	-	-	-	-	-	-	RNA analysis	(Florell *et al.*, 2001; Vink *et al.*, 2005)
16	Yes	RNAlater	4°C	Over-night	Dry	-20°C	-	-	-		
17	Yes	HWK	>80°C	>30s	Dry	4°C	-	-	-	External morphology and DNA analysis	-
18	Yes	HWK	>80°C	>30s	Dry	-20°C	-	-	-		
19	Yes	70% ethanol	4°C	-	-	-	-	-	-	External morphology and DNA analysis	(Cox *et al.*, 2006; Linville *et al.*, 2004; Koch *et al.*, 1998; Post *et al.*, 1993; Tantawi & Greenberg 1993)
20	Yes	70% ethanol	-20°C	-	-	-	-	-	-		
21	No	Dry	-80°C	-	-	-	-	-	-	RNA analysis	(Cox *et al.*, 2006)

Table 2.17. Pupal preservation solutions and methods. 1092 pupae were collected and preserved using 21 different methods. Pupae were pierced before placement in all solutions (see Appendix II Table A2), except dry storage at -80°C. Subsequent storage solutions and times held in those solutions are indicated. The primary purpose for each preservative is indicated, along with studies that have previously used that method.

preserved in each final solution for up to two weeks or between 6-8 months. The extended storage period allowed examination of the effects of prolonged exposure.

2.14.2 Morphological analyses

For external morphological analysis, five live pupae (at 4d and 7d) provided reference (control) samples for discolouration, turgor and size. Puparia were removed from five pupae in each solution. Length, width and mass were measured for each pupa, and discolouration and turgor were each graded on a scale of 1-5. Discoloured pupae were always darker when compared to live samples. Discolouration was scored 1 if the pupa was completely putrefied/black and 5 if the pupa was similar in appearance to a live sample. Turgor was rated according to that of Adams and Hall (Adams & Hall 2003), 1 being collapsed, 5 being firm.

The effects of hot water killing (HWK) were also investigated. Boiled water was placed in a petri-dish and the temperature monitored. Once the water had cooled to 90, 80, 70 or 60°C, pupae were pierced and placed in the water for either 0.5 or 2 min, before preservation in 80% ethanol and stored at room temperature or 4°C. Puparia were removed ~1 week later and discolouration assessed.

Histological analysis to document internal morphology was carried out using 4 pupae from each preservative following removal of puparia. Two pupae were re-fixed in Kahles solution (if they were not already in formalin-based fixatives; the standard for histology) prior to clearing and embedding alongside two pupae taken directly from preservative. Lateral and medial sections were cut from each pupa, mounted on standard slides, and stained. Mounting was most effective when 0.5% gelatin was added to the water-bath at 37°C.

2.14.3 Molecular species identification

DNA was extracted from 2-3 pupae from each preservative (both 4d and 7d pupae) and a 1270bp COI gene fragment was amplified. The PCR products obtained were sequenced to determine whether preservatives (particularly formalin-based fixatives) prevent species identification. High fidelity Taq polymerase was used to amplify COI for pupae preserved in 70% ethanol (4 and 7 days, after 2 weeks and 6-8 months), Kahles, Bouins and Bouins/Carnoys solutions (4 and 7 days, after 6-8 months). Forward and reverse reference sequences for comparison were obtained from NCBI *(*Appendix II, Table A3).

2.14.4 Gene expression analysis

RNA was extracted from a homogenised single intact 4d or 7d pupa (including puparium) from each preservative. The protocol did not include a Proteinase K step. Pupae preserved in formaldehyde-based fixatives, i.e. Kahles, Bouins and Bouins/Carnoys solution were subjected to a cross-link reversal step, which involved homogenisation followed by incubation with 6.8 mg/mL proteinase K for 3 hours to 3 days at 55°C adapted from Godfrey *et al.,* (2000), with the addition of 6.8 mg/mL proteinase K at 24 hour intervals.

1 µg total RNA was reverse-transcribed to cDNA, and cDNA (~1200 µg) was PCR amplified using primers for actin (85 bp) and arylphorin receptor (133 bp) fragments (Ames, Turner & Daniel, 2006). Products were visualised on a 2% agarose TBE gel containing ethidium bromide.

2.15 Statistical analyses

Statistical analyses were carried out using Minitab v.15-16. Differences in pupal stage and lifecycle lengths between sexes and trials were analysed using Chi-squared and ANOVA tests.

For the analysis of discolouration and turgor data obtained from pupae in different preservatives, data were normally distributed (where necessary) using Box-Cox transformations prior to comparison to control pupae using T-tests and ANOVA. Pupae that had died prior to preservation were excluded in the analyses (<1%).

Variation in gene expression C_T values between each age and samples was examined using ANOVA analyses and visualised using Box-Plots. Regression analysis was used to develop equations for age estimation based on external morphological development and gene expression data from all genes.

2.16 Waste disposal

The release of any living organism into the wild was minimized by the following procedures: Any waste meat remaining after larvae had entered the post-feeding stage (wandered away) was frozen at -20°C to kill any remaining immature insects, prior to immediate disposal with the general waste. All unused immature insects were either frozen or killed with boiling water prior to disposal. Adult colonies either died of natural causes, or were frozen prior to disposal.

Chapter 3 – Assessment of Natural Variation in Pupal Age

3.1 Introduction

PMI estimates are given with a window of error, based on the increasing variation in stage length with increasing age. These errors can be quantified and minimized by the analysis of adult laying behavior, age variation in eggs at oviposition and natural variation between age range of the pupal stage and lifecycle.

3.1.1 Egg laying behaviour

Oviposition of the first eggs by flies such as *C. vicina* is typically used to indicate the start of the period of insect activity (PIA). The maximum PIA, calculated in ADH for each species, is used to estimate minimum post-mortem interval (PMI) (Amendt *et al.,* 2007). By nature of the process, oviposition of a single batch of eggs is not an instantaneous event occurring immediately after cadaver location. Examination of the time taken to oviposit and the variation in the age range of a batch of eggs would enable more accurate estimation of the start of PIA and minimum PMI.

Unlike males, which contain sperm only one day after emergence (Lowne, 1895), ovaries in females reach maturity after 6-7 days dependent on temperature and a protein feed (Vinogradova 2009; Pitts & Wall 2004; Hobson 1937). On copulation, females store sperm within the spermatheca ready for fertilization once a suitable oviposition site is located.

The Calliphoridae will, in general, lay in any cadaver orifice (Amendt *et al.,* 2007); *Lucilia sericata* preferred oviposition sites are known to include humid cracks and crevices within sheep fleece (Davies 1948; Wallis 1962). Detection of these sites involves multiple chemoreceptors on the antennae, labella and ovipositor that can detect decay compounds including volatile organic compounds such as cadaverine (1,5-pentanediamine) and putrescine (1,4-butanediamine) from the food source (Easton & Feir 1991; Dekeirsschieter *et al.,* 2009; Statheropoulos *et al.,* 2005; Wallis 1962).

Little is known about *C. vicina* oviposition behaviour and factors such as selection of laying site, duration of oviposition, or the age of individual eggs on oviposition. It is also unknown if pupation and emergence of the first laid eggs in a batch occurs earlier or whether the eggs are laid at a single site or scattered across the substrate. Investigation of these issues will inform possible egg collection protocols for both developmental studies and at the crime scene, and indicate a PIA range that should be considered when estimating PMI.

3.1.2 Precocious egg development

Precocious egg development is a phenomenon that has been noted in the Calliphoridae and Drosophilidae. Eggs are normally only fertilized immediately prior to laying, however, in certain conditions a fertilized egg can held in the genital tract for an extended period of time and undergo embryogenesis. Extending the time between food source/cadaver detection and oviposition by prevention of access (e.g. burial) increases the chance of this happening, especially if adults are starved for three weeks following a protein meal (Wigglesworth 1968; Wells & King 2001; Erzinclioglu 1996; Demerec 1950).

Consequently, this retained egg may be older than the remaining eggs, possibly by only a few minutes (Wells & King 2001), but potentially by the length of the entire embryonic stage (~24 hours at 22°C). Although this will only be one egg in a batch, many batches of eggs are laid on a cadaver, and it may therefore not be possible to distinguish which insects are the oldest (from which PMI is estimated) and which ones are precocious, in cases of large numbers (tens of thousands) of immature insects. PMI estimation from precocious insects would therefore be erroneously long, if occurrence is common. In winter (California, USA), two *C. vicina* females were collected, and one held a precociously developed egg; a 50% occurrence rate (Wells & King 2001). As this is a unique study with a small sample size, further examination is required, such that sampling protocols for developmental studies can minimise the collection of precocious eggs, and their possible impact on PMI estimation can be assessed.

3.1.3 Variation in lifecycle length

With an understanding of the variation occurring at the egg stage, quantification of pupal stage length variation is needed for accurate age and PMI estimation. As noted from previous studies, the point at which pupation occurs (the time between first and last larvae in a batch to pupate) varied by 93 hours at ~23°C in *C. vicina*, and the emergence point ranged 59 hours similarly (Finell & Jarvilehto 1983; Kamal 1958; Anderson 2000). This variation indicates that similar differences in the occurrence times of developmental age markers will be present. As such, age estimates based on pupal morphology should consider the range of times when specific developmental features are observed. A similar approach should be applied to temporal gene expression data. This issue has been tackled in different ways, depending on the purpose of the timeline created.

Robertson (1936) and Sivasubramanian & Biagi (1983) acknowledged the presence of natural variation in lifecycle length in their work, however failed to provide errors to their timelines, limiting their accuracy for age estimation. Bainbridge & Bownes (1981) documented morphological characteristics between the sexes and individuals of *Drosophila*, by displaying the extreme times at which each feature was noted. An average was used for general staging purposes; a more useful approach for PMI estimation.

Finell & Jarvilehto (1983) used eye development and general head morphology changes to stage the *Calliphora erthrocephala (vicina)* pupa. They commented on the variation of development times within and between batches of flies but not on differences between the sexes. Most significantly, it was noted that pupation occurred from 5.3 to 11.6 days after egg hatching. Within a single batch, the time taken for all larvae to pupate ranged from a period of ~3 to ~10 days. The lifecycle length range (from hatching to eclosion) was on average 5.3 days. These ranges will vastly limit the accuracy of age estimation. One way of circumventing this error, is to assign development to percentage point throughout the stage, as demonstrated by the authors; whether this was an average point at which the development was noted is unclear. In order to attempt pupal age estimation within a short time frame, e.g.12-24 hours, a more detailed study into pupal stage variation is required which quantifies error ranges in ADH.

3.1.4 Conclusions and aims

Overall, in order to estimate the age of *C. vicina* pupae with the greatest possible accuracy, oviposition behaviour, occurrence of precocious eggs and natural variation in lifecycle and pupal stage length should be examined, as there is insufficient data at present to estimate age within a known error range. Data obtained may then be used to estimate PMI using pupae, with greater reliability than currently possible.

Therefore, the aims of these experiments were to:

- Examine oviposition behavior in *C. vicina* and determine the duration and habits during egg-laying.

- Examine precocious egg development and occurrence, using standard rearing protocols and collection of eggs after set oviposition intervals, in order to quantify errors in PMI estimation.
- Develop a suitable egg collection protocol to define the start point of ADH measurement, so that the ages of the eggs are known within a small timeframe.
- Examine natural variation of lifecycle length within a batch of eggs laid within a restricted interval, allowing an error range to be applied to pupal age estimates.

3.2 Results

3.2.1 Observation of oviposition behaviour

Observation of oviposition behaviour was carried out in real time using a web-cam. With understanding of how a female distributes her egg batch and how long it takes, appropriate errors can be applied to the calculation of PIA and PMI. Optimisation of egg collection protocols for developmental studies would also be possible, with the aim of reducing within-batch age variation.

Flies began to congregate on the meat after 3 hours to feed or clean themselves. Before laying, flies were observed feeding on the meat and probing suitable sites with their ovipositor. They began to lay after 3.11 hours (Table 3.1) with mean initial laying time after 4.26 hours (S.D. = 0.9 hours). Eggs were laid in crevices between pieces of meat, or next to the meat on the moist paper. Each fly laid in multiple locations (mean = 3.6, S.D. = 2.63) sometimes laying their egg batches as whole clumps, others singly (Fig. 3.1 – Dark green fly). Flies spent an average of 5 minutes laying at each visit (S.D. = 5.37 minutes), with an observed maximum total laying time of 24 minutes. Between laying episodes, flies continued to probe meat for an average of 6.5 minutes (S.D. = 8.2 minutes). After oviposition, flies often cleaned their wings and legs.

Table 3.1. Statistical analysis of fly oviposition behaviour. Ten females were observed laying their eggs over a six hour period. Microsoft Excel was used to calculate summary statistics for initial and total oviposition times, number and time between visits to the meat.

	Intitial laying from T0 / hrs	Total time laying / mins	Time between laying episodes / mins	Number of oviposition locations
Mean	4.26	5.12	6.50	3.60
S.D.	0.90	5.37	8.23	2.63
Min	3.11	0.08	0.00	0.00
Max	5.51	24.13	37.58	8.00
Range	2.40	24.05	37.58	8.00

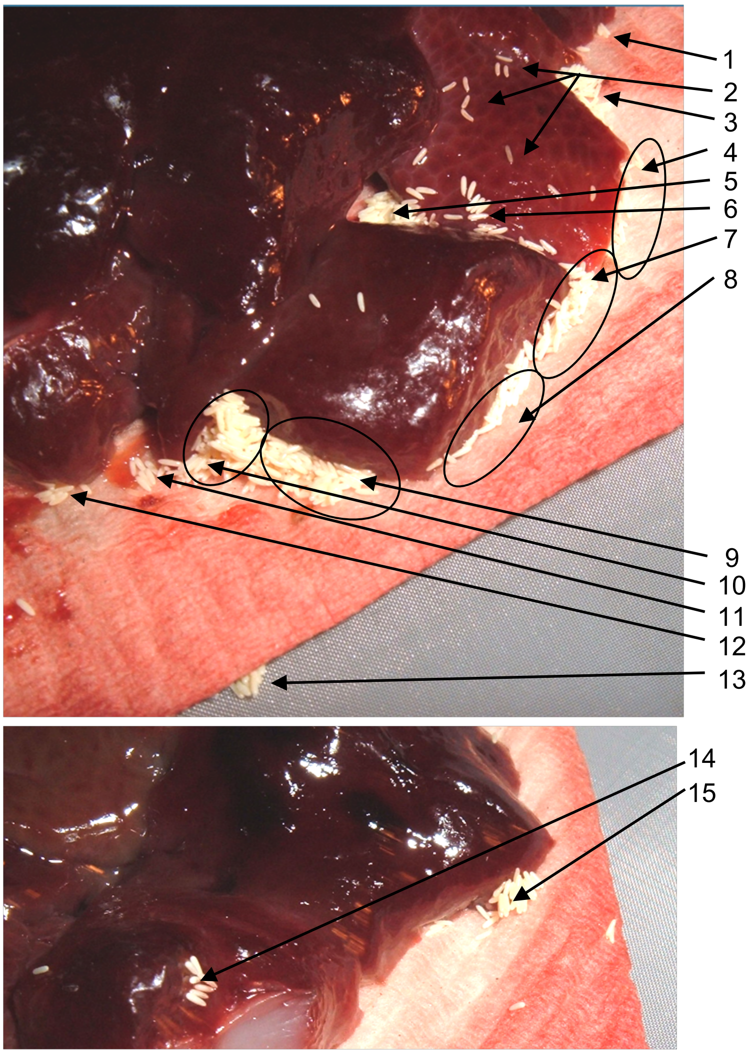

Site	Colours of ovipositiong flies
1	Light blue
2	Dark green
3	Blue
4	Blue, Red
5	Dark green, Blue, Red
6	Dark green, Light blue
7	Vermillion, Blue, Purple, Light blue, Red
8	Vermillion, Light blue, Red
9	Blue, Dark green, Light blue, Purple, Yellow ochre
10	Vermillion, Dark green, Blue, Light blue, Purple, Yellow ochre
11	Vermillion, Light blue
12	Vermillion
13	Vermillion
14	Light blue
15	Light green, Lemon yellow

Figure 3.1 Oviposition sites of *C. vicina*. A web cam was used to monitor oviposition behaviour of ten flies painted different colours, over six hours. The positions of all eggs laid are shown, with the colours of flies laying at each site (number) noted. For example, only the 'light blue' fly laid at site 1. 'Dark green', 'blue' and 'red' flies all laid at site 5. The 'dark green' fly also laid at sites 2, 6, 9 and 10.

3.2.2 Occurrence of precocious egg development

The occurrence of precocious egg development has the potential to cause large error when conducting developmental studies (such as timeline production), and when estimating PMI from the eldest insects at the crime scene. The occurrence of this phenomenon was examined in captive bred colonies and wild-caught adults by observation of larvae (larviposition) at oviposition of the egg batch, or remaining in the genital tract.

3.2.2.1 Influence of protein starve and permitted oviposition period

Precocious egg occurrence was analysed after starving adults of meat for one, two and three weeks and for 15 and 30 minute oviposition periods. Percentage of precocious eggs per batch, as noted by larvae present amongst eggs, was calculated to account for total egg number and colony size variation.

Visible, but not significant differences (as tested by ANOVA) were noted between batch collections (Fig. 3.2a), oviposition period (Fig. 3.2b) and protein starve (Fig. 3.2c). Higher mean levels and variation in number (standard deviation) of precocious eggs were found on the meat from the first of the three consecutive collections and in a shorter oviposition period as expected, but also after a shorter protein starve. The overall proportion of precocious eggs (from 17 batches) was 1.6% (S.D. = 4.79%). This figure includes a 20% precocious egg occurrence obtained from a 15 minute oviposition period, 1-week starve, batch one (not displayed in Fig. 3.2). This was possibly anomalous, due to the small sample size of 5 eggs compared to other samples ranging from 146 – 2717 eggs. Removal of this result resulted in a reduction in the average precocious egg occurrence to 0.47% (S.D. = 0.75%).

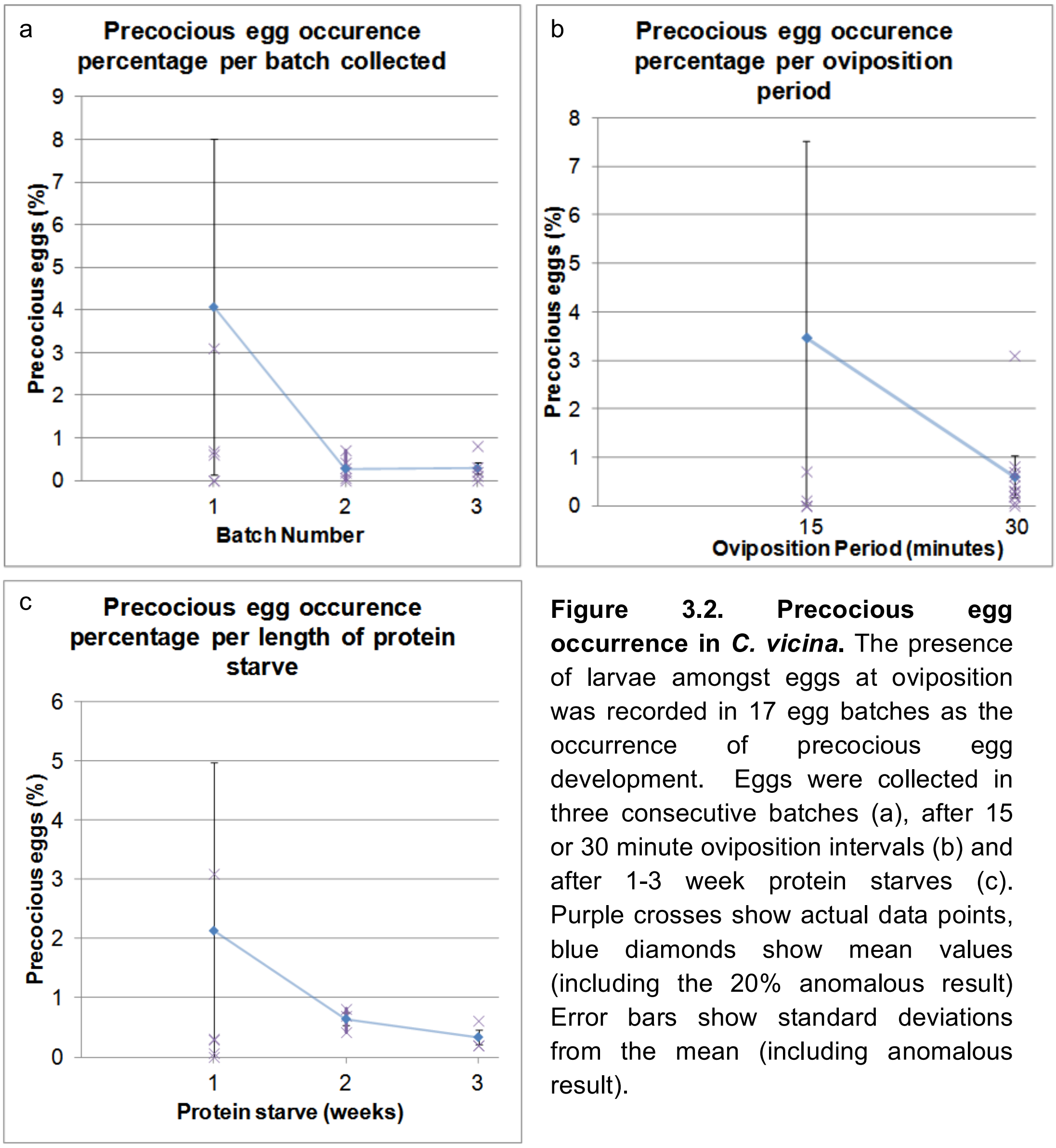

Figure 3.2. Precocious egg occurrence in *C. vicina*. The presence of larvae amongst eggs at oviposition was recorded in 17 egg batches as the occurrence of precocious egg development. Eggs were collected in three consecutive batches (a), after 15 or 30 minute oviposition intervals (b) and after 1-3 week protein starves (c). Purple crosses show actual data points, blue diamonds show mean values (including the 20% anomalous result) Error bars show standard deviations from the mean (including anomalous result).

3.2.2.2 *Timing of egg-hatching throughout embryonic development*

Timing of egg-hatching was monitored to determine the variation in egg ages upon oviposition and to define what constitutes a precocious egg. To collect enough eggs for a suitable sample size with a small colony (100 adults), oviposition was permitted over a one-hour period instead of the 15-30 minutes used previously with colonies comprising hundreds of adults. This resulted in an increase of overall precocious egg occurrence from 0.05% to a total of 2.6%.

Initially, embryogenesis was monitored in its entirety; eggs were collected over a 24-hour period from the same colony. No significant differences in precocious egg occurrence were noted (F = 1.98, P = 0.219), thus results were pooled with the second data set, which focused on the range of larval hatching at the end of embryogenesis. Precocious eggs (present as larvae) were observed within 50 ADH of oviposition, and comprised 2.55% of an egg batch (S.D. = 3.85%). ~1.5% of the batch hatched between 300 – 480 ADH (Table 3.2); these could be precocious but most likely hatched early as a result of natural variation in embryogenesis. 85-95% of eggs hatched between 500 - 580 ADH (Figs. 3.3 & 3.4). Batch 1 gave unusual results; 14.3% hatched within 50 ADH and 16.7% between 401 - 450 ADH. This resulted in precocious egg occurrence increasing from a mean of 1.6% (S.D. = 1.62) to 2.55% (as in Table 3.2).

Table 3.2. Hatching of precocious eggs throughout embryogenesis. The entire period of embryogenesis was monitored in 13 batches for hatching of eggs. Eggs hatched <50 ADH and 300 – 480 ADH from oviposition. Percentages of larvae hatching (per egg batch) are given and averaged for each time period (<50 ADH and 300 – 400 ADH).

Batch number	Total eggs laid	Larvae <50 ADH	% total	Larvae 300-480 ADH	% total
1	36	6	14.29	7	16.67
2	35	0	0.00	0	0.00
3	55	2	3.51	0	0.00
4	800	10	1.23	0	0.00
5	1000	3	0.30	7	0.70
6	300	1	0.33	0	0.00
7	30	1	3.23	0	0.00
8	1000	8	0.79	0	0.00
9	1000	1	0.10	4	0.40
10	60	2	3.33	1	1.67
11	1000	11	1.10	2	0.20
12	800	3	0.38	0	0.00
13	65	3	4.62	0	0.00
		Mean %	2.55		1.51

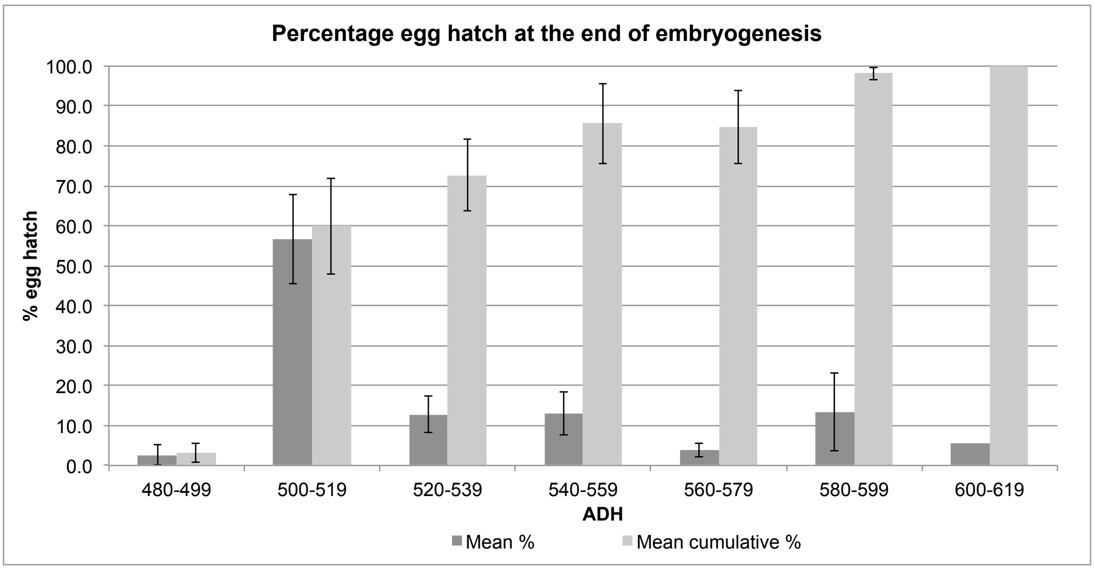

Figure 3.3. Egg hatching at the end of embryogenesis. The final hours of embryogenesis were observed in four batches for egg hatching. Mean and cumulative mean % egg hatching are shown from 480 to 620 ADH. Error bars indicate standard deviation of the mean.

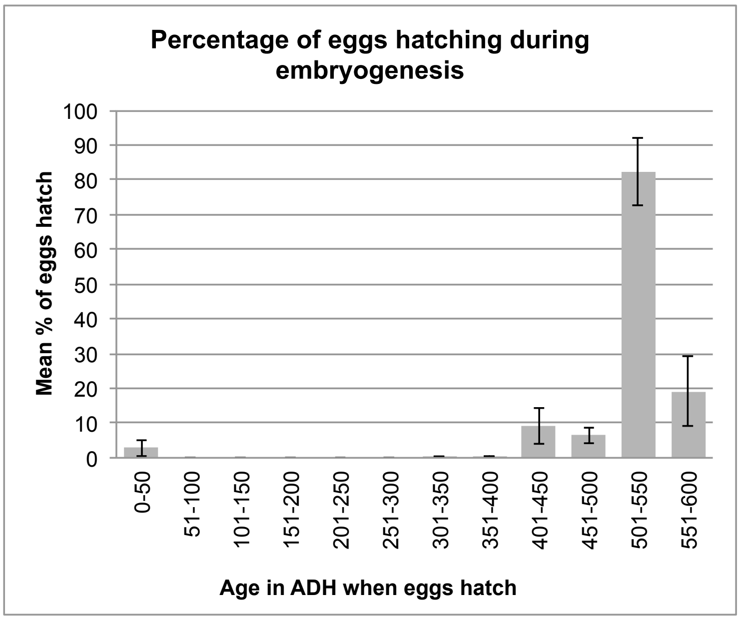

Figure 3.4. Hatching of eggs throughout embryogenesis. The numbers of larvae present immediately after oviposition and those observed hatching throughout embryogenesis were noted in nine batches. Data were recorded in set time intervals and calculated as percentages of the total batch. The mean percentages per time interval are shown, with standard deviation error bars. Hatching % between 300 – 400 ADH was so low it is not visible here.

3.2.2.3 Assessment of precocious eggs occurrence in wild-caught adults

The ovary and egg maturation states of wild female flies were examined to quantify levels of precocious egg occurrence, to assess its possible detrimental effects on PMI estimation.

In total, 53 adult females were collected immediately upon entering the trap (prior to oviposition) and observations regarding ovary development made using stereomicroscopy. 64% (34/53) were classed as gravid, i.e. ovaries fully developed. Of these, 27/34 (79%) held an egg in the genital tract in the abdomen (Fig. 3.5a) or ovipositor (Fig. 3.5b). 3/34 (9%) showed no egg in the genital tract. A further 3/34 (9%) had a 1st instar larva in the genital tract (Fig. 3.6) and one (3%) contained a dead larva.

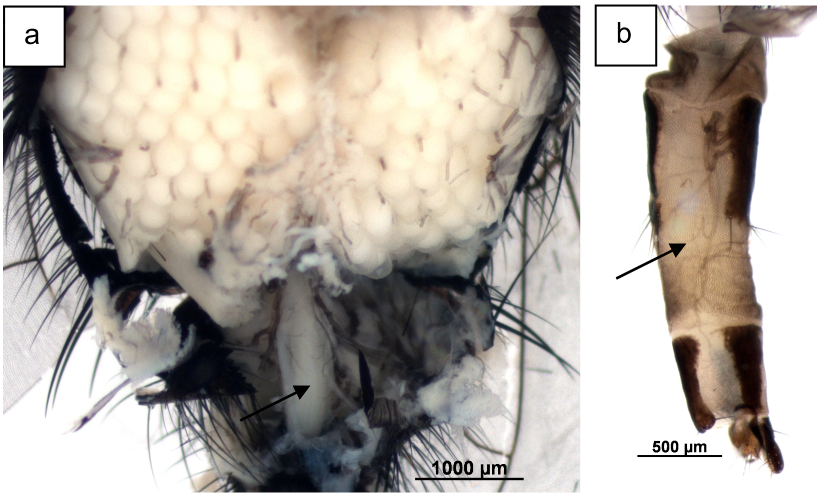

Figure 3.5. Eggs present in the genital tracts of females. Eggs (arrows) were held fertilised in the genital chamber (a) or ovipositor (b), ready for oviposition, in 27/34 flies. The opacity of the chorion prevents age estimation from stage of embryogenesis.

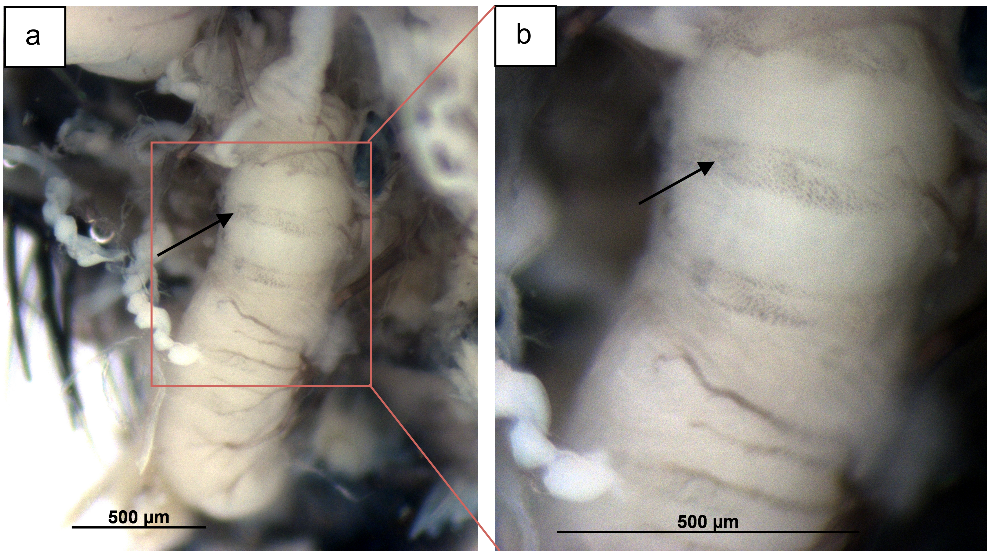

Figure 3.6. Precocious larva in the genital chamber. In 3/34 flies, embryogenesis was complete and the 1st instar larva could be seen (a), indicated by the inter-segmental spines (arrows in a and b). This denotes complete precocious egg development.

3.2.3 Variation in pupal stage length

3.2.3.1 Larvae reared on an unlimited food supply

The variation in pupal ages noted from eggs laid during a set oviposition interval and fed *ad libitum* was quantified. This indicated the window of error that should be applied to all age estimates based on morphological or molecular markers.

Pupation rates of third instar larvae were 98.5% and 100% for $T_{FF}1$ and $T_{FF}2$ respectively. Emergence rates were $T_{FF}1$ = 93% and $T_{FF}2$ = 99%. Also, no differences were observed in both trials between control and test colonies in pupation and emergence times.

Chi squared analysis indicated that in both trials, the number of males and females was not significantly different from a 50:50 ratio ($T_{FF}1$: $\chi^2 = 0.23$, n=1, P=0.619; $T_{FF}2$: $\chi^2 = 0.01$, n=1, P=0.906). No gender differences were noted for most time points (Table 3.3). $T_{FF}2$ did however highlighted significant differences (P<0.01) between male and female emergence times, with males emerging at a mean of 09:00h (S.D. = 5.9), and females later at 12:30h (S.D. = 4.8). Pupae in $T_{FF}1$ were only monitored at 10:00, hence this observation was not noted (Table 3.3).

Table 3.3. Gender differences in pupal stage lengths and emergence times for *C. vicina*, fed on meat *ad libitum*. Two trials of pupal stage/lifecycle length monitoring were conducted using fully fed larvae; $T_{FF}1$ (1047 pupae) and $T_{FF}2$ (71 pupae). Mean and standard deviation (S.D.) values for each gender and analysis shown stated in ADH, days or times. Lifecycle and pupal stage length ADH values were calculated using mean pupation and emergence days from oviposition. P values given are for comparison between males and females in each trial. The shading indicates the only significant difference (P<0.01) for time emerged in $T_{FF}2$. Where standard deviation was 0, the P value is not applicable (N/A).

Trial	$T_{FF}1$					$T_{FF}2$				
Gender	Male		Female		M/F P value	Male		Female		M/F P value
Statistic	Mean	S.D	Mean	S.D.		Mean	S.D	Mean	S.D.	
Pupal stage length (ADH)	6050.1	347.8	6043.8	328.7	>0.05	6016.9	200.7	5982.4	224.2	>0.05
Lifecycle length (ADH)	10837	281	10839	287	>0.05	10653	195	10702	134	>0.05
Day pupated	8.649	0.524	8.665	0.482	>0.05	8.611	0.494	8.771	0.426	>0.05
Time pupated	10:00	0	10:00	0	N/A	07:00	0	07:00	0	N/A
Day emerged	20.107	0.532	20.112	0.543	>0.05	20.083	0.280	20.029	0.169	>0.05
Time emerged	10:00	0	10:00	0	N/A	08:57	5.942	12:31	4.755	<0.01

Comparisons were then made between the two trials (Table 3.4). The mean time of emergence was significantly different between trials which was also reflected in the significantly different lifecycle lengths (in ADH), however the lifecycle length in days were similar. $T_{FF}2$ indicated bias towards eclosion early on in the day; 42% of pupae emerged between 01:00h and 11:00h and a further 21% between 11:00h and 13:00h (Figure 3.7). No significant differences were found between trials in mean pupal stage length in ADH, mean days to pupation or emergence and mean lifecycle length in days (Table 3.4).

Table 3.4. Comparison of variation in pupal stage and lifecycle length in both fully-fed trials. Mean and standard deviation values are given for each trial ($T_{FF}1$ = 1047 pupae; $T_{FF}2$ = 71 pupae), and the P value indicates significant difference between them. Lifecycle length (ADH) and time emerged were significantly different (shaded rows).

Trial	$T_{FF}1$		$T_{FF}2$		P value
Statistic	Mean	S.D	Mean	S.D.	
Pupal stage length (ADH)	6047.0	338.1	5999.9	211.8	>0.05
Lifecycle length (ADH)	10838	284	10678	169	<0.001
Day pupated	8.657	0.492	8.690	0.466	>0.05
Time pupated	10:00	0	10:00	0	N/A
Day emerged	20.109	0.537	20.056	0.232	>0.05
Time emerged	10:00	0	10:42	5.645	<0.001

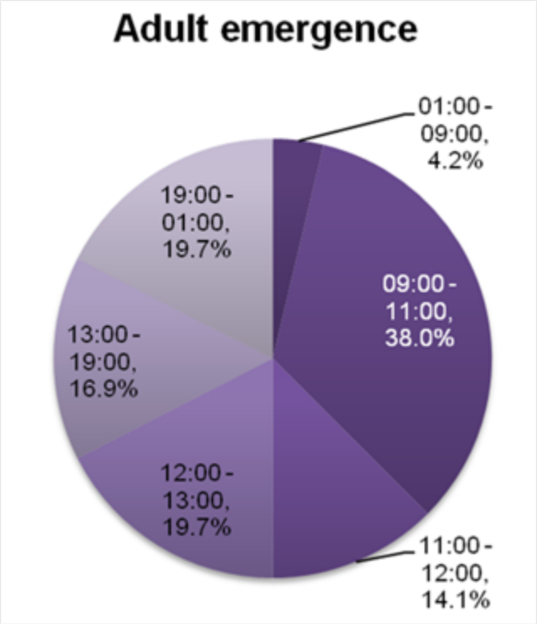

Figure 3.7. Emergence rates of adults within a 24 hour period. The emergence times of 70 adults were noted in trial $T_{FF}2$. Data for males and females, as well as both days of emergence were combined; data thus represents the entire batch of eggs. Percentages indicate the proportion of the batch that emerged between the times stated.

The differences between the maximum and minimum length of the pupal stage (ADH) were similar for both $T_{FF}1$ and $T_{FF}2$. An overall range of ~1000 ADH included 100% of pupae analysed and ~540 ADH included 95% of pupae, i.e. excluded unusually long or short pupal stage durations (Table 3.5, Figure 3.8). These ranges however did not overlap (Figure 3.8); $T_{FF}1$ had an overall shorter pupal stage than $T_{FF}2$ (Table 3.5). In contrast, the difference between the minimum and maximum lifecycle length (ADH) that included either 100% or 95% of pupae analysed were considerably shorter in $T_{FF}2$ than in $T_{FF}1$ (Table 3.5). These ranges did however coincide with each other (Figure 3.8). The difference between the trials could be attributed to the increased sampling frequency in $T_{FF}2$, thus 694 - 759 ADH may be more representative of natural variation range in lifecycle length. This range therefore quantifies the window of error which must be applied to pupal age estimates based on morphological or molecular markers.

Table 3.5. Pupal stage and lifecycle length variation between two trials of fully-fed larvae. The minimum and maximum pupal stage and lifecycle lengths were calculated in ADH for both trials ($T_{FF}1$ and $T_{FF}2$), for all pupae (100%) and >95 of pupae (excluding outliers). This indicates the variation/range (R) in ADH that occurs within the pupal stage and lifecycle when larvae are given food *ad libitum*.

Trial	$T_{FF}1$						$T_{FF}2$					
% Samples	100			>95			100			>95		
ADH	Min	Max	R	Min	Max	R	Min	Max	R	Min	Max	R
Pupal stage length	4444	5500	1056	4444	4972	528	5599	6510	911	5816	6380	564
Lifecycle length	9724	11836	2112	10252	11308	1056	10438	11197	759	10438	11132	694

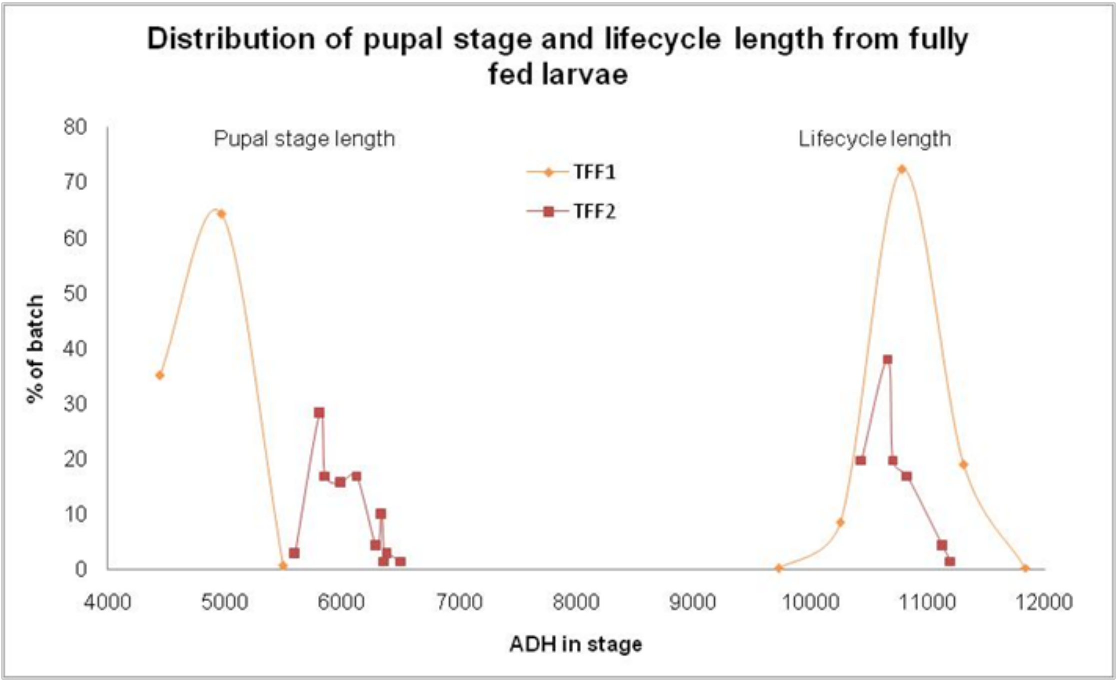

Figure 3.8. Distribution of pupal stage and lifecycle length for fully-fed larvae. The pupal stage and lifecycle lengths of all pupae ($T_{FF}1$ = 1407 and $T_{FF}2$ = 71) were recorded and calculated in ADH. The distribution of the ADH values is displayed for all pupae as percentages of the total batch. The distributions for both trials ($T_{FF}1$ and $T_{FF}2$) are displayed; discrete pupal stage lengths and overlapping lifecycle lengths are evident.

Overall, when development occurs at 22°C, pupation and eclosion occur on average 8.65 days and 20.08 days after oviposition (within a 30 minute interval) respectively, with these events predominantly occurring before 13:00. The mean lifecycle length is ~10700 ADH from oviposition (from $T_{FF}2$ data) and the pupal stage length lasts ~6024 ADH; 11.4 days at 22°C, 56% of the lifecycle. Natural variation results in a mean pupal stage length variation of 564 ADH (26 hours at 22°C) and a mean lifecycle variation of 694 ADH (32 hours at 22°C) ($T_{FF}2$) that includes 95% of samples.

3.2.3.2 Starved larvae

The pupal stage and lifecycle lengths were also examined for starved third instar larvae, mimicking the effects of a small carcass or inadequate food supply (developmental studies). Pupation rates of third instar larvae were 100% and 95% for T_S1 and T_S2 respectively. Emergence rates from pupae were T_S1 = 100% and T_S2 = 97%.

$T_{CS}1$ (control colony) pupation and emergence times were the same as the fully-fed colony $T_{FS}1$ monitored in parallel, indicating pupae selection by sieving had no visible effects. In contrast, $T_{CS}2$ (control colony) pupated 173 ADH earlier than the fully-fed colony ($T_{FS}2$) and emerged 513 ADH earlier.

Similarly to the fully-fed larvae ($T_{FF}1$ & $T_{FF}2$), chi-squared analysis showed no significant male/female bias (T_S1: $\chi^2 = 0.9$, n=1, P=0.343; T_S2: $\chi^2 = 1.97$, n=1, P=0.161). There were no significant age differences between males and females in either trial at any point in the lifecycle (Table 3.6).

In both trials, eclosion of starved larvae occurred over a wider timeframe and also later on in the day than the fully fed larvae ($T_{FS}1$ & $T_{FS}2$). In T_S1, 88% emerged after 12:00, compared to 67% in the fully fed colony $T_{FS}1$. Similarly, fewer starved larvae eclosed before 08:00 (42%) than fully-fed flies (51%) (Figure 3.9).

Comparisons were then made between the two trials as previously for fully fed larvae ($T_{FF}1$ & $T_{FF}2$), however in all analyses (pupal stage and lifecycle length, days/times pupated and emerged), the trials were statistically significant from each other (Table 3.7). The least significant difference between trials, as expected, was pupation day. The distributions of pupation and emergence and ADH ranges of pupal stage and lifecycle length for starved larvae are indicated in Table 3.8 and Figure 3.10. The sample size for T_S2 was 4x greater than T_S1, thus the pupal stage length range of 1071 ADH encompassing 95% of the sample is more reliable than the first trial (521 ADH for T_S1). Only 10 ADH separated the lifecycle lengths for the 100% and 95%

Table 3.6. Gender comparison between starved larvae trials. Larvae (T_S1 = 16, T_S2 = 73) were starved at the third instar stage, and their pupation and eclosion was monitored. Mean and standard deviation (S.D.) values for each gender and analysis shown stated in ADH, days or time as recorded. P values are for comparison between males and females in each trial.

Trial	T_S1					T_S2				
Gender	Male		Female		M/F P value	Male		Female		M/F P value
Statistic	Mean	S.D	Mean	S.D.		Mean	S.D	Mean	S.D.	
Pupal stage length (ADH)	5915.1	262.2	5867.6	170.7	>0.05	5392.7	247	5398.9	336	>0.05
Lifecycle length (ADH)	10126	391	10291	184.2	>0.05	9120.9	252.7	9165.7	349.3	>0.05
Day pupated	7.625	0.518	8.000	0	>0.05	7.444	0.504	7.586	0.501	>0.05
Time pupated	10:56	3.36	11:45	3.47	>0.05	04:43	4.243	03:13	3.902	>0.05
Day emerged	18.875	0.641	19.125	0.354	>0.05	18.278	0.554	18.370	0.721	>0.05
Time emerged	13:22	3.01	15:00	0	>0.05	10:15	2.383	10:11	2.331	>0.05

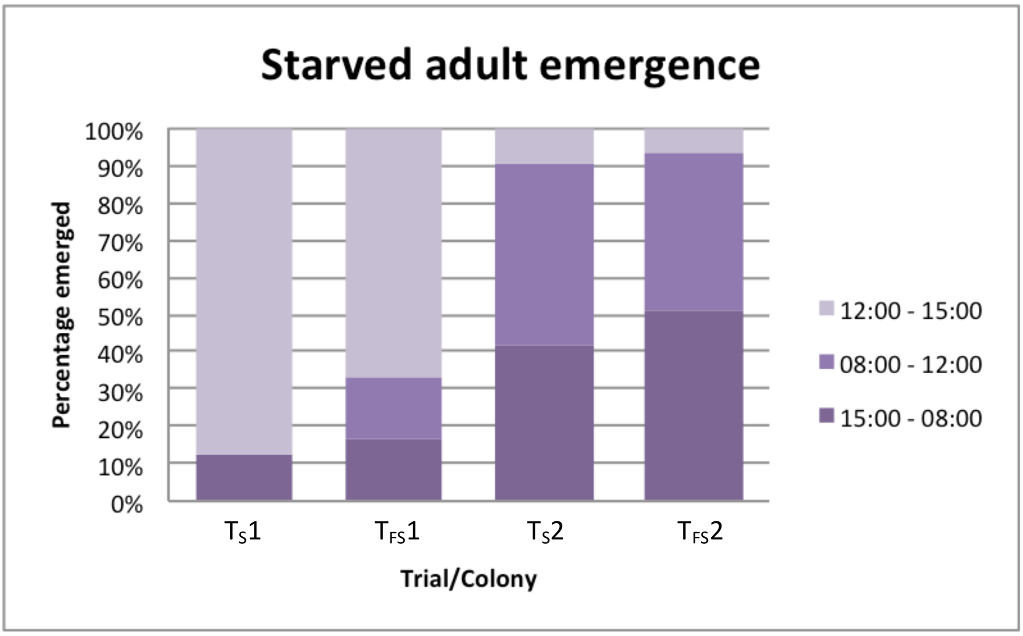

Figure 3.9. Emergence throughout the day of starved and control fed larvae. Larvae were starved at the third instar, and their emergence monitored (pupae emerged: T_S1 = 16, T_S2 = 66). Emergence time is compared for starved and control colonies (pupae emerged: $T_{FS}1$ = 24, T_S2 = 181) for the two trials. Data are displayed as the percentage batch of adults emerging within each timeframe.

Table 3.7. Comparison of pupal stage and lifecycle length between starved larvae trials. Pupal stage and lifecycle lengths of starved larvae (T_S1 = 16, T_S2 = 73) were calculated in ADH from time between oviposition and pupation/emergence. Mean and standard deviation values are given for each trial, and the P value indicates significant difference between them. In all aspects, the trials were significantly different from each other.

Trial	T_S1		T_S2		P value
Statistic	Mean	S.D	Mean	S.D.	
Pupal stage length (ADH)	5891.4	215.1	5554.5	288.1	<0.01
Lifecycle length (ADH)	10209	307	9141	298	<0.01
Day pupated	7.813	0.403	7.508	0.504	<0.05
Time pupated	11:21	3.330	04:06	4.132	<0.01
Day emerged	19.000	0.516	18.292	0.631	<0.01
Time emerged	14:11	2.220	10:13	2.342	<0.01

sample inclusion levels for T_S2 (Table 3.8). This is in contrast with the large spread of lifecycle lengths observed for fully-fed larvae (compare to Table 3.5). For both trials the pupal stage and lifecycle ranges were similar and also the starved larvae had shorter pupal stage and lifecycle lengths than fully-fed larvae (Fig. 3.10).

Despite difficulties in making quantitative comparisons, the data suggest that starved larvae pupate earlier and have a shorter pupal stage length and lifecycle (in days and ADH) than fully-fed larvae. Starved larvae also emerge and pupate later on in the day than fully-fed larvae (Table 3.9).

Table 3.8. Pupal stage and lifecycle length variation between two trials of starved larvae. The minimum and maximum pupal stage and lifecycle lengths were calculated in ADH for both trials (T_S1 and T_S2), for all pupae (100%) and >93/95 of pupae (excluding outliers). This indicates the variation/range (R) in ADH that occurs within the pupal stage and lifecycle when larvae are starved in the third instar.

Trial	T_S1						T_S2					
% Samples	100			>93			100			>95		
ADH	Min	Max	R	Min	Max	R	Min	Max	R	Min	Max	R
Pupal stage length	5732	6394	662	5732	6253	521	4927	6008	1081	4937	6008	1071
Lifecycle length	9564	10747	1183	9564	10747	1183	8463	9932	1469	8524	9605	1081

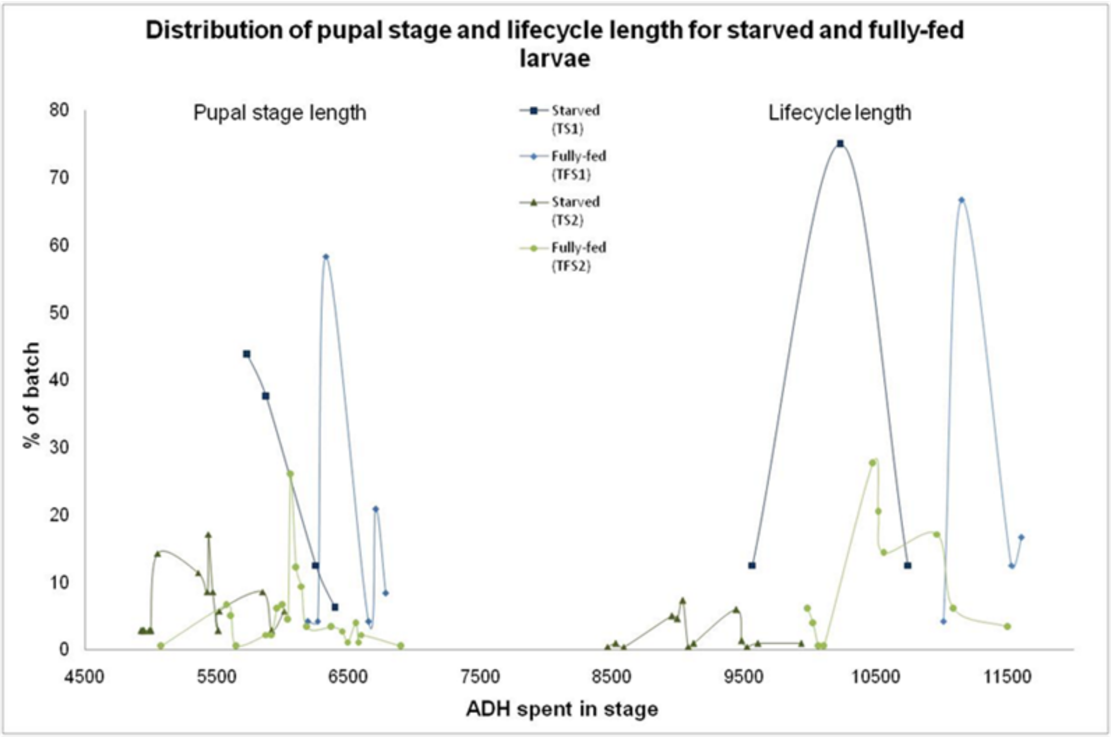

Figure 3.10. Distribution of pupal stage and lifecycle length for starved larvae and fully-fed control larvae. The pupal stage and lifecycle lengths of all pupae (T_S1 = 16, $T_{FS}1$ = 23, T_S2 = 73, $T_{FS}2$ = 198) were recorded and calculated in ADH. The distribution of the ADH values is displayed for all pupae as percentages of the total batch. The distributions for starved and accompanying control (fully-fed) trials are displayed. Starved larvae pupated and emerged earlier than fully fed larvae.

Comparing the starved and fully fed trials with the largest sample sizes (T_S2 and $T_{FS}2$), pupation and eclosion occur 1.6 and 2.9 days (at 22°C) earlier in starved larvae than in fully-fed, respectively (Table 3.9). The following are observed for starved larvae: The mean lifecycle length and pupal stage are 1418 ADH (2.7 days at 22°C) and 667 ADH shorter (1.3 days at 22°C) respectively. The average lifecycle length is therefore 9141 ADH with a pupal stage length of 5555 ADH; 10.5 days at 22°C. The pupal stage and lifecycle length variation (encompassing 95% of samples) is 1071 ADH and 1081 ADH (~2 days at 22°C) respectively (Table 3.9).

Table 3.9. Comparison of pupal stage and lifecycle lengths in starved and fully-fed control larvae. Pupal stage and lifecycle lengths were calculated as previously for fully-fed trials. The following pupae were counted: T_S1 = 16, $T_{FS}1$ = 23, T_S2 = 73, $T_{FS}2$ = 198. Mean and standard deviation for each analysis is given for each trial. P values less than <0.05 indicate significant differences. Shaded means indicate the lowest figure between starved and fully fed for each trial.

Trial	TS1		TFS1		P value	TS2		TFS2		P value
Statistic	Mean	S.D	Mean	S.D.		Mean	S.D	Mean	S.D.	
Pupal stage length (days)	11.306	0.413	12.505	0.382	<0.01	11.706	0.588	13.005	0.530	<0.01
Pupal stage length (ADH)	5891.2	215.1	6449.3	196.9	<0.01	5554.5	288.1	6221.4	260.9	<0.01
Lifecycle length (days)	19.591	0.589	21.851	0.391	<0.01	19.718	0.609	22.586	0.674	<0.01
Lifecycle length (ADH)	10209	307	11269	210	<0.01	9141	298	10599	332	<0.01
Day pupated	7.813	0.403	8.958	0.359	<0.01	7.508	0.504	9.166	0.489	<0.01
Time pupated	11:21	3.33	09:18	2.141	<0.05	04:06	4.132	01:58	3.161	<0.01
Day emerged	19	0.516	21.292	0.464	<0.01	18.292	0.631	21.188	0.665	<0.01
Time emerged	14:11	2.22	13:25	2.509	>0.05	10:13	2.342	09:33	1.872	<0.05

3.3 Discussion

3.3.1 Observation of oviposition behaviour

C. vicina females appear to display similar behaviour to *Lucilia sericata*, which start to oviposit 15-30 minutes after presentation of a suitable substrate (Barton Browne, 1958). The meat presented in the present study was initially cold (as it was not left to thaw overnight), resulting in oviposition being delayed for three hours after presentation. Painting of the thoraces would not have affected chemodetection of the meat as receptors are located on the antennae, labellum and ovipositor (Wallis, 1962). After this time, there were often multiple flies congregating on the meat, even if only to feed or clean. This may indicate possible delayed colonization of incompletely thawed or refrigerated cadavers used in research, extending the post mortem interval estimate, however insect succession does not appear to be affected (Huntington, 2007).

Individual flies waited for chemosensory detection of decaying compounds by the labellum, antennae and palps from the meat before oviposition, which has been shown to be the primary stimulus for oviposition in other Calliphoridae species (Amendt, *et al.,* 2008; Barton Browne, 1960; Easton & Feir, 1991; Wallis, 1962). Adults initially fed on the meat and showed ovipositor probing behavior associated to egg-laying, similar to *Phormia regina* (Barton Browne, 1960)*,* which allows olfactory and tactile sensation by the anal leaflet sensillae (Wallis, 1962). The effects of visual stimulation were not tested, however have been shown to be important in Calliphoridae (Amendt *et al.,* 2008). The time between flies first feeding/testing the meat and oviposition was different for individual flies with no clear consensus. This indicates variation in readiness to lay, even when ovary maturation occurred simultaneously in all females 7 days previously (*P. regina* are ready to lay similarly after 6 days (Barton Browne, 1958)).

Female groups appeared to prefer laying eggs in crevices in meat, most likely with the aim of optimizing egg survival. Similarly, *L. sericata* have been observed laying in groups in dark, humid crevices in sheep fleece (Barton Browne, 1958). Typically, flies laid eggs at multiple sites, some of which were re-used by the same and other flies, and some females displaying interruptions of up to ~30 minutes between laying eggs. Most females were observed laying their batch of eggs within a 30 minute timeframe, indicating the age range upon oviposition. These observations have not been recorded for other blowfly species, and could play important roles in collection of eggs from cadavers and for future study of specific-aged batches of eggs.

Overall, this study indicates *C. vicina* display similar ovary maturation and oviposition behaviours to *P. regina* and *L. sericata*, with new data presented for the age range of eggs at oviposition. To obtain accurate developmental data, eggs collected and studied should be of similar age. The selection of individual egg batches is unlikely to represent the full cohort of eggs from a single fly since they visit ~4.5 times and lay in multiple sites, with ~6.5 minutes in between laying periods. To minimise the age range of a single batch of eggs for developmental studies, these studies suggest an oviposition interval of 30 minutes should be employed, and all eggs from that period used. Fortunately, these findings have reduced implications for PMI estimation. If eggs are sampled from the cadaver, it cannot be assumed they are: (i) from the same fly, (ii) represent the entire batch or (iii) have similar ages, however the earliest hatching are taken to indicate the first-laid eggs, even if there is a large range amongst each batch.

3.3.2 Occurrence of precocious egg development

Whilst the age of the majority of the egg batch can be predicted, precocious egg development is prevalent in *C. vicina*; the present study indicated levels ranging from 2.55% to 9% in captive and wild populations respectively. The effects this may have on post-mortem interval (PMI) estimation and developmental studies must therefore be considered.

In captivity, levels of precocious egg occurrence can be minimised by using specific collection protocols. It was initially hypothesised that longer protein starves would increased levels of precocious egg occurrence. In contrast, the highest levels of occurrence were noted after a one-week starve. This may be explained by insufficient time provided for meat feeding, for initial ovary maturation of the entire colony to occur. This would result in multiple ovary maturation states and only those with complete development would lay their eggs, as noted after 5 days of meat exposure. Some flies may have initiated oocyte maturation of some eggs past the point of resorbtion (Spradbery & Schweizer 1981), and these may have been laid as precocious eggs/larvae on the meat after the one week starve or unnoticed in the BugDorm after longer starves. Lower levels of precocious egg occurrence after two-three week starves may be due to complete egg resorbtion after incomplete ovary maturation, which has been shown to improve chances of further oviposition (Cook & Dadour 2011; Papaj 2000; Vogt, *et al.,* 1985a & b). Equally, egg maturation may have been completed in the two or three week starve using the sucrose provided at all times (Chapter 2.1) (Barton Browne 1981).

It was expected that the first batch of eggs collected would contain higher numbers of larvae than later ones, since females containing a developing embryo may be more receptive to the meat in order to expel the precocious egg or larva; many *C. vicina* and *P. terraenovae* females starved for extended period of time lay eggs in the BugDorm (K Brown, personal observation). Once these advanced-stage embryos have been laid, the remainder of the batch can be laid all within 30 minutes of each other, most likely in the second round of egg collection after the time for chemosensory detection has increased. Despite the absence of statistically significant changes in precocious egg occurrence between the different batches (as revealed by ANOVA analysis) it is suggested that it would be prudent to avoid use of batch one eggs for developmental studies.

Testing the length of oviposition periods showed higher ratios of precocious eggs were observed with 15 minutes oviposition time. Adults require about 30 minutes to lay their full cohort (~200) of eggs, often at multiple sites with about 7 minutes between laying periods (Davies 2006; personal observation). Extending the oviposition period to 60 minutes made an insignificant change in proportion of precocious egg levels (0.05% increase over that found after 30 minutes). It is therefore recommended to use a 30 minute oviposition interval where possible.

The potential impact of precocious eggs on developmental studies should be considered. The mean precocious egg occurrence across all batches (laid within 50 ADH) was 2.55%, i.e. this proportion of samples could be ~500 ADH older than expected. The low percentage of eggs (1.51%) that hatched between 300-480 ADH were presumed to have done so due to natural variation in the stage length. If these were the result of early fertilisation, this would have occurred a maximum of 200 ADH previously, and the low number of samples this would affect in developmental studies would be insignificant. However, precocious egg development could have an undesired effect on the mean ADH ages given for each lifecycle stage. For example, studies examining pupal development may involve sampling the first larvae to pupate, and an age in ADH calculated for the start of the pupal stage. These pupae may have developed from precocious eggs and not truly represent the development at the mean batch age, causing error in the developmental data.

To minimise the effects of precocious egg occurrence it is desirable to collect eggs from a 30 minute oviposition period, after the first 30-minute exposure of a colony to the meat feed, following a >7 day protein starve. This method is similar to that of Parks and Sonnenblick in Demerec (1950) and should result in less than 2.5% of the eggs being precocious.

The frequency of precocious eggs (larvae in genital tract) in the wild was surprisingly high (9%) when compared with the study of Wells & King (2001), which failed to find *any* live larvae in the genital tract of *C. vicina* females in autumn or winter. Had such larvae been laid alive, they would have been at least one day older (at 22°C) than the rest of the batch. In the present study, a single dead larva was observed but this was not recorded as precocious as it would not contribute to PMI estimation. The dead larva may have been fertilised ~24 hours previously, and as no suitable oviposition substrate was located it was being reabsorbed, as seen in the larvae of *Calliphora dubia* (Cook & Dadour 2011). *C. dubia* is primarily larviparous but also lays generally unviable eggs; the embryogenic development and oviposition behaviour may be therefore markedly different, therefore the cause and fate of the *C. vicina* 'dead' larva is unknown.

Wells & King (2001) found that 11% (3 of 27) gravid *C.vicina* females collected in autumn and 50% (1 of 2) gravid females collected in winter contained an egg in the genital tract. In the present study 79% (27 of 34) gravid *C. vicina* females contained an egg in the genital tract. The large difference in percentage precocious egg occurrence is most likely attributed to small total female collections (present study n = 53, summer, Wells and King study in autumn n = 33 and winter n = 2). Eggs present in the genital tract are likely to be fertilised, as they have passed the spermathecal ducts, however in the absence of gene expression data it is impossible to determine their developmental stage (Tarone *et al.,* 2007). Fertilisation was likely to have occurred immediately prior to collection/preservation, as the presence of an egg in the genital tract was a common occurrence (79%) in comparison to the presence of larvae (9%). The eggs would be very young and under normal oviposition conditions would be laid with the rest of the batch (i.e. no precocious development occurred). The ages of these eggs would therefore have no significant effect on age or PMI estimation using older stages (larvae etc).

It was expected that in summer with the increased temperatures, fly activity, and distribution of decomposition odours, precocious egg occurrence would be lower as oviposition sources would be easily detectable. The high precocious egg occurence in *Calliphora vicina* found in this study may reflect the predicted low availability of carrion and other oviposition sites available for *C. vicina* in an urban environment (Portsmouth – Chapter 2). Faeces and rubbish are more prevalent however frequency of oviposition on these sites by *C. vicina* is unknown. The effects of oviposition site availability on precocious egg occurrence could be examined using *Lucilia sericata*, which readily oviposit on faeces, rubbish and carrion, hence should display lower levels of precocious egg occurrence. Further work should be carried out on other forensically important Diptera, as at present precocious egg occurrence appears to show a strong bias towards the blue-bottle flies (e.g. *C. vicina* and *Calliphora vomitoria*), with limited data to support its presence in other species.

Estimation of PMI from *C. vicina* immature stages that have developed from precocious eggs could result in the estimate being decreased by 24 hours (at 22°C) or more. As ~10% of a batch of eggs is likely to be precocious, and the eldest immature stages are used to estimate PMI, it should be expected that some precocious samples may be collected. Therefore, the estimated PMI window should be lengthened accordingly (by ~24 hours) based on the entomologists judgement of the case and samples obtained, as suggested by Wells & King (2001). Upon collection of a large sample batch (>500), it may not be possible to distinguish between a sub-section as the genuine eldest, or a precocious proportion of the eldest batch. In smaller samples however, it may be easier to distinguish a small number of samples as being precocious in relation to the batch, such as when <10 large larvae are present amongst hundreds of smaller larvae. Careful judgement should always be made and an extra period of time equal to that of the embryonic stage calculated from crime scene temperatures should be removed from the age of the eldest samples to estimate a PMI.

Overall, precocious egg presence has been shown to be an important feature influencing both developmental studies and PMI estimation. It should always be considered and where possible its effects minimised.

3.3.3 Variation in pupal stage length

To calculate pupal age and allow PMI estimation from eggs with a known small age interval, an indication of the natural variation in the lifecycle length and pupal stage is also needed, so that appropriate errors (age limits) can be placed on all estimates based on morphological and molecular analyses.

Pupation and emergence levels were much higher than previously stated for *C. vicina*: Kamal (1958) found a 'high' mortality rate for 'pre-pupae', i.e. failed to pupate, and an emergence rate of 31-43% at 27°C; Putman (1977) found survival rates of 79% pupation and 67% emergence at 24°C, however some larvae were starved of meat. The survival rates found in this study were always above 93% for both pupation and emergence, even in protein-starved larvae, thus indicating environmental conditions used did not have any detrimental effect on development. The methods used here permitted mild starvation of larvae with no gross effects on mortality, mimicking the scenario in which development of the eldest larvae occurs on a small carcass or with limited food. It is proposed that extending the period of protein starvation (i.e. removal of food in earlier instars) increases mortality rates, with consequently greater effects on pupal stage and lifecycle lengths.

Unlike in *Drosophila melanogaster* (Bainbridge & Bownes 1981), male/female bias in lifecycle and pupal stage length (in ADH) was not observed in these studies (Table 3.5), and no compensation for pupal sex needs to be made. It is likely that ADH errors caused by temperature fluctuations within maggot masses are more significant. A significant bias in emergence time was observed in $T_{FF}2$, with males emerging around 9:00 and females around 12:30h. This phenomenon has been previously noted by Erzinclioglu (1996), but was not observed in any other trials in the present study and it did not produce significant lifecycle length (in ADH) differences between males and females. Male/female emergence bias has been noted in other insect species (Rivero

& West 2005; Fagerström & Wiklund 1982; Bainbridge & Bownes 1981; Zwaan *et al.,* 2008) and although contested in *Drosophila*, this should be investigated further in *C. vicina*.

A significant bias towards early eclosion (before 14:00h) was noted in all fully-fed trials. This indicates a circadian eclosion rhythm, such as has been recorded for *Lucilia cuprina*, *Protophormia terraenovae, Musca domestica,* the Sarcophagidae and in other Diptera (Smith 1985; Aschoff & Von Saint Paul 1990; Codd *et al.,* 2007; Yocum *et al.,* 1994; Saunders 1979; Watari & Arai 1997; Konopka & Benzer 1971). This rhythm appeared to be disrupted in the protein starved larvae, indicating starvation may affect the genetic modulation of this process, which also occurs when a 24 hour light cycle is imposed (Codd *et al.,* 2007), however no previous research on this aspect could be found. PMI estimation from starved larvae could thus be problematic if laboratory rearing is required, since larvae may be more sensitive to artificial conditions. It is also unknown if the extent or period of starvation affects the degree of circadian rhythm change, thus possibly affecting lifecycle ADH further.

Comparison between fully-fed and starved trials showed significant variation in pupal stage and lifecycle length occurred under identical conditions, making conclusion of results difficult. Differences between trials are most likely due to the following:

a) Natural variation between batches is common at 20°C, as indicated by Finell and Jarvilehto, and is likely due to natural variation between colonies (Figure 3.11).

b) Within maggot-masses, some larvae will develop at 37°C, some at 20-22°C. Even with a low larva:meat ratio, larvae are observed to congregate in masses in the third instar, making such temperature effects difficult to eliminate.

c) Sampling intervals were chosen as the most suitable at the time of the trial, hence vary slightly. A balance was required between obtaining detailed information about pupation and emergence, and disturbing larvae/pupae such that information obtained would be inaccurate, as demonstrated by over-sampling in $T_{FS}2$, which caused the undisturbed control colony to emerge earlier. Further repeats of all trials with a balanced sampling approach would eliminate such differences.

d) Selection of egg masses for specific monitoring. Eggs were collected in 30 minute intervals, and only in $T_{FF}1$ were all eggs used; counting and analysis of such large numbers was extremely difficult and likely to introduce errors. In later trials, a selection of eggs was collected for analysis, and divided into test and control colonies. This reduced maggot-mass effects, lessened the need for sieving (which was shown to reduce lifecycle length in starved colonies) and facilitated sexing of adults upon emergence. Selecting only a small portion of the eggs may have reduced the possible natural variation, as seen in $T_{FF}1$ (Figure 3.11), but equally such variation may have been caused by maggot-masses in the other trials. Overall, all fully fed and starved trials showed similar trends on a daily basis.

The mean pupal stage and lifecycle lengths were shorter in starved larvae, by approximately 2-3 days at 22°C (Fig. 3.10 and Table 3.9). Similar results were obtained by Arnott & Turner (2008), which suggests larvae with a long post-feeding stage (i.e. fully fed) also have an extended pupal stage, resulting in a longer lifecycle length. Identification of starved larvae is therefore imperative for PMI estimation, as age estimates based on developmental markers need to be adjusted accordingly for the variation in lifecycle length caused by lack of food (this study) or similarly by chemical compounds (O'Brien & Turner 2004; Bourel *et al.,* 1999; Bourel *et al.,* 2001).

Comparison of all starved and fully-fed trials shows a similar pupal stage length which is distinctly different to the variability evident in Finell and Jarvilehto's data (Fig. 3.13). The data presented here indicate that there is a minimum energy requirement for metamorphosis: a) starved larvae reduce their wandering time (indicated by shorter lifecycle length) in order to conserve limited energy stores for the pupal stage, if they have enough to enter metamorphosis and b) starved larvae commit themselves to a shorter pupal stage, using the minimal level of energy for metamorphosis (which may not be successful); fully fed larvae consume more food and wander longer than is required to ensure successful pupation. Increased levels of feeding (as in fully-fed larvae) may also increase adult size and fecundity (Greenberg (1973) in Catts (1992)) or improve their chances of finding a better pupation site; more research into this is required.

The range noted in pupation and emergence periods in the current study were much shorter than that observed by Finell & Jarvilehto (1983) (Fig. 3.11). This may be a result of the higher temperature (22°C) in the current study; however this should affect the entire lifecycle length, which was shown to be similar at both temperatures. Variation in sample size may also cause these stage length differences as shown in the current study; a larger sample displayed larger variation in stage length, as expected. The most probable causes for large variation are rearing conditions, which are difficult to control. Further trials with large sample sizes should be conducted at multiple temperatures to reliably quantify the variation in the stage lengths.

Overall, using the ADH values for the pupal and lifecycle stage lengths, and the confidence intervals given, it should be possible to estimate age with a 95% certainty

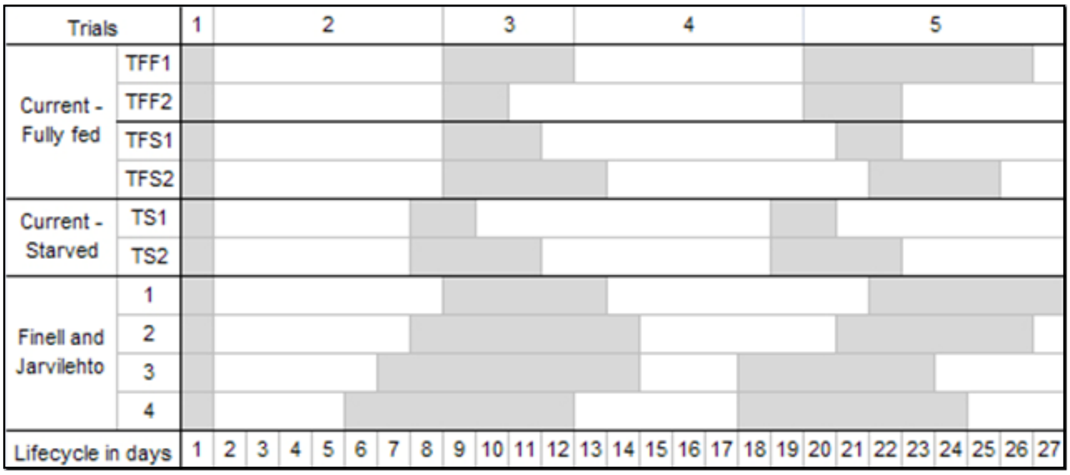

Figure 3.11 Comparison between current and previous findings for pupal stage length. Data from the present study, conducted at 22°C was compared to that obtained by Finell & Jarvilehto (1983) at 20°C (Figure 1 – only comparable data available). 1 = embryonic development; 2 = larval development; 3 = pupation period – from first to last larvae to pupate; 4 = pupal period – all samples are pupae; 5 = emergence period – from first to last pupae to emerge.

within +/- 500 ADH (1 day at 22°C), and correlate development to an approximate percentage in time through the stage lengths (e.g. 50% developed). This results in a reliable data set that can be compared to development at different temperatures, facilitating PMI estimation under different environmental conditions.

3.4 Conclusion

To obtain eggs of a known age-interval, permitting accurate developmental timelines to be constructed, the following protocol should be followed:

1. Flies must be subjected to protein starvation after ovary maturation for a minimum of 7 days.
2. Frozen meat should be thawed and allowed to equilibrate to room temperature (~22°C) overnight.
3. The second batch of eggs from a 30 minute oviposition interval should be collected for rearing.

This protocol should result in collection of the entire egg batch from each female, with an age variation of <30 minutes. <2.55% of the eggs collected may be precocious, which will have minimal effects on age estimation and developmental studies. When estimating PMI from *C. vicina*, 9% of a sample should be considered as precocious, and 550 ADH added on to the estimate as a precaution.

Collection of pupae for morphological and molecular timeline production should continue for 3 days following first significant emergence, to ensure >95% of pupae have emerged. Pupal age can be estimated (from fully-fed larvae) with 95% confidence to be within a minimum range of a) 564 ADH (25.6 hours at 22°C) for a point within the pupal stage, and b) 694 ADH (31.5 hours at 22°C) for a point within the lifecycle. If larvae appear to be starved, the range increases to 1071 ADH for the pupal stage and 1081 ADH for the lifecycle.

The mean pupal stage length for fully-fed larvae is 6023 ADH; 11.4 days and a lifecycle length of 10678 ADH, or 20.2 days. Starved larvae have a shorter mean pupal stage length of 5550 ADH, equivalent to 10.5 days at 22°C, and a shorter lifecycle length of 9141 ADH, or 19.7 days. These figures should be used to calculate developmental percentages relative to the pupal stage and lifecycle, to facilitate development comparison between closely-related species.

Chapter 4 – Preservation Methods

Protocols for collection of pupae with known age and variation, for the purpose of developmental studies, have been established. Correct preservation and storage of pupae for this purpose, and those collected from the crime scene for age and PMI estimation, is vital. This chapter tests various existing and new preservation methods for *Calliphora vicina* pupae.

4.1 Introduction

4.1.1 Insect collection and PMI estimation

For PMI estimation, insects collected from the crime scene are sent to the entomologist in two forms; alive and preserved. Living insects are transported to the lab under specific temperature-controlled conditions (Amendt *et al.,* 2007) for rearing to the adult stage, enabling confirmation of species identification of preserved samples. The developmental time to adult eclosion (in ADH) is then subtracted from the total development time to indicate the ages of insects upon collection. This is then used to back-calculate the time of oviposition and PMI. Rearing of insects can, however, require considerable time, e.g. 19-21 days at 23°C for *C. vicina* (Anderson 2000), which can delay the calculation of the PMI estimate. Also, depending on development and transportation temperatures, insects may enter diapause, which would increase the time to, or completely prevent, emergence, or even die preventing PMI estimation from these samples (Villet *et al.,* 2010).

Age estimation from preserved samples is clearly less time-consuming than rearing. In addition, the error associated with age estimation from older stages, e.g. adult eclosion, is minimised (Foran 2007). Although species identification of the immature insects is possible using morphological characteristics, it is not as reliable as that obtained from adults, due to limited published data. As a consequence, PMI is estimated using the analysis of both reared and preserved insects.

Age estimation depends on adherence to specific collection, transport, preservation and storage conditions (Adams & Hall 2003; Day & Wallman 2008). Preservation can be done at the crime scene but is more often carried out after transportation of insects to the lab (again under temperature-controlled conditions). Standards and guidelines for optimal preservation of adults, eggs and larval stages are given in Amendt *et al.,* (2007) however preservation methods for pupae are not established, therefore hindering their use in PMI estimation.

Species identification and age estimation is conducted using multiple stage and species-specific features. Preservation methods can therefore be stage-specific, as currently proposed (Amendt *et al.,* 2007), to ensure the features used are retained in their natural state.

4.1.2 Preservation of eggs and larvae

Eggs are rarely found as the oldest stage on a cadaver (Anderson 2004), as crime scenes are not often discovered within the short timeframe required for development to 1st instar (hatching). Rearing of eggs enables age estimation using the developmental time to first instar (Bourel *et al.,* 2003), and species identification at adult eclosion. Eggs should also be preserved in 70-95% ethanol for morphological species identification by scanning electron microscopy (Mendonça *et al.,* 2008). Age estimation of *Lucilia sericata* eggs fixed in RNAlater and frozen at -80°C is possible using developmental gene expression (Tarone *et al.,* 2007), however it is not known whether this is possible from eggs preserved in 70-95% ethanol, as proposed (Amendt *et al.,* 2007).

Larvae are preserved by hot-water-killing (HWK) and stored in 80% ethanol. This prevents putrefaction, ensures full larval size extension for biometric measurement and preserves features such as spiracles and intersegmental spines for both morphological species identification and age estimation. Larval DNA is also preserved using this method, permitting molecular species identification. Larvae remain unchanged in this preservative for at least one year (Richards *et al.,* 2012), which is a necessary requirement for cold cases that may be revisited many months later.

4.1.3 Pupal preservation for multiple purposes

Similarly to eggs and larvae, preservation of pupae must facilitate species identification and multiple age estimation methods, which require different features to be used. Species identification is conducted using both morphological characters of the puparium (Sukontason *et al.,* 2007; Amorim & Ribeiro 2001; Whitworth 2003) and by amplification and sequence analysis of the COI gene (Mazzanti *et al.,* 2010). Critical to the preservation method is therefore the conservation of the puparium characteristics and high molecular weight DNA. Preservation of puparia in 70-95% ethanol adequately preserves morphological characteristics (Amendt *et al.,* 2007). DNA is suggested to be best preserved by storage at -80°C, however preservation in 70-95% ethanol has also been suggested to be suitable for insect samples for short periods of time (Post *et al.,* 1993).

Pupae dimensions do not change and other development features are used to estimate age. Within the first 24 hours, analysis of the degree of puparium tanning and respiratory horn eversion can indicate age (Greenberg & Kunich 2005). Given the short duration during which these changes occur, the subjectivity of colour assessment (prior to preservation) and the inter-individual variation, these methods have limited applicability.

After puparium removal, morphological development of various features including eye colour and bristle formation can be used to indicate age (Greenberg & Kunich 2002; Gaudry *et al.,* 2001). Careful removal of the puparium is facilitated by gentle boiling of pupae (Greenberg & Kunich 2002), but a suitable preservative for the prevention of discolouration and putrefaction has not been established for *C. vicina* pupae. Alcohol based preservatives have been used for morphology preservation in other Diptera and Hymenoptera (Quicke *et al.,* 1998; Tantawi & Greenberg 1993; Amendt *et al.,* 2007).

An emerging pupal age estimation method is the examination of internal development using histology. Changes in thoracic muscle, brain and optical structures can be examined by sectioning and staining of pupae, as noted previously in *C.vicina* (Lowne 1895; Perez 1910; Jarvilehto & Finell 1983) and *Drosophila melanogaster* (Robertson 1936; Bainbridge & Bownes 1981). Whilst no histological preservatives are indicated for calliphorid pupae, formalin fixation has commonly been used in other organisms (Buesa 2008) however insects kept in these fixatives for extended periods become brittle and it is therefore unsuitable for long term storage or for combined external morphological analysis (Cox *et al.,* 2006).

The analysis of temporal gene expression is also being developed as a method for quantitative age estimation (Ames *et al.,* 2006; Zehner *et al.,* 2006; Zehner *et al.,* 2009). This requires the most stringent pupal preservation methods, due to the inherently unstable nature of mRNA. Flash freezing and storage of samples at -80°C, or preservation in RNAlater at -20°C are suggested as the best options for preventing degradation by RNases (Cox *et al.,* 2006; Florell *et al.,* 2001).

4.1.4 Conclusions and aims

Species identification and age estimation methods require the preservation of multiple characteristics and a variety of procedures are available for this purpose. Since at the time of preservation the age estimation method/s to be employed may be unknown, in addition to establishing the optimal preservative for each analysis, the identification of a universal preservation method, such as that used for larvae (HWK, 80% ethanol), would be valuable.

Preservatives must use readily available materials and easy to achieve storage temperatures, and be cost-effective if they are to be adopted for use in the field and/or lab. They must also be suitable for both short and long-term storage to allow for reanalysis as would be needed if revisiting cold cases.

In summary, the absence of standardised pupal preservation protocols necessitates reliance on rearing of this stage for age estimation. This results in larger error windows than necessary and general underutilisation of the stage in PMI estimation. The aim of this study was therefore to:

- Test multiple preservatives and identify optimal protocols for age estimation by:
    - External morphology
    - Histology
    - Temporal gene expression

  and finally molecular species identification.
- Identify a universal preservative suitable for all pupal age estimation methods that facilitates a multidisciplinary approach to PMI estimation.

4.2 Results

4.2.1 External morphological analysis

Morphological age estimation of preserved pupae requires retention of their living-state colouration, size and adequate turgor to prevent damage upon examination. Two pupal ages, 4 and 7 days after puparium formation, were examined after 2 weeks in the appropriate preservative, and again after 6-8 months. At 4d, pupae retain many of their larval characteristics, such as an abundance of fat and white colouration. By 7d, pupae have pigmented eyes and bristles, and development of thoracic muscle and sclerotisation of the epidermis has begun. Selection of these two ages therefore provides variation in tissue structure, and any differential effects of preservative due to age/relative development of pupae can be monitored.

The fresh live (control) pupae (Fig. 4.1) were scored five (meaning no discolouration) and three for turgor (fairly soft). After two weeks in preservative, ANOVA analysis with Dunnetts comparison to the control pupa indicated that significant discolouration ($P<0.05$) occurred in both 4d and 7d pupae in most histological fixatives (Table 4.1), such as significant yellowing and pierce-hole putrefaction in Bouins (Fig. 4.2). 4d pupae were also discoloured in modified methacarn, isopropanol and after HWK with dry storage. 4d and 7d pupae were discoloured in 70% ethanol and propylene glycol.

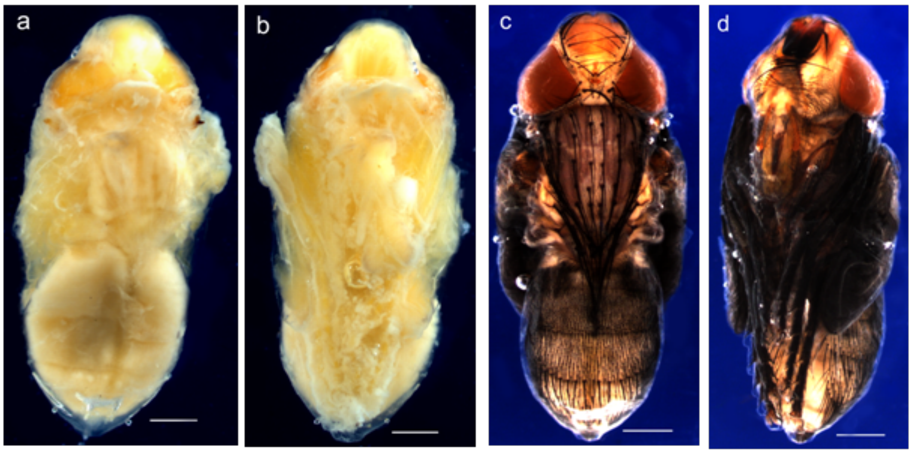

Figure 4.1. Control pupae showing native colouration. Puparia were removed from 4 day old (a & b) and 7 day old (c & d) pupae, which were imaged alive from both dorsal (a & c) and ventral (b & d) aspects. These pupae were used for comparison to preserved samples. The epidermis in both young and old pupae is white. The blue backgrounds are the same throughout all images. Scale bar = 1mm

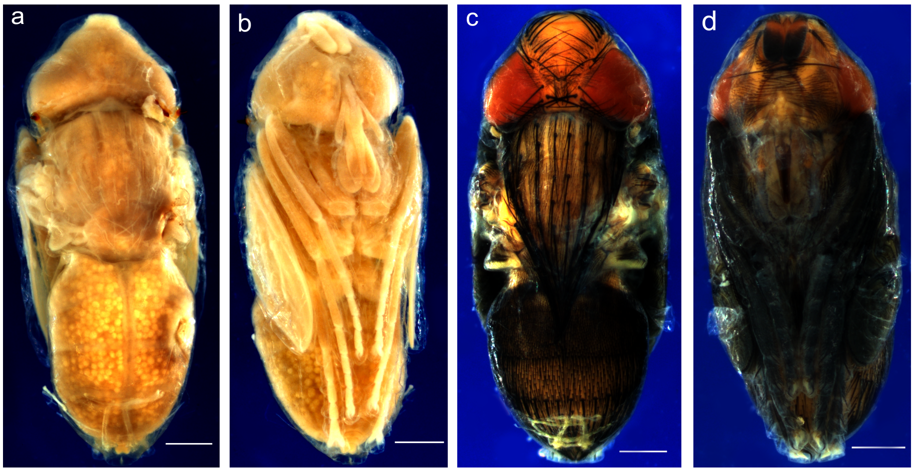

Figure 4.2. Discolouration of pupae fixed in Bouins. Pupae imaged after fixation in bouins for four hours and preservation in 70% ethanol for 6 months. The epidermis of all pupae was stained yellow, with 4 day old pupae (a & b) more notably than 7 day old (c & d). Scale bar = 1mm

Pupal width and length were not affected by any solution. Mass was affected in 4 preservatives, three of which were at 4°C; 4d pupae were significantly lighter, 7d pupae significantly heavier. Turgor significantly decreased ($P<0.05$) in 4d pupae preserved in RNAlater (4°C and -20°C) and 7d pupae preserved by HWK and stored without solution or in propylene glycol at -20°C (Table 4.1). An increase in turgor from live pupae (scored 3) was considered beneficial, as this facilitated puparium removal.

Analysis		External																				Internal				DNA				RNA				Total Score /76	% Score	Rank
Preservative time		<2 weeks										6-8 months										<2 weeks		6-8 months		<2 weeks		6-8 months		<2 weeks		6-8 months				
		4 days old					7 days old					4 days old					7 days old																			
Preservative	Temperature	Discolour	Turgor	Length	Width	Mass	Discolour	Turgor	Length	Width	Mass	Discolour	Turgor	Length	Width	Mass	Discolour	Turgor	Length	Width	Mass	4 days old	7 days old	4 days old	7 days old	4 days old	7 days old	4 days old	7 days old	4 days old	7 days old	4 days old	7 days old			
HWK, 80% EtOH	4°C	▨	▨	▨	▨		▨	▨	▨	▨	▨	▨	▨	▨	▨	▨	▨	▨	▨	▨	▨	2	2	2	2	5	5	5	5	2	2	2	2	75	99	**1**
	-20°C	5	2	1	1	1	5	2	1	1	1	5	2	1	1	1	5	2	1	1	1		▨	▨		▨	▨	▨	▨	▨	▨	▨	▨	72	95	**2**
Kahles	4°C		▨	▨	▨	▨		▨	▨	▨	▨		▨	▨	▨	▨	▨	▨	▨	▨	▨	▨		▨		▨	▨	▨	▨					49	64	17
	-20°C		▨	▨	▨	▨	▨	▨	▨	▨	▨		▨	▨	▨	▨	▨	▨	▨	▨	▨	▨	▨	▨	▨	▨	▨	▨	▨					58	76	11
Bouins	4°C		▨	▨	▨	▨		▨	▨	▨	▨		▨	▨	▨	▨		▨	▨	▨	▨			▨	▨	▨	▨	▨	▨					44	58	20
	-20°C		▨	▨	▨			▨	▨	▨			▨	▨	▨	▨		▨	▨	▨	▨		▨	▨	▨	▨	▨	▨	▨					44	58	20
Bouins/ Carnoys	4°C		▨	▨	▨	▨		▨	▨	▨	▨		▨	▨	▨	▨	▨	▨	▨	▨	▨			▨	▨	▨	▨	▨	▨					49	64	17
	-20°C	▨	▨	▨	▨	▨		▨	▨	▨	▨		▨	▨	▨	▨		▨	▨	▨	▨			▨	▨	▨	▨	▨	▨					49	64	17
Modified Methacarn	4°C		▨	▨	▨		▨	▨	▨	▨	▨		▨	▨	▨	▨	▨	▨	▨	▨	▨		▨		▨	▨	▨	▨	▨	▨	▨	▨	▨	61	80	7
	-20°C		▨	▨	▨	▨	▨	▨	▨	▨	▨		▨	▨	▨	▨	▨	▨	▨	▨	▨		▨	▨		▨	▨	▨	▨	▨	▨	▨	▨	62	82	5
Isopropanol	4°C		▨	▨	▨	▨	▨	▨	▨	▨	▨		▨	▨	▨			▨	▨	▨	▨		▨	▨	▨	▨	▨	▨	▨	▨	▨	▨	▨	58	76	11
	-20°C		▨	▨	▨	▨	▨	▨	▨	▨	▨		▨	▨	▨	▨	▨	▨	▨	▨	▨			▨	▨	▨	▨	▨	▨	▨		▨	▨	60	79	8
RNAlater	4°C	▨		▨	▨		▨	▨	▨	▨		▨		▨	▨	▨	▨	▨	▨	▨	▨			▨	▨	▨	▨	▨	▨	▨				58	76	11
	-20°C	▨		▨	▨	▨	▨	▨	▨	▨	▨	▨		▨	▨	▨		▨	▨	▨	▨					▨	▨	▨	▨	▨	▨	▨	▨	59	78	10
HWK, Dry	4°C		▨	▨	▨	▨	▨	▨	▨	▨	▨			▨	▨	▨	▨	▨	▨	▨	▨		▨	▨	▨	▨	▨	▨	▨	▨	▨		▨	60	79	8
	-20°C	▨	▨	▨	▨	▨	▨		▨	▨	▨	▨	▨	▨	▨	▨	▨		▨	▨	▨	▨		▨	▨	▨	▨	▨	▨	▨	▨	▨	▨	70	92	3
70% EtOH	4°C		▨	▨	▨	▨		▨	▨	▨	▨		▨	▨	▨	▨		▨		▨	▨		▨	▨	▨	▨	▨	▨	▨	▨	▨		▨	51	67	15
	-20°C		▨	▨	▨	▨	▨	▨	▨	▨	▨		▨	▨	▨	▨		▨		▨	▨			▨		▨	▨	▨	▨	▨		▨	▨	52	68	14
Propylene Glycol	4°C		▨	▨	▨	▨		▨	▨	▨	▨		▨	▨	▨	▨		▨	▨	▨	▨		▨	▨		▨	▨	▨	▨		▨	▨	▨	50	66	16
	-20°C	▨	▨	▨	▨	▨	▨		▨	▨	▨		▨	▨	▨	▨		▨	▨	▨	▨		▨	▨	▨	▨	▨	▨	▨	▨	▨	▨	▨	62	82	5
Dry	-80°C	▨	▨	▨	▨	▨	▨	▨	▨	▨	▨	▨		▨	▨	▨	▨			▨	▨			▨		▨	▨	▨	▨	▨	▨	▨	▨	65	86	4

Table 4.1. The effects of preservation protocols on pupal morphology and molecular integrity. Four- and seven-day old pupae were preserved using 21 protocols for two weeks and six to eight months prior to analysis of morphology and molecular integrity. In each preservative, 52 pupae were examined using all methods. Grey shaded boxes indicate non-significant (P<0.05) or no observed differences detected between preserved and fresh pupae. Weightings are based on the importance in preservation for PMI estimation, allowing preservatives to be ranked for overall usage. Discolouration and DNA integrity were ranked the most important factors, thus given a value of 5. Turgor, internal and RNA analyses were scored at 2, as these were considered of average importance, based on current PMI estimation methods in development. Least important factors such as mass were given a score of 1. Only non-significant results (grey boxes) were included in the overall score and rank.

After 6-8 months, 4d pupae showed significant additional changes in discolouration, when using preservatives such as Bouins and propylene glycol (-20°C). Seven-day-old pupae in Kahles and Bouins were no longer significantly discoloured when compared to live pupae, however they were discoloured in additional solutions; isopropanol at 4°C and RNAlater, 70% ethanol and propylene glycol at -20°C. Seven-day-old pupae preserved in 70% ethanol shrank presumably through dehydration. In some solutions turgor of 4d decreased significantly (Table 4.1). However, T-tests indicated that after 6-8 months, overall turgor of 7d pupae had improved and length had decreased ($P<0.01$). Overall significant increases in 4d pupae length, width and mass ($P<0.01$) were observed.

Discolouration was significantly worse, especially around pierce incisions, in the absence of a hot-water-kill prior to preservation. This prompted investigation into the importance of the HWK conditions, on both 4d and 7d pupae. All pupae showed significant discolouration ($P<0.01$) by temperatures below 80°C; putrefaction around pierce holes was evident in 4d and 7d pupae and significant darkening of the legs and wings occurred in 4d pupae (Fig. 4.3). There were no significant differences in discolouration above water temperatures of 80°C for immersion times of 0.5 and 2 minutes and storage at 4°C and room temperature. Discolouration and putrefaction were considered the most important factors for age estimation using analysis of morphology. Minimising these effects was vital; the optimal preservation method was; pierce three times, HWK >80°C for at least 0.5 minutes, store in 80% ethanol, below 4°C, preferably at -20°C (Tables 4.1 and 4.2).

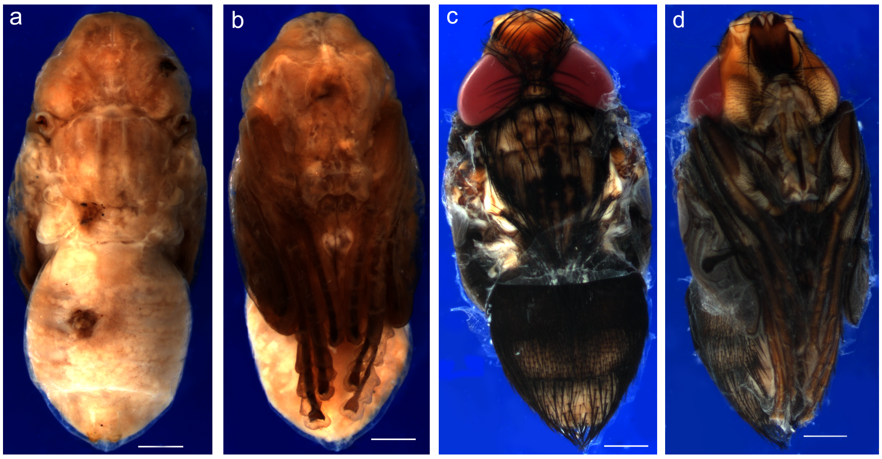

Figure 4.3. Putrefaction caused by low temperature hot-water-killing. Ten pupae were pierced three times, killed by submersion in hot water at 60°C for 30 seconds and preserved in 80% ethanol. 4 day old pupae (a & b) putrefied rapidly, and 7 day old pupae (c & d) displayed discolouration in the thoracic and abdominal epidermis, preventing reliable judgment of colour development. Scale bar = 1mm.

4.2.2 Histological analysis

External morphological analysis primarily required preservation of colour and prevention of putrefaction. Histological analysis required preservation of structure, achieved by consistent intact pupal section cutting, which was found to be dependent on preservative uptake and wax impregnation.

The best preservatives for histological analysis of pupae after short-term storage were Kahles (-20°C) and HWK, 80% ethanol (4°C) (Fig. 4.4 and Table 4.1). Sections from pupae in these preservatives were generally intact, however problems were experienced with tissue fragmentation during sectioning and section loss during staining from pupae in most solutions. This was examined using Hsu's multiple comparison with best (MCB) test, the best method being HWK, followed by preservation in 80% ethanol at 4°C, as previously stated. For 4d pupae, section adhesion to the slides was poor and probably due to the large quantities of fat body at this stage (Fig. 4.4a). Seven-day-old pupae comprised thoracic muscle (Fig. 4.4b) which was brittle and sections frequently crumbled and slipped off the slides during the staining process.

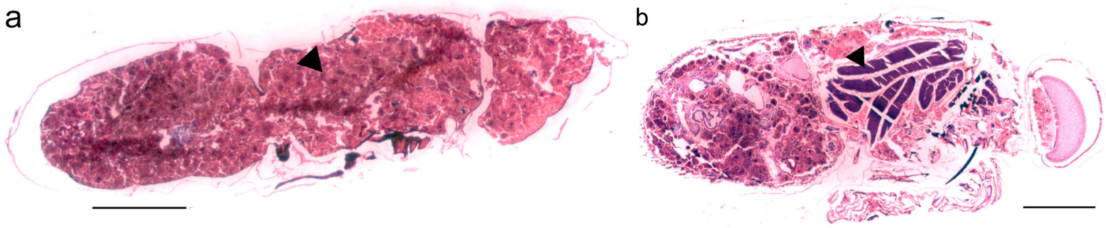

Figure 4.4. Variation in tissue type in 4d and 7d pupal sections. Sections were taken of four, 4 day old (a) and 7 day old (b) pupae killed by HWK and preserved in 80% ethanol at 4°C. Sections are mostly complete with very few tissue cracks. The differences in composition of tissues can be noted between the ages; fat body abundance in 4d pupae and muscle in 7d pupae (arrow heads). Scale bar = 1mm

For 4d pupae after 6-8 months storage, complete sections were significantly more easily obtained as examined using T-test ($P<0.01$) though 7d pupae were unaffected (Table 4.1). Refixing pupae in Kahles after both 2 weeks and 6-8 months preservation had neither beneficial nor detrimental effects on sectioning, and this step was deemed unnecessary (results not shown). The most consistent preservation conditions for long term storage were HWK, 80% ethanol, stored at 4°C or Kahles stored at -20°C (Table 4.2).

Further alterations to the method were tested, with the aim of improving section adhesion that had been observed for all preservatives. Firstly, pupae were bisected between the thorax and abdomen before clearing (Chapter 2.11.1). Secondly, 0.5%

gelatin was added to the water used for transferring sections on to slides. These adaptations greatly improved section retention from both the optimal and poor preservatives; HWK, 80% ethanol at 4°C (Fig. 4.5) and Kahles at 4°C (not shown) respectively.

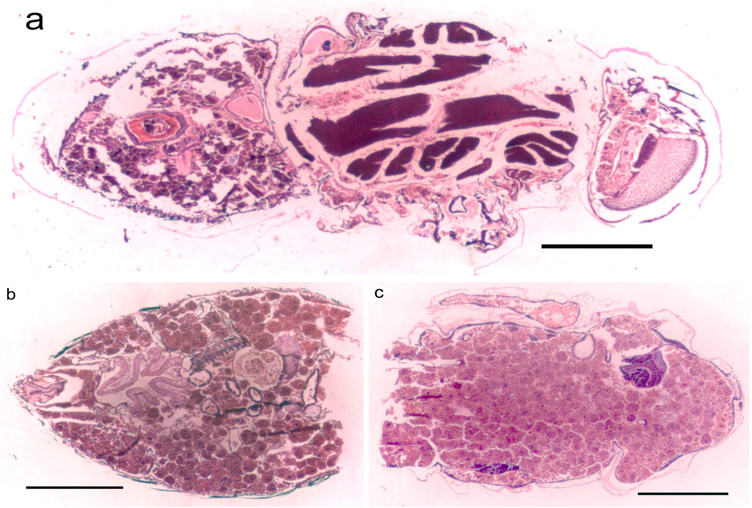

Figure 4.5. The use of pupal bisection and gelatin improve tissue integrity. Three whole (a) and bisected pupae (b & c) were preserved by HWK and stored in 80% ethanol at 4°C. they were mounted on to glass slides using gelatin. Fat body abundance mostly in 4 day old pupae (c) and combination of fat with sclerotisation of tissue in 7 day old pupae (b) resulted in tissue cracks without the use of gelatin. Scale bar = 1mm

4.2.3 Molecular species identification

Molecular species identification is often required to confirm morphological assessment. DNA was extracted and a 1270bp region of the COI gene was amplified by PCR. Preservative suitability was based on sequencing this PCR product from both short and long-terms storage in the 70% ethanol and formalin-based fixatives (Fig. 4.6 and Table 4.1). Lower yields of PCR product were obtained from 7d preserved in 70% ethanol (Fig. 4.6c) and 4d pupae preserved in Bouins after 6m (Fig 4.6g), possibly due to increased degradation, however complete sequences were obtained from all pupae. Individual sequence differences were detected, as expected from an F1 colony. All sequences clustered with existing *Calliphora vicina* sequences from NCBI

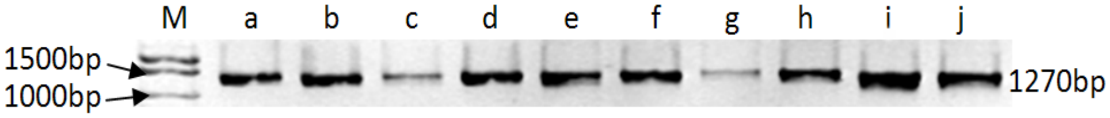

Figure 4.6. 1270bp COI gene PCR products from sequenced pupal samples. DNA was extracted from three pupae (of each age) in each preservative and a 1270bp COI gene fragment was amplified from all pupal extracts. PCR products shown here are those sent for sequencing, from 4d and 7d pupae preserved at 4°C in 70% ethanol after two weeks (a-b), 70% ethanol after 6 months (c-d), Kahles after 6 months (e-f), Bouins after 6 months (g-h) and Bouins/Carnoys after 6 months (i-j).

(www.ncbi.nlm.nih.gov) with 100% support, suggesting that even for formaldehyde-based preservatives, prolonged preservation does not prevent species identification. Neighbour-joining (Tamura-Nei model) and maximum parsimony analyses with boostrap support (50-1000 replicates) displayed 100% support for divergence from the nearest available relative, *Calliphora vomitoria* (Appendix III, Fig. A3). COI gene amplification and species identification was therefore possible from pupae preserved in all solutions tested, with preservation at -80°C considered optimal as this is known to minimise degradation of large DNA fragments (Post *et al.,* 1993) (Table 4.2).

4.2.4 Analysis of RNA integrity and gene expression

Temporal gene expression offers a method of quantitative age estimation, hence the preservation of RNA was assessed in pupae stored in each of the solutions.

The overall integrity of RNA, extracted after two weeks in the preservatives, was assessed by direct analysis of extracts on a 2% agarose TBE gel. The presence of a defined ribosomal 18S rRNA bands (running at ~1000bp dsDNA) was used as an indicator of RNA quality (Fig. 4.7); the 28S band is not distinct as it dissociates into two and migrates to the same position as the 18S rRNA band. RNA was extracted from all pupae (data not shown), and as expected, extracts from fresh 4d and 7d pupae and those stored at -80°C were least degraded. Extracts from the RNAlater

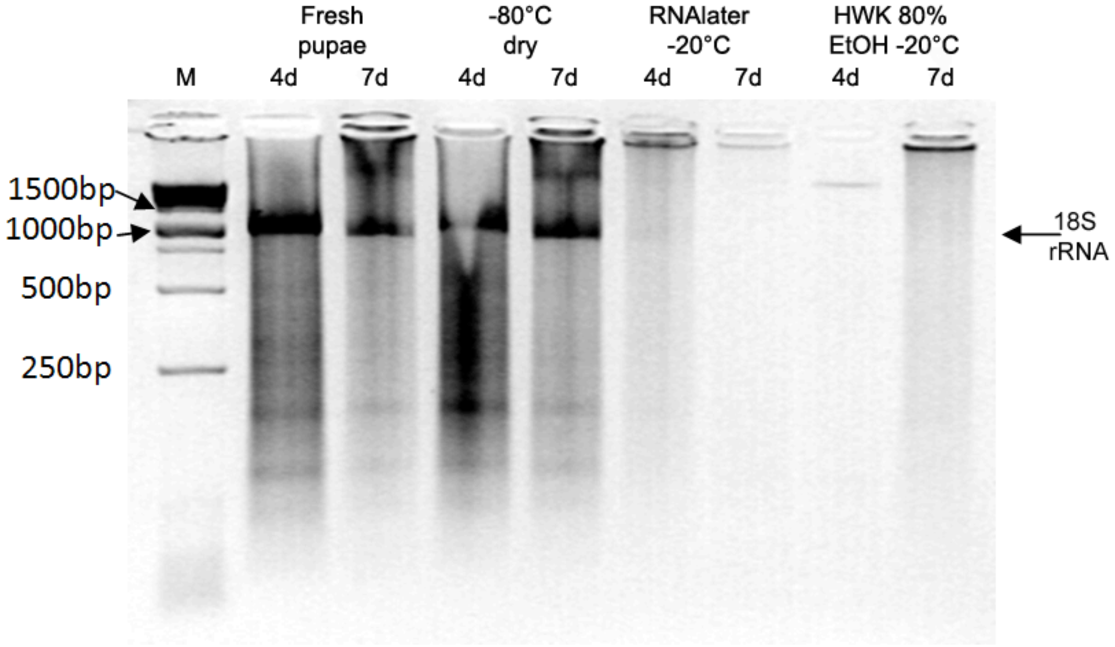

Figure 4.7. RNA extracts showing minimal degradation. RNA was extracted from one pupa of each age preserved in all preservatives, and visualised on a non-denaturing 2% agarose gel. Extracts shown are from 4- and 7-day old fresh pupae, compared with extractions from -80°C frozen without solution, RNAlater (-20°C) and HWK 80% ethanol (-20°C). The 18S and 28S rRNA bands migrate to ~1000 bp on a dsDNA ladder.

and HWK 80% ethanol pupae are faint (equal volumes were loaded), showing low RNA quantity. Assessment of integrity is therefore difficult, however as high molecular weight RNA is visible, a lack of low molecular weight (below 250 bp) smearing, which tended to be more prominent (Fig. 4.8), indicates the RNA remained intact.

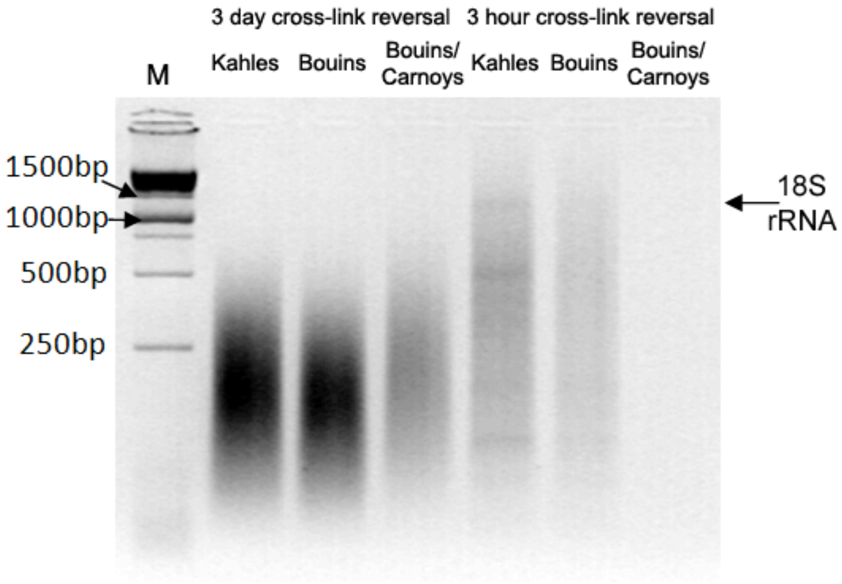

Figure 4.8. RNA extracts after cross-link reversal. RNA extractions after formaldehyde cross-link reversal from one pupa in each preservative were analysed on a non-denaturing 2% agarose gel. A 3-day reversal was carried out on 4d pupae preserved for 2 weeks at 4°C in Kahles, Bouins and Bouins/Carnoys. A 3-hour reversal was carried out on pupae preserved in the same manner for 6-8 months. The arrow indicates the expected position of the 18S rRNA band.

After 6-8 months in solution, RNA was extracted and analysed in the same manner (data not shown). RNA was recovered from all pupae other than those stored at 4°C in RNAlater (4d and 7d pupae) and 4d pupae in 70% ethanol. The least degraded RNA extracts were obtained from pupae preserved in RNAlater (-20°C) and -80°C dry.

No RNA was recovered from formalin-based fixatives such as Kahles and Bouins without prior formaldehyde-crosslink removal by extended incubation coupled with proteinase K digestion (3 days at 55°C). Highest yields were recovered from pupae preserved in Kahles and Bouins however this treatment resulted in recovery of highly degraded RNA from all pupae, as evidence by low molecular weight smears at the base of the gel (Fig. 4.8 lanes 2-4). A shorter crosslink removal (3 hours at 55°C) was performed on pupae preserved similarly for 6-8 months, with the aim of minimising RNA degradation. RNA was still degraded as 18S rRNA bands could barely be identified (Fig. 4.8 lanes 5-7). Lower yields of RNA were also recovered. These data therefore suggest that formaldehyde-based fixatives are unsuitable for RNA preservation.

Assessment of RNA yield and integrity performed by gel electrophoresis gave an initial indication of overall quality. To fully assess suitability for gene expression analysis, cDNA was reverse-transcribed from the extracted RNA and actin and arylphorin receptor fragments were amplified by PCR. After short-term storage, actin (85 bp) was amplified 32 out of 33 times (97%), in all except 4d pupae preserved in propylene glycol (4°C) (Fig. 4.9 and Table 4.1). PCR reactions that showed no product were repeated at least once to ensure no PCR product could be obtained.

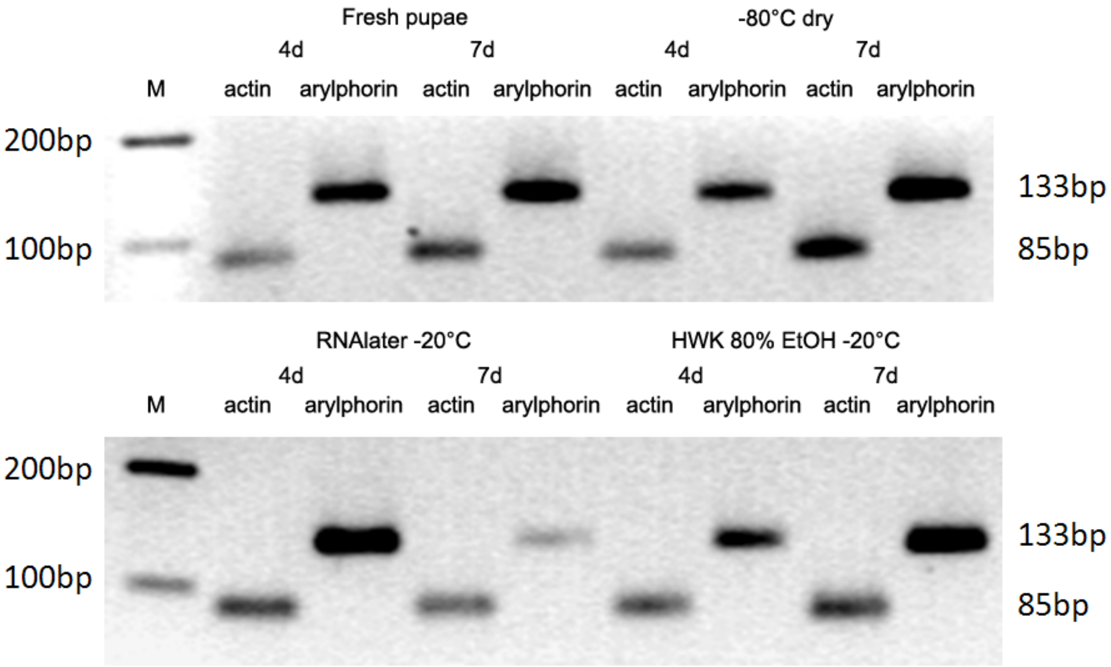

Figure 4.9. PCR amplification of cDNA after short term storage. Amplification of actin (85 bp) and arylphorin receptor gene fragments (133 bp) was carried out on all pupae (one at each age from each preservative). Those shown are from fresh 4d and 7d pupae and after two weeks in the following preservatives; -80°C frozen, RNAlater (-20°C), HWK 80% ethanol (-20°C).

Arylphorin receptor (133 bp) failed to amplify in 6 out of 33 PCRs; The data for 7d pupae in isopropanol (-20°C), RNAlater (4°C) and 70% ethanol (-20°C), and in formaldehyde-based fixatives are summarised in Table 4.1 and discussed below. Amplification failure of the arylphorin fragment indicated these solutions contained highly degraded RNA, resulting in the requirement of amplification of both genes to indicate acceptable RNA preservation for qRT-PCR analysis. The intensity of the bands gave an indication of the RNA quality, as PCR amplifications were continued until the final plateau phase (36 cycles). Variability was noted amongst all pupae in all solutions (Fig. 4.9) indicating inter-individual and inter-preservative variation in RNA integrity and yield.

After long-term storage, PCR products of the expected sizes were obtained from actin (30 out of 33 amplifications) and arylphorin (29 out of 33 amplifications). This included isopropanol (-20°C) and 70% ethanol (-20°C) (Fig. 4.10 and Table 4.1), which failed to yield PCR products after short-term storage. PCR products were also obtained from pupae preserved in Kahles, Bouins and Bouins/Carnoys (Fig. 4.10 and Table 4.1), indicating increased retention of RNA integrity from the 3-hour incubation in comparison to the 3-day. PCR products were not obtained from pupae preserved by HWK and stored dry, and also in 70% ethanol (at 4°C), which were obtained after short term storage.

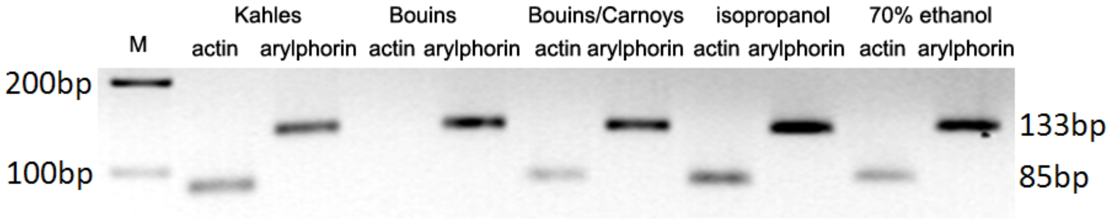

Figure 4.10. PCR amplification of cDNA after long-term storage. PCR amplification of actin (85 bp) and arylphorin receptor gene fragments (133 bp) was conducted from three 4d pupae preserved in formaldehyde-based fixatives for 6 months at 4°C after a 3-hour cross-link reversal. PCR products from two 7d pupae preserved for 6 months isopropanol (-20°C) and 70% ethanol (-20°C) are also shown.

Overall, due to the failure of PCR amplification of actin and/or arylphorin from pupae preserved in RNAlater (4°C), HWK, dry (4°C) and 70% ethanol (4°C) after long term storage, these solutions would not be suggested as suitable for RNA analysis. Also, the formaldehyde-based fixatives are considered unsuitable, due to degradation of RNA caused by the cross-link reversal resulting in inconsistent gene amplification. The optimal preservation method would be dry storage at -80°C, as this retains greatest RNA integrity (Table 4.2).

Table 4.2. Optimal solutions. The optimal solutions for each analysis are given. Pupae requiring a HWK should be pierced three times and placed in >80°C water for >30 seconds. Pupae preserved for nucleic acid analyses should be placed in -80°C storage in a dry state.

Type of analysis	Preservation method	Storage Temperature
External Morphology	HWK, 80% ethanol	-20°C
Histology	HWK, 80% ethanol	4°C
Species Identification	Dry	-80°C
Gene expression	Dry	-80°C

4.3 Discussion

Appropriate preservation of pupae is essential to minimise error in species identification, age and subsequent PMI estimation. Ideally, the preservation method selected should facilitate any later analyses required.

4.3.1 External morphological analysis

Since age estimation by external morphological analysis is based on qualitative features such as compound eye colour and bristle tanning (Sivasubramanian & Biagi 1983), putrefaction and associated colour changes are the most adverse effect of attempted preservation and have the potential to significantly reduce the accuracy of age estimation. Putrefaction was sometimes noted surrounding the piercing incisions in the pupa, and was likely caused by slow penetration of the killing solution (hot water or fixative). This was a major source of discolouration in otherwise well-preserved pupae. Piercing the pupa is essential for full preservative penetration through the pupal cuticle and tissues. It also facilitates heat transfer, as water can directly access the pupa through the chitinous puparium. The piercing of larvae is not necessary for heat transfer as their epidermis is thinner and less heat-resistant than the puparium. It is also not necessary for solution penetration in larvae, as this readily occurs through spiracles and mouthparts (Carvalho *et al.,* 2005), in comparison to the only permeable area in the pupal cuticle, the respiratory horns, which are insufficient.

Preservation of turgor was considered, as examination of soft or brittle pupae results in damage to and loss of features, which reduces the accuracy of the age estimate. Even after long-term (6-8 month) storage, pupae did not appear brittle, even in formalin-based fixatives which has been reported to harden tissue significantly (Cox *et al.,* 2006). 7d pupae have a higher turgor than 4d pupae, which is likely a result of the muscle that has formed by this stage. 4d pupae are comprised mainly of fat. Therefore, choice of solution was more important for 4d pupae as the turgor needs to be raised to facilitate puparium removal for morphological analysis. This was readily achieved using the hot water kill, or any of the preservatives tested except RNAlater. RNAlater is suggested to poorly penetrate brain tissues (Sanna *et al.,* 2005), explaining the maintenance of naturally low pupal turgor, but it is also known to cause brain tissue to become brittle (Noriega *et al.,* 2009), which was not observed in pupae preserved in this solution. It was therefore concluded that dry storage or preservation in RNAlater for morphological analyses was inappropriate, but pupae for this are instead preserved in solution to increase turgor, facilitating puparium removal and feature manipulation.

Length, width and mass were generally unaffected by long-term storage in all of the tested preservatives, although 70% ethanol should be avoided as this causes pupae to shrink. This highlights the need to ensure pupae are hot-water-killed before preservation, and any morphological measurements must be taken as soon as possible and using an internal reference, such as with adult wing vein length (Ireland & Turner 2006; Crossley 1972). Statistically significant changes in mass were observed in five of the preservation methods. This could be due to natural variation in pupal size, however differences in length were not noted in similar solutions. It was therefore likely that mass changes were caused by differential uptake of solution, indicated by four of the five methods being at 4°C storage, which would facilitate perfusion faster than -20°C. Therefore, mass of 'wet' pupae is likely to be a poor age indicator.

The hot-water-kill (HWK) procedure greatly improved the preservation of pupae, in agreement with observations made by Adams & Hall (2003) and Amendt *et al.,* (2007) for larval preservation. Similar conditions must be employed; >80°C, for a minimum of 30 seconds. This is easily achieved by pouring 'just-boiled' water from a kettle on to pierced pupae. The HWK prevents any further enzymatic degradation of the pupa, fixing it and preventing putrefaction. This combined with the dehydration effects of 80% ethanol, and storage at -20°C preserve pupal morphology, for at least 6 months. If access to -20°C storage is not immediately available, samples should be refrigerated at 4°C (as this was also a suitable preservative; see Table 4.2) and transferred to -20°C storage at the earliest opportunity (Table 4.3). In general, pupae should be analysed as soon as possible after preservation, as no preservatives were tested for longer than 8 months thus long-term effects are unknown.

4.3.2 Histological analysis

Analysis of internal morphological features has the potential to improve age and PMI estimates based on the use of additional developmental features not examinable by external morphology, such as tracheal, alimentary system, muscle, salivary gland, and imaginal disc development (Bainbridge & Bownes 1981; Crossley 1972; Berridge *et al.,* 1976; Condic *et al.,* 1991).

Observation of morphology required consistent production of complete slides. Excessively hardened or brittle tissue caused sections to crumble and fall off slides, resulting in absence of tissues. 7d pupae are highly muscular, especially in the thorax (flight muscle), and the newly forming adult epidermis is becoming sclerotised. This causes pupae to be naturally hard, brittle and crumbly when sectioning, which was compounded by preservation in formalin-based fixatives hence their poor performance in this study. Tissue hardness is also caused by insufficient preservative and wax penetration, caused by low surface area created by piercing and natural tissue type. 4d (and the abdomen of 7d) pupae consist mainly of hydrophobic fat, which resisted wax penetration at the embedding stage preventing clean sectioning and reduced the adhesion of sections to glass slides.

The solutions which produced the best results were the HWK 80% ethanol at 4°C, and Kahles at -20°C. 80% ethanol facilitated penetration of wax at the clearing stage better than some formalin-based fixatives and prevented excessive hardening of tissues. The low temperature and formalin content of Kahles (-20°C) preservation minimises hardening in comparison to Bouins, which rarely resulted in good sections.

Even in the best solution, sections from 4d pupae were still variable in quality. In order to improve sectioning consistency, two aspects of the problem were tested; wax penetration and section adhesion. Bisection and 0.5% gelatine was required to produce consistently acceptable slides (Davies & Harvey 2012). After piercing and fixing, pupae were bisected between the thorax and abdomen before clearing, to allow complete ethanol and wax penetration, facilitating stabilisation of tissue. Using this method inevitably causes tissue damage, as the pupa is in two halves, and care must be taken to leave the legs and wings intact, but the quality (integrity) of section (i.e. fewer tissue cracks and voids) was vastly improved. 0.5% gelatin helped keep the pupal sections intact on the slide whilst staining, resulting in a dramatic improvement to the histological method. Both adaptations improved the quality of sections from optimal (HWK, 80% ethanol, 4°C) and suboptimal (Kahles, 4°C) preservatives, thus it is likely that histological analysis can be performed to an acceptable standard on pupae preserved in any solution. HWK 80% ethanol is recommended over Kahles as the optimal solution however, as it is used as a standard at present and is less toxic.

4.3.3 Molecular species identification

DNA extraction and PCR amplification of a cytochrome oxidase I gene fragment was successful in all solutions, as previously noted (Vink *et al.,* 2005; Post *et al.,* 1993). Differences in band intensities were noted (Fig. 4.6); this was most likely due to variation in homogenisation (grinding) consistency, resulting in differential amounts of DNA released. Sequencing was performed on PCR fragments amplified from pupae preserved in 70% ethanol and formalin-based fixatives; the species was correctly identified as *C. vicina* from all products. Formaldehyde-based preservatives have been shown to cause mutations in DNA sequence (Tsai 2006), however nucleotide differences in any sequence did not prevent species identification by phylogenetic analysis. As these solutions were expected to cause the most DNA damage, it can therefore be said any solution tested can be used for preservation of DNA for species identification. As formaldehyde-based solutions did not perform well in other analyses however, it is suggested that these are avoided for the purpose of DNA extraction also. Preservation by HWK 80% ethanol, stored at -20°C is a suitable preservative but the -80°C freeze is recommended as an optimal method.

4.3.4 Analysis of RNA integrity and gene expression

Critical to reliable gene expression analysis is the ability to extract high levels of high integrity RNA. This was achieved from pupae in most preservatives, but pupae stored at -80°C and in RNAlater at -20°C showed least degradation as expected. RNA extraction from pupae preserved in alcohol-based solutions (including HWK, 80% ethanol) at -20°C also showed limited mRNA degradation.

High quality RNA extracts were obtained by rapid and complete homogenisation of pupae using a bead homogeniser, followed by debris removal (such as puparia) prior to binding the RNA on to the spin column. Samples preserved in formaldehyde required reversal of crosslinks and proteinase K digestion to recover RNA, however the extensive incubation (3 days) at 55°C resulted in increased RNA degradation. Shorter incubation (3 hours) reduced this problem but yields were poor, thus although RNA can be extracted and amplified from formalin-fixed samples, this is not a recommended preservative. The use of a short proteinase K digestion with pupae in other preservatives is however beneficial in increasing the RNA yield, as pupae have high protein content (Ring 1973).

Despite consistent amplification of actin (94% (62 of 66)), arylphorin failed to amplify in 15% (10 of 66) samples. Arylphorin failed to amplify in 75% of pupae (3 of 4) preserved in RNAlater at 4°C, indicating this preservation method was not suitable however reproducible amplification was achieved by direct transfer to -20°C in this solution. The noted amplification failures of actin and arylphorin fragments from pupae preserved in the same manner (isopropanol, 70% ethanol, HWK dry, propylene glycol - Table 2) indicated that it was likely that some may have died prior to preservation, which was not observable, as pupae are homogenised intact. These variable data may indicate a poor preservation method, however confirmation would require further trials; in this study these amplification failures were included in ranking of solutions, thus were assessed as unsuitable for gene expression analysis.

Small amplicon size (75-150bp) can result in possible amplification of degraded transcripts, which could mask true gene expression levels. As a result, amplicons should be nearer the 150bp length, and RNA extracts should be of high integrity to ensure true gene expression level is measured. As a result, future qRT-PCR primers for gene expression analysis in pupae for age estimation should be designed to amplify as large a fragment (up to 150bp) as possible, to ensure the sample mRNA is of high integrity and a reliable measurement of expression level is conducted.

In summary, for age estimation using differential gene expression, pupae should be preserved under optimal conditions; either in RNAlater after piercing 3 times through the entire pupa for immediate -20°C storage, or in the absence of preservative at -80°C as soon as possible. Pupae should be shipped alive under controlled conditions prior to preservation if on-site preservation is not feasible. RNA extraction is also possible from HWK, 80% ethanol (-20°C) preserved pupae, provided RNA is extracted as soon as possible to prevent degradation. This is suitable for pupae collected for multiple analyses, or when preservation using the preferred methods is not possible.

4.3.5 A multidisciplinary approach

As methods for age and subsequent PMI estimation develop, it is expected that preservation and care of samples for the processes required will also change. The purpose of this study was to find suitable preservatives for pupal age estimation methods used at present and under development, therefore providing collaborative age estimates for those obtained from rearing of pupae to adult stage. As methods for pupal age estimation are developed, a sample of pupae may need to be preserved in a specific optimal solution for a preferred technique. However, the general preservative proposed is also suitable for all age estimation methods tested here and using multiple methods on a pupal sample gives corroborative age estimates, increasing its reliability.

PMI estimates are generally based on multiple samples, and estimating the age of a batch of pupae using a multidisciplinary approach will provide reliable data for corroboration of PMI estimation using other immature stages. It is potentially possible to perform all methods highlighted in this paper on a single pupa fixed by HWK and preserved in 80% ethanol at -20°C, should limited samples be available. Age analysis should start with molecular species identification using the removed puparium (Mazzanti *et al.,* 2010). External, followed by internal morphological analysis of the pupa can then be carried out. As only a few sections are retained for histological analysis, those cut but not used should be reserved for gene expression analysis; RNA can be extracted using multiple kit methods (Bohmann *et al.,* 2009). Using a multidisciplinary method on each pupa in a batch also has the potential to provide more accurate age and PMI estimates based on a multitude of distinguishing features, something that has not previously been reported in the literature.

4.4 Conclusion

Morphological age estimation and DNA species identification are the most likely methods of choice for PMI estimation using blowfly pupae. The preservation method suggested for these methods should involve piercing the pupa three times, a hot-water-kill >80°C for >30 seconds, followed by preservation in 80% ethanol at -20°C (Table 4.2). This is a simple method to implement and use at a scene, using readily available equipment. This method is suitable for gene expression analysis also, thus it is suggested as the overall crime scene preservative. Should temporal gene expression analysis be specifically required, preservation in RNAlater at -20°C or a -80°C freeze is optimal. Overall, the general preservative: HWK, preservation in 80% ethanol, storage at -20°C, should be used, such that a multidisciplinary approach to pupal age estimation can be employed. Age estimates from preserved pupae can then provide corroborative data for other insect stages, improving the reliability of a PMI estimate.

Chapter 5 – Age Estimation using External Morphology

Large morphological changes are known to occur during metamorphosis. This chapter documents these developmental changes in *C. vicina* with pupal age in ADH, to establish an age estimation methodology for use in PMI estimation.

5.1 Introduction

5.1.1 Dipteran morphology and metamorphosis

As discussed in Chapter 1, extensive literature has been published on the adult morphology of various insects, including dipteran species (Lowne 1895; Peterson 1916; Snodgrass 1930; Wigglesworth 1954). Early accounts of pupation and metamorphosis describe puparium structure and formation, and provide observations of development of major features for a variety of Diptera (Weissman 1874a, b, c; Kirby & Spence 1828).

Dipteran metamorphosis is described as the histolysis of larval tissue and development of adult structures from either larval tissue rearrangement or from imaginal discs (Fig. 5.1) (Weissman 1874a). Imaginal disc growth begins in the embryo (Wigglesworth, 1954), and eversion to their adult forms is initiated during the late larval (Chen 1929; Ranade 1977; Taylor & Adler 2008) or early pupal stage (Lakes & Pollack 1990; Weissman 1874b; Zdarek & Friedman 1986).

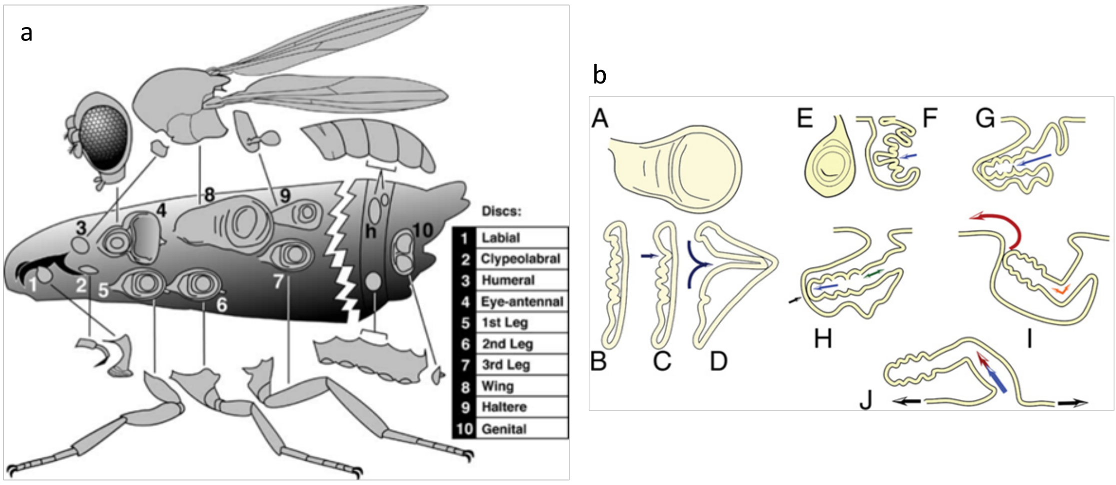

Figure 5.1. Locations and morphology of imaginal discs in the Drosophilidae. a: Imaginal discs are roughly drawn to scale and position. The abdominal wall is constructed from histoblasts, (h) (Held, 2002). b: wing (A-D) and leg (E-J) imaginal disc eversion. A and E show the disc *en face*. B-D and F-J show the cross section of the everting wing and leg discs respectively (Taylor & Adler 2008).

Development of *Musca domestica* has been described in limited detail, including the initial pupariation and pupation processes together with head, appendage and abdomen development (Hewitt 1907; Karandikar & Ranade 1965). Table 5.1 shows a comparison of data from these groups. Eclosion occurred on similar days despite different rearing temperatures and may reflect variation in rearing methods. Absence of temporal data in Karandikar & Ranade (1965) prevents detailed comparison of developmental timing, however sequences are similar. Eclosion occurred after 6 days at 25°C (Callahan 1962), which equates to 3600 ADH which is comparable to that observed by Hewitt (1907) to 4 days at 35°C (3360 ADH). However, due to lack of morphological detail provided neither account can be used to estimate pupal age.

Table 5.1. External morphological development of *Musca domestica*. The external morphology highlighted by both authors are compared, along with ages of occurrence when given. N/A = no correlating age given.

Hewitt (1907)		**Karandikar & Ranade (1965)**	
Age	Development (35°C)	Age	Development (28°C)
<12 hours	Tracheal system shed, adheres to puparium	<6 hours	Larva-pupa intermediate
			12 segmented
	Puparium colouration complete		No head or appendages
	Cephalophayngeal skeleton adheres to puparium	N/A	Cryptocephalic pupa
30 hours	Head everted	N/A	Phanerocephalic pupa
	Mouthparts split into labellum and labrum		Eyes and antennae are swollen areas
	Wings sac-like		Longer legs and wings
	Femoral and tibial segments in one membraneous sheath		Abdomen 8 segmented
3-4 days	Eclosion	4 days	Eclosion

Morphological development of the flesh fly *Sarcophaga bullata* is described Hewitt (1907) and is correlated to age in days and stages (Table 5.2). The developmental sequence is similar to that of *M. domestica* despite the 3 times longer pupal stage of *S. bullata*. The timeline therefore has utility for staging purposes, but has low temporal resolution (days), and it would be of limited use for age estimation.

Detailed studies of *Drosophila melanogaster* development describe external and internal (histological) morphology from fixed pupae (Robertson 1936) and changes seen *in vivo* through the puparium (Bainbridge & Bownes 1981). In addition to the descriptions of morphology, drawings and images present in these studies enable accurate age estimation and staging of *D. melanogaster* pupae (Fig. 5.2). Table 5.3 shows comparison of morphological features from these authors. Despite the use of

Table 5.2 External morphological development of *Sarcophaga bullata*. The metamorphosis timeline of *S. bullata*. Development occurred at 25°C

Stage	Age/days	Development
P1	0	Untanned pupa
P2	0.4	Fully tanned pupa
P3	1.5	Uneverted head; partly everted legs and wings
P4	2	Head and thoracic appendages fully everted
P5	6	Thorax, abdomen and legs segmented
P6	8	Eye yellow colouration develops
P7	9	Eyes red, macrochaetae begin to tan
P8	10	Chaetae tanned
P9	11	Genitalia tanned, development complete

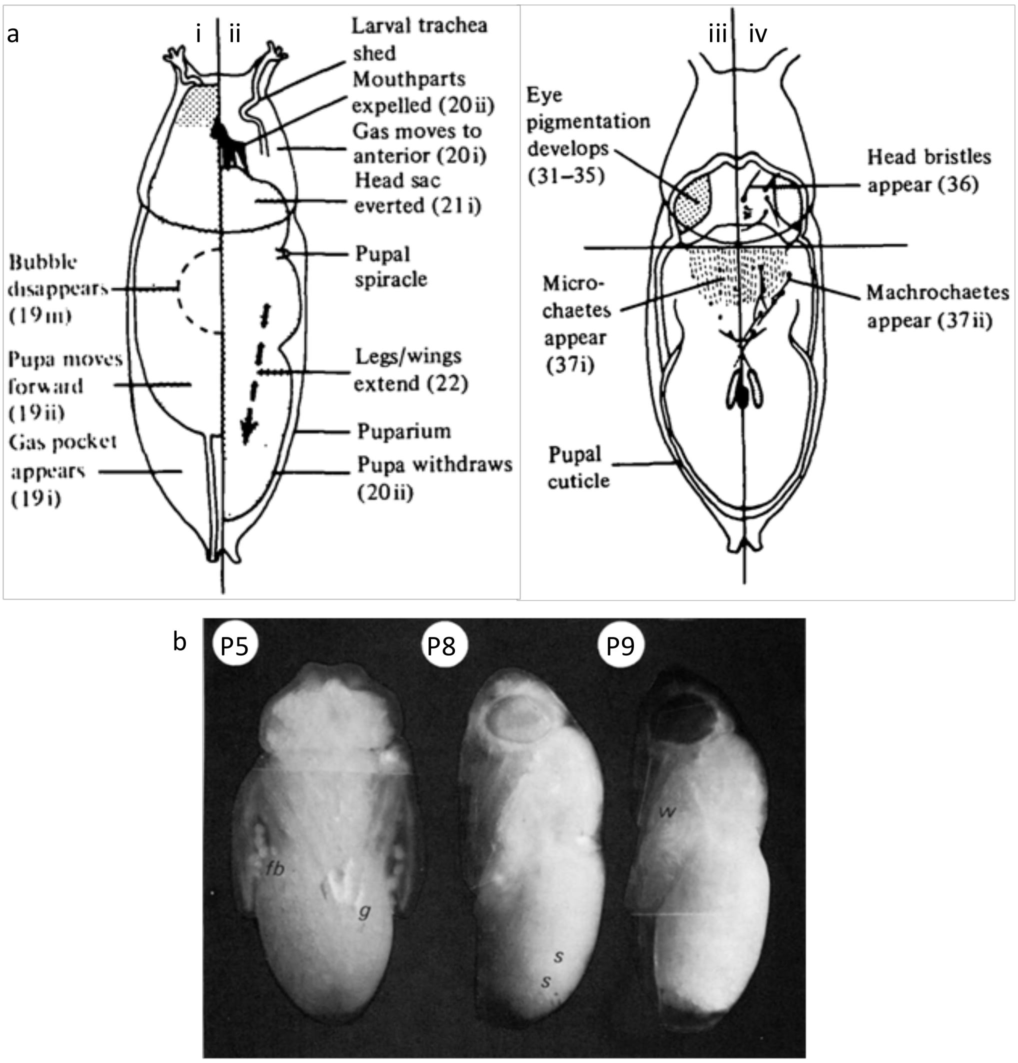

Figure 5.2. Morphological development stages of *Drosophila*. a: drawings produced by Bainbridge & Bownes (1983) of the morphological changes that occur during stages P4 (i), P5 (ii), P8 (iii) and P11 (iv), as described in Table 5.3. Numbers (e.g. Legs/wings extend (22) in aii) refer to original paper. b: photographs of stages as labelled. Fat body cells (fb), gas pockets (g), abdominal segment margins (s) and wings (w) are labelled.

Table 5.3. A comparison between the morphological developments noted by authors on *Drosophila melanogaster.* The table outlines external morphological developments and their associated mean timings through the pupal stage, used for estimating the age of or staging *D. melanogaster*. *Internal development* indicates times at which when internal morphology is developing and no external morphological change was noted.

Robertson (1936)		**Bainbridge & Bownes (1981)**		
Age/ hours	**Development**	**Stage**	**Age/ hours**	**Development**
0	Puparium formation	L2	0	Body contracts
1	_*Internal development*_	P1	1.7	Larva ceases movement, puparium tans
2				
3				
4		P2	4.8	*Internal development*
5	Tarsi are in 'pockets'	P3	5.8	Ridge of operculum becomes distinct, pupa becomes buoyant
6	Legs and wings exposed			
7	Halteres remain covered	P4i	8	Wings and legs become visible
8		P4ii	8.2	Head is everted
9		P5i	9.3	Legs and wings achieve full extension, eye development begins
10	Legs elongate			
11	Head eversion			
11.5				
12	Haltere exposed, rapid elongation of legs,	P5ii	18.7	_*Internal development*_
13-27	_*Internal development*_			
30	Bristles and hairs appear	P6	32.4	
36	Wings now thin and well formed			
42	_*Internal development*_	P7	44.3	Eyes become yellow at perimeter
48	Wing structure is completed			
54	_*Internal development*_	P8	56.6	Eyes become amber
60				
72	Bristles and hairs darken	P9	70.6	Eyes become pink
		P10	74.6	Eyes become red and associated bristles darken
		P11i	75.9	Thoracic chaetae visible
		P11ii	76.6	Tips of wings become grey
		P12i	77.5	Bristles on abdominal tergites become visible, wings become grey
		P12ii	78.6	Sex comb darkens, wings blacken
84	_*Internal development*_	P13	81.9	Tarsal bristles and claws darken
		P14	91.5	_*Internal development*_
96	Emergence	P15i	99.6	Tergites become tanned, ptilinum expands
		P15ii	100	Eclosion complete

the same temperature (25°C), significant differences in timings were observed e.g. head eversion was observed at 8 hours for Bainbridge and Bownes but 11 hours for Robertson. Similar differences are seen in the latter stages; bristle colouration is recorded at 72 hours and 82 hours (Table 5.3: shaded cells). Such differences may result from differing rearing conditions due to the time elapsed between the studies (45 years) and inter-specific differences due to location (Edinburgh and New York respectively). Though this is not a forensically important species, it shows that accurate age estimation is possible with a complete dataset.

5.1.2 Metamorphosis in the Calliphoridae

Published work on *C. vicina* metamorphosis is limited to two studies in English (Lowne 1895; Finell & Jarvilehto 1983) and one in French (Perez 1910). Limited information can be obtained from Perez (1910); few drawings and descriptions are presented.

Lowne (1895) describes the histology of larvae, prepupae, imago and adult together with limited description of external morphology summarised in Table 5.4. Major events such as head eversion, mouthpart development and eye colouration are correlated to an age in days, however since growth temperature is not stated, this is of limited value for age estimation purposes. Day of emergence was not provided and was predicted from timings of other developments (see Table 5.4).

Finell & Jarvilehto (1983) document compound eye, antennae and bristle development at 20°C and correlate these to age as a percentage of the pupal stage duration to divide metamorphosis into eight stages. Table 5.4 shows the approximate ages in days calculated using mean lifecycle data given to allow for comparison with Lowne (1895). Facets (Table 5.4) refer to the individual ommatidia shape which progress from round to hexagonal during metamorphosis, which is useful for age estimation. It was noted that yellow eye colouration was present at ~5 days, which does not progress to light brown until almost day 10. This contrasts with Lowne (1895) who indicated colouration did not start at all until day 9 (Table 5.4). Correlation of morphology to percentage of the pupal stage of lifecycle length allows age estimation at different developmental temperatures using time to pupation and/or eclosion, which can be obtained from various developmental studies (Anderson 2000; Greenberg 1991; Kamal 1958). This could be most useful when development is not linearly correlated with temperature, such as near LDT and UDTs (upper developmental thresholds), or when fluctuations are great (Kaufmann (1932) in Nabity *et al.,* (2006)). Therefore, although *C. vicina* morphological data are available, disparities between

Table 5.4 External morphological development of *Calliphora vicina*. The external morphological development of *C. vicina* as described by Lowne (1895) and Finell & Jarvilehto (1983). Developments have been temporally aligned where possible.

Lowne (1892)		Finell & Jarvilehto (1983)			
Age/ Days	Development	Stage	Age		Development
			%	days	
1	-	III	0	0	Only anterior spiracles seen at front of pupa
2-3	Short legs and wings visible at the anterior end	IV	15	2.0	Eyes white, facets round, white antennae and bristles
		-	-	-	-
4	Head eversion	-	-	-	-
	Cephalopharyngeal skeleton released				
	Mouthparts visible but undeveloped				
5	Pupa is fully formed	V	35	5.0	Eyes yellow, round facets
	No setae				
7	Oral lobe development complete	-	-	-	-
	All setae visible				
8	Joints formed	-	-	-	-
9	Eye colouration begins	VI	70	9.5	Eyes light brown, facets bounded, antenna/bristles tanned
10	Internal developments until emergence (including sclerotisation)				
11+	Emergence?	VII	95	12.0	Eyes red/brown, hexagonal facets, black antennae and bristles, cuticle soft
		VIII	100	13.5	Eyes red/brown, facets hexagonal, black antennae and bristles, cuticle hard

studies and low temporal resolution of observations prevent its use for age and PMI estimation.

Pupal development in *Musca (Calliphora) vomitoria* has been reported and similar external and internal morphology observations to those reported for *C. vicina* by Lowne (1895) were made (Weissman 1874a, b & c). Metamorphosis lasts 18-20 days, but temperature data are not present and widely spaced observations are made, and the data are unsuitable for accurate age estimation.

Phormia regina external pupal morphology has been described and imaged in a more recent study, with timelines of development at 22°C (Table 5.5) and 29°C produced

(Greenberg 1991; Greenberg & Kunich 2002). A standard colour chart was used to describe compound eye colour development from 81 hours onwards. This reduces the subjectivity and improves reliability of age estimation based on this feature. These data are the most comprehensive produced to date. However, the low temporal resolution permits only an approximate age estimate to be obtained, with a large window of error.

Table 5.5. External morphological development of *Phormia regina*. Developments observed by Greenberg (1991) over the pupal stage, at 22°C.

Age (hours)	Development
0	Prepupa
9-17	Puparium colouration complete
	Cryptocephalic pupa stage
	Head invaginated
	Body segmented
	Respiratory horns at anterior end
	Short legs and wings visible
23.5	Phanerocephalic pupa stage
	Head everted
	Respiratory horns puncture membrane
42	Membrane encloses appendages
52	Membrane encloses entire pupa
60	Abdomen segmented
81-88	Eye colouration begins
120	Setae tanned on head and thorax
134	Setae tanned on abdomen
149	Eclosion

In summary, though timelines of external pupal morphology for *C. vicina* and other forensically important species have been published, they have limited utility for age estimation purposes. In order to maximise the value of pupae recovered from crime scenes in PMI estimation, a detailed study of development under controlled conditions must be recorded with high temporal resolution, allowing accurate age estimates to be obtained.

5.1.2 Imaging techniques

Much of the previous research into morphological development during metamorphosis was carried out decades ago, using light microscopy. Whilst this is a cost-effective technique, other more powerful methods such as scanning electron microscopy (SEM) have also been used to analyse pupal development (Finell & Jarvilehto 1983; Beno *et al.,* 2007). There are distinct advantages to both methods, which are discussed below.

Stereo light microscopy is readily available in most laboratories, and requires minimal expertise. Pupae do not usually require any preparation post-preservation, and external morphology can be observed under ethanol and recorded by digital photography (Fig. 5.3). This technique is often used for species identification and length measurement of larvae (Sanford *et al.,* 2011; Sukontason *et al.,* 2005). The

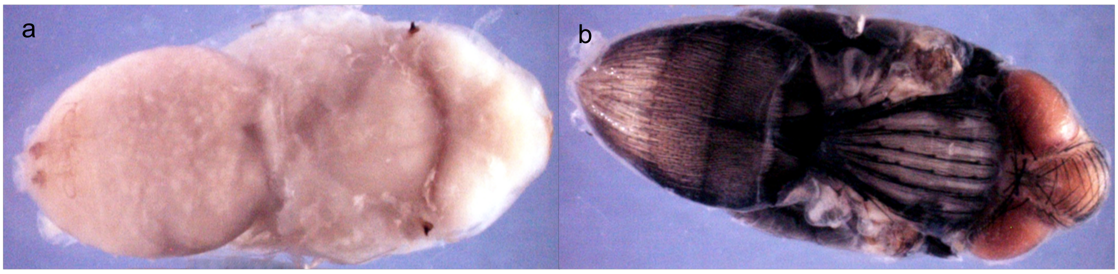

Figure 5.3. *C. vicina* pupae viewed under light microscopy. These images of a recently head-everted pupa (a) and a completely developed imago (b) were taken using a Nikon DN100 camera attached to a Leica WILD M3Z stereomicroscope.

main limitations of stereo microscopy are the low power of magnification and resolution, limiting observation of smaller features.

SEM utilises the shorter wavelength of a focussed electron beam to produce high resolution, greatly magnified, three-dimensional images (Bozzola & Russell 1999). Specimens for SEM must be chemically fixed and dried; specific methods have been developed for soft-bodied insects in order to prevent tissue damage (Beno *et al.,* 2007; Grodowitz *et al.,* 1982), but the most recent techniques are yet to be trialled on blowfly pupae. SEM is particularly useful for identification of eggs, 1st and 2nd instar larvae and puparia, as the species-specific features are easier to observe under high magnification (Siriwattanarungsee *et al.,* 2005; Sukontason *et al.,* 2006; Sukontason *et al.,* 2007). The compound eyes of *C. vicina* have been observed using SEM (Fig. 5.4) (Finell & Jarvilehto 1983) and more recent studies show higher resolution images are now achievable for soft and comparatively small *Drosophila* pupae (Fig. 5.5) (Beno 2007). SEM is however more expensive and labour-intensive than standard microscopy and sample preparation procedures may prevent further analyses such as DNA species identification. Forensic investigation requires the use of rapid techniques at minimal cost, thus stereomicroscopy remains the most commonly used method at present. Should SEM become more cost-effective and required for observation of smaller developmental changes then this method may also be adopted.

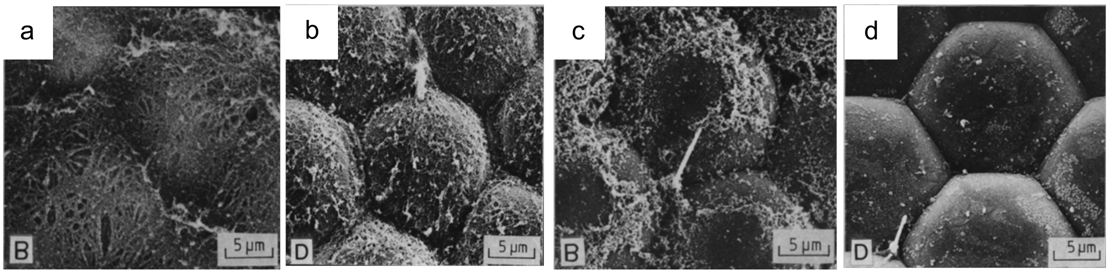

Figure 5.4. Development of *C. vicina* compound eyes. Finell and Jarvilehto (1983) produced SEM images of the developing pupal compound eyes, as follows: Juvenile pupa with white, round facets (a), Histogenetic pupa (stage of tissue formation from undifferentiated cells) with yellow eyes and inter-facetal hair development (b), Premature pupa with light brown, bordered facets (c), Mature pupa with red-brown, hexagonal facets (d).

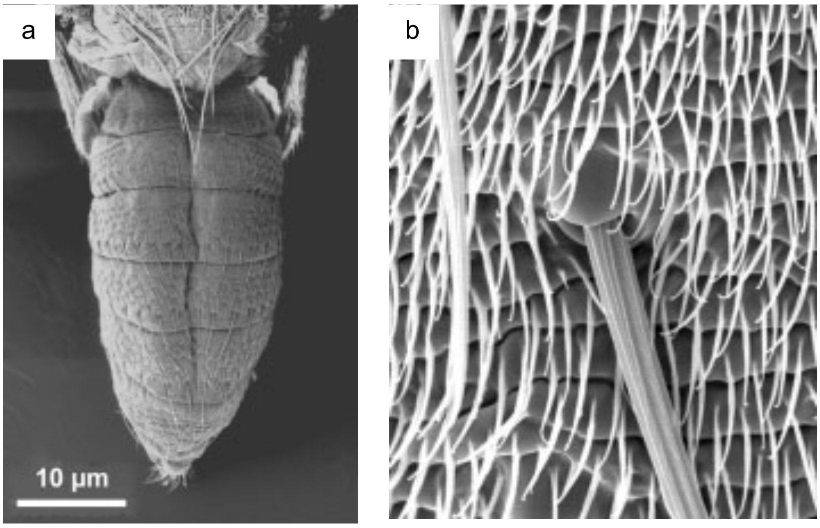

Figure 5.5. *Drosophila* pupae viewed under SEM. These images of a *Drosophila* pupal abdomen (a) and abdominal setae (b) were obtained by Beno *et al.* (2007), using a new fixing technique and a high-resolution scanning electron microscope.

5.1.3 Conclusions and aims

After considering previous research, there are insufficient data at present to fully exploit the potential of the *C. vicina* pupal stage for PMI estimation. Data are available on development of individual features of various species, and the complete timeline of *Drosophila melanogaster* development demonstrates that accurate age estimation is possible. To date no complete developmental analysis of the *C.vicina* pupal stage has been carried out.

The aim was to produce an accurate timeline documenting the development of external morphological features of *C. vicina,* correlated to age in ADH as well as a percentage through the lifecycle and pupal stages. This will require:

- Rearing pupae under controlled conditions and collection at set times, to allow precise age calculation in ADH.
- External morphological analysis using stereomicroscopy (and SEM if required).
- Correlation of morphological development of multiple features to specified age ranges.
- Development of age estimation methods/algorithms, derived from combination of age ranges and regression analyses.
- Blind testing of methods to ensure validity.

It is anticipated that the age of *C.vicina* pupae will be able to be estimated to within ~500 ADH (24 hours at an average of 22°C), given the limits of natural variation (see Chapter 3.2.3).

5.2 Results

Examination of the external morphological development of 1494 pupae was conducted and features correlated to age in ADH, with the aim of producing a timeline for pupal age estimation of crime-scene samples.

5.2.1 Pupal age calculation

To ensure accuracy, the ages of the two sets of test pupae analysed (T1 & T2) were calculated using developmental temperatures recorded every 15 minutes. The overall mean developmental temperature for all cohorts in T1 was 23.2°C and T2 was 21.8°C, resulting in similar lifecycle durations. The ADH ages of pupae collected varied from 3911 ADH (first larvae to pupate) to 11358 ADH (final pupae to remain un-emerged). Over all sample cohorts (T1 & T2), larvae started pupation at a mean age of 4036 ADH, and emerged at 10289 ADH (Table 5.6). The mean pupal stage length, measured from the first pupa collected to the emergence of the first adult, was 6223 ADH (11.8 days at 22°C).

5.2.2 External morphological analysis

The development of 23 features was documented; changes observed in each feature were divided into categories for assessment of developmental stage. In each trial, the earliest and latest ages for each feature category were noted. These ADH ages were used to calculate lifecycle % data using the youngest and eldest pupae collected; 3911 & 11358 ADH for T1 and 3982 & 11314 ADH for T2 (Table 5.6, yellow and green highlighting; Table 5.7a & b). The minimum and maximum values from both trials for both ADH age and lifecycle % were selected (Table 5.9ci & ii, blue, red, tan and purple shading), and converted to the lifecycle % or ADH ages respectively, using the maximum 11358 ADH from T1. The overall maximum and minimum data were then identified as the combined range for each feature category (Table 5.8ciii), outside which the specific development was not observed.

The complete ADH and lifecycle % ranges for all feature categories are shown in Table 5.8. Development is also expressed as a percentage age through the pupal stage (% TPS) calculated using the same ADH values. This measure allows for possible natural variation in lifecycle length, non-linear development and permits inter-species comparison.

Table 5.6 Pupal ages for Trial 1 and 2. Ages of 1494 pupae (Trial 1 = 493, Trial 2 = 1001) are shown in hours after puparium formation (APF) at 22°C, which was constant between both trials. The individual ADH of each sample in each trial is also given, calculated from continuously monitored larval mass temperatures. Yellow highlighting indicate when emergence of the first flies occurred in each trial and cohort. Emergence of pupae is highlighted in red; the eldest pupae to be collected in each trial are highlighted in green. '-' indicates no pupae remained for sampling (i.e. they were all collected).

Sample #	Age (h APF)	Trial 1	Trial 2			
			1	2	3	4
		Age (ADH)				
1	0	3911	4138	-	-	-
2	6	4047	4275	3993	3982	-
3	12	4186	4414	-	4108	4154
4	18	4325	4555	4267	4237	4285
5	24	4463	4694	4406	4379	4422
6	30	4600	4835	4544	4521	4560
7	36	4739	4975	4682	4663	4698
8	42	4876	5117	4820	4804	4837
9	48	5013	5259	4959	4945	4977
10	54	5148	5400	5099	5085	5115
11	60	5285	5539	5238	5225	5254
12	66	5423	5679	5378	5364	5392
13	72	5558	5822	5520	5504	5532
14	78	5693	5962	5661	5644	5673
15	84	5831	6102	5801	5784	5812
16	90	5969	6243	5942	5923	5951
17	96	6106	6384	6082	6063	6090
18	102	6244	6526	6224	6206	6231
19	108	6383	6669	6367	6349	6372
20	114	6521	6812	6510	6493	6514
21	120	6659	6953	6651	6635	6656
22	126	6795	7092	6791	6777	6797
23	132	6933	7233	6932	6918	6938
24	138	7072	7374	7073	7059	7078
25	144	7209	7515	7213	7199	7218
26	150	7347	7656	7354	7341	7358
27	156	7485	7797	7496	7482	7498
28	162	7623	7940	7638	7624	7639
29	168	7761	8081	7776	7765	7780
30	174	7899	8222	7916	7906	7922
31	180	8037	8364	8058	8049	8063
32	186	8175	8506	8201	8192	8205
33	192	8313	8648	8342	8334	8346
34	198	8451	8788	8481	8474	8486
35	204	8589	8930	8624	8615	8627
36	210	8727	9073	8767	8758	8769
37	216	8865	9215	8909	8900	8910
38	222	9003	9355	9049	9042	9050
39	228	9141	9496	9190	9185	9191
40	234	9279	9637	9332	9329	9332
41	240	9419	9778	9471	9471	9472
42	246	9559	9920	9613	9611	9613
43	252	9697	-	9755	9749	9755
44	258	9836	-	-	9884	9897
45	264	9976	-	-	10021	10037
46	270	10115	-	-	10162	10178
47	276	10254	-	-	10303	10320
48	282	10392	-	-	10441	10463
49	288	10530	-	-	10578	10605
50	294	10668	-	-	10719	10747
51	300	10806	-	-	10861	10888
52	306	10944	-	-	10999	11029
53	312	11082	-	-	11135	11171
54	318	11220	-	-	11274	11314
55	324	11358	-	-	-	-

ADH age ranges for each feature category are shown graphically in Fig. 5.6, enabling identification of age markers for early and late pupal stages, which could be useful for approximate age estimation of damaged samples. Early developing features (up to ~6500 ADH) included eversion of the cephalopharyngeal skeleton, leg width, abdominal segments and antennae shape. Features that developed during the latter part of the stage (from ~8500 ADH) were thoracic bristles, wing colour and abdominal macro- and microchetae.

Table 5.7. Calculation of maximum age ranges for observation of each category and feature. The ADH ages and lifecycle % limits for each feature category are shown for trials 1 and 2 (a & b respectively). The maximum and minimum ADH values (ci) over both trials (red and blue shading) were converted to lifecycle % values. The maximum and minimum lifecycle % values (cii) over both trials (purple and tan shading) were converted to ADH values. The combined overall maximum and minimum ADH and lifecycle % values over both trials are then selected for the maximum age range (cii). The orange shaded figure was the minimum age lifecycle %, converted from trial 1 ADH data. Green and aqua shading highlights the origins of the combined, final data set (ciii); minimum % lifecycle values calculated from original T1 ADH data (ci - green), and maximum ADH values calculated from original T2 % lifecycle data (cii - aqua).

a

Feature	Categories	Trial 1			
		Min Age (ADH)	Max Age (ADH)	Min Age (% lifecycle)	Max Age (% lifecycle)
Antennae shape	Full length	5693	11358	50.1	100.0
	Elongated	5243	5831	46.2	51.3
	Round and central	5243	5831	46.2	51.3
	Round and wide	5148	5831	45.3	51.3
	Round and lateral	4876	5831	42.9	51.3
	Absent	3911	5558	34.4	48.9

b

Feature	Categories	Trial 2			
		Min Age (ADH)	Max Age (ADH)	Min Age (% lifecycle)	Max Age (% lifecycle)
Antennae shape	Full length	5661	11314	50.0	100.0
	Elongated	5520	6349	48.8	56.1
	Round and central	5364	6349	47.4	56.1
	Round and wide	5364	6349	47.4	56.1
	Round and lateral	5400	5812	47.7	51.4
	Absent	3982	5801	35.2	51.3

ci cii ciii

Lifecycle (original min/max ADH)				Lifecycle (original min/max %)				Combined ADH		Combined %	
Age limits (ADH)		Convert to %		Age limits (%)		Convert to ADH					
Min	Max	Min	Max	Min	Max	Min	Max	Min	Max	Min	Max
5661	11358	49.8	100.0	50.0	100.0	5683	11358	5661	11358	49.8	100.0
5243	6349	46.2	55.9	46.2	56.1	5243	6374	5243	6374	46.2	56.1
5243	6349	46.2	55.9	46.2	56.1	5243	6374	5243	6374	46.2	56.1
5148	6349	45.3	55.9	45.3	56.1	5148	6374	5148	6374	45.3	56.1
4876	5831	42.9	51.3	42.9	51.4	4876	5835	4876	5835	42.9	51.4
3911	5801	34.4	51.1	34.4	51.3	3911	5824	3911	5824	34.4	51.3

Table 5.8. External morphological characteristics assessed for age estimation, with age ranges. The development of each of the features assessed was sub-divided into categories. The youngest and oldest age (in ADH) at which that the category was observed is recorded. Percentages of the lifecycle and pupal stage (TPS) are also shown.

Feature	Categories	ADH age		Lifecycle %		% TPS	
		Min	Max	Min	Max	Min	Max
Compound eye colour	Brown	9042	11358	79.6	100.0	68.9	100.0
	Red	8192	10076	72.1	88.7	57.5	82.8
	Pink	7765	9419	68.4	82.9	51.8	74.0
	Pale pink	7515	9003	66.2	79.3	48.4	68.4
	Cream	5013	8589	44.1	75.6	14.8	62.8
	Absent	3911	5824	34.4	51.3	0.0	25.7
Orbital/facial bristles	Black	8865	11358	78.1	100.0	66.5	100.0
	Brown	8589	9793	75.6	86.2	62.8	79.0
	White	6659	9509	58.6	83.7	36.9	75.2
	Absent	3911	7899	34.4	69.5	0.0	53.6
Jowl bristles	Black	8865	11358	78.1	100.0	66.5	100.0
	Brown	8589	11080	75.6	97.6	62.8	96.3
	White	6791	9509	59.8	83.7	38.7	75.2
	Absent	3911	8451	34.4	74.4	0.0	61.0
Antennae shape	Full length	5661	11358	49.8	100.0	23.5	100.0
	Elongated	5243	6374	46.2	56.1	17.9	33.1
	Round and central	5243	6374	46.2	56.1	17.9	33.1
	Round and wide	5148	6374	45.3	56.1	16.6	33.1
	Round and lateral	4876	5835	42.9	51.4	13.0	25.8
	Absent	3911	5824	34.4	51.3	0.0	25.7
Antennae colour	Black	9141	11358	80.5	100.0	70.2	100.0
	Brown	9003	10646	79.3	93.7	68.4	90.4
	1/2 brown	5693	10218	50.1	90.0	23.9	84.7
	White	5013	10076	44.1	88.7	14.8	82.8
	Absent	3911	5824	34.4	51.3	0.0	25.7
Arista colour	Black	9329	11358	82.1	100.0	72.8	100.0
	Brown	9003	10218	79.3	90.0	68.4	84.7
	White	7347	9922	64.7	87.4	46.1	80.7
	Bald	5013	9077	44.1	79.9	14.8	69.4
	Absent	3911	5824	34.4	51.3	0.0	25.7
Labellum shape	Complete	9419	11358	82.9	100.0	74.0	100.0
	Oral hair dev	6383	11072	56.2	97.5	33.2	96.2
	Double end lobed	6082	7827	53.5	68.9	29.2	52.6
	End lobed	5693	6795	50.1	59.8	23.9	38.7
	Double lobed	5243	6551	46.2	57.7	17.9	35.5
	Slightly lobed	5148	6397	45.3	56.3	16.6	33.4
	Square	4876	5985	42.9	52.7	13.0	27.9
	Absent	3911	5824	34.4	51.3	0.0	25.7
Labellum colour	Brown	9884	11358	87	100.0	80.2	100.0
	White	4876	11358	42.9	100.0	13.0	100.0
	Absent	3911	5824	34.4	51.3	0.0	25.7
Oral Lobe Hairs	Brown	8865	11358	78.1	100.0	66.5	100.0
	Absent	3911	9935	34.4	87.5	0.0	80.9
Palp shape	Full length	5962	11358	52.5	100.0	27.5	100.0
	Long or clubbed	5520	7403	48.6	65.2	21.6	46.9
	Slightly elongated	5243	6551	46.2	57.7	17.9	35.5
	Round	5243	6397	46.2	56.3	17.9	33.4
	Absent	3911	5985	34.4	52.7	0.0	27.9
Palp colour	Pale brown	9003	11358	79.3	100.0	68.4	100.0
	Brown/Black hairs	8758	9976	77.1	87.8	65.1	81.4
	Dev/White	5013	9793	44.1	86.2	14.8	79.0
	Absent	3911	5824	34.4	51.3	0.0	25.7

Table 5.8. Continued.

Feature	Categories	ADH age		Lifecycle %		% TPS	
		Min	Max	Min	Max	Min	Max
Labrum shape	Split	5822	11358	51.3	100.0	25.7	100.0
	Full length	5784	7623	50.9	67.1	25.2	49.8
	Pointed	5243	6795	46.2	59.8	17.9	38.7
	Elongated	5285	6397	46.5	56.3	18.5	33.4
	Arrow	4876	6448	42.9	56.8	13.0	34.1
	Absent	3911	5824	34.4	51.3	0.0	25.7
Labrum colour	Brown	9329	11358	82.1	100.0	72.8	100.0
	Pale Brown	8769	11220	77.2	98.8	65.2	98.1
	White	4876	9976	42.9	87.8	13.0	81.4
	Absent	3911	5824	34.4	51.3	0.0	25.7
Cephalopharyngeal skeleton	Everted	4876	11358	42.9	100.0	13.0	100.0
	Membrane-enclosed	4663	5561	41.1	49.0	10.1	22.2
	Loosened	4463	5279	39.3	46.5	7.4	18.4
	Attached	3911	4996	34.4	44.0	0.0	14.6
Thoracic Bristles	Black	8865	11358	78.1	100.0	66.5	100.0
	Brown	8758	10066	77.1	88.6	65.1	82.7
	1/2 brown	8589	9650	75.6	85.0	62.8	77.1
	White	6521	9509	57.4	83.7	35.0	75.2
	Developing	6106	7672	53.8	67.5	29.5	50.5
	Absent	3911	7668	34.4	67.5	0.0	50.4
Wing Folding	All folded	6918	11358	60.9	100.0	40.4	100.0
	Partially folded	6231	8451	54.9	74.4	31.2	61.0
	All unfolded	5558	7668	48.9	67.5	22.1	50.4
	Fat veins	5148	6397	45.3	56.3	16.6	33.4
	Tissue mass	4275	6267	37.6	55.2	4.9	31.6
	Absent	3911	4996	34.4	44.0	0.0	14.6
Wing Colour	Dark silver	9329	11358	82.1	100.0	72.8	100.0
	Silver	9141	11358	80.5	100.0	70.2	100.0
	Pale silver	8865	10076	78.1	88.7	66.5	82.8
	White	4275	9935	37.6	87.5	4.9	80.9
	Absent	3911	5285	34.4	46.5	0.0	18.5
Leg length	Full	4876	11358	42.9	100.0	13.0	100.0
	Short	4663	5831	41.1	51.3	10.1	25.8
	Very Short	4275	5693	37.6	50.1	4.9	23.9
	Absent	3911	4996	34.4	44.0	0.0	14.6
Leg width	Fine	5243	11358	46.2	100.0	17.9	100.0
	Inflated	4876	5831	42.9	51.3	13.0	25.8
	Absent or short	3911	5561	34.4	49.0	0.0	22.2
Leg Bristle Colour	Thick black	9329	11358	82.1	100.0	72.8	100.0
	Fine black	8589	10218	75.6	90.0	62.8	84.7
	White	6383	9509	56.2	83.7	33.2	75.2
	Absent	3911	7485	34.4	65.9	0.0	48.0
Abdominal segments	Adult	5085	11358	44.8	100.0	15.8	100.0
	Pupal	3982	5824	35.1	51.3	1.0	25.7
	Larval	3911	5558	34.4	48.9	0.0	22.1
Abdomen Macrochatae	Black	9141	11358	80.5	100.0	70.2	100.0
	Brown	8865	10218	78.1	90.0	66.5	84.7
	White	6659	9935	58.6	87.5	36.9	80.9
	Absent	3911	7668	34.4	67.5	0.0	50.4
Abdomen Microchatae	Black	8865	11358	78.1	100.0	66.5	100.0
	Brown	8865	9935	78.1	87.5	66.5	80.9
	Developing brown	8758	9935	77.1	87.5	65.1	80.9
	White	6795	9650	59.8	85.0	38.7	77.1
	Absent	3911	7668	34.4	67.5	0.0	50.4

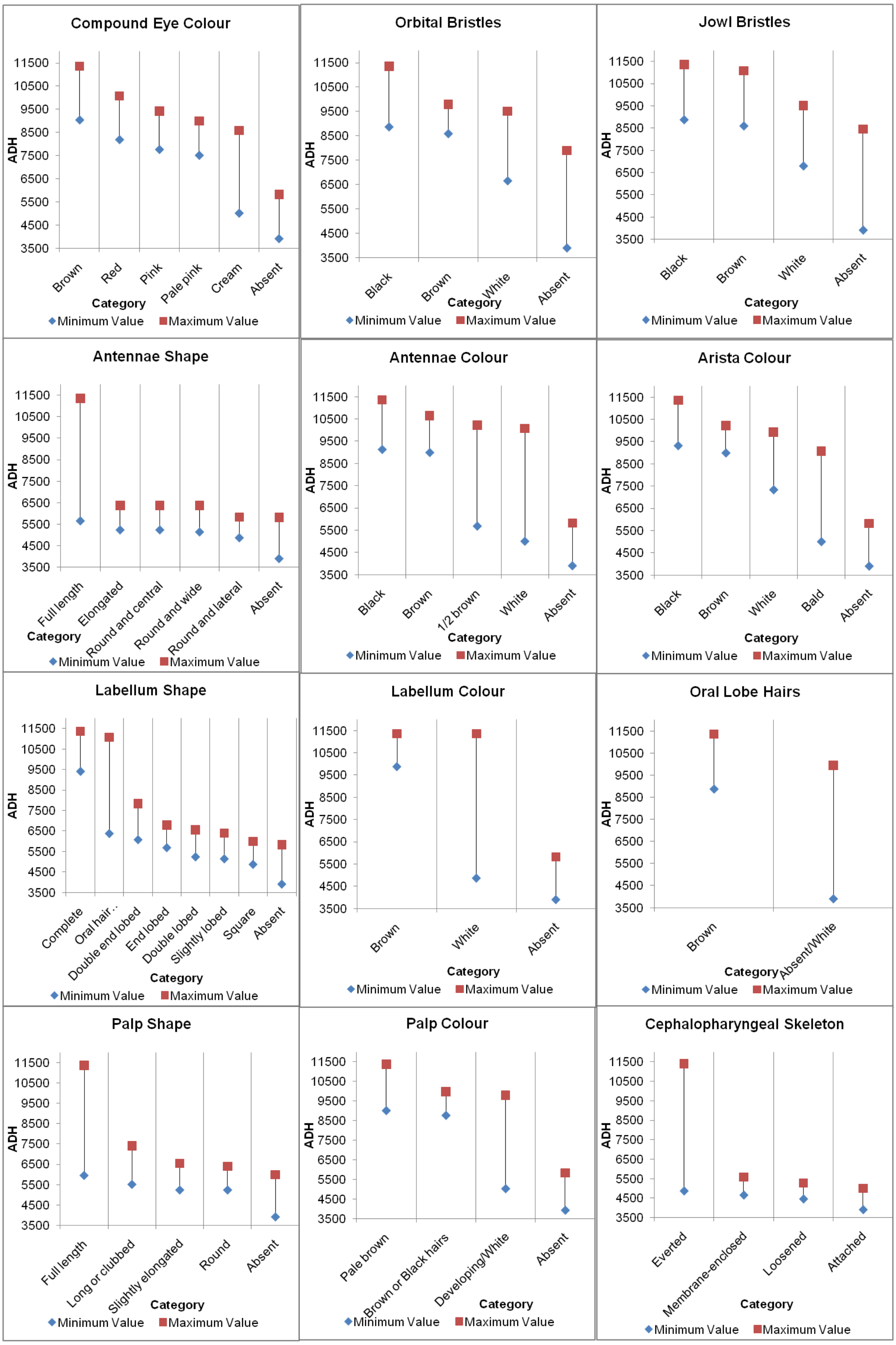

Figure 5.6. Age ranges in ADH of each category of each feature. The charts depict the minimum and maximum ADH ages at which that category of each feature occurs.

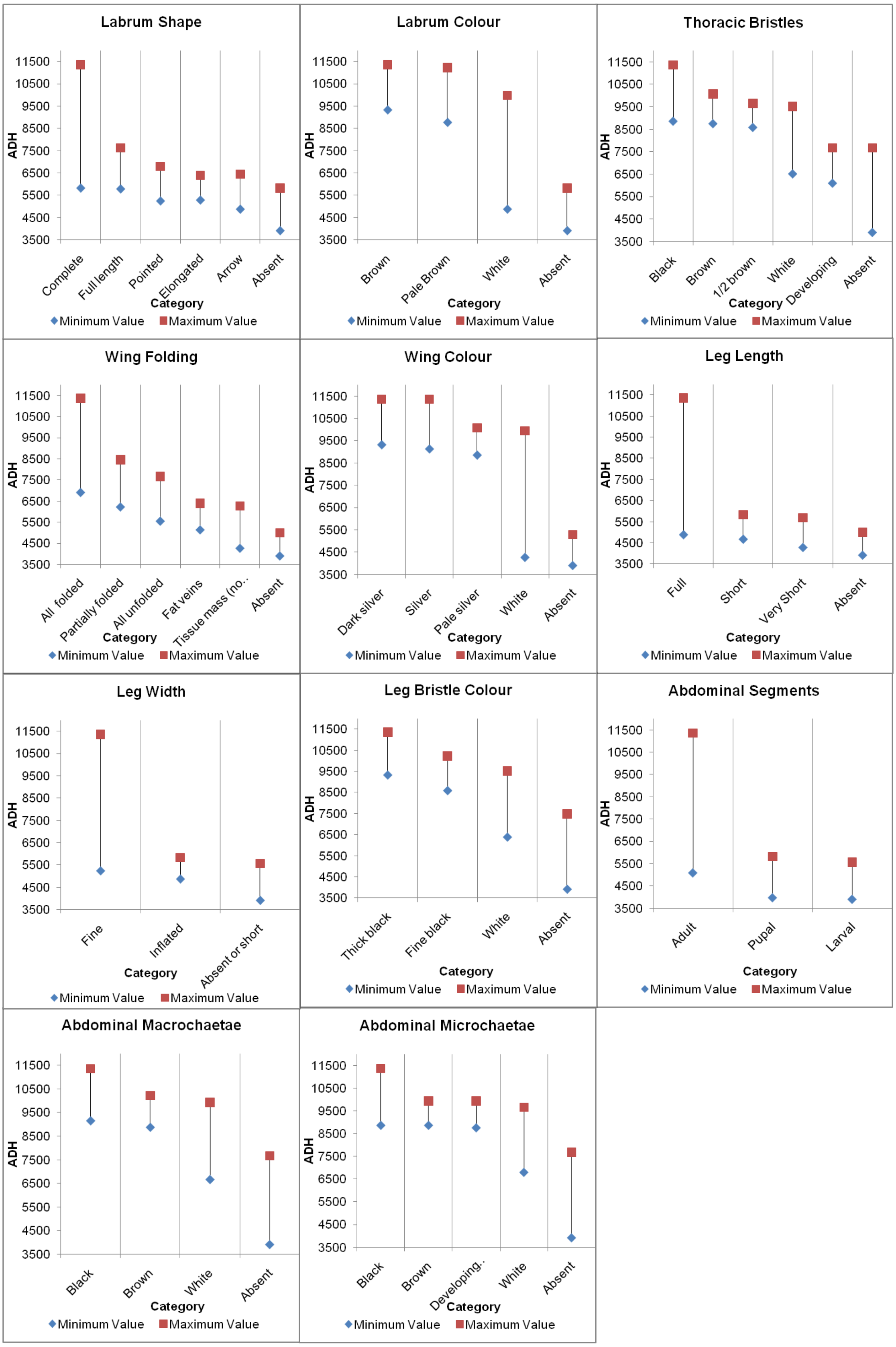

Figure 5.6. Continued.

5.2.2.2 Developmental timeline of cephalic features

A custom colour chart (Table 2.6 and Fig. 5.7), which was read vertically then horizontally, was used to assess eye colour. Colour ranges were then grouped into larger categories for the purpose of age estimation. Compound eyes are absent during the pre-pupal and cryptocephalic pupal stages. Eye colour remains cream until 48-63% TPS, after which the pigment cells start to develop a pale pink colour. Colour steadily develops though pink and red, and finally to brown from 69-83% TPS.

The ‘orbital/frontal bristles’ feature also described the postocular setae, ocellar and postocellar bristles. These become visible from 37-54% TPS, and colouration starts and completes within 63-79% TPS, developing brown through to black (Fig. 5.8). The ‘jowl bristles’ or vibrissae appear at a similar time through the pupal stage (39-61%) as the orbital/facial bristles. They begin to develop brown colouration at 63% TPS yet complete to black much later, up to 96% TPS (Fig. 5.9).

Antennal shape (Fig. 5.10) develops prior to its colour (Fig. 5.11). Antennae are visible from the phanerocephalic pupa stage, with initial circular buds noted laterally on the ventral surface of the head from 13% TPS. These buds rapidly migrate medially until 18-33% TPS, when they appear centrally and elongation of the flagellomere begins. Elongation completes as early as 24% TPS, which coincides with detection of distal brown colouration. Colour develops proximally and tanning (to black) completes from as early as 70% TPS. Aristae (Fig. 5.12) develop from a small bud on the round lateral antennae, from 15% TPS. This gradually elongates until 46-70% TPS when white setae are observed. Setae tan from the distal end, from 68% TPS, and appear black from 73% TPS.

Development of labellum shape (Fig. 5.13), oral lobe setae (Fig. 5.14) and colour (Fig. 5.15) occur over the entire phanerocephalic pupal stage. Labellum development begins as a square structure from 13-28% TPS. It takes shape at the distal (slightly lobed) and then proximal (double lobed) ends, up to 24-36% TPS when the proximal end becomes constricted and the labial palps begin to form (end lobed). These increase in size (double end lobed) until the setae develop at 33-53% TPS. Fully formed labella are visible from 74% TPS. The ‘oral lobe hairs’ feature describes their colouration, which begins at 67-81% TPS. Whole labellum colouration from white to brown begins from 80% TPS and persists up to eclosion in some pupae.

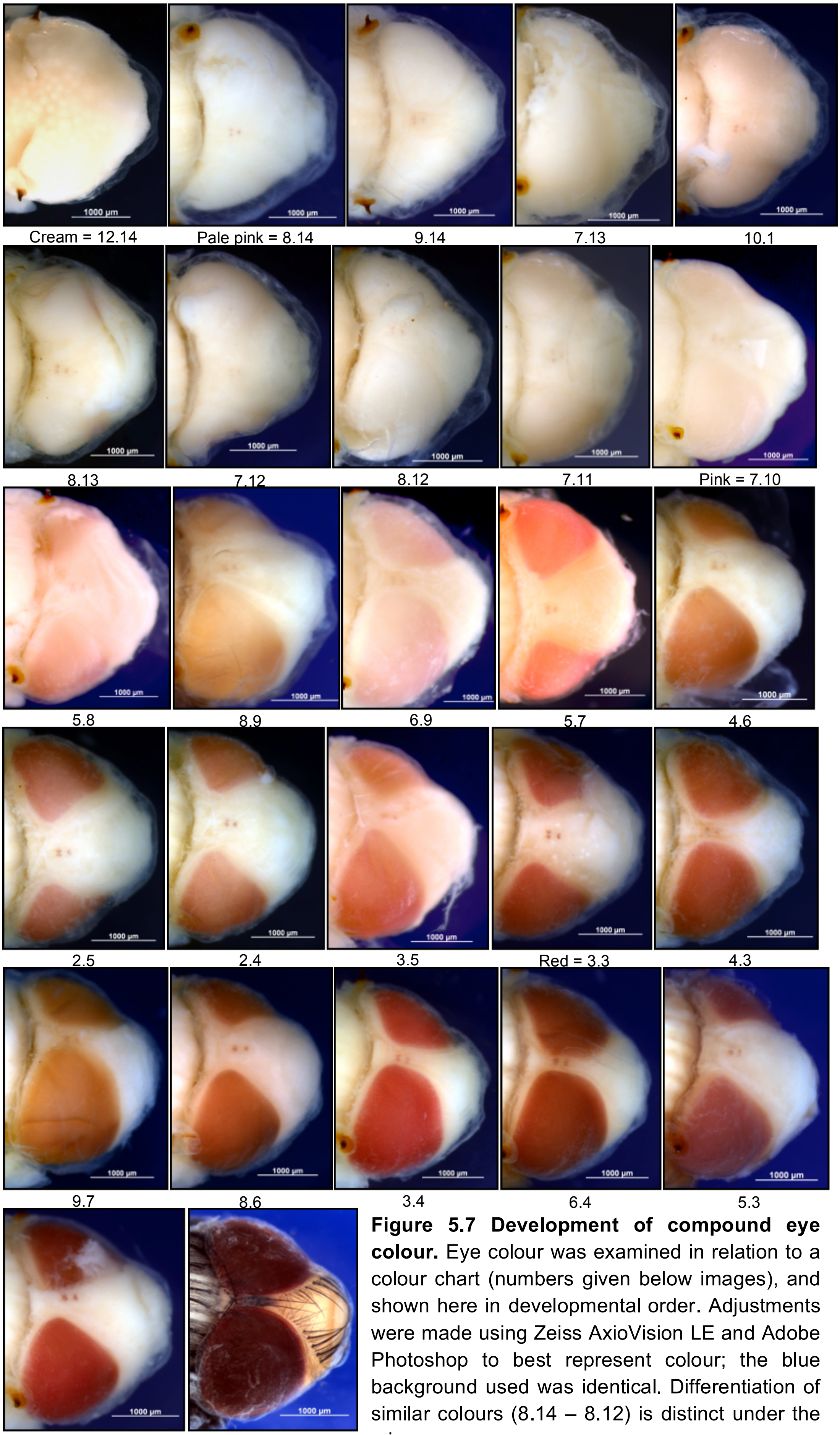

Cream = 12.14
Pale pink = 8.14
9.14
7.13
10.1
8.13
7.12
8.12
7.11
Pink = 7.10
5.8
8.9
6.9
5.7
4.6
2.5
2.4
3.5
Red = 3.3
4.3
9.7
8.6
3.4
6.4
5.3
6.2
Brown = 51.36

Figure 5.7 Development of compound eye colour. Eye colour was examined in relation to a colour chart (numbers given below images), and shown here in developmental order. Adjustments were made using Zeiss AxioVision LE and Adobe Photoshop to best represent colour; the blue background used was identical. Differentiation of similar colours (8.14 – 8.12) is distinct under the microscope.

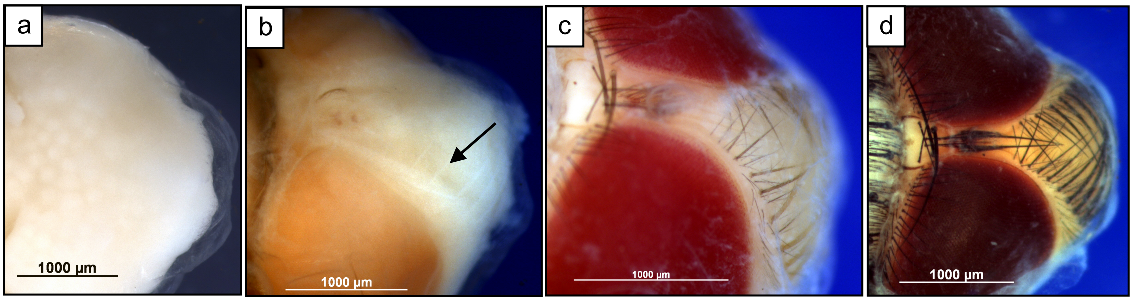

Figure 5.8 Development of orbital and frontal bristles. Bristles developed from being initially absent (a), to white (b - arrow), and to brown (c) and black (d). The blue background was retained as a standard throughout.

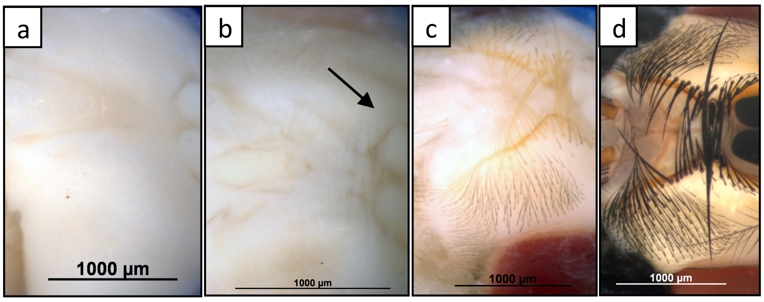

Figure 5.9 Development of jowl bristles. Bristles developed from being absent (a), to white (b - arrow), and then to brown (c) and black (d).

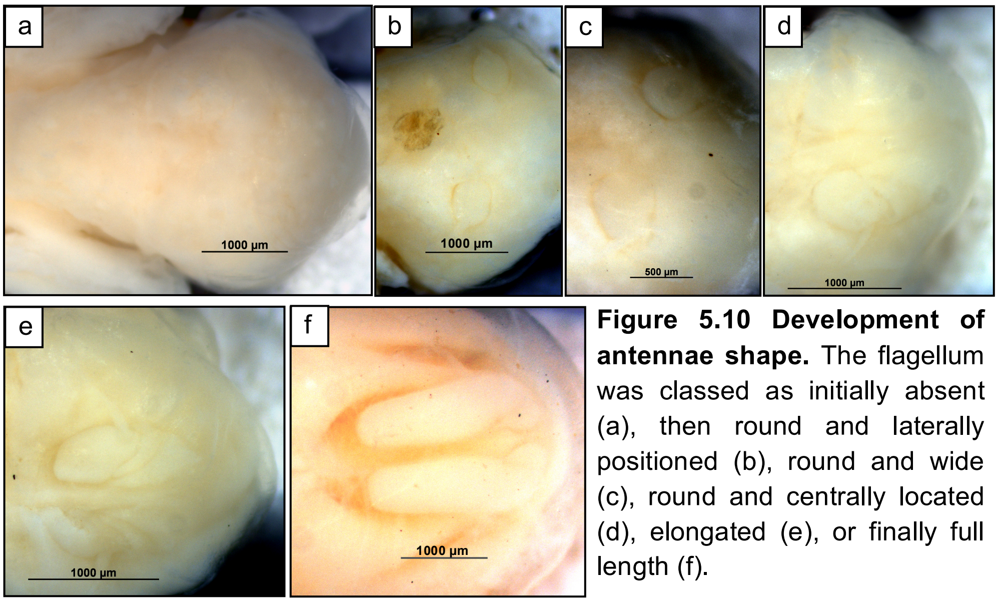

Figure 5.10 Development of antennae shape. The flagellum was classed as initially absent (a), then round and laterally positioned (b), round and wide (c), round and centrally located (d), elongated (e), or finally full length (f).

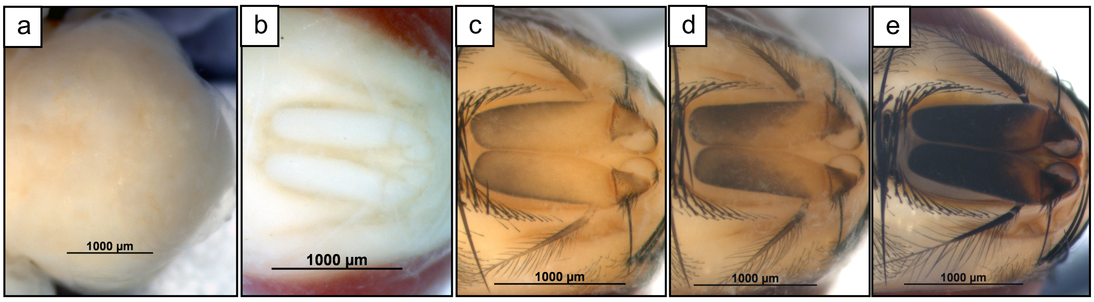

Figure 5.11 Development of antennae colour. Antennae were either classed as absent (a), white (developing or full length) (b), developing brown (c), brown (d) or black.

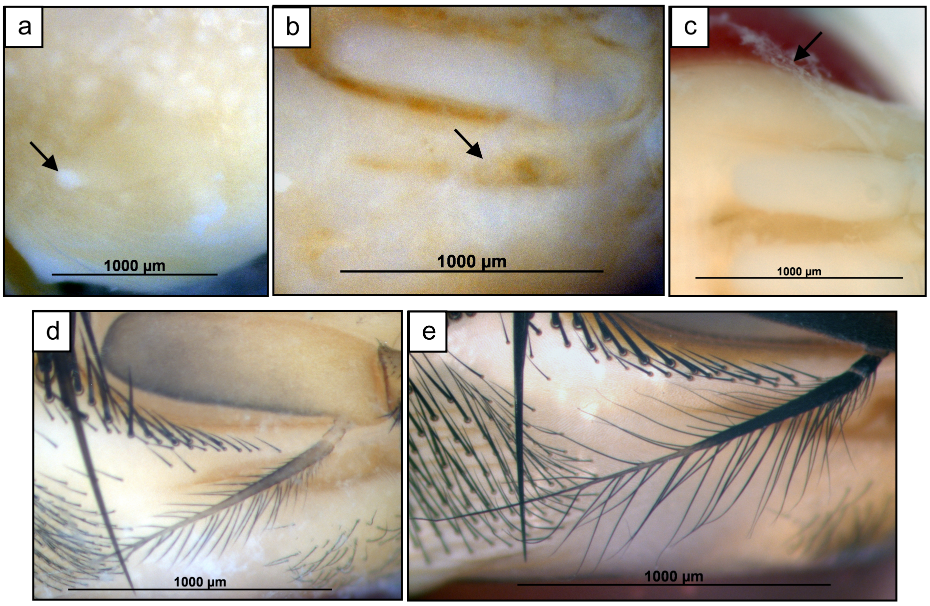

Figure 5.12 Development of arista colour and form. Aristae were either classed as absent (a – arrow = developmental start point), bald (b - arrow), white (c - arrow), brown (d) or black (e). Bald aristae had not yet developed visible setae along their length; white aristae had very fine white setae present.

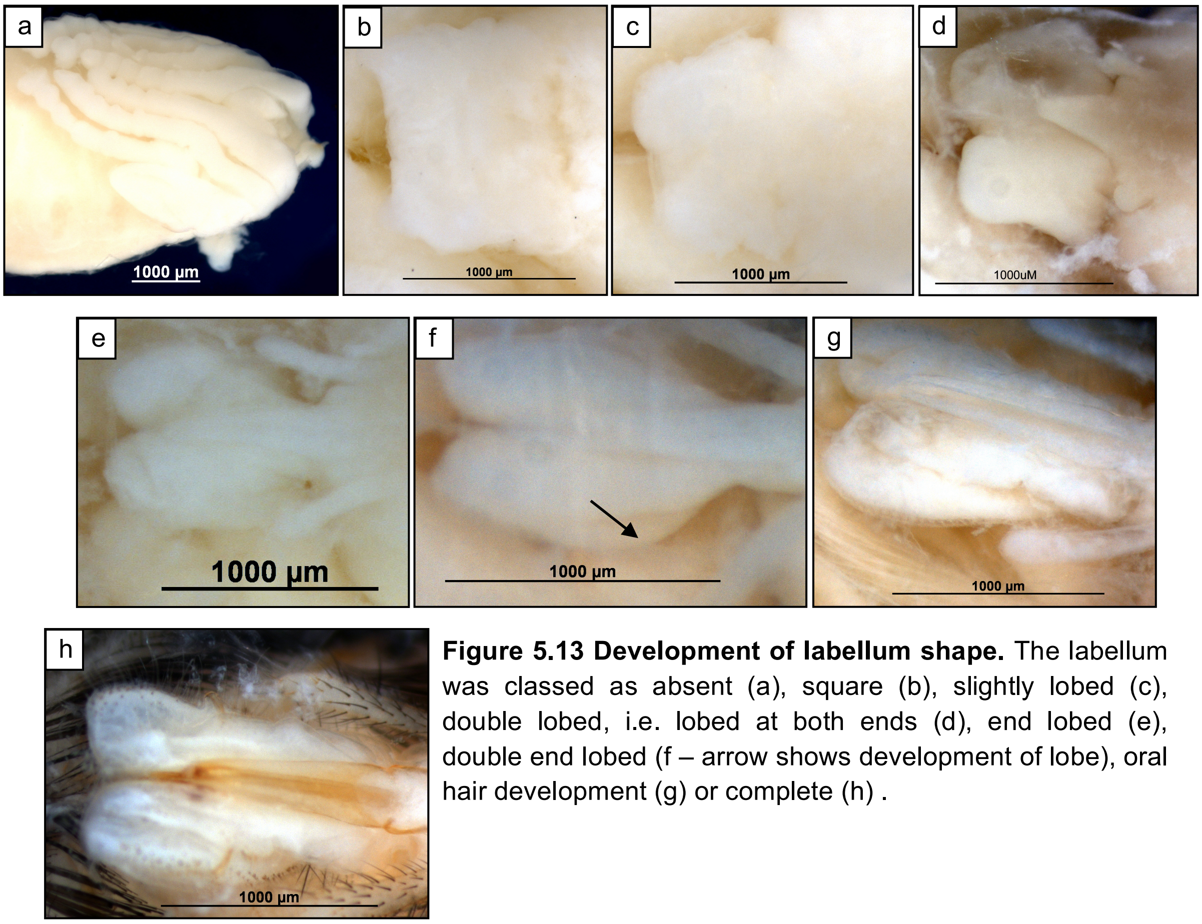

Figure 5.13 Development of labellum shape. The labellum was classed as absent (a), square (b), slightly lobed (c), double lobed, i.e. lobed at both ends (d), end lobed (e), double end lobed (f – arrow shows development of lobe), oral hair development (g) or complete (h) .

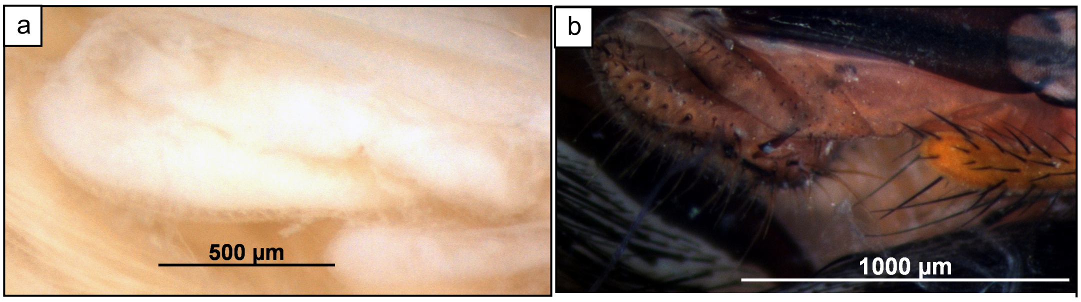

Figure 5.14 Development of oral lobe setae colour. Setae were either classed as absent or white (a - arrow) or brown/black (b).

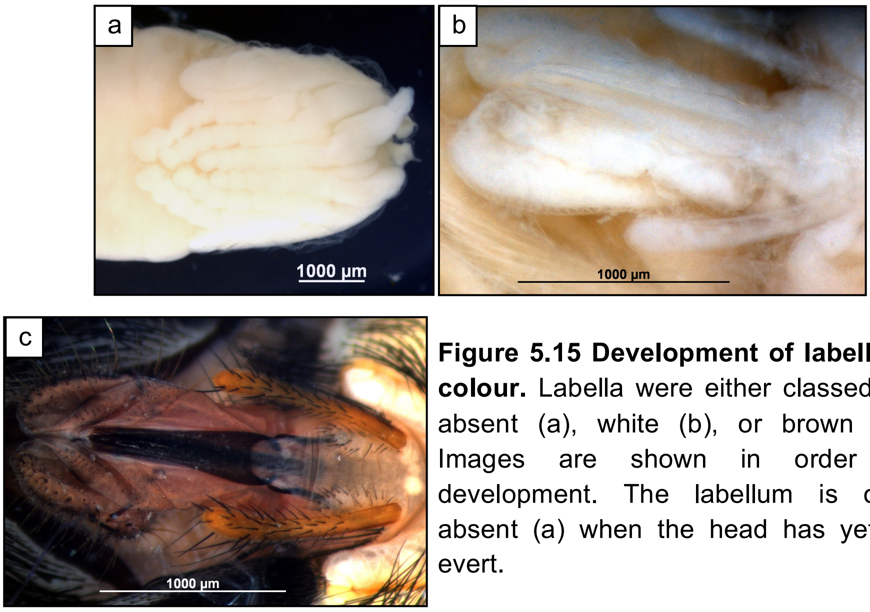

Figure 5.15 Development of labellum colour. Labella were either classed as absent (a), white (b), or brown (c). Images are shown in order of development. The labellum is only absent (a) when the head has yet to evert.

Palps first appear as small round protuberances (Fig. 5.16) at 18-28% TPS that slowly elongate and reach full length from 28-47% TPS. Colour (Fig. 5.17) development follows with setae tanning from 65-79% TPS, with their final pale brown colour achieved from 68-81% TPS.

The labrum is first visible as a small arrow (Fig 5.18), which elongates gradually until its full length is achieved from 25-39% TPS. The medial groove is visible from 26-50% TPS. Labrum colouration (Fig. 5.19) develops from pale brown from 65-81% TPS, and is complete from 73-98% TPS (brown).

The larval cephalopharyngeal skeleton (Fig. 5.20) is everted and released from the head at the start of the phanerocaphalic pupal stage. Its position within the pupa changes during early development; initially it is attached to the surrounding tissue, however it becomes loosened (pushed out of the head) as the thorax everts from 7-18% TPS. As the legs evert and elongate, the cephalopharyngeal skeleton is enclosed in a membrane and is readily separated from the pupa (from 10% TPS), prior to being fully released from the pupa and adhering to the puparium, from 13-22% TPS.

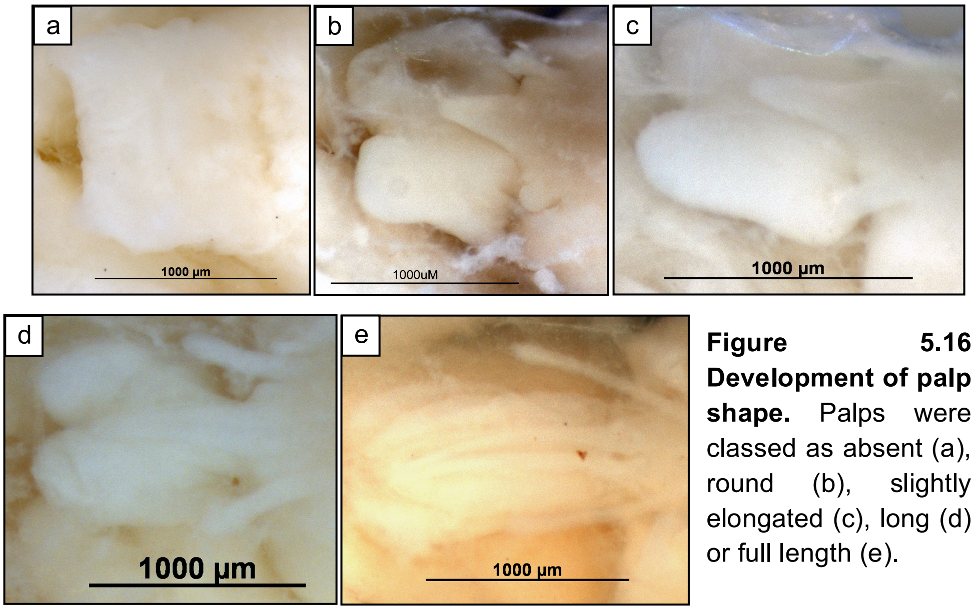

Figure 5.16 Development of palp shape. Palps were classed as absent (a), round (b), slightly elongated (c), long (d) or full length (e).

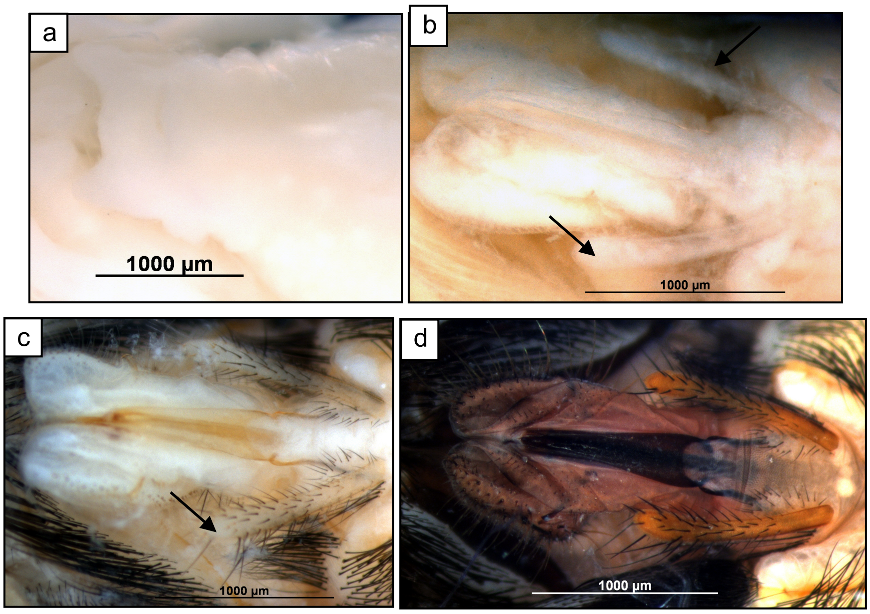

Figure 5.17 Development of maxillary palp colour. Palps were either classed as absent (a), developing/white (b - arrow), with brown/black setae (c - arrow), or completely brown (d).

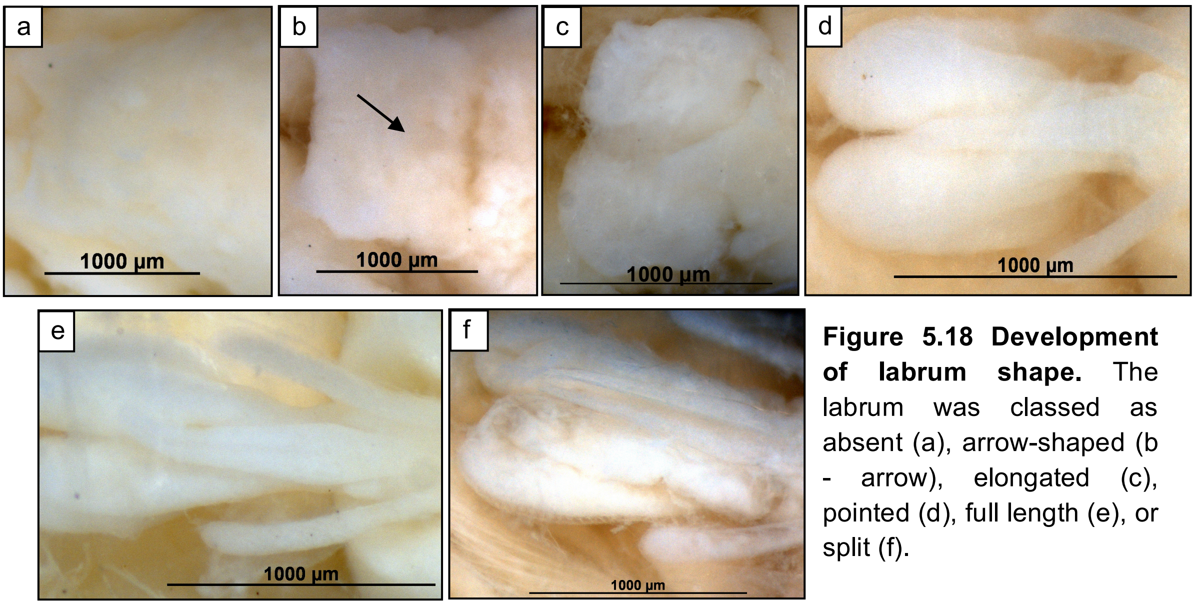

Figure 5.18 Development of labrum shape. The labrum was classed as absent (a), arrow-shaped (b - arrow), elongated (c), pointed (d), full length (e), or split (f).

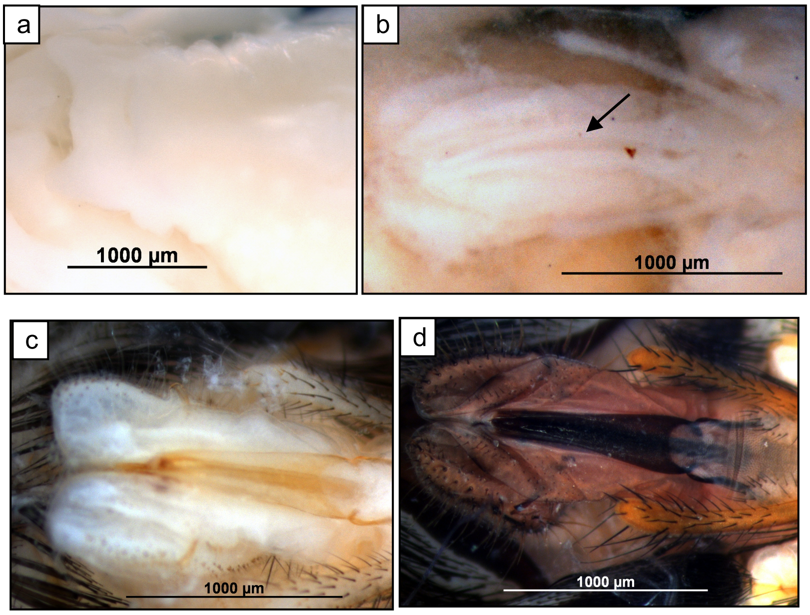

Figure 5.19 Development of labrum colour. Labrum colour was either classed as absent (a), developing/white (b), pale brown (c) or brown (d).

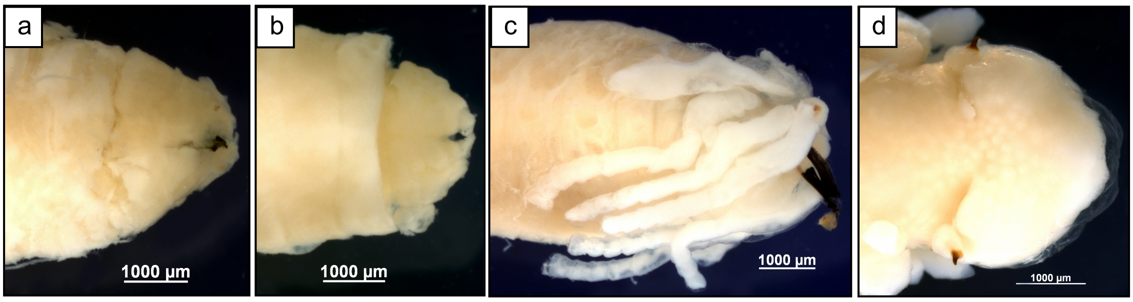

Figure 5.20 Progression of head eversion. Progression of head eversion was indicated by the ease of removal of the cephalopharyngeal skeleton. The mouthparts were considered attached to the pupa (a), slightly loosened within the head (b), enclosed in a membrane ready for eversion (c) or fully everted (d).

5.2.2.3 Development of thoracic features

Thoracic bristles (Fig. 5.21) develop after head eversion, at 30-50% TPS. They appear short and disorganised, lengthen rapidly and achieve full length from 35-51% TPS. The scutellar bristles develop brown colouration at 63-75% TPS which progresses anteriorly to the bristles on the scutum ('brown' category) from 65-77% TPS. Complete black colouration is observed from 67-83% TPS.

Wings evert early in the pupal stage (Fig. 5.22), from 5-14.6% TPS, and appear as a small triangular masses of tissue initially. Veins appear as thick lines ('fat veins' category) from 17-32% TPS, and the wing appears more translucent, displaying complete venation from 22-33% TPS. Wing folding initiates at 31-50% TPS and is complete by 40-61% TPS. Colouration (Fig. 5.23) changes from pale silver from 67-81% to the final dark silver colour from 73% until eclosion.

Legs evert with the wings and thorax, prior to the head (Fig. 5.24), from 5-15% TPS. Initially they are the same length as the thorax but extend down the abdomen ('short' category) from 10-26% TPS, reaching their full length at head eversion from 13% TPS. Intially, legs appear as inflated tubes of undifferentiated tissue (Fig. 5.25), which persist until the adult cuticle was formed from 18-26% TPS after which the segments appear more defined ('fine' category). Leg bristle growth (Fig. 5.26) is detected from 33-48% TPS on the femur and tibia. Tanning of the setae begins from 63-75% TPS, which darken alongside leg colouration (darkening) from 73-85% TPS.

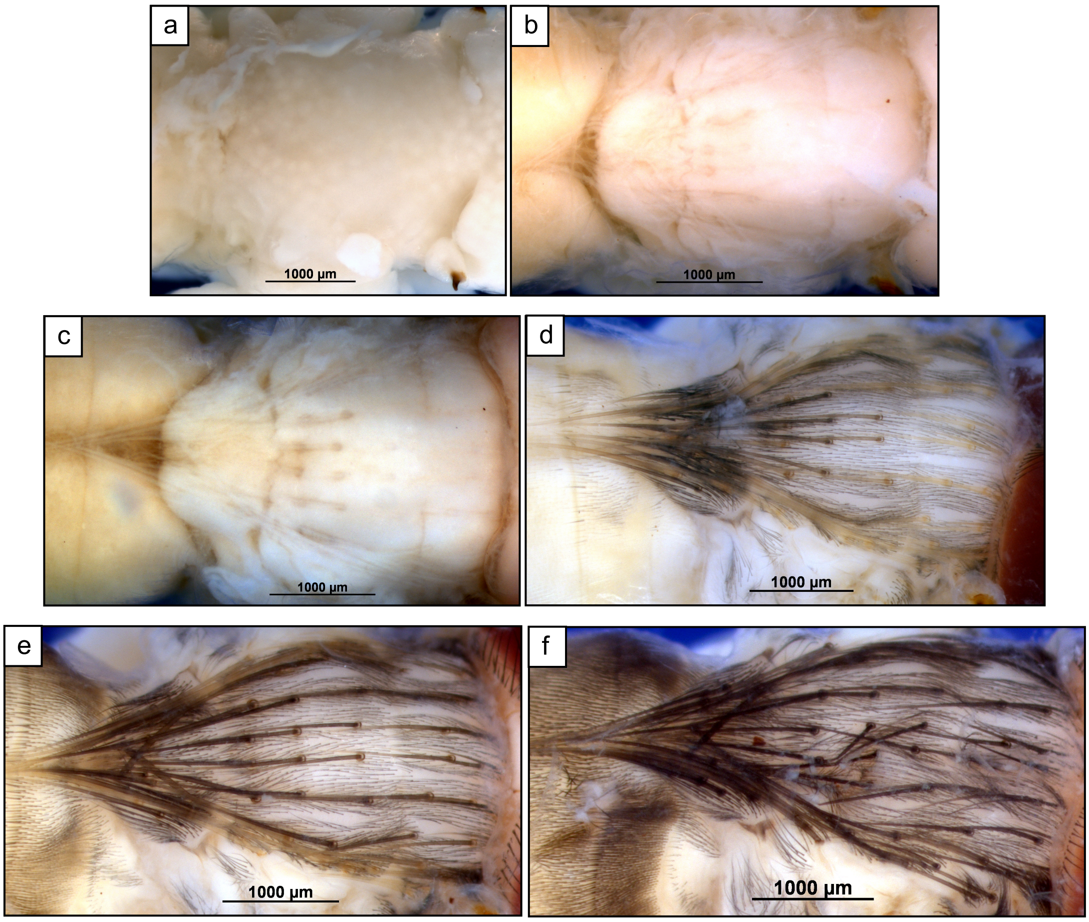

Figure 5.21 Development of thoracic bristles. Bristles were either classed as absent (a), developing (b), white (c), developing (1/2) brown (d), brown (e) or black (f). '1/2 brown' indicates the incomplete tanning of all thoracic bristles. Tanning of scutellar bristles occurred initially and progressed anteriorly to the bristles situated on the scutum. Brown bristles had yet to develop the colour intensity of black bristles.

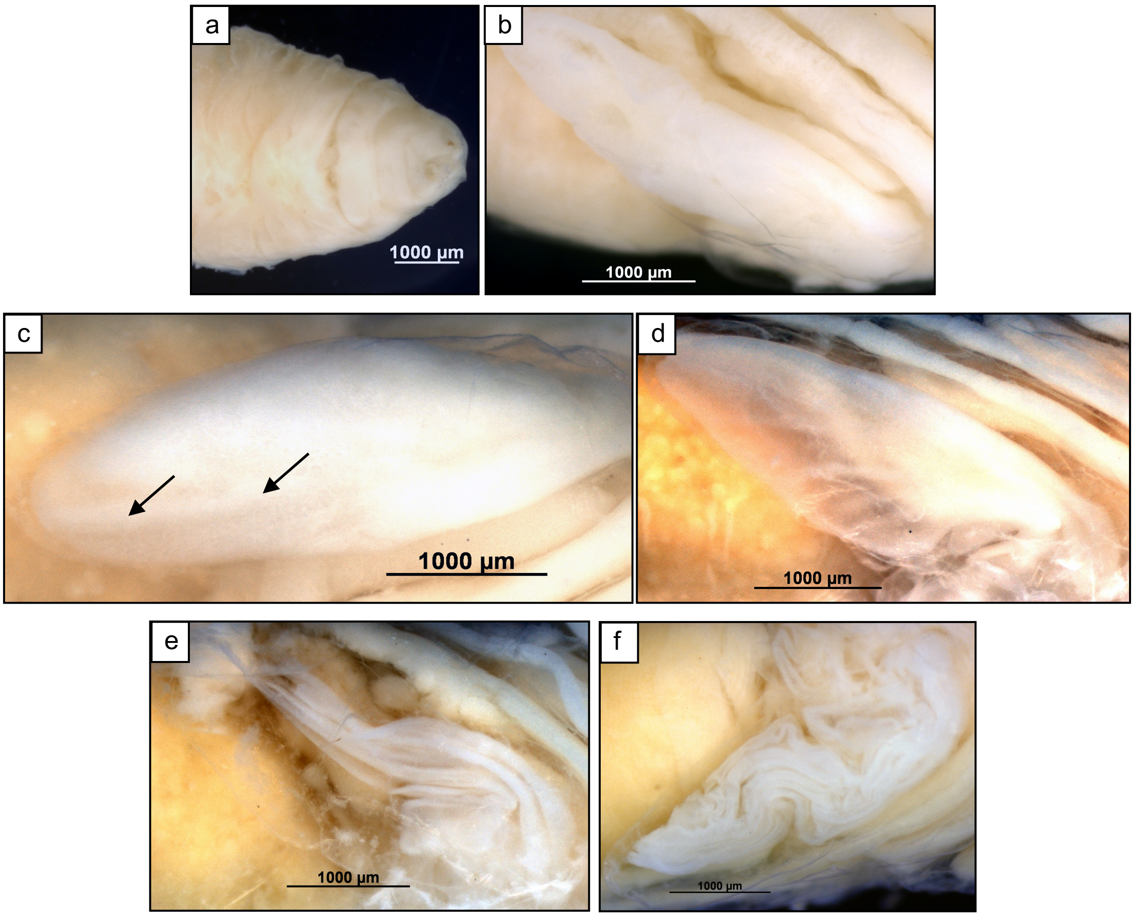

Figure 5.22 Development of wing folding. Wings were either classed as absent (a), a mass of undifferentiated tissue (b), vein differentiation started ('fat veins') (c), wings unfolded, veins visible (d), partially folded (e) or fully folded (f). Wings were absent prior to thorax eversion.

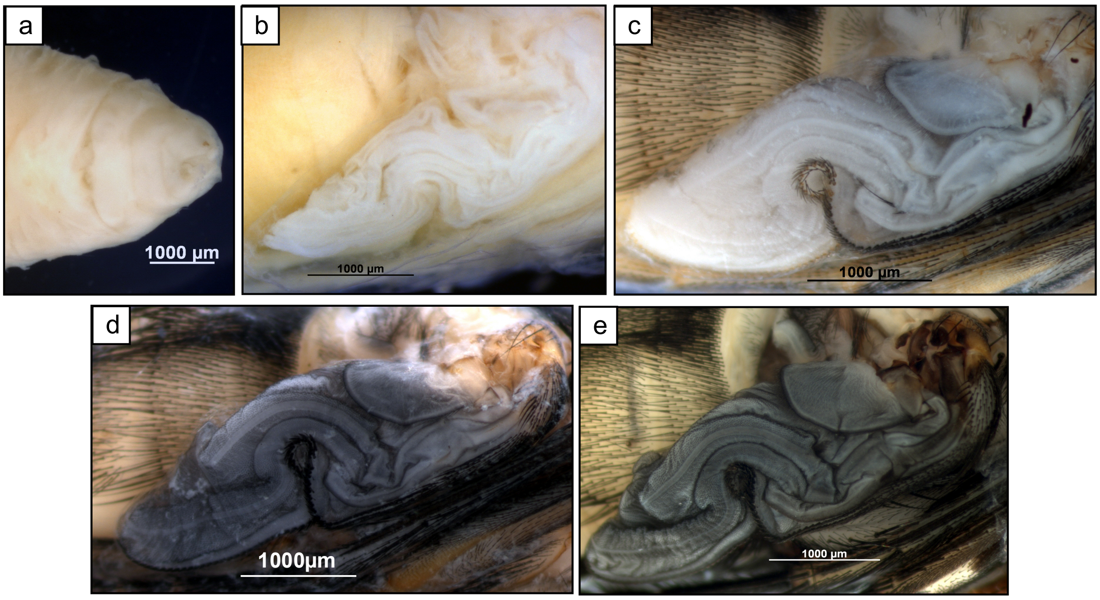

Figure 5.23 Development of wing colour. Wings were either classed as absent (a), white (b), pale silver (c), silver (d) or dark silver (e). White wings described all stages of wing development (folding).

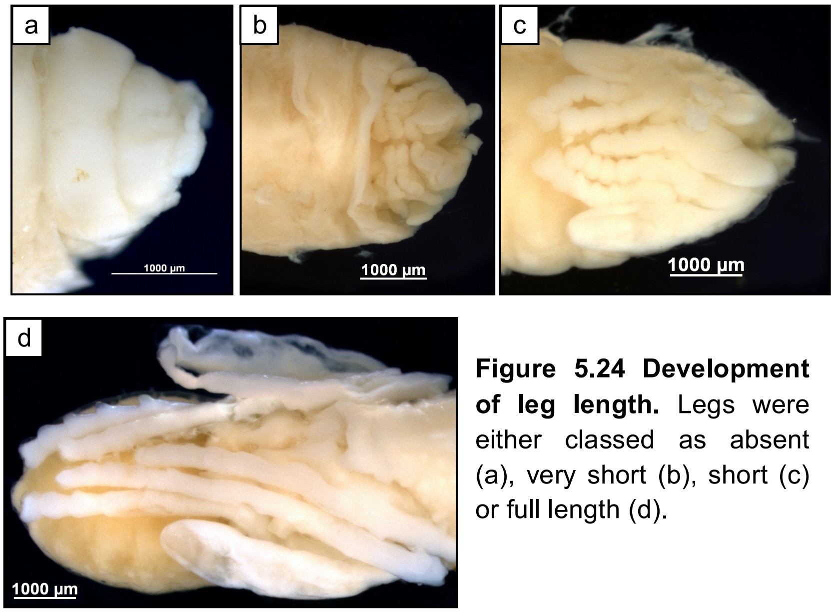

Figure 5.24 Development of leg length. Legs were either classed as absent (a), very short (b), short (c) or full length (d).

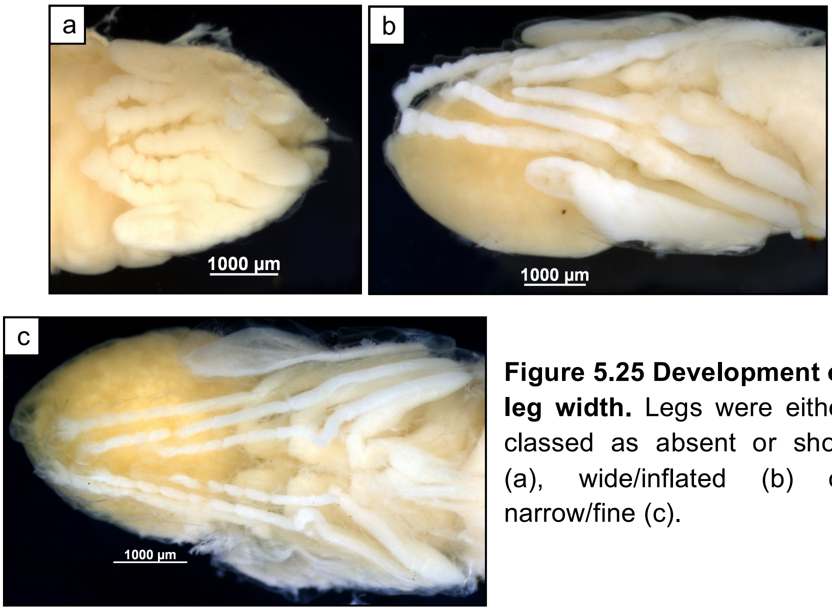

Figure 5.25 Development of leg width. Legs were either classed as absent or short (a), wide/inflated (b) or narrow/fine (c).

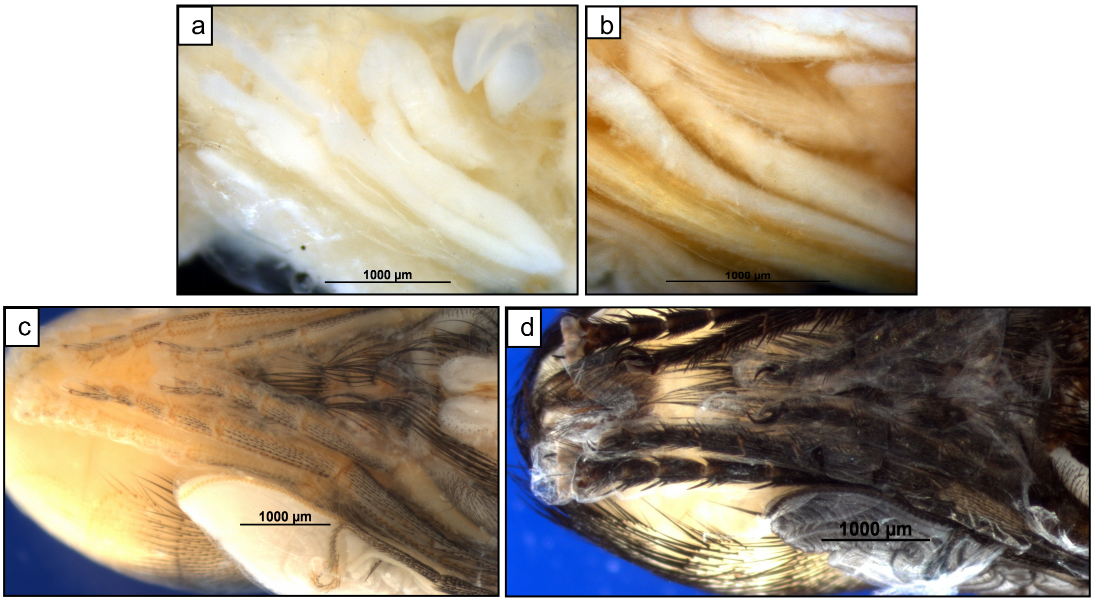

Figure 5.26 Development of leg bristles. Bristles were either classed as absent (a), white (b), fine black (c) or dense black (d).

5.2.2.4 Development of abdominal features

Histoblasts are visible in the abdominal segments (Fig. 5.27) until 22% TPS. As the thorax and head evert, histoblasts develop the abdominal cuticle. Pupae are more easily dissected from the puparium after this occurs. Following head eversion (16-26% TPS), the abdomen adopts its adult form, with definitive segmentation visible.

Development of the long macrochetae (Fig. 5.28) at the posterior end of the abdomen (5th segment onwards) begins at 37-50% TPS and tanning initiates at 67-81% TPS. Complete black colouration is observed from 70-85% TPS.

The abdominal microchetae (Fig. 5.29) appear at a similar time to the macrochetae, at 39-50% TPS. Anterior microchetae begin to tan ('developing brown' category) from 65-77% TPS, which rapidly develops to full brown and black colouration over a similar time frame, from 67-81% TPS.

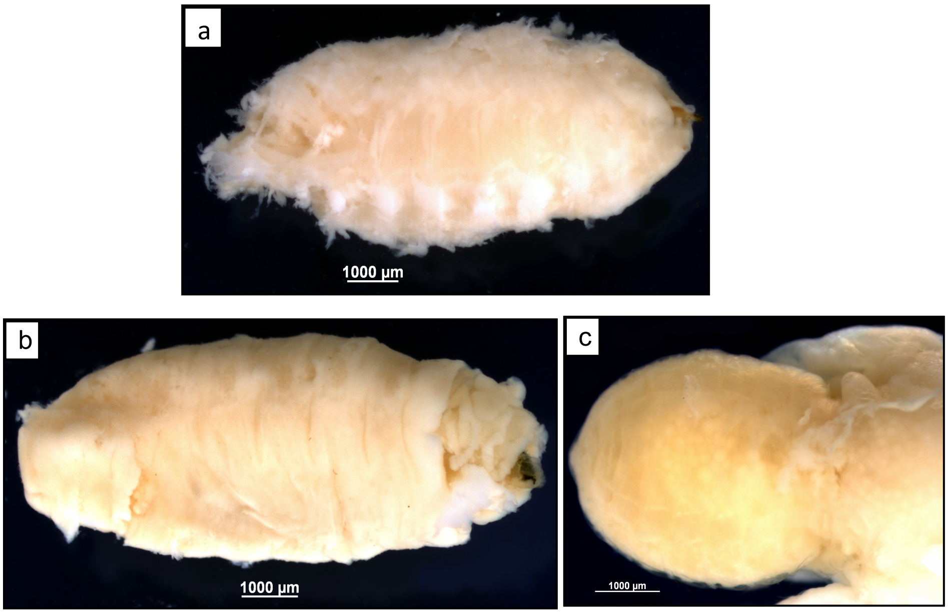

Figure 5.27 Development of the abdomen. The abdomen was either classed as larval, with a rough cuticle and distinguished larval segments (a), pupal, with smoothened segments (b) or adult, comprising full tagmosis (c).

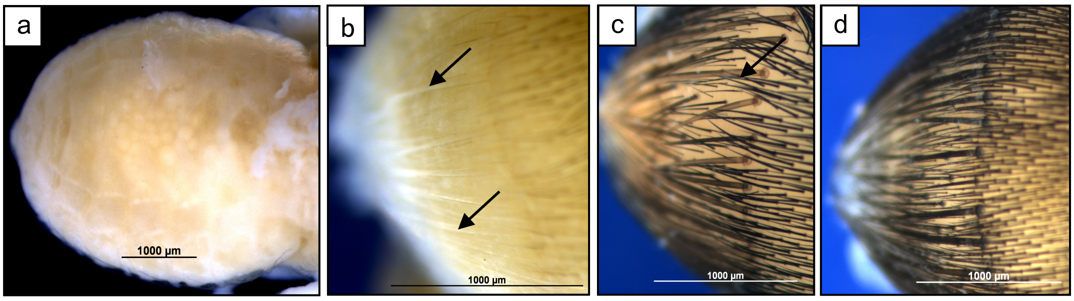

Figure 5.28 Development of abdominal macrochetae. Macrochetae were either classed as absent (a), white (b - arrows), brown (c - arrow) or black (d).

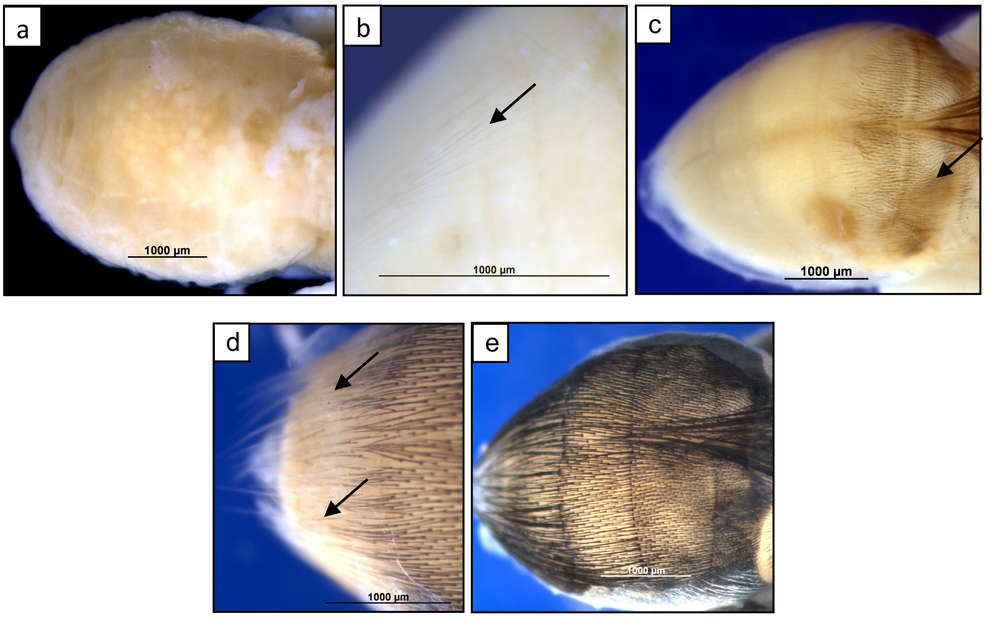

Figure 5.29 Development of abdominal microchetae. Microchetae were either classed as absent (a), white (b - arrow), developing brown (c - arrow), brown (d - arrows) or black (e). Brown indicates all microchetae have started to tan, with the majority of the abdomen covered in dark brown microchetae.

5.2.3 Age estimation using manual age-range correlation

Age estimation was attempted using the complete developmental timeline established. The manual age-range correlation method was based on the principle that if a given categorization of a feature was observable during a defined ADH range, then the *combination* of all these ranges would provide a refined age range, as illustrated in Fig. 5.30 using just eight features. In this example, the antennae and arista ‘brown’ colouration limits the minimum age of the pupa to 8823 ADH, whilst the white orbital/frontal bristles and the developing brown thoracic bristles limit the maximum age to 9094 ADH.

To facilitate data input and comparison, an Excel spreadsheet was developed (Fig. 5.31). Categorization of features was also assigned a numerical scale shown in the figure alongside the feature, A and category, B, to permit flexibility in data input, format and to facilitate regression analysis (see 5.3.4). Minimum and maximum ADH age ranges are shown for each category (C & D) as in Table 5.9. The input table comprises features (E) and a drop-down menu for categories (F). Once a category is selected, this automatically determines the category number (G). This number is used with the corresponding feature to ‘look up’ and select the minimum and maximum ages (H & I). An equivalent table was constructed for selection of categories by number (data not shown).

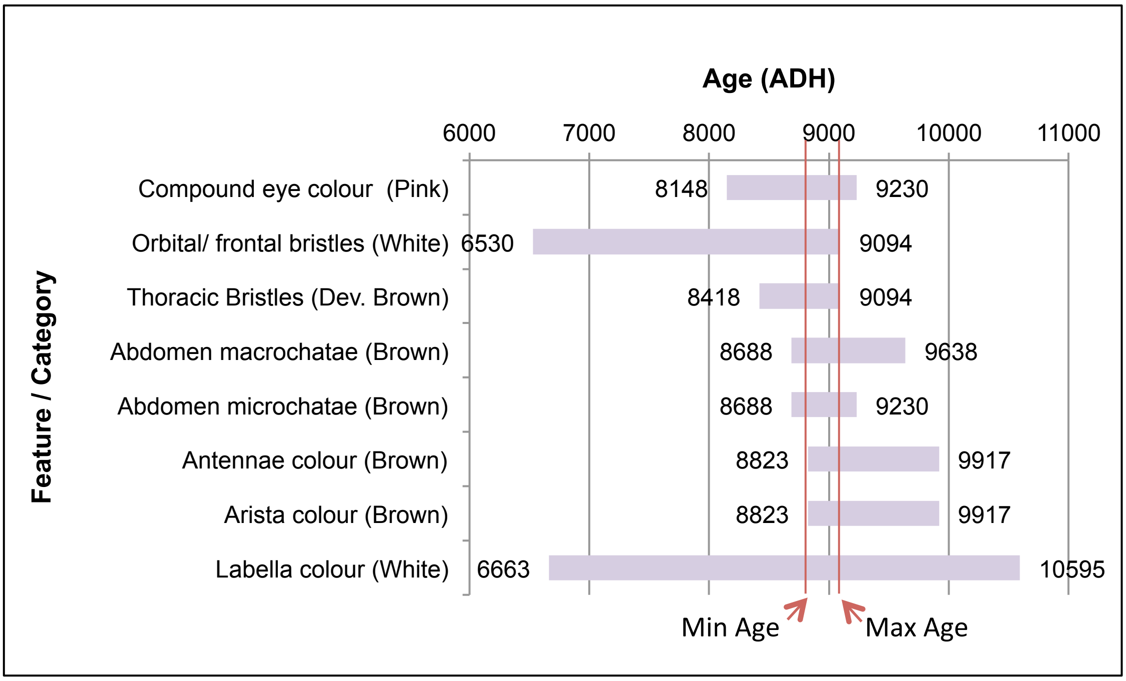

Figure 5.30 The principle of the manual age range correlation method. The age ranges of each feature category are displayed, and the overlapping range covered by all features indicates the derived age range. In this case the age of this pupa was between 8823 – 9094 ADH.

The maximum and minimum values from columns H & I respectively were displayed as the minimum and maximum age range of the analysed pupa (J). A small error of +/- 49 ADH (K) was applied to account for oviposition time and temperature fluctuations between colonies in T1. The spreadsheet then displays the range of ages calculated in ADH (L) with the total range (N), days at 22°C (O) and the lifecycle % limits (M).

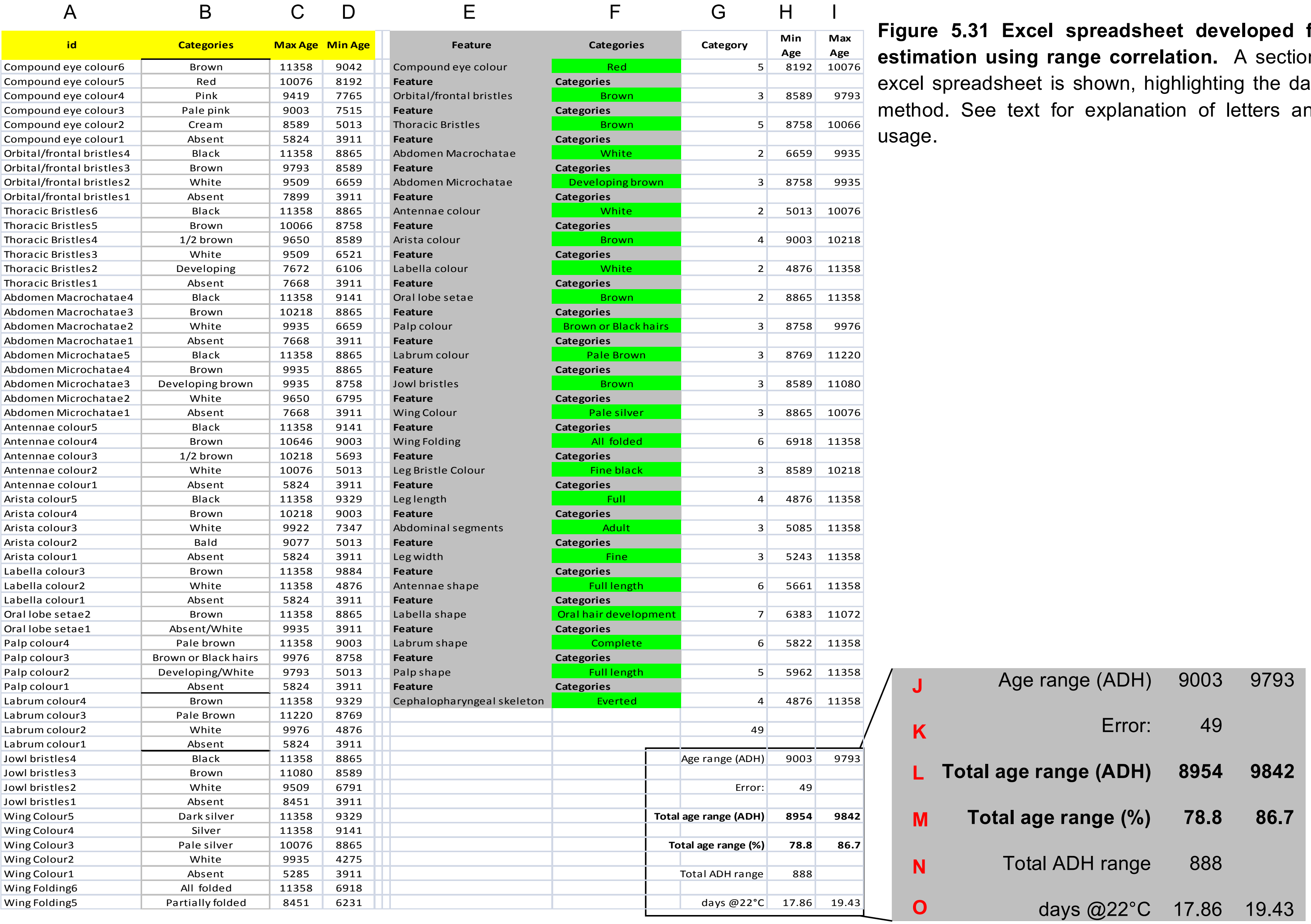

id	Categories	Max Age	Min Age	Feature	Categories	Category	Min Age	Max Age
Compound eye colour6	Brown	11358	9042	Compound eye colour	🟩 Red	5	8192	10076
Compound eye colour5	Red	10076	8192	**Feature**	**Categories**			
Compound eye colour4	Pink	9419	7765	Orbital/frontal bristles	🟩 Brown	3	8589	9793
Compound eye colour3	Pale pink	9003	7515	**Feature**	**Categories**			
Compound eye colour2	Cream	8589	5013	Thoracic Bristles	🟩 Brown	5	8758	10066
Compound eye colour1	Absent	5824	3911	**Feature**	**Categories**			
Orbital/frontal bristles4	Black	11358	8865	Abdomen Macrochatae	🟩 White	2	6659	9935
Orbital/frontal bristles3	Brown	9793	8589	**Feature**	**Categories**			
Orbital/frontal bristles2	White	9509	6659	Abdomen Microchatae	🟩 Developing brown	3	8758	9935
Orbital/frontal bristles1	Absent	7899	3911	**Feature**	**Categories**			
Thoracic Bristles6	Black	11358	8865	Antennae colour	🟩 White	2	5013	10076
Thoracic Bristles5	Brown	10066	8758	**Feature**	**Categories**			
Thoracic Bristles4	1/2 brown	9650	8589	Arista colour	🟩 Brown	4	9003	10218
Thoracic Bristles3	White	9509	6521	**Feature**	**Categories**			
Thoracic Bristles2	Developing	7672	6106	Labella colour	🟩 White	2	4876	11358
Thoracic Bristles1	Absent	7668	3911	**Feature**	**Categories**			
Abdomen Macrochatae4	Black	11358	9141	Oral lobe setae	🟩 Brown	2	8865	11358
Abdomen Macrochatae3	Brown	10218	8865	**Feature**	**Categories**			
Abdomen Macrochatae2	White	9935	6659	Palp colour	🟩 Brown or Black hairs	3	8758	9976
Abdomen Macrochatae1	Absent	7668	3911	**Feature**	**Categories**			
Abdomen Microchatae5	Black	11358	8865	Labrum colour	🟩 Pale Brown	3	8769	11220
Abdomen Microchatae4	Brown	9935	8865	**Feature**	**Categories**			
Abdomen Microchatae3	Developing brown	9935	8758	Jowl bristles	🟩 Brown	3	8589	11080
Abdomen Microchatae2	White	9650	6795	**Feature**	**Categories**			
Abdomen Microchatae1	Absent	7668	3911	Wing Colour	🟩 Pale silver	3	8865	10076
Antennae colour5	Black	11358	9141	**Feature**	**Categories**			
Antennae colour4	Brown	10646	9003	Wing Folding	🟩 All folded	6	6918	11358
Antennae colour3	1/2 brown	10218	5693	**Feature**	**Categories**			
Antennae colour2	White	10076	5013	Leg Bristle Colour	🟩 Fine black	3	8589	10218
Antennae colour1	Absent	5824	3911	**Feature**	**Categories**			
Arista colour5	Black	11358	9329	Leg length	🟩 Full	4	4876	11358
Arista colour4	Brown	10218	9003	**Feature**	**Categories**			
Arista colour3	White	9922	7347	Abdominal segments	🟩 Adult	3	5085	11358
Arista colour2	Bald	9077	5013	**Feature**	**Categories**			
Arista colour1	Absent	5824	3911	Leg width	🟩 Fine	3	5243	11358
Labella colour3	Brown	11358	9884	**Feature**	**Categories**			
Labella colour2	White	11358	4876	Antennae shape	🟩 Full length	6	5661	11358
Labella colour1	Absent	5824	3911	**Feature**	**Categories**			
Oral lobe setae2	Brown	11358	8865	Labella shape	🟩 Oral hair development	7	6383	11072
Oral lobe setae1	Absent/White	9935	3911	**Feature**	**Categories**			
Palp colour4	Pale brown	11358	9003	Labrum shape	🟩 Complete	6	5822	11358
Palp colour3	Brown or Black hairs	9976	8758	**Feature**	**Categories**			
Palp colour2	Developing/White	9793	5013	Palp shape	🟩 Full length	5	5962	11358
Palp colour1	Absent	5824	3911	**Feature**	**Categories**			
Labrum colour4	Brown	11358	9329	Cephalopharyngeal skeleton	🟩 Everted	4	4876	11358
Labrum colour3	Pale Brown	11220	8769					
Labrum colour2	White	9976	4876			49		
Labrum colour1	Absent	5824	3911					
Jowl bristles4	Black	11358	8865			Age range (ADH)	9003	9793
Jowl bristles3	Brown	11080	8589					
Jowl bristles2	White	9509	6791			Error:	49	
Jowl bristles1	Absent	8451	3911					
Wing Colour5	Dark silver	11358	9329			**Total age range (ADH)**	**8954**	**9842**
Wing Colour4	Silver	11358	9141					
Wing Colour3	Pale silver	10076	8865			**Total age range (%)**	**78.8**	**86.7**
Wing Colour2	White	9935	4275					
Wing Colour1	Absent	5285	3911			Total ADH range	888	
Wing Folding6	All folded	11358	6918					
Wing Folding5	Partially folded	8451	6231			days @22°C	17.86	19.43

J	Age range (ADH)	9003	9793
K	Error:	49	
L	**Total age range (ADH)**	**8954**	**9842**
M	**Total age range (%)**	**78.8**	**86.7**
N	Total ADH range	888	
O	days @22°C	17.86	19.43

Figure 5.31 Excel spreadsheet developed for age estimation using range correlation. A section of the excel spreadsheet is shown, highlighting the data input method. See text for explanation of letters and table usage.

5.2.4 Age estimation using regression analysis

Observations from 1494 pupae, at defined ages (in ADH), were used to establish the regression equation. The dependent variable was age in ADH, and the independent variables were all the features analysed. The resulting regression equation (Equation 5.1) was set up in Excel for automatic selection of category numbers from the age range method.

```
The regression equation is
Age in ADH = 3237 + 275 x Compound eye colour + 161 x Orbital/facial bristles
               + 60.0 x Thoracic Bristles + 30.8 x Abdomen Macrochatae
               + 115 x Abdomen Microchatae + 81.2 x Antennae colour
               + 261 x Arista colour + 431 x Labella colour
               - 200 x Oral Lobe Hairs - 237 x Palp colour
               - 155 x Labrum colour + 40.5 x Jowl bristles
               + 27.5 x Wing Colour + 205 x Wing Folding
               + 94.6 x Leg Bristle Colour + 24.2 x Leg length
               - 2.5 x Abdominal segments - 293 x Leg width at full length
               - 34.4 x Antennae shape + 192 x Labellum shape
               + 57.0 x Labrum shape - 3.8 x Palp shape
               + 82.5 x Cephalopharyngeal skeleton
```

Equation 5.1 The regression equation for age estimation of pupae. This equation was derived using raw data from 1494 pupae, using all features as the predictors (independent variables). The numbers in the equation are multiplied by the category number for each feature, e.g. pale pink compound eyes, white bristles: ADH = 3237 + (275 x 3) + (161 x 2) + … etc.

This regression equation had a high correlation coefficient (adjusted R^2 value) of 97.9%. The error approximated from the pupal stage/lifecycle length natural variation was +/- 500 ADH. This was later refined (see below) using analysis of residual values from blind sample testing to +/- 320 ADH (+/- 15 hours at 22°C), which was applied to semi-blind and blind samples.

The age estimate given using the regression equation should coincide with the predicted age range (manual age range correlation method) for the same pupa. However, when this was not the case it highlighted user error with category selection, either at the pupal assessment or data input stage. It was therefore advantageous to ensure that for all age estimates, both methods were used as a partial control for correct assessment and data entry by the user.

Regression analysis also indicated which characteristics were the least ($P > 0.05$) and most ($P < 0.001$) significant contributors to the age estimation equation (Table 5.9). The most significant contributors were therefore used to create another regression equation (Equation 5.2), with an adjusted R^2 value of 97.8%. Four of five test-sample age estimates obtained using this equation did not align with corresponding manual (age-range correlation) estimates, indicating limited utility of the minimised equation.

Predictor	Coef	SE Coef	T	P
Constant	3236.92	76.25	42.45	0.000
Compound eye colour	**275.01**	**17.08**	**16.10**	**0.000**
Orbital/facial bristles	**160.54**	**44.54**	**3.60**	**0.000**
Thoracic Bristles	60.02	24.88	2.41	0.016
Abdomen Macrochatae	**30.79**	**38.52**	**0.80**	**0.424**
Abdomen Microchatae	114.78	40.39	2.84	0.005
Antennae colour	**81.18**	**23.14**	**3.51**	**0.000**
Arista colour	**261.14**	**29.24**	**8.93**	**0.000**
Labella colour	**430.61**	**34.96**	**12.32**	**0.000**
Oral Lobe Hairs	-199.52	76.10	-2.62	0.009
Palp colour	**-237.27**	**44.65**	**-5.31**	**0.000**
Labrum colour	**-154.97**	**36.24**	**-4.28**	**0.000**
Jowl bristles	**40.52**	**38.57**	**1.05**	**0.294**
Wing Colour	**27.52**	**27.33**	**1.01**	**0.314**
Wing Folding	**205.32**	**22.44**	**9.15**	**0.000**
Leg Bristle Colour	94.57	41.01	2.31	0.021
Leg length	**24.17**	**43.58**	**0.55**	**0.579**
Abdominal segments	**-2.45**	**29.45**	**-0.08**	**0.934**
Leg width at full length	**-293.22**	**57.48**	**-5.10**	**0.000**
Antennae shape	**-34.42**	**24.55**	**-1.40**	**0.161**
Labellum shape	**191.83**	**19.89**	**9.65**	**0.000**
Labrum shape	57.05	26.22	2.18	0.030
Palp shape	**-3.76**	**32.60**	**-0.12**	**0.908**
Cephalopharyngeal skeleton	**82.45**	**42.88**	**1.92**	**0.055**

Table 5.9 Assessment of significance of features for age estimation by regression analysis. The features in yellow had P > 0.05, indicating they did not play a significant role in the estimation of age, using this method. The features highlighted in green were the most significantly correlated to age in ADH (P < 0.001).

```
The regression equation is
Age in ADH = 3200 + 300 x Compound eye colour + 337 x Orbital/facial bristles
             + 153 x Antennae colour + 262 x Arista colour
             + 473 x Labella colour - 219 x Palp colour
             - 128 x Labrum colour + 276 x Wing Folding
             - 336 x Leg width at full length + 205 x Labellum shape
```

Equation 5.2 The truncated regression equation for pupal age estimation. This equation was created using the ten features most significantly correlated to age, as indicated by the original regression analysis.

5.2.5 Age estimation method testing

The manual age-range correlation and full length regression equation age estimation methods were stored in Microsoft Excel as the Pupal Age Estimator tool. This tool was first trialed semi-blind (SB1 and 2) on the test sets of pupae. In SB1, 15 pupae were selected blindly (by another researcher) at random from the test pupae used to establish the age estimation methods. These were separately analysed and ages estimated using both methods. By combining both methods a minimised age range was calculated using the highest minimum and lowest maximum ages. This was conducted to reduce the overall age/PMI estimate range given for each pupa (Table 5.10). Of the SB1 samples the ages of one and three pupae were incorrectly predicted using the regression equation with +/- 500 ADH or +/- 320 ADH errors respectively. The age estimate obtained using the manual method was correct (Table 5.10). Twenty pupae were selected for individual analysis in SB2, which resulted in correct age estimation of all pupae using the complete Pupal Age Estimator tool (both manual and regression methods) with an error of +/- 500 ADH. Fifteen of the twenty pupal ages were estimated correctly using the +/- 320 ADH error.

Table 5.10 Semi-blind age estimation SB1 & SB2. Semi-blind testing of all 35 test-set pupae was conducted. The predicted age range (manual method) and regression (& error) estimates are given. Shading indicates correct/incorrect age predictions with errors of +/- 320 ADH (green and pale red) and +/- 500 ADH (dark red).

SB1

Pupa No.	Predicted Age range		Regre-ssion	Regression +/- 320 ADH		Overall range		Range	Actual ADH
	Min	Max		Min	Max	Min	Max		
1	5735	6446	5893	5573	6213	5735	6213	478	5923
2	7716	9468	8510	8190	8830	8190	8830	640	8788
3	6610	7717	7279	6959	7599	6959	7599	640	7213
4	9835	11407	10699	10379	11019	10379	11019	640	10441
5	4414	5328	4786	4466	5106	4466	5106	640	4698
6	6057	6844	6293	5973	6613	6057	6613	556	6656
7	7298	7721	7655	7335	7975	7335	7721	386	7639
8	8954	9699	9034	8714	9354	8954	9354	400	9496
9	4614	5610	4893	4573	5213	4614	5213	599	4796
10	7298	8500	7755	7435	8075	7435	8075	640	7473
11	9835	11407	10726	10406	11046	10406	11046	640	10578
12	5036	5873	5812	5492	6132	5492	5873	381	5525
13	9370	11407	10268	9948	10588	9948	10588	640	11171
14	4614	5610	4893	4573	5213	4614	5213	599	5052
15	4414	5328	4786	4466	5106	4466	5106	640	4694

SB2

Pupa No.	Predicted Age range		Regre-ssion	Regression +/- 320 ADH		Overall range		Range	Actual ADH
	Min	Max		Min	Max	Min	Max		
1	9280	10086	9780	9460	10100	9460	10086	626	9775
2	8954	9842	9013	8693	9333	8954	9333	379	9230
3	7298	8638	7960	7640	8280	7640	8280	640	7608
4	4414	5328	4786	4466	5106	4466	5106	640	4698
5	8143	9558	8785	8465	9105	8465	9105	640	8615
6	3862	5054	4450	4130	4770	4130	4770	640	4267
7	5194	5880	5571	5251	5891	5251	5880	629	5392
8	5644	6844	6233	5913	6553	5913	6553	640	6224
9	8143	9126	8524	8204	8844	8204	8844	640	8334
10	3862	5054	4450	4130	4770	4130	4770	640	4414
11	9370	10267	9986	9666	10306	9666	10267	601	9749
12	8954	9842	9044	8724	9364	8954	9364	410	9496
13	4614	5610	4893	4573	5213	4614	5213	599	4837
14	5735	6844	6290	5970	6610	5970	6610	640	5962
15	9370	10125	9612	9292	9932	9370	9932	562	9897
16	9835	11407	10726	10406	11046	10406	11046	640	11141
17	4614	5610	4893	4573	5213	4614	5213	599	4787
18	6746	7876	7302	6982	7622	6982	7622	640	7203
19	9835	11407	10699	10379	11019	10379	11019	640	10303
20	6742	7717	7127	6807	7447	6807	7447	640	7213

In summary, age was estimated with the following success rates:

- The manual age-range correlation method = 100%
- Regression/overall range with +/- 500 ADH = 97% (34/35 pupae)
- Regression/overall range with +/- 320 ADH = 77% (27/35 pupae)

To further test the Pupal Age Estimator, two independent blind sampling trials were conducted (B1 & B2). For each trial 10-15 pupae were collected at ten intervals throughout the pupal stage. Sets of pupae were used to mimic crime scene collection procedures in which age estimates are made from multiple individuals rather than a single pupa. Initially, the ADH ages of all pupae in the set were estimated individually using both the manual method and full regression equation. The overall age range for each pupa was derived from the overlapping age ranges obtained from the manual and regression methods (+/- 320 ADH). For each set of pupae the mean regression age was calculated from all individuals. The maximum and mean pupal age ranges were also determined from the manual method, using the minimum and maximum ages and the mean of all min/max ages respectively (Table 5.11 and Fig. 5.32). This process was repeated for all time points for each trial (Table 5.12). Ages as a percentage of the lifecycle were also derived.

The blind samples were used to calculate the error of the regression equation. The mean and the standard error of the residual differences between the predicted and actual ages of 244 pupae were calculated and used to work out 95% confidence intervals (296 +/- 22 ADH). This gave a maximum error of +/- 320 ADH.

Table 5.11 Individual pupal age estimation within a sample set. The predicted ages of 15 pupae collected at one of the sampling times are shown. Dead pupae were excluded from the analysis. The overall range was derived from the overlapping range from the manual and regression methods. The pupal age ranges obtained from the manual method are combined into mean and maximum ranges for the sample set.

Sample 1

Pupa No.	Age range		Regre-ssion	Regression +/- 320 ADH		Overall range	
	Min	Max		Min	Max	Min	Max
1	7716	9468	8510	8190	8830	8190	8830
2	7716	9468	8510	8190	8830	8190	8830
3	7716	9468	8510	8190	8830	8190	8830
4	8143	9558	8785	8465	9105	8465	9105
5	8143	9558	8785	8465	9105	8465	9105
6	7716	9468	8510	8190	8830	8190	8830
7	7716	9468	8510	8190	8830	8190	8830
8	7716	8500	8305	7985	8625	7985	8500
9	7716	9468	8510	8190	8830	8190	8830
10	7716	9468	8510	8190	8830	8190	8830
11	7716	9468	8510	8190	8830	8190	8830
12	7716	9468	8510	8190	8830	8190	8830
13	7716	9126	8249	7929	8569	7929	8569
14	Dead						
15	Dead						
Mean range	7782	9381	8516	8196	8836	8196	8827
Max range	7716	9558		7929	9105	7929	9105

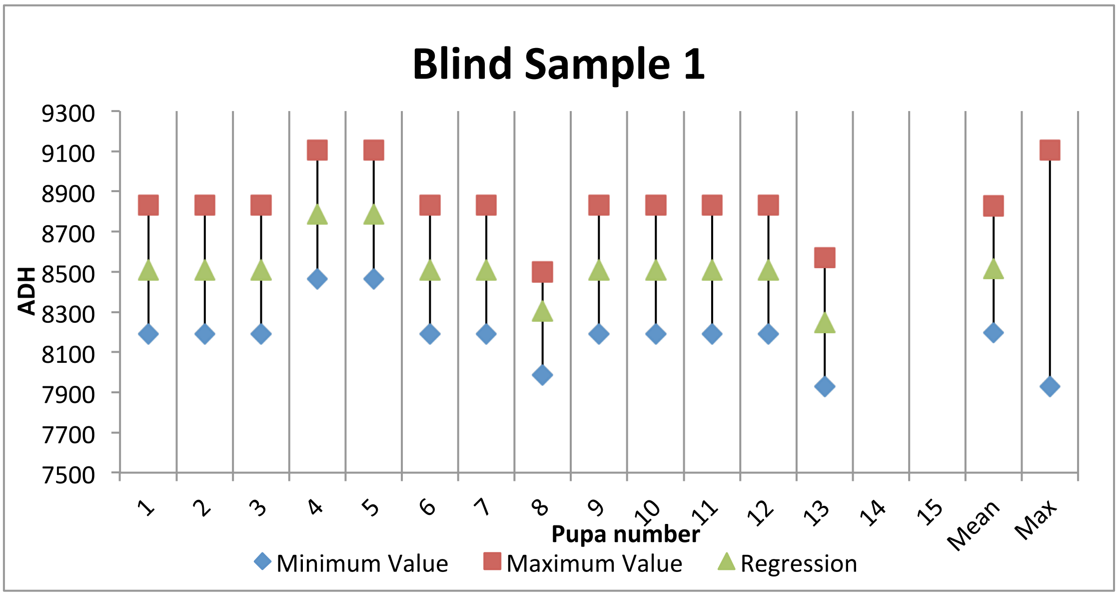

Figure 5.32 Comparison of pupal ages in blind sample set 1. The overall age ranges of each pupa in the first sample set are displayed alongside each other, with the mean and maximum overall range shown.

In B1 (Table 5.12a), all ten sample set ages were predicted correctly using the maximum age range and nine of ten by the mean age ranges. The difference between actual and predicted ADH (from mean regression of the set of pupae) was within +/- 320 ADH for all of the sets. The predicted lifecycle % was always within +/- 5% of the actual lifecycle %. In B2 (Table 5.12b), eight of ten pupal ages were predicted correctly using the maximum range, however only 20% were predicted using the mean range. 90% of pupal ages were predicted +/- 500 ADH of the mean regression and within +/- 5%. 30% of ages were predicted within +/- 320 ADH.

Predicted ages for B2 were less accurate than B1. In both trials ages were calculated using accumulated temperatures measured by iButtons placed in the larval mass. These are easily moved by the larvae, which may cause errors in ADH age calculation. Instead, the mean growth room temperature (21.62°C) was used to calculate age (Table 5.13); this may represent a more accurate mean growth temperature for all larvae. Despite the small temperature difference between this and the mean colony temperature (21.37°C), using 21.62°C improved B2 age estimation success. 80% of ages were predicted correctly using the mean range, and all were within +/- 5% of the actual age. Unfortunately, using this approach for B1 data resulted in decreased estimation accuracy using the mean range, which reduced from 100% to 60% (data not shown). This indicates the importance of accurate developmental temperature measurement.

Table 5.12 Blind testing of age predictions. Ages of 10-15 pupae collected in ten sets in two blind sample trials (B1: a, B2: b) were estimated using the Pupal Age Estimator (manual and regression equation (+/- 320 ADH error) methods). The maximum and mean overall ranges are shown for each sample set. Actual age in ADH and lifecycle/pupal stage % are highlighted in grey. Green shading highlights correctly predicted ages within the age range (maximum or mean) or if the difference between actual and predicted age was within +/- 500 ADH or 5%. Red shading indicates incorrectly predicted ages (not within ranges) or a difference to the actual age of greater than +/- 320 ADH (pale red) or +/- 500 ADH and 5% (dark red).

a

Sample #	Maximum range			Mean range			Mean regression (ADH)	Predict. lifecycle %	Actual Age (ADH)	Actual lifecycle %	Actual pupal stage %	Diff. (ADH)	Diff. (%)
	Start ADH	End ADH	Range (ADH)	Start ADH	End ADH	Range (ADH)							
1	7929	9105	1176	8196	8827	630	8516	75.0	8617	75.9	63.2	100	1
2	6033	7051	1018	6206	6831	625	6521	57.4	6629	58.4	36.5	108	1
3	9439	10267	828	9487	10078	590	9782	86.1	9621	84.7	76.7	-162	-1
4	8465	10229	1764	8758	9312	554	8992	79.2	9124	80.3	70.0	132	1
5	7466	8830	1364	7804	8424	620	8106	71.4	8229	72.4	58.0	123	1
6	5550	6423	873	5629	6213	584	5949	52.4	6133	54.0	29.8	184	2
7	7929	9105	1176	8338	8978	640	8658	76.2	8731	76.9	64.7	73	1
8	8709	9984	1275	9025	9603	578	9294	81.8	9232	81.3	71.5	-61	-1
9	4466	5873	1407	5081	5643	562	5386	47.4	5677	50.0	23.7	291	3
10	7114	8089	975	7233	7700	467	7548	66.5	7623	67.1	49.8	75	1

b

Sample #	Maximum range			Mean range			Mean regression (ADH)	Predict. lifecycle %	Actual Age in ADH	Actual lifecycle %	Actual pupal stage %	Diff. (ADH)	Diff. (%)
	Start ADH	End ADH	Range (ADH)	Start ADH	End ADH	Range (ADH)							
1	5735	7485	1750	6283	6892	610	6576	57.9	6599	58.10	36.1	23	0
2	8465	9781	1316	8720	9345	625	9025	79.5	8635	76.03	63.4	-390	-3
3	8816	10125	1309	9326	9843	517	9523	83.8	9150	80.56	70.4	-373	-3
4	4466	5213	747	4555	5158	603	4838	42.6	4723	41.58	10.9	-115	-1
5	7985	9105	1120	8129	8714	584	8449	74.4	8124	71.53	56.6	-325	-3
6	7466	9105	1639	8214	8827	613	8532	75.1	8213	72.31	57.8	-319	-3
7	9948	11046	1098	10301	10941	640	10621	93.5	9822	86.48	79.4	-799	-7
8	8726	10025	1299	8961	9515	554	9208	81.1	8768	77.20	65.2	-440	-4
9	5251	6423	1171	5402	5930	527	5722	50.4	5222	45.98	17.6	-500	-4
10	7074	8350	1276	7201	7819	618	7519	66.2	7188	63.29	44.0	-331	-3

Table 5.13 Predicted ages of B2 pupae using growth room temperature. Age estimations for each sample set in B2 and comparisons to actual ages in ADH and lifecycle % were calculated as before. The actual age in ADH was calculated using the mean growth room temperature, rather than the individual temperatures monitored every 15 minutes over the lifecycle as previously.

Sample #	Maximum range			Mean range			Mean regression (ADH)	Predict. lifecycle %	Actual Age in ADH	Actual lifecycle %	Actual pupal stage %	Diff. (ADH)	Diff. (%)
	Start ADH	End ADH	Range (ADH)	Start ADH	End ADH	Range (ADH)							
1	5735	7485	1750	6283	6892	610	6576	57.9	6778	59.67	38.5	202	2
2	8465	9781	1316	8720	9345	625	9025	79.5	8828	77.73	66.0	-197	-2
3	8816	10125	1309	9326	9843	517	9523	83.8	9334	82.18	72.8	-188	-2
4	4466	5213	747	4555	5158	603	4838	42.6	4773	42.02	11.6	-66	-1
5	7985	9105	1120	8129	8714	584	8449	74.4	8318	73.24	59.2	-131	-1
6	7466	9105	1639	8214	8827	613	8532	75.1	8405	74.00	60.3	-128	-1
7	9948	11046	1098	10301	10941	640	10621	93.5	9999	88.04	81.8	-622	-5
8	8726	10025	1299	8961	9515	554	9208	81.1	8956	78.85	67.7	-252	-2
9	5251	6423	1171	5402	5930	527	5722	50.4	5304	46.70	18.7	-418	-4
10	7074	8350	1276	7201	7819	618	7519	66.2	7383	65.00	46.6	-136	-1

Combining results from all 20 pupal sets, using original temperatures, it was therefore concluded that accurate age estimation was achieved with the following success rates:

- Maximum overall range = 90%
- Mean overall range = 55%
- Mean regression +/- 320 ADH = 65%
- Mean regression +/- 500 ADH = 95%
- Mean regression +/- 5% (lifecycle) = 95%

5.3 Discussion

Accurate and reliable pupal age estimation is a prerequisite for successful PMI estimation. The data presented here indicate age estimation using external morphology with an accuracy of +/- 500 ADH is consistently achieved, using a combination of two methods in the Pupal Age Estimator.

5.3.1 Pupal age calculation

Pupal ages were accurately calculated using temperatures recorded every 15 minutes to minimize averaging effects that can reduce the accuracy of PMI estimates (Amendt *et al.,* 2007; Rankin & Harvey, Pers. comm.). As the temperature of larval masses can increase significantly above the ambient (Anderson & VanLaerhoven 1996; Slone & Gruner 2007; Amendt *et al.,* 2007), the high resolution of temperature recording allowed corresponding ADH changes to be calculated.

As with many other developmental studies this work was conducted at a constant ambient temperature (Anderson 2000; Greenberg 1991; Grassberger & Reiter 2001). The rate of development alters under constant and fluctuating temperatures (Anderson, 2000; Erzinclioglu, 1996). This affects the use of ADH to calculate age, the principle of which is that each stage requires a set accumulation of heat to reach regardless of temperature within developmental limits. The results of this study are therefore accurate for pupal age estimation occurring at a mean developmental temperature of approximately 22°C.

The precision of the temperature measurement is an important factor in age calculation. Calculation of ADH ages using the mean environmental (growth room) temperature recorded throughout the pupal stage (as is often carried out at crime scenes) gave more accurate age estimates for B2, indicating possible errors in colony temperature measurement. The growth room temperature was only 0.25°C higher than the mean colony temperature, highlighting the need for precise temperature measurement of the samples throughout all stages, and multiple replicates to ensure reliability and validity of the data set. Accurate ambient and colony temperatures must also be taken at the crime scene. Infra-red thermometers may indicate actual developmental temperatures more precisely than contact thermometers (as these are often shifted around the larval mass), however larvae would be repeatedly disturbed, affecting development (personal observation). Controlling sample sizes to reduce larval mass (as conducted here) may aid in controlling temperature fluctuations and in turn error in temperature measurement.

In this study, an LDT of 0°C was applied to ADH ages, to allow location-specific *C. vicina* LDTs to be used, such as 1°C for London, UK or 2°C in St Petersburg, Russia (Donovan *et al.,* 2006; Marchenko 2001). There are various ways of estimating LDT, such as using the observed minimum developmental temperature or by calculation from developmental curves by using the x-intercept value (Higley and Haskell in Byrd & Castner 2009). There is general disagreement about what LDT should be incorporated and variable results are gained when the same LDTs are used from different studies (VanLaerhoven 2008). This dataset was therefore constructed to allow for the discrepancies in the field. To obtain the ADH ages for the development of each feature using a specific LDT Equation 5.3 should be used.

$$\mathrm{ADH\ [with\ LDT]} = \mathrm{ADH\ [0°C]\ x}\ \frac{22.5°\mathrm{C} - \mathrm{LDT}}{22.5°\mathrm{C}}$$

Equation 5.3. Incorporation of LDT into existing pupal development data. The data presented include an LDT of 0°C. To calculate ADH values for pupae with a known LDT value, this equation should be used. The ADH [0°C] value is that presented here. 22.5°C is the mean developmental temperature for T1 and T2.

5.3.2 External morphological development timeline

Analysis of 23 meta-morphological changes observed in the large calibration data set enabled production of a detailed developmental timeline, suitable for age and PMI estimation. The head showed the greatest number of readily monitored changes in individual features during the pupal stage. However, some of the most difficult features to observe reliably were the mouthparts (labellum, labrum and maxillary palps). Development of shape and size of these white features was difficult to distinguish from the overall white colour of the head and thorax upon which they were located. Movement of the structures was required to observe differences, however due to their delicate nature damage was difficult to avoid. The potential for damage to these regions is exacerbated by their proximity to piercing sites at the preservation stage. Complete destruction was not evident in any pupae analysed, however in some pupae the mouthparts were distorted or pushed to the side. The damage presumably occurred as the pin was pushed through and whilst analysis was not prevented in any of these pupae it was made more difficult. Piercing of the head is necessary for full preservative preservation (Chapter 4), and with numerous important features, minimisation of damage is difficult.

To permit comparison to other dipteran studies, pupal ages were described as a percentage through the pupal stage. Limited similarity to previous timelines of *C. vicina* was noted (Lowne 1895; Finell & Jarvilehto 1983), for example eye colouration began from 35 or 82% through the pupal stage in previous studies, compared to 48-68% in the present study (Table 5.14). These differences may be explained by older methods of temperature measurement or few sampling intervals. Age ranges for feature development observed in this study were most similar to those described for *P. regina* and *D. melanogaster* (Table 5.14) (Greenberg 1991; Bainbridge & Bownes

Table 5.14 Timeline comparison with previous studies. The % TPS for the current study were compared to *Phormia regina* (Greenberg 1991), *Drosophila melanogaster* (Bainbridge & Bownes 1981), *Sarcophaga bullata* (Sivasubramanian & Biagi 1983) and *Calliphora vicina* (Finell & Jarvilehto 1983; Lowne 1895). Green/red shading indicates agreement/disagreement from the current study. Previous studies are shown in order of similarity to the current work. '–' indicates data was not available.

Development	**Current Study**	**F&J *C. vicina***	**Lowne *C. vicina***	**Greenberg *P. regina***	**B&B *D.melano-gaster***	**S&B *S. bullata***
Untanned pupa	0	0	0	0	0	0
Cryptocephalic pupa	5-15	-	18-27	9	8	14
Head everted	13-15	-	36	16	9	18
Eyes white, antennae and bristles white	15-83	15	-	-	9-33	-
Abdomen segmented	16-28	-	-	40	-	-
No setae	30-75	-	45.5	-	<75	-
Eye colouration begins	48-68	35	82	56	44	73
Eyes red, macrochetae start to tan	56-81	70	-	-	75	82
Eyes red/brown, tanned antennae and bristles	56-100	95	-	-	76-78	-
All chetae tanned	67-96	-	-	81	75-82	91
Oral lobe development complete	74-96	-	64	-	-	-
Development complete	100	100	100	100	100	100

1981), indicating intra- and inter-family similarities in metamorphosis. These similarities are useful for comparison of similarly-staged individuals for developmental studies. For PMI estimation ADH and percentage lifecycle/pupal stage timelines are needed for all forensically important species.

Morphological age estimation using the features proposed here is based on subjective analysis, resulting in discrepancies in categorisation and therefore errors in age estimation. Errors are minimised by using large numbers of features (such as the 23 used here), and also the combination of methods provides a check on the estimate given. To reduce subjectivity further, age estimation using quantitative methods such as developmental gene expression has been previously trialled and is performed (Chapter 7) (Ames *et al.,* 2006; Zehner *et al.,* 2009; Tarone & Foran 2011).

5.3.3 Development and testing of age estimation methods

Methods of pupal age estimation suitable for application to PMI estimation have not been previously described. Hitherto only limited development timeline data have been available and these must be interpreted and used with caution. Entirely novel methods are developed here for this purpose.

Two error ranges are proposed; +/- 500 ADH based on lifecycle length variation observed in this study (Chapter 3.2.3) and +/- 320 ADH based on statistical analysis of residual values from blind samples. These errors are applied to the individual pupal age estimates obtained using the regression equation and are subsequently incorporated into the maximum and mean ranges given for sample sets (BST1 and 2). Age estimation using the manual age-range correlation method with the +/- 320 ADH error proved to be 90% accurate for individual and groups of pupae of similar age (as found at crime scenes). This was reduced to 55% accuracy for the mean range. In addition, the mean regression was accurate to +/- 500 ADH in 95% pupae, compared to 65% for +/- 320 ADH error. These data suggest that whilst the residuals indicate an error of +/- 320 ADH is suitable, actual analysis of data indicate that the age estimate window applied should be +/- 500 ADH to incorporate >90% of samples. This larger error was derived from the natural variation in lifecycle range (Chapter 3), which correlates to the maximum and minimum ages of morphological development observation in all 1494 pupae. The residual error was only obtained from 244 pupae; a larger sample set may increase this error as it could include a larger age range with a wider range of residual values.

Whilst no published data was found describing the use of this method for this purpose elsewhere, the regression equation method developed is similar to the most widely accepted method of age determination for teeth used by forensic odontologists. Originally, 6 age-correlated variables were used to develop a single multiple component regression equation (Johanson in Willems, 2001), however recent improvements to age estimation of teeth have been achieved using multiple regression formulae constructed from different sample populations (such as Indian and Italian) (Saxena 2011). This suggests that though the regression equation for pupal age estimation may be accurate for the current (local) population and under similar developmental conditions, it might require supplementation with data from further developmental studies from different *C. vicina* populations for more universal application.

Regression analysis also identifies the most important features for age estimation, reducing the total number of required observations from 23 to 10. All features except leg width at full length develop over the majority of the pupal stage, providing a large range of age estimation data. Leg width only develops within the first 5500 ADH, when few other features develop, thus being an important indicator of early developmental stages. With the eye colour chart produced, and mouthparts being primarily assessed for colour change, the equation minimizes the need for analysis of form, which is more difficult to observe and categorise. However, with its lower adjusted R^2 value of 97.8% and only 80% success rate, the shortened regression equation is less suitable for age estimation than the full-length equation. Should damage to non-significant features occur, age can still be estimated using the truncated equation. Use of the age range method employing only the significant features has yet to be trialled for accuracy as this would require extensive development of the Pupal Age Estimator tool but it is likely that fewer variables would result in larger age range estimates.

5.4 Conclusion

Prior to this work it was anticipated that based on the limits of natural variation, the age of *C.vicina* pupae could be estimated to within ~500 ADH (24 hours at an average of 22°C) of the actual age. By analysing the development of 23 morphological features and using a combination of both the age range and regression analysis methods (the Pupal Age Estimator), it was possible to estimate age of *C. vicina* pupae sample sets to within +/- 500 ADH or +/- 5% of their actual age with 95% reliability. 90% of sample set ages were estimated correctly using the maximum overall range, which had a maximum error window of 1800 ADH.

Chapter 6 – Internal morphological timeline of pupal development

As presented in Chapter 5, pupal age estimation based on external morphological development is achievable to a high degree of accuracy, with an error window of +/- 500 ADH. Alongside changes in external morphology, the internal anatomy undergoes substantial metamorphic development, which has the potential to provide further developmental markers for age and PMI estimation.

6.1 Introduction

6.1.1 Previous research

Metamorphosis, as previously described, involves histolysis of larval tissue and histogenesis of adult structures *de novo*, from both imaginal discs and existing tissue. As with external morphology, the most extensive research into internal morphological development has been conducted on the model organism, *Drosophila melanogaster*, using a variety of analytical techniques.

6.1.1.1 Dissection and histology

Dissection and histology were commonly used for examination of internal morphological development, prior to the development of more advanced methods (Chapter 6.1.1.2). In *Drosophila melanogaster*, the development of the reproductive organs and tracheal systems (Dobzhansky (1930) in Demerec, 1950; Whitten, 1957), leg and wing muscle and the digestive system (Robertson 1936) (Table 6.1) have been described using these techniques. These and other published timelines of morphology enable a) the age of a pupa to be approximated (Bodenstein (1950) in Demerec (1950)) or b) selection of living pupae at a particular stage of development (Bainbridge & Bownes 1981) (Table 6.1). All studies describe morphology to a temporal resolution of a few hours, with only that by Bainbridge and Bownes indicating windows of variation for each feature described and providing a comprehensive collection of images for feature identification. The similarities in metamorphosis amongst the Diptera suggest the *D. melanogaster* studies can be used to indicate candidate features for observation in *C. vicina*.

Work conducted on *Musca domestica* and *Sarcophaga bullata*, which are more closely related to *C. vicina*, only described the final internal anatomical form of the imago (not metamorphosis) and development until 96 hours after puparium formation respectively (Hewitt 1907; Fraenkel & Bhaskaran 1973). Feature identification is again facilitated using these data, however insufficient detail is provided for age estimation of these species.

Table 6.1 A comparison between the internal morphological developments observed in *Drosophila melanogaster*. Development noted through the translucent puparium are noted alongside age in hours and designated stage. **External development** indicates points at which only external morphological development is occurring (see Table 5.3).

Robertson (1936)		**Bainbridge & Bownes (1981)**		
Age/hrs	**Feature**	**Stage**	**Age/hrs**	**Feature**
0	Puparium formation	L2	0	Pupation
1	Imaginal discs increase in size	P1	1.7	
2	Gut replacement cells proliferate			
3	Gut epithelium separates from basement membrane			
4	Anterior segment muscles histolyse, mid gut ends close	P2	4.8	Heart stops pumping, gas bubble visible within abdomen
5	Lumen of gut larger	P3	5.8	**External development**
6	Wing muscle development starts			
7	Peristalsis visible	P4i	8	Abdominal peristalsis visible
8		p4ii	8.2	Bubble in puparium moves towards anterior end
9		P5i	9.3	Malpighian tubules move from the thorax to the abdomen.
10	Epithelium of foregut replaced			
11	Air bubble disappears, trachea shed			
11.5				
12	Peristalsis stopped	P5ii	18.7	Malpighian tubules become prominent and green
13	Hindgut shortened			
14	Most of abdominal muscles gone, crop forms			
15	Salivary glands break into pieces			
18	Differentiation of wing muscle			
21	Rectal pouch and proventriculus appear			
24	Leg muscle begins to develop, midgut spindle shaped	P6	32.4	Yellow body appears between anterior ends of malpighian tubules.
27	Wing muscle a third formed			
42	Wing muscle two-thirds formed	P7	44.3	**External development**
54	Striations appear in wing muscle	P8	56.6	
60	Leg muscle well formed			
84	Wing muscle complete	P13	81.9	
		P14	91.5	Meconium appears
96	Meconium voided, emergence	P15i	99.6	Tergites become tanned, ptilinum expands
		P15ii	100	Eclosion complete

In the Calliphoridae, various timelines of development have been described. The earliest study of *Musca vomitoria* (*Calliphora vomitoria*) development details few morphological changes (Table 6.2) (Weissman 1874a) and lacks images and information on rearing conditions to allow accurate age estimation. *C. vicina* metamorphosis was also studied around a similar time; the age of the work limits obtainable information to summarised descriptions of gut (Table 6.3), reproductive system and muscle development, correlated to age in days (Perez 1910; Lowne 1895). Since temperatures were not recorded, developments cannot be correlated to physiological time. However, the line drawings presented offer valuable morphological information and may identify important indicators of age; for example the corps jaune (Fig. 6.1) which is initially located in the thorax and migrates to the abdomen at ~13 days. It comprises degenerated larval salivary glands, epithelial cells, gastric caecae, muscle and fat body, indicating the end of histolysis of these tissues (Perez 1910).

Table 6.2 Development of *M. vomitoria* throughout metamorphosis. The internal development of various tissues in *C. vomitoria* as described by Weissman (1874), related to approximate age in days.

Age (Day)	Feature
1-2	Destruction of muscles, pharynx, oesophagus and stomach
3-4	Tracheal system forming, formation of brain and anterior gut, destruction of posterior gut, growth of appendages
5-6	Antennae formed
7	Thoracic muscle begins to form, small intestine and rectum form
7-12	Compound eye neurones extend from brain
12-18	Dorsal system remodelled, tracheal system develops, sclerotisation of features
18-20	Development complete, emergence.

Table 6.3. Histological analysis in *C.erythrocephala.* The table gives a summary of the work carried out by Perez (1910) on the metamorphosis of the pupal/adult digestive system in *C. vicina*. The full table includes other parts of the pupa including respiratory systems and muscle.

Age (days)	Foregut	Midgut	Hindgut
1	Larval crop disappeared	Imaginal cells visible	Imaginal cells visible
2	Crop imaginal cells visible	Formation of corpus luteum (see figure 6.1)	Degeneration of larval anus
6	Adult crop developing	Ventriculus now appears tubular in structure	Rearrangement of the rectum
13	Folding of crop wall	Corpus luteum moves to abdomen	Invagination of the rectal wall
17	Differentiation complete	Differentiation complete	Accumulation of meconium

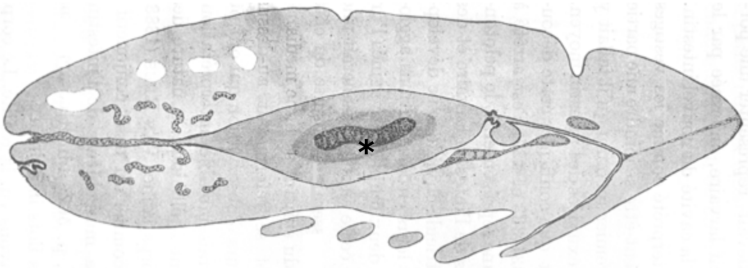

Figure 6.1 The ‘corps jaune’ in the pupa. Section of a 3 day old pupa showing the development of the corps jaune (*) in the metathoracic area (Perez, 1910).

Barritt & Birt (1971) produced a developmental timeline for *Lucilia cuprina* (Table 6.4). Pupae were reared at 30°C and examined at regular intervals after cessation of larval movement until eclosion. Muscle histolysis and generation were well detailed, and some information on gut development was given. Due to the close evolutionary relationship between the species these data could be used in comparison with *C. vicina* for developmental order. It may aid in the age estimation of *L. cuprina* pupae, however the temporal resolution is low.

Recnt histological analysis has been prevented by the lack of current and suitable protocols. Previously, pupae have been fixed by hot-water-killing (HWK) or placement in Carnoys or Bouins solution (Bodenstein (1950) in Demerec (1950)). HWK is preferred as it is more readily available, less hazardous and does not cause excessive hardening (Chapter 4). Pupae then required bisection (Chapter 4) or dissection of individual organs for adequate solution penetration, prior to embedding in paraffin wax and sectioning at 7-10 μm (Lowne 1895; Sprey 1970). The addition of egg albumin or glycerine to the water bath assisted section adhesion (Lowne 1895; Davies & Harvey 2012). Many stains have been utilised to highlight different tissues, such as Lang’s picrocarmine and haematoxylin & eosin (Lowne 1895; Sprey 1970; Davies & Harvey 2012) for general tissue structure, the paraldehyde-fuchsin method for chitin (Sprey 1970). The abundance of glycogen in the everting leg was observed using PAS stain (Fig. 6.2) (Sprey 1970). Brain and compound eye development was observed using the Allochrome method (Fig. 6.3) which highlighted development between juvenile, histogenic and premature pupae (representing 15, 35 and 70% development points of the pupal stage respectively) as another possible morphological age marker (Finell & Jarvilehto 1983). For age estimation of pupae for forensic purposes, a general all-purpose and readily available stain is preferred, such as haematoxylin and eosin (Davies & Harvey 2012).

Table 6.4 Histological development of *L. cuprina* throughout metamorphosis. The internal development of various tissues as described by Barritt and Birt (1970), correlated to age in hours from puparium formation.

Age (hours)	Feature
Wandering	• Increasing number of granular haemocytes • Oenocytes visible • Imaginal discs grow rapidly
0-8	• Granular haemocytes more dispersed and in greater numbers • Larval muscle breakdown • Salivary glands start to degenerate
8-12	• Imaginal discs and thorax everted • Thorax contains remains of crop, salivary gland, muscle and fat bodies • Imaginal epidermis forming
12-16	• Imaginal muscle development and abdominal muscle breakdown • Oesophagus shortened • Foregut muscle histolysis and imaginal cells present • Pupal cuticle distinct and and head everted
16-24	• Midgut closed off at each end • 'Corps jaune' (Perez, 1910) contains gastric caecae cells • Hindgut shortened • Salivary glands smaller • Imaginal epidermal cells cover abdomen
24-40	• Thoracic and leg muscle growth • Small amount of imaginal muscle in head and abdomen • Salivary glands disintegrated, • Adult proventriculus clearly visible • Epithelium is imaginal throughout
40-66	• Striated larval muscles disintigrated • Dorsal longitudinal flight muscle extended in length • Leg muscle developing • Dorsal thoracic profile beginning to take shape.
66-96	• Further flight muscle development • Imaginal cuticle formed and thickness increasing • Eye pigment develops • Legs segmented with setae and tarsal claws
Until emergence	• Continued growth of all existing structures • Striated imaginal thoracic and abdominal muscle • Air sacs and crop well developed • Flight muscle at full volume

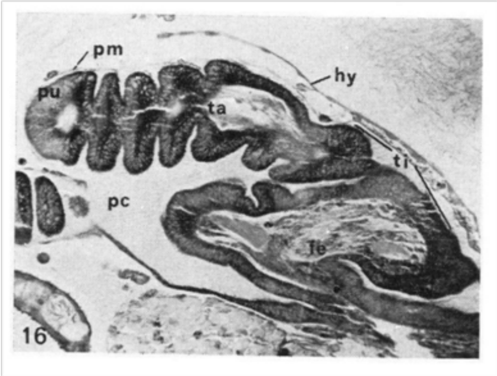

Figure 6.2 *C. vicina* cryptocephalic pupal leg. The everted imaginal leg disc in a cryptocephalic pupa is shown to have abundant glycogen content in most parts of the disc (dark PAS staining), with none in the pulvilli (pu). pm = peripodal membrane, hy = hypoderm, pc = peripodal cavity, ta = tarsalia, ti = tibia, fe = femur (Sprey 1970).

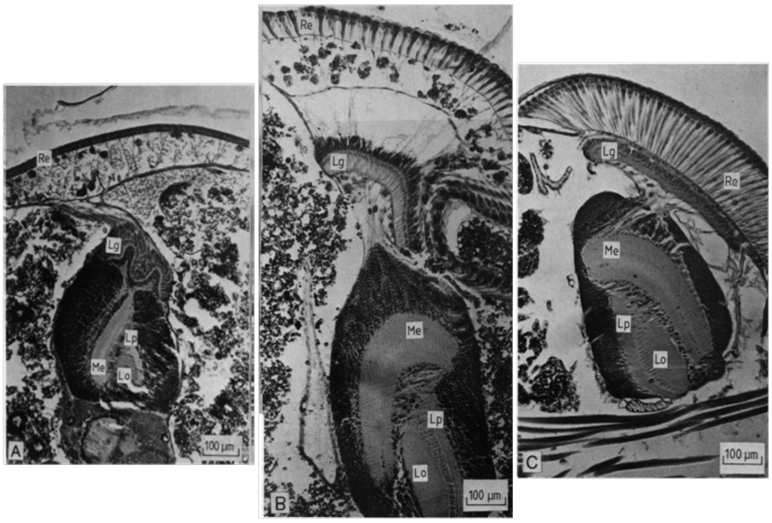

Figure 6.3 *C. vicina* compound eye development. Sections of a juvenile pupa (A), histogenic pupa (B) and premature pupa (C) indicate changes in eye and brain development over time. The retinal layer (Re) is initially thin, with cells growing centrally over time. Lg = The lamina ganglionaris (Lg), initially in the brain area, migrates towards the retina. The medulla (Me) initially lies anteriorly, however turns 90° to a lateral position. Lo = lobula, Lp = lobular plate (Finell & Jarvilehto 1983).

Additional detail is revealed by immunohistochemical staining methods. Primary (1°) antibodies raised against specific molecules and proteins bind to their counterparts on histological sections. Enzyme conjugated secondary (2°) antibodies are then used to highlight 1° antibody locations typically by the precipitation of a coloured product or fluorescent labelling of the 2° antibody. Ommatidial cell plasma membrane development in *D. melanogaster* pupae (Grzeschik & Knust 2005) has been observed using Anti-DE-cadherin (1°) and Cy2/3 (2°) antibodies (Fig. 6.4).

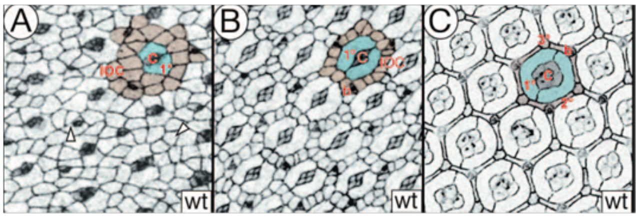

Figure 6.4. The development of ommatidial cells in pupal imaginal discs. Immunohistochemistry highlights changes in these cells over time, with pigment cells (1° (blue shading), 2° and 3°), cone (c), bristle cells (b) and inter-ommatidial cells (brown shading) shown (Grzeschik & Knust, 2005).

Fluorescent staining has also been used to identify specific structures in *Drosophila* whole mounts, such as the *omb* domain in imaginal discs, indicating a developmental timeline (Fig 6.5) (Taylor & Adler 2008).

Although not used to observe development, antibody staining has been used in *C. vicina*. The α5-IgG fluorescent antibody highlights the distribution of Na+/K+-ATPase α-subunit in cryogenic sections of salivary gland tissue. Fluorescent phalloidin staining indicates F-actin for comparison (Fig. 6.6) (Zimmermann 2003; see also Rotte *et al.,* 2008). Also, biotinlated IgG 2° antibodies detected using the avidin-biotin-peroxidase complex revealed the incorporation of morphine and codeine (detected by 1° antibody) in third instar larval cuticle (Bourel *et al.,* 2001).

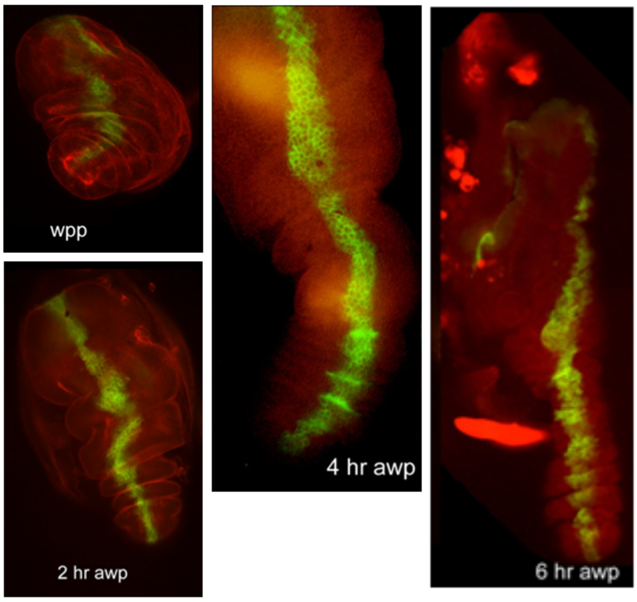

Figure 6.5 *Drosophila* leg development. Whole mount fluorescent staining indicates the *omb* domain (optomotor blind gene - green), which along with F-actin staining (red) aided visualisation of pupal leg development (Taylor & Adler 2008).

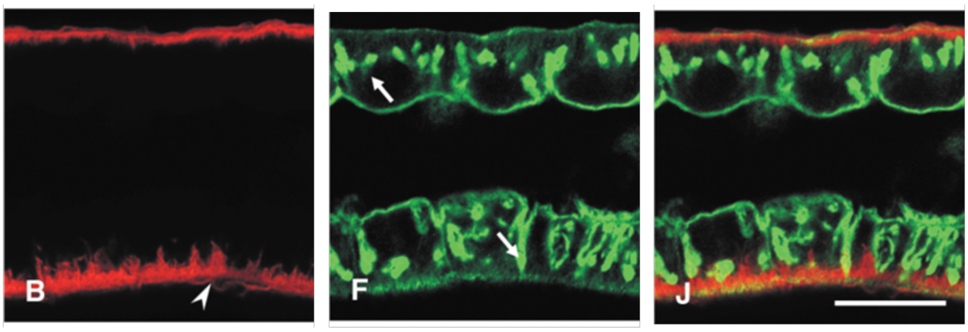

Figure 6.6 *C. vicina* salivary glands imaged using fluorescent antibody staining. The sodium-potassium pump (red) is shown to be restricted to the basolateral membranes of the salivary gland cells (green). Primary antibodies visualised using Cy3 secondary antibodies: Red = Na+/K+-ATPase α-subunit, green = F-Actin (Zimmermann 2003).

Immunohistochemistry approaches are limited by the availability of suitable antibodies for *C. vicina*. The absence of genomic data makes it difficult to generate antibodies from the derived protein sequence. Fluorescent staining methods require the use of genetically modified organisms, therefore although *C. vicina* pupal development could possibly be visualized in this manner it is unsuitable for age estimation of crime scene samples. Therefore, well established histological methods are more currently suitable and have been used in this investigation to document the development of a detailed internal morphological timeline of *C. vicina*. However, it must be considered that the accuracy of age estimation may be limited by the risk of loss of tissue when selecting sections for staining, causing features to be missed.

6.1.1.2 Live imaging

Observation of whole living or preserved pupae using magnetic resonance imaging, x-rays or optical coherence tomography (OCT) avoids tissue loss through sectioning. Traditionally, these methods have been used for medical imaging and various adaptations have been made for use on smaller samples. Live imaging techniques also permit further analyses or rearing on to the adult stage.

X-ray microscopy has developed from producing a single image of the developing pupa (Davies *et al.,* 1988) to a stacked, 3D rendered approach using micro computed tomography (CT) (Greco *et al.,* 2006; Metscher 2009). Live imaging is possible, and this enables rearing to the adult stage (to back-calculate PMI). However, greater resolution has been achieved with freeze-dried insects (Davies *et al.,* 1988) or even more so with phosphotungstic acid (PTA) staining (Metscher 2009) of preserved specimens (Fig. 6.7) though processing pupae in PTA may hinder molecular species ID or age estimation based on external morphology.

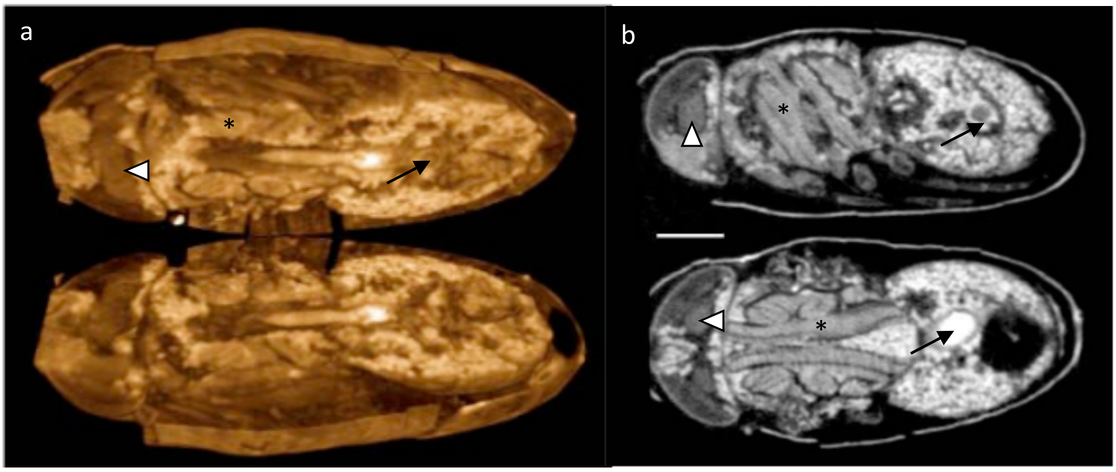

Figure 6.7. MicroCT scan of a fully developed *C. vicina* pupa. The pupa was fixed with hot ethanol and stained with PTA (after piercing). Scale bar = 1mm. Scan was produced using SkyScan 1174 scan, with a voxel size (resolution) of 7.7μM. a) is a volume rendered 3D image of the pupa, and b) are sagittal and transverse 2D sections (Metscher 2009). * = thoracic muscle, arrow head = brain tissue, arrow = gut morphology.

Magnetic resonance microscopy (MRM) uses nuclear magnetic resonance (NMR) to image small objects at higher resolution than traditional medical magnetic resonance imaging (MRI). Early insect studies only highlighted fat and water distributions of large lepidopteran pupae (Goodman *et al.,* 1995). Now, with the use of contrast agents and higher magnetic fields, relatively detailed images of smaller Drosophildae pupae (Null *et al.,* 2008) are achievable, however the slice thickness of ~100 μm remains a limitation.

A critical review of MRM for entomological studies (Hart *et al.,* 2003) suggests visualization of *in vivo* development is possible, with obvious advantages over histological methods. However, like CT, resolution is generally poor in comparison to standard histology. Imaging of living insects is particularly complex, due to movement (such as abdominal peristalsis) causing blurring. High quality images of organs such as the brain have been obtained (Haddad *et al.,* 2004; Hallock 2005; Jasanoff & Sun 2002; Michaelis *et al.,* 2005), due to the lack of movement. Cooling the insects reduces movement and improves imaging (Null *et al.,* 2008; Michaelis *et al.,* 2005) but the best images are produced using preserved specimens (Wecker *et al.,* 2002) or contrast agents, which can be introduced in the feed or by microinjection prior to killing (Null *et al.,* 2008). MRM has been used to visualize the movement of the gas bubble within the pupa and subsequent head eversion of the flesh fly, *Sarcophaga peregrina* (Fig. 6.8) (Price *et al.,* 1999). The images produced are of high enough resolution and show significant differences between stages to enable age estimation to within a few hours. Generally the technique is still considered complementary to histology on larger insects (Hart *et al.,* 2003).

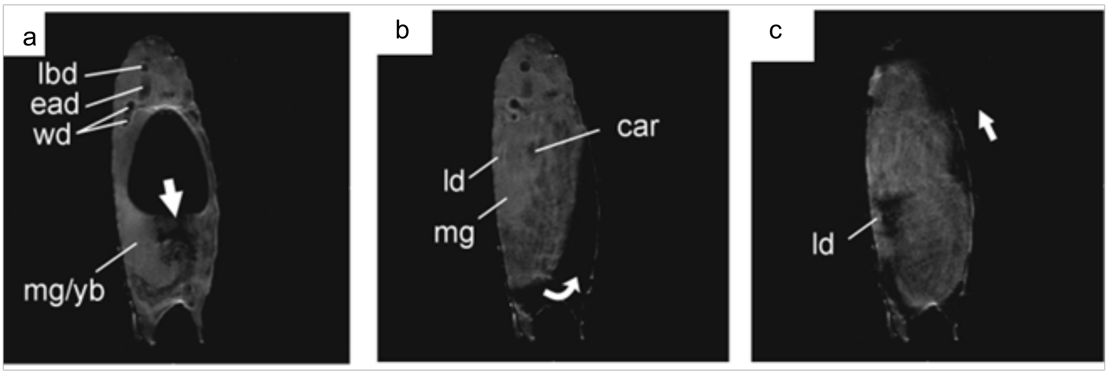

Figure 6.8. Hourly growth of the *Sarcophaga peregrina* pre-pupa. a: development at 45 hours after puparium formation (AP), the bubble is moving posteriorly. b: 46 hours AP, the bubble now moves around the outside of the pre-pupa between the pupal cuticle and the puparium. c: 47 hours AP the bubble is nearly at the anterior end of the pre-pupa. The following are labelled: labial disc (lbd), eye-antennal disc (ead), wing disc (wd), midgut/yellow body (mg/yb), leg disc (ld) and cardia (car) (Price *et al.* 1999).

Optical coherence tomography (OCT) is a more recent development and involves scanning the object with single or multiple lasers, and uses the attenuated and backscattered near-infrared light to produce two dimensional cross sectional images. OCT microscopy can be used to image samples *in vivo*, negating the need for histological fixation and sectioning. The OCT microscope is considerably smaller (bench-top sized), relatively simple to operate and cheaper than MRM and microCT. Resolution of <5 μm is achievable, with imaging depths of up to 3 mm, depending on tissue type (Fujimoto 2003). Slice thicknesses of 2-20 μm are achievable (Jenkins 2011), so provides better comparison to histological preparations.

OCT has been used for retina, blood vessel and skin carcinoma examination (summarised in Fujimoto (2003); see also Matheny *et al.,* (2004)), however its uses in developmental biology are being explored as the resolution it provides on mammals (Larina & Larin 2011) and non-mammals such as *Xenopus* spp. (Boppart *et al.,* 1996; Boppart *et al.,* 1997; Mariampillai *et al.,* 2007) and *Drosophila* spp. (Choma *et al.,* 2006; Bradu *et al.,* 2009) are superior to those achievable using MRI and CT. Insects can be difficult to image, as their transparent organs lie beneath an opaque cuticle which causes much of the light backscattering before penetration of the sample can occur. This was evident in *Drosophila* larvae (Bradu *et al.,* 2009), however OCT was used to image daily development of lepidopteran wings (Fig. 6.9) as they lie just beneath the surface of the puparium (Kambe *et al.,* 2008), indicating its possible use in the age estimation of calliphorid pupae. Microsphere contrast agents have been developed to improve the depth of image, however these must be injected (Boppart & Suslick 2006), and may interfere with other age estimation methods.

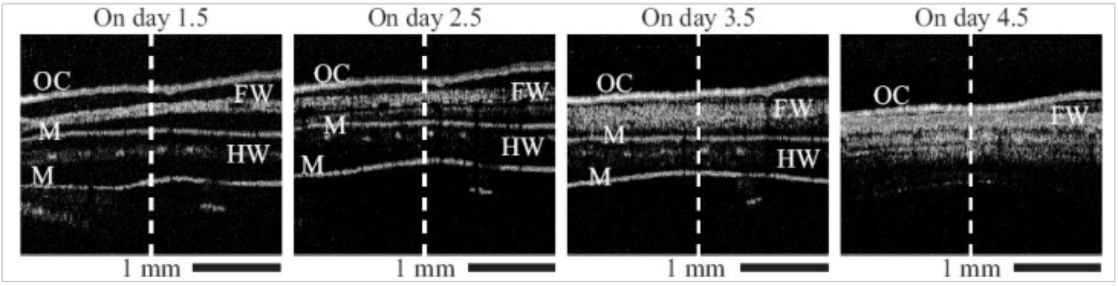

Figure 6.9. Daily development of butterfly wings. OCT was used to monitor development of butterfly wings during metamorphosis of a live pupa. Scans were performed daily for 5 days, at a speed of 0.125 m/sec, using a ~1300 nm laser. Depth resolution = 18.2 μm, lateral resolution = 4.4 μm. OC = outer cuticle, M = membrane surrounding wing, FW = forewing and HW = hindwing (Kambe *et al.* 2008).

6.1.2 Conclusions and aims

In summary, examination of internal morphological development has the potential to provide additional age markers, and provide complementary data for age estimation by external morphological analysis. In cases where pupal epidermal discolouration or putrefaction prevent external morphological analysis, internal morphological analysis may enable age estimation from an otherwise poorly-preserved pupa.

Studies to date indicate that standard histological techniques allow the highest resolution observations of pupal internal morphological development. At present, there are insufficient data available for age estimation of *C. vicina* using this method; its production has been hindered by lack of suitable histological protocols. OCT is a potential complementary approach to examine morphology of living and preserved pupae; despite its lower resolution, it is non-destructive and less time consuming than histology.

The specific aims of this study were therefore to:

- Develop an effective protocol for histological analysis of *C. vicina* pupae.
- Produce an internal morphological development timeline, and test its potential for use in pupal age estimation.
- Conduct *in vitro* and *in vivo* morphological analysis of pupae using an OCT microscope to test the potential of the technique for age estimation purposes.

6.2 Results

Similarly to external morphological analysis, internal development was observed in 42 individuals. The ages of larvae and pupae in ADH were calculated as described in Chapter 5.3.1, with those utilized for histological analysis given in Table 6.5.

Table 6.5 Ages of all pupae used for histological analysis in hours after APF and ADH. Three pupae were collected at each timepoint, resulting in analysis of 42 pupae, The ages of pupae are given in hours after puparium formation (APF) at 22°C, and in ADH. The individual ADH of each sample in each trial is given, calculated using larval mass temperatures.

Sample #	Age (h APF)	Trial 1
		Age (ADH)
1	0	3911
5	24	4463
9	48	5013
13	72	5558
17	96	6106
21	120	6659
25	144	7209
29	168	7761
33	192	8313
37	216	8865
41	240	9419
45	264	9976
49	288	10530
53	312	11082

6.2.1 Histological timeline

Internal development of the pupa was observed from over 500 slides (36-48 slides per time-point). Consistently identifiable and traceable morphological developments that are candidate for age indicators are described.

Unfortunately, as pupae collected were prioritised for external morphology and gene expression analyses, no pupae aged 3911 – 4463 ADH were collected for histological analysis. Instead, late post-feeding larvae (collected at 3911 – 4463 ADH) were analysed and the first few hours prior to appendage eversion in pupae were not observed histologically.

6.2.1.1 The Head

The two main features observed in the head were the brain (Fig. 6.10) and compound eyes (Fig. 6.11), whose development is also intricately linked. Mouthparts and antennae were small and fragile, and so were often discarded during sectioning. They were infrequently detected and their development could not be correlated with age.

The brain develops from its larval form at 3911 ADH (Fig. 6.10a), without histolysis, to its adult counterpart at 10530 ADH (Fig 6.10j-k), described in Table 6.6. In summary, the medulla, lobula and lobular plate differentiate from the larval mushroom bodies, noted distinctly at 5558 ADH (Fig. 6.10d). These structures migrate laterally across the head towards the compound eyes. The protocerebrum is visible from 6659 ADH (Fig. 6.10f). From the same age, the lamina ganglionaris extends from the medulla and flattens out underneath the retinal cells. Brain development appears complete from 9149 ADH (Fig. 6.10i).

Compound eyes originate as eye imaginal discs (Fig. 6.11 a, b) until head eversion at 5558, when a single layer of retinal cells is visible (Fig. 6.11c). Elongation of the cells starts at 6106 ADH (Fig. 6.11d) as optical neurons begin to form. Elongation continues throughout development and eye development is complete at 10530 ADH (Fig. 6.11i).

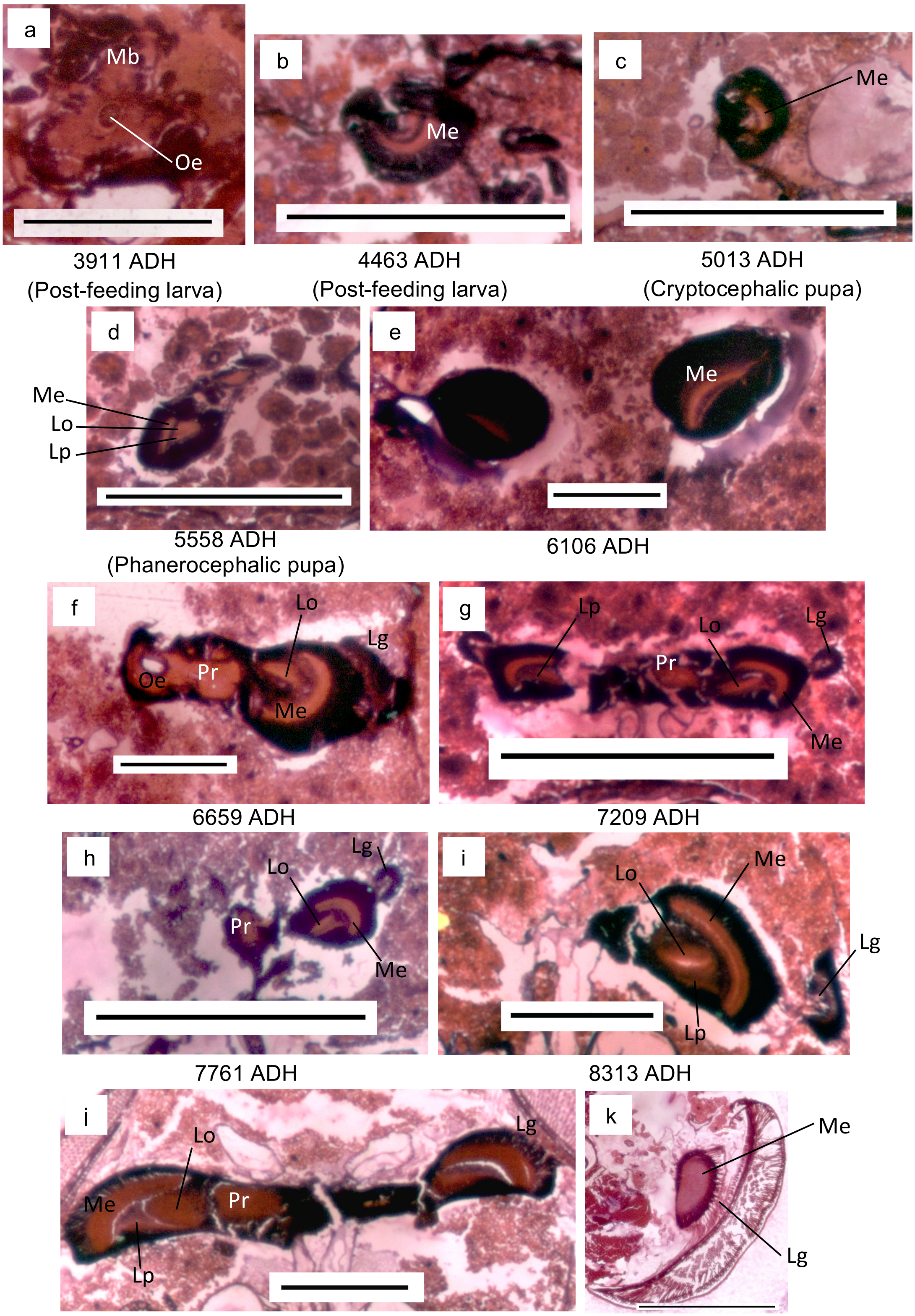

3911 ADH (Post-feeding larva)

4463 ADH (Post-feeding larva)

5013 ADH (Cryptocephalic pupa)

5558 ADH (Phanerocephalic pupa)

6106 ADH

6659 ADH

7209 ADH

7761 ADH

8313 ADH

9419 ADH

10530 ADH

Fig. 6.10 Brain development in *Calliphora vicina*. Transverse (a, e, f, i, j & k) and longitudinal sections (b, c, d, g, & h) of the developing brain are shown from post-feeding larvae through to fully developed adults, in chronological order. Ages in ADH are given beneath each image. Lg = lamina ganglionaris, Lo = Lobula, Lp = Lobular plate, Mb = Mushroom body, Me = Medulla, Oe = Oesophagus, Pr = Protocerebrum. All scale bars = 1000 µm.

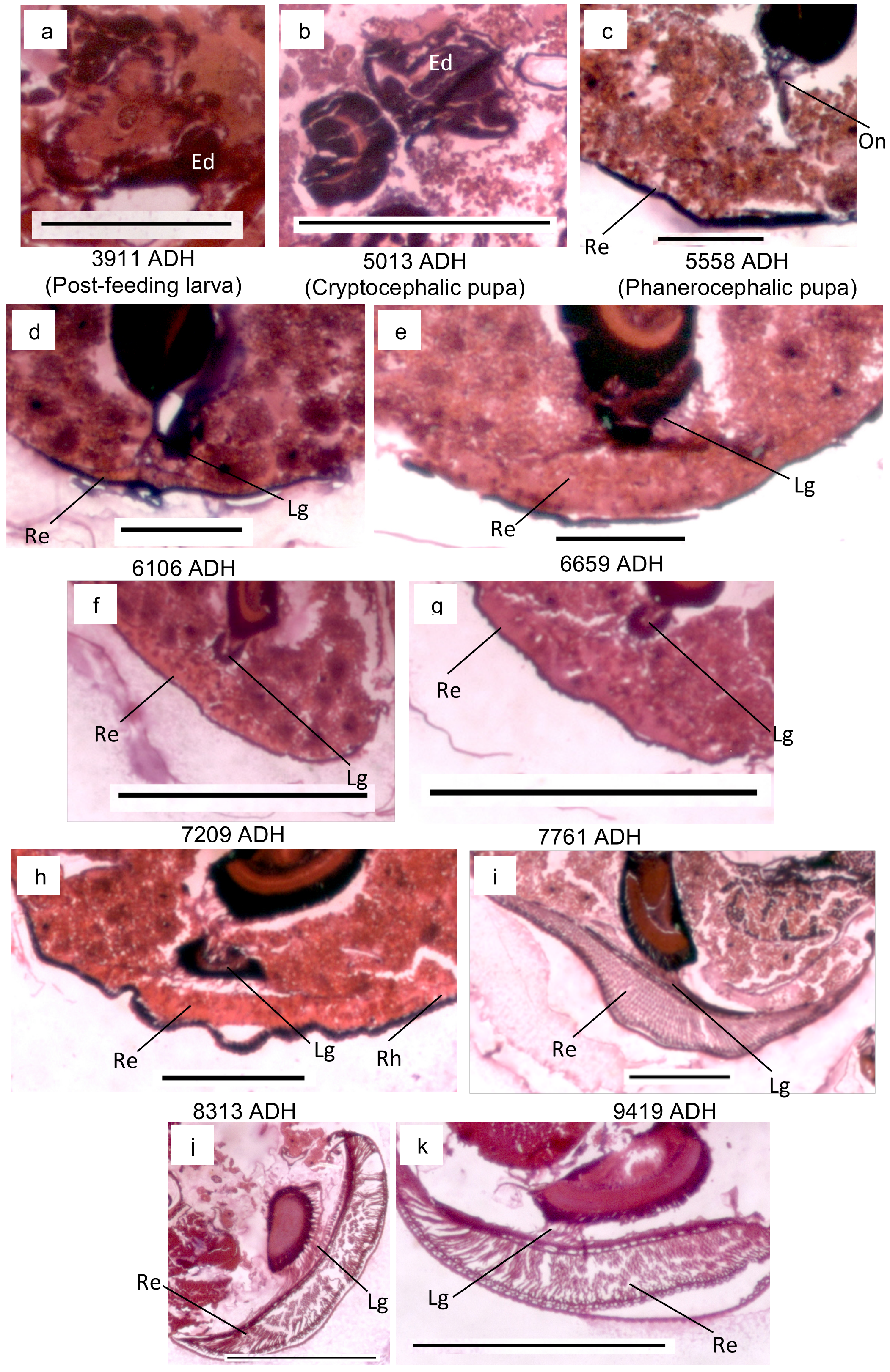

3911 ADH (Post-feeding larva)

5013 ADH (Cryptocephalic pupa)

5558 ADH (Phanerocephalic pupa)

6106 ADH

6659 ADH

7209 ADH

7761 ADH

8313 ADH

9419 ADH

10530 ADH

11082 ADH

Fig. 6.11 Compound eye development in *Calliphora vicina*. Transverse (a, c, d, e, h, i, j & k), Sagittal (b) and longitudinal sections (f, g) of the developing compound eye are shown from post-feeding larvae through to fully developed adults, in chronological order. Ages in ADH are given beneath each image. Ed = Eye imaginal disc, Lg = Lamina ganglionaris, On = optical neurones, Re = Retinal cells, Rh = Rhabdomeres. All scale bars = 1000 µm.

Table 6.6 Summary of internal development of the head of *Calliphora vicina*. The table details development of the brain and compound eyes, as shown in Figures 6.10 and 6.11. TS = transverse section, LS = longitudinal section, SS = sagittal section. n/a indicates no additional data of value was obtainable from the sections, e.g. feature was not noted.

Age	Brain	Compound eye
3911	TS: Larval form. Oesophagus positioned through mushroom bodies.	TS: Eye imaginal discs present on the dorsal lateral surface of the brain.
4463	LS: Medulla visible in post-feeding larva	n/a
5013	LS: Cryptocephalic pupa, no change noted.	SS: Eye imaginal discs migrate anteriorly away from the brain.
5558	LS: Lobula and lobular plate centrally located within the head.	TS: Eyes have everted. Retinal cells now a thin layer. First optic neurons noted.
6106	TS: no change	TS: Retinal cells spreading along epidermal surface, starting to increase depth as neurons form.
6659	TS: Medulla rotated ~90°. Lamina ganglionaris separated from medulla. Protocerebrum now distinct. Overall increased width.	TS: Retinal cells now ~0.5mm thick in centre. Connection with the laminar ganglionaris is definitive.
7209	LS: Lamina ganglionaris formed a loop laterally to medulla.	LS: All retinal cells continue to increase in depth.
7761	LS: no change	LS: No change
8313	TS: Lobular plate increased in thickness. Lamina ganglionaris flattening out beneath retinal cells.	TS: Rhabdomeres in retinal cells starting to be distinguishable
8865	n/a	n/a
9419	TS: Medulla, lobula and lobular plate completed development. Lamina ganglionaris still flattening over retinal cells.	TS: Retinal cells (inc. Rhabdomere) development appears complete
9976	n/a	n/a
10530	TS: Lamina ganglionaris development complete.	TS: Lamina ganglionaris fully distributed beneath retinal cells.
11082	n/a	TS: No change

6.2.1.2 The Thorax

The most prominent features to develop within the thorax are the flight muscle (Fig. 6.12) and appendages (Fig. 6.13); details are given in Table 6.7. Nearing pupation, the intersegmental muscles start to degenerate between 4463 – 5013 ADH (Fig. 6.12a-c). Small amounts of precursor muscles remain, which develop into adult thoracic muscle from 6106 ADH (Fig. 6.12e). Development of longitudinal (Fig. 6.12f) and transverse muscle (Fig. 6.14i) progresses slowly until completion at 9976 ADH (Fig. 6.12k).

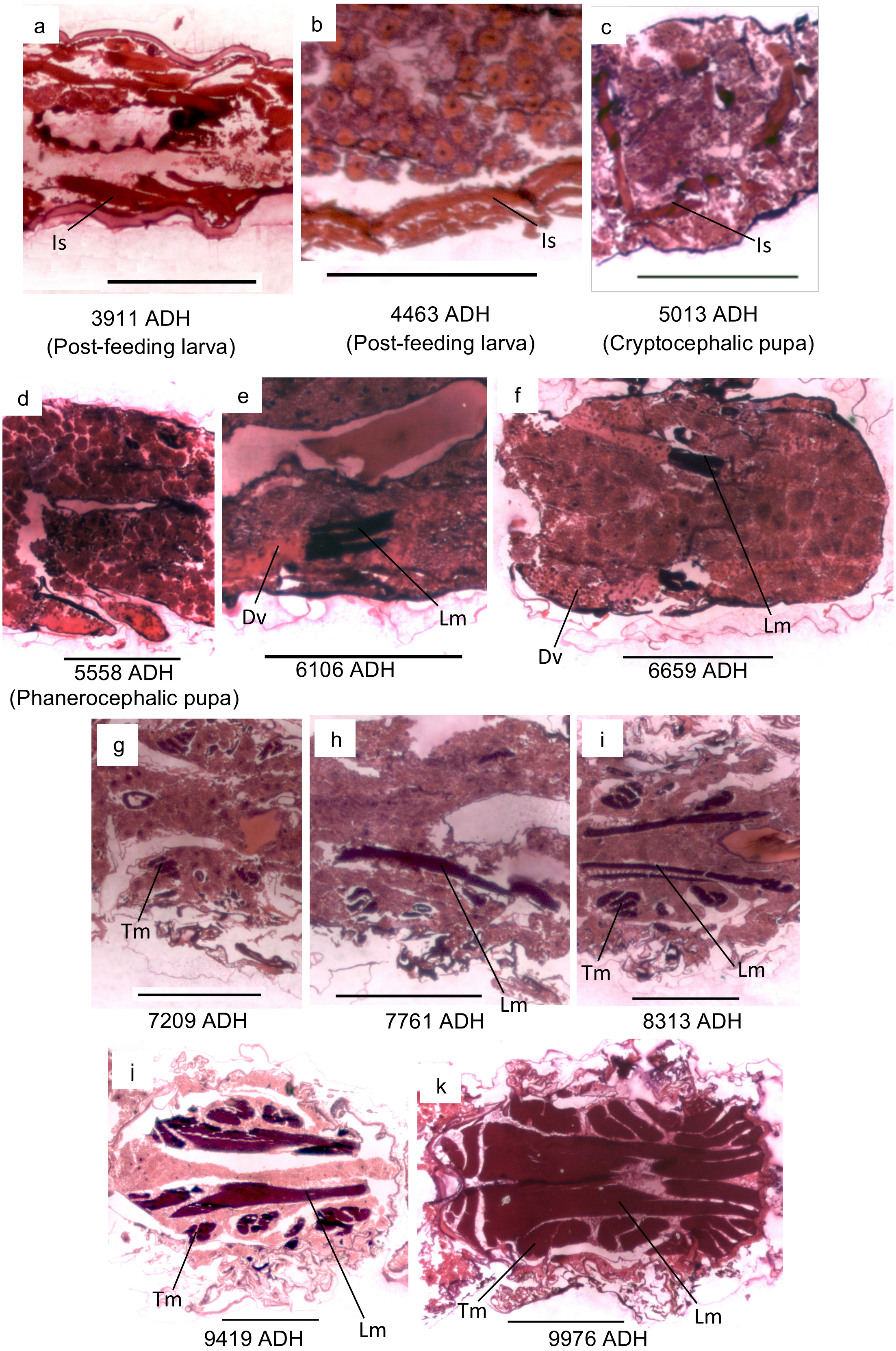

3911 ADH
(Post-feeding larva)

4463 ADH
(Post-feeding larva)

5013 ADH
(Cryptocephalic pupa)

5558 ADH
(Phanerocephalic pupa)

6106 ADH

6659 ADH

7209 ADH

7761 ADH

8313 ADH

9419 ADH

9976 ADH

Fig. 6.12 Thoracic muscle development in *Calliphora vicina*. Sagittal (c, d & e) and longitudinal sections (a, b, f, g, h, i, j & k) of the developing thoracic muscle are shown from post-feeding larvae through to fully developed adults, in chronological order. Ages in ADH are given beneath each image. Dv = development zone, Is = Intersegmental muscle, Lm = longitudinal muscle, Tm = transverse muscle. All scale bars = 1000 µm.

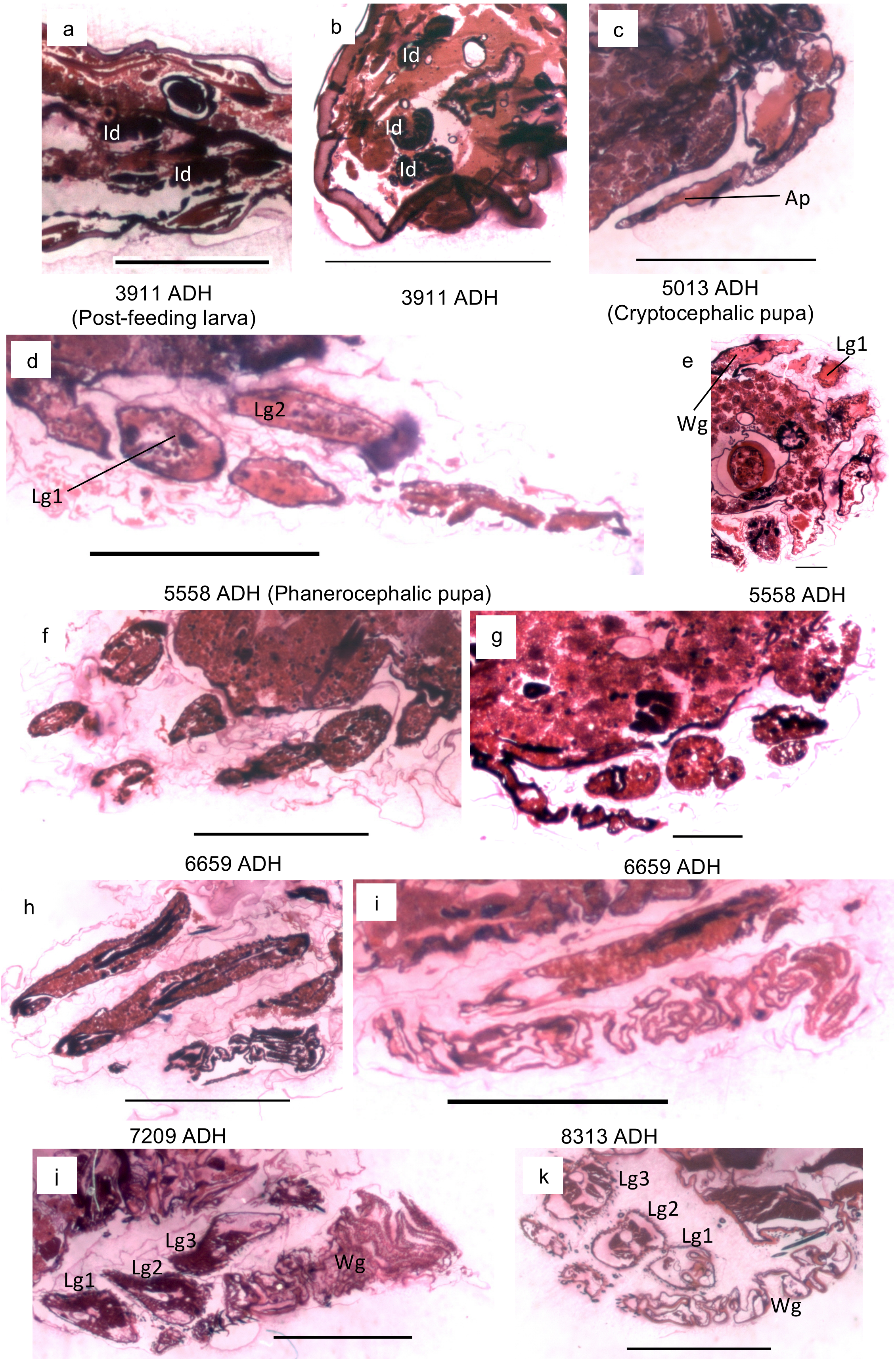

3911 ADH (Post-feeding larva)

3911 ADH

5013 ADH (Cryptocephalic pupa)

5558 ADH (Phanerocephalic pupa)

5558 ADH

6659 ADH

6659 ADH

7209 ADH

8313 ADH

9976 ADH

11082 ADH

Fig. 6.13 Appendage development in *Calliphora vicina*. Sagittal (c, d, f, h & j), transverse (b, e, g & k) and longitudinal sections (a & i) of the developing appendages are shown from post-feeding larvae through to fully developed adults, in chronological order. Ages in ADH are given beneath each image. Ap = Appendage, Id = Imaginal disc, Lg1 = Prothoracic leg, Lg2 = Mesothoracic leg, Lg3 = Metathoracic leg, Wg = wing. All scale bars = 1000 µm.

Imaginal discs are visible in larval sections (3911 ADH) (Fig 6.13a, b) however their individual identification is not possible. Leg and wing imaginal discs evert at 5013 ADH (Fig. 6.13c). After head eversion at 5558 ADH, appendages appear full length and individual legs and wings are distinguishable histologically (Fig. 6.13d, e). Wings gradually become more folded and convoluted until 8313 ADH (compare Figs. 6.13e and i), whereas legs develop muscles from 6659 – 9976 ADH (Fig. 6.13g-i), after which no morphological changes are observed.

Salivary glands are detectable in post-feeding larvae aged 3911 ADH (Fig 6.14a) but degenerate in early pupae aged 5558 ADH (Fig 6.14b). The thoracic ganglion is noted sporadically (due to small size and section losses) at 5558 ADH (Fig. 6.15), 6106 ADH and 8313 ADH (not shown), with no visible developmental changes. After 8313 ADH, thoracic muscle dominates the cavity, preventing further observation of the thoracic ganglion.

Table 6.7 Summary of internal development of the thorax of *Calliphora vicina*. The table details development of the thoracic muscle and appendages, as shown in Figures 6.12 and 6.13. TS = transverse section, LS = longitudinal section, SS = sagittal section. n/a indicates no additional data of value was obtainable from the sections, e.g. feature was not noted or remained unchanged.

Age	Thoracic muscle	Appendages
3911	LS: Intersegmental muscle persists in the larva.	LS/TS: Imaginal discs visible (uneverted).
4463	LS: Intersegmental muscle starting to diminish.	n/a
5013	SS: Intersegmental muscle degrading within thorax.	SS: Appendages just everted (cryptocephalic pupa).
5558	SS: No remnants of muscle visible.	SS/TS: Legs and wings comprise undifferentiated tissue and haemolymph.
6106	SS: Small sections of longitudinal muscle start to develop.	n/a
6659	LS: Longitudinal muscle development continues spanning the thorax.	SS/TS: Small amounts of muscle visible in metathoracic leg. Wings show some folding.
7209	LS: Transverse muscle bundles are noted.	TS: Longitudinal muscle in all legs. Wing folding increased.
7761	LS: Longitudinal muscle developed across thorax.	n/a
8313	LS: Minimal change.	SS: No change in legs. Wing folding increased.
8865	n/a	n/a
9419	LS: Density increase in all muscle types.	n/a
9976	LS: Maximum muscle density reached.	LS: No change in wings. Legs now fully muscular.
10530	n/a	n/a
11082	n/a	TS: No change.

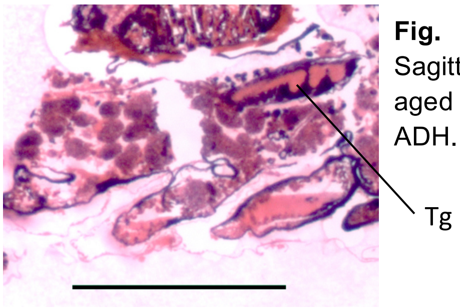

5558 ADH (Phanerocephalic pupa)

Fig. 6.14 The thoracic ganglion in *Calliphora vicina*. Sagittal section of the thoracic ganglion in an early pupa, aged 5558 ADH. Noted again at 6106 ADH and at 8313 ADH. Tg = thoracic ganglion. Scale bar = 1000 µm.

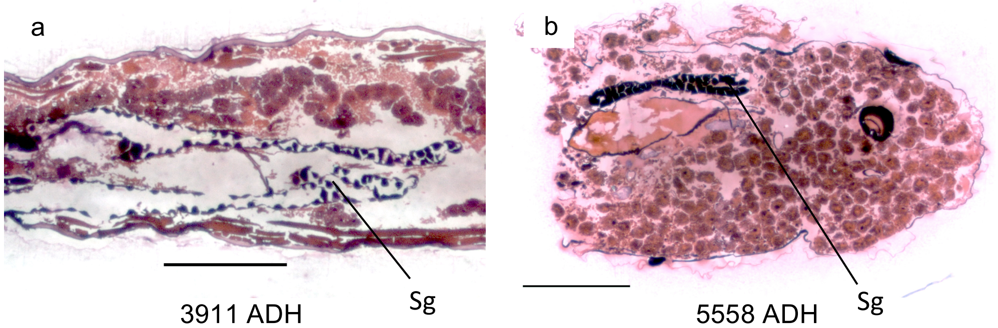

3911 ADH (Post-feeding larva)

5558 ADH (Phanerocephalic pupa)

Fig. 6.15 Salivary gland degeneration in *Calliphora vicina*. Longitudinal sections of the degenerating salivary glands are shown from post-feeding larvae through to early pupae, in chronological order. Ages in ADH are given beneath each image. Sg = salivary glands. All scale bars = 1000 µm.

6.2.1.3 The Abdomen

The abdomen contains few features that were potentially useful for age estimation. It comprises mainly fat body (Fig. 6.16) and the digestive system displays the greatest developmental change (Fig. 6.17). Development is summarised in Table 6.8. Reproductive organs are also identified (Fig. 6.18).

The larval fat body (Fig. 6.16a) becomes more eosinophilic (more basic – pink-coloured), with peak levels at 5013 ADH (Fig. 6.16c). By 6106 ADH (Fig. 6.16d), the nuclei decrease in size and eosin staining had faded.

Up to and including the cryptocephalic pupal stage (5013 ADH), the larval gut exists as a slim tube in the thorax (Fig 6.17a, b, c), with only a small amount of larval food remaining. The larval gut appears fully degraded as meconium at 5558 ADH (Fig. 6.17d), located in the thoracic midgut of the pupa; the abdominal midgut (pupal) is undergoing development (Fig. 6.17e). The thoracic midgut has migrated to the abdomen by 6659 ADH (Fig. 6.17h), and is visible through to at least 8865 ADH (Fig. 6.17l). The gut develops convolutions and differentiates into specific structures such as the gastric caecae, malpighian tubules and rectal papillae from 6106 to 10530 ADH (Fig. 6.17g-m). From 9976 ADH, numerous fine tracheal branches are observed (Fig. 6.17m).

The reproductive organs are observable as early 5013 ADH, shown in Fig 6.18 at 8313 ADH. In the sections taken, it is not possible to differentiate between testes and ovaries or to determine developmental changes due to their sporadic appearances.

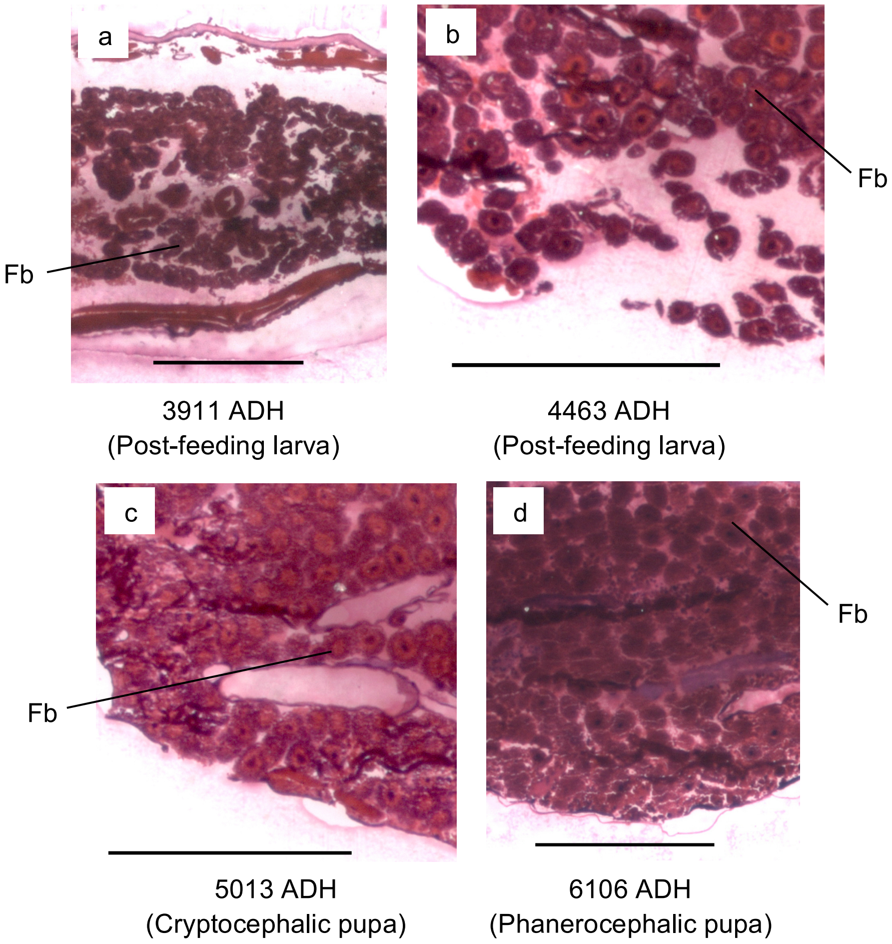

Fig. 6.16 Fat body development in *Calliphora vicina*. Longitudinal sections of the degenerating larval fat body are shown from post-feeding larvae through to early pupae, in chronological order. Ages in ADH are given beneath each image. Fb = fat body. All scale bars = 1000 μm.

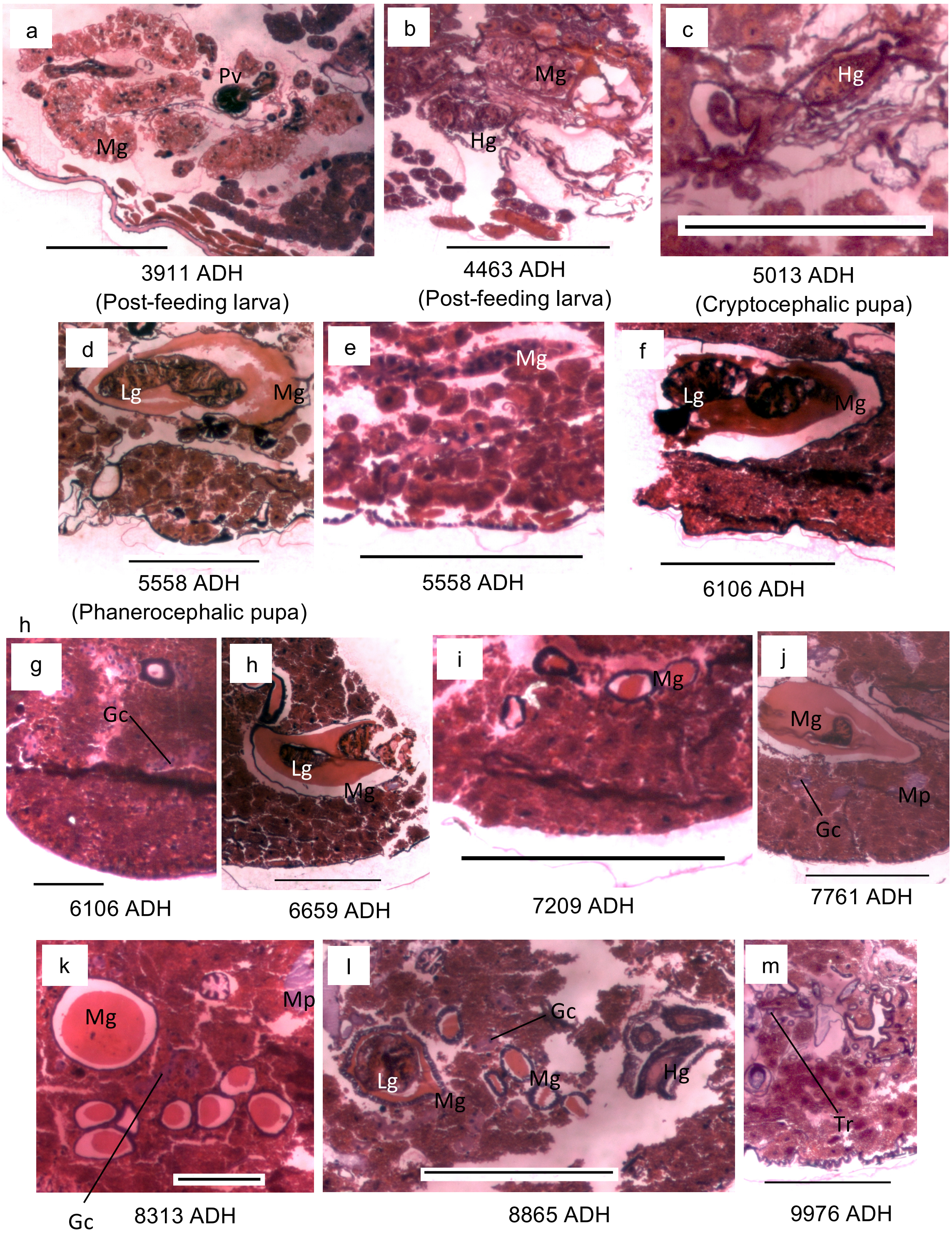

3911 ADH
(Post-feeding larva)

4463 ADH
(Post-feeding larva)

5013 ADH
(Cryptocephalic pupa)

5558 ADH
(Phanerocephalic pupa)

5558 ADH

6106 ADH

6106 ADH

6659 ADH

7209 ADH

7761 ADH

8313 ADH

8865 ADH

9976 ADH

Fig. 6.17 Digestive system development in *Calliphora vicina*. Sagittal (f, g, h, i), longitudinal (b, c, d, e, j, l, m) and transverse (a, k) sections of the developing digestive system are shown from post-feeding larvae through to fully developed adults, in chronological order. Ages in ADH are given beneath each image. Gc = Gastric caecae, Hg = Hindgut, Lg = Larval gut, Mg = Midgut, Mp = Malpighian tubules, Tr = Trachea. All scale bars = 1000 µm.

Table 6.8 Summary of internal development of the abdomen of *Calliphora vicina*. The table details development of the fat body and digestive system, as shown in Figures 6.16 and 6.17. TS = transverse section, LS = longitudinal section, SS = sagittal section. n/a indicates no additional data of value was obtainable from the sections, e.g. feature was not noted or remained unchanged.

Age	Fat body	Digestive system
3911	LS: Cells are uninucleated, containing oil droplets, appears granulated	TS: Larval midgut and proventriculus present.
4463	LS: Some cells more eosinophilic (starting to release contents)	LS: Small amount of digesting food remains in hindgut. Midgut visible.
5013	LS: Most cells eosinophilic	LS: Larval food still visible in hindgut (cryptocephalic pupa).
5558	n/a	LS: The degenerated larval gut is present as meconium in the pupal/adult midgut in the thorax. The abdominal midgut is developing.
6106	LS: Nuclei diminished, and no longer eosinophilic.	SS: The midgut (with old larval gut) migrating posteriorly. Gastric caecae visible in abdomen.
6659	n/a	SS: The midgut (with old larval gut) now in abdomen.
7209	n/a	SS: Midgut convolutions now visible in posterior abdomen.
7761	n/a	LS: Malpighian tubules visible.
8313	n/a	TS: Gastric caecae, malpighian tubules and midgut convolutions noted.
8865	n/a	LS: Old larval gut still visible. No change.
9419	n/a	n/a
9976	n/a	LS: Many trachea present surrounding digestive tissues.
10530	n/a	n/a
11082	n/a	n/a

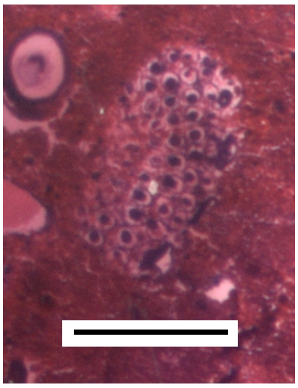

8313 ADH
(Phanerocephalic pupa)

Fig. 6.18 The reproductive organs in *Calliphora vicina*. Transverse section of a reproductive organ, at 8313 ADH. Scale bars = 1000 μm.

6.2.2 Optical Coherence Tomography Microscopy

Live intact pupae and preserved pupae with puparium removed, 4 and 10 days after puparium formation, were examined using the Optical Coherence Tomography (OCT) microscope. It was hoped that this method would yield enough pupal morphological detail *in vivo* to reduce the reliance on destructive observation methods.

3D surface rendered images of preserved 4d pupae showed no identifiable features (Fig. 6.19a), however virtual cutaway sections taken in dorsal and sagittal planes from a ventral aspect clearly revealed eyes, legs and mouthparts (Fig, 6.19b, c). 3D surface rendered images of preserved 10d pupae showed compound eyes and thoracic bristles (Fig. 6.20a). Cut away sections of 10d pupae revealed the optic nerves and brain (Fig. 6.20b), compound eyes, thoracic and abdominal bristles and wings Fig 6.20c, d, e).

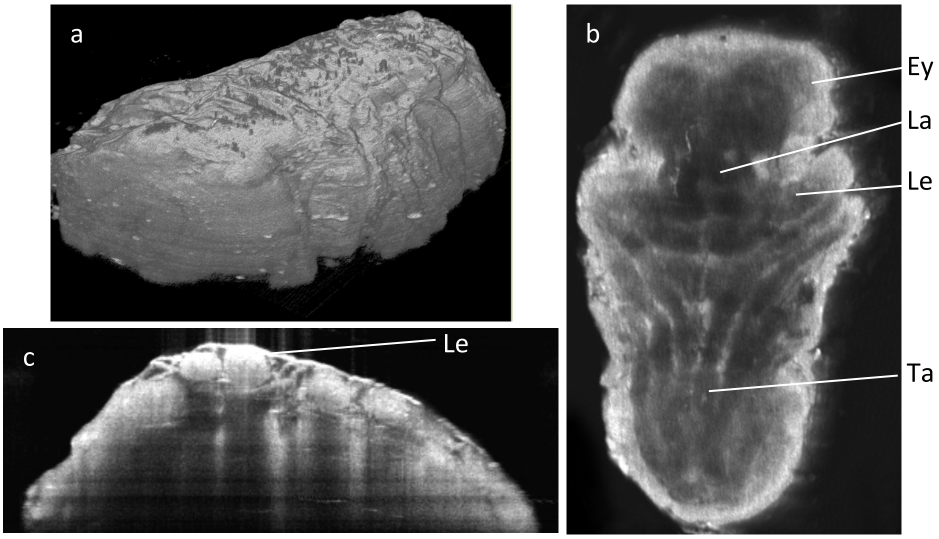

Fig. 6.19 OCT images of a preserved 4 day old pupa. The pupa was preserved by HWK, and the puparium was removed prior to ventral surface scanning with the OCT microscope. a) a 3D rendered image of the pupal external surface. Virtual 3D cut-away longitudinal (b) and transverse (c) sections of the pupa. Ey = Compound eye, La = Labellum, Le = Legs, Ta = Tarsi.

3D rendering of live pupae only resulted in a view of the external puparium surface and no features were visible (data not shown). Longitudinal and sagittal sections of 4d live pupae allowed visualisation of some internal structures through the puparium such as the abdomen, wings, everted trachea (Fig. 6.21a) and respiratory horns (Fig 6.21b), as well as the brain (Fig. 6.21a, b, d). Longitudinal and transverse sections of live 10d pupae similarly revealed external features such as the mouthparts and legs (Fig. 6.22b, c, d) and also the brain (Fig. 6.22c).

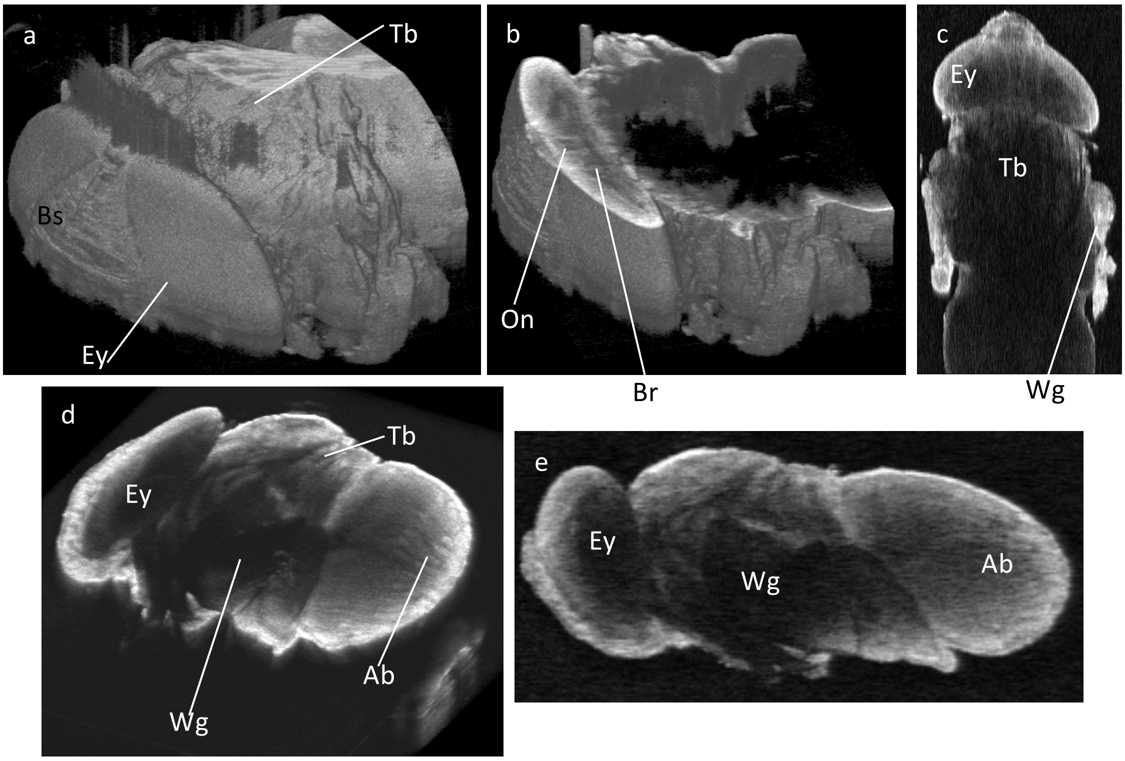

Fig. 6.20 OCT images of a preserved 10 day old pupa. The pupa was preserved by HWK, and the puparium was removed prior to dorsal surface scanning with the OCT microscope. Full (a) and cut-away (b) 3D rendered images of the head and thorax. Virtual longitudinal (b) and 3D cut-away transverse and sagittal (c-d) sections of the pupa. Ab = Abdominal macrochetae, Br = Brain, Bs = Orbital/frontal bristles, Ey = Compound eye, On = Occelar nerves, Tb = Thoracic bristles, Wg = Wing.

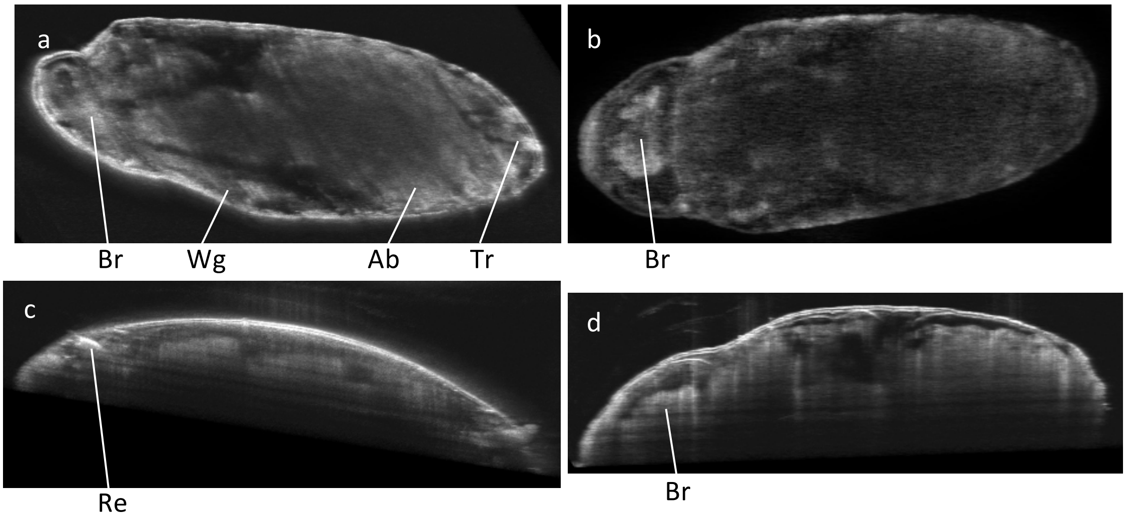

Fig. 6.21 OCT images of a live 4 day old pupa. The pupa remained alive, in its puparium, whilst its dorsal surface was scanned with the OCR microscope. a) 3D cut-away cross section image of the pupal external surface. Virtual longitudinal (b) and 3D cut-away transverse and sagittal (c-d) sections of the pupa. Ey = Compound eye, La = Labellum, Le = Legs, Ta = Tarsi.

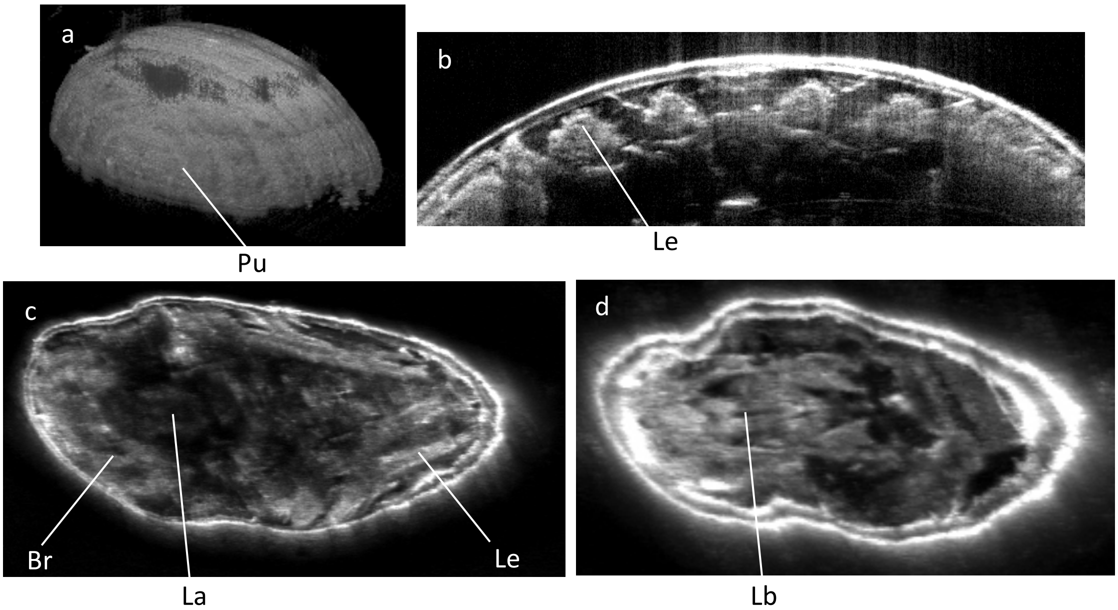

Fig. 6.22 OCT images of a live 10 day old pupa. The pupa remained alive, in its puparium, whilst its dorsal surface was scanned with the OCR microscope. (a) Full 3D rendered image of the puparium. Virtual transverse section of the abdomen (b) and 3D rendered longitudinal sections of the entire pupa (c-d). Br = Brain, La = Labellum, Lb = Labrum, Le = Legs, Pu = Puparium.

6.3 Discussion

Morphological development of *C. vicina* pupae was examined using histology and optical coherence tomography. Timelines for multiple features were constructed, correlated to age in ADH, for the purpose of accurate age and PMI estimation.

6.3.1 Methodology

Histological examination of insect morphology has been used for over a century, prior to the works of Lowne (1895) on *Calliphora vicina*. Protocols for histological study often lack detail and so the work is difficult to replicate, or outdated and/or hazardous solutions are used (such as boiling Bouins, which contains picric acid (Bodenstein in Demerec, 1950)). This study has employed a simple method, based on that of Bodenstein in Demerec (1950) for *Drosophila melanogaster*, which uses a non-formalin based preservative that produces excellent morphological detail.

Bodenstein (1950) recommends puparium removal after boiling pupae for ‘special needs’ however routine use of hot-water-killing for fixation was employed here to prevent tissue damage. Bodenstein also suggested piercing of the pupa, but after primary fixation and puparium removal. This risks inadequate heat transfer, and may result in subsequent putrefaction. In the present study pupae were pierced with the puparium intact prior to fixation. Dehydration by ethanolic solutions (as suggested by

Bodenstein in Demerec (1950)) was effective if calliphorid pupae were bisected; specimens were embedded in paraffin and stained with haematoxylin and eosin as described. The present study required the use of gelatin as a section-to-slide adhesive. This was not required for *D. melanogaster* pupae (Bodenstein in Demerec (1950)), or in *Lucilia sericata* (Davies & Harvey 2012). This was probably due to the smaller sizes of these pupae (*C. vicina* pupae ~ 10 mm long, *L. sericata* pupae ~ 6 mm long, *D. melanogaster* pupae ~2 mm long) which facilitated better penetration of solutions and wax to support the tissue on the slide. Splitting of tissue (detected by the presence of fissures in sections) caused (presumably) by brittle tissue type was exacerbated by poor wax penetration (Davies & Harvey 2012). Damage was minimised by cutting pupae to expose the raw surface, and placing this in ice-cold water for a few minutes; this softened the immediate few micrometers of tissue. This has not previously been reported for other dipteran pupae.

In conclusion, a protocol suitable for histological examination of *C. vicina* pupae has been developed. This protocol uses standard equipment and solutions, and allows pupal age and PMI estimation.

6.3.2 Histological development timeline

Developmental features were documented histologically by examination of three pupae sampled at 24-hour intervals between the ages of 3911 -11082 ADH. Pupae were sectioned through three planes, prominent features were examined, and timelines of development were produced. These timelines were compared to that previously produced for *C. vicina* and *Drosophila melanogaster* (Finell & Jarvilehto 1983; Perez 1910; Lowne 1895; Bodenstein in Demerec 1950). These data was not correlated to age in ADH, and with differences in developmental protocols and lifecycle lengths, developments were correlated to age in percentage time through the pupal stage for comparison.

Due to section damage or loss not every feature was detected in all pupae. Timelines presented in this study therefore show the major histological changes correlated to ADH, to facilitate comparison between known-age and unknown-age pupae sections.

6.3.2.1 The head

In the head, features such as the brain and compound eyes were most readily observed. Upon comparison of development with previous *C. vicina* and *D. melanogaster* studies, morphological similarities and temporal differences were noted.

Finell & Jarvilehto (1983) showed three stages of brain and compound eye development at 15, 35 and 70% (in time) through the pupal stage. As no ages in ADH were given, the developments noted approximately correlated to observations made in this study at 5558, 6659 and 8313 ADH respectively (Fig. 6.10d, f, i), which equate to 23%, 38% and 60% development through the pupal stage; different times from those previously found. This was unexpected as both studies were conducted on *C. vicina*, however it may be accounted for in pupal rearing methods, such as temperature measurement.

The *Drosophila* larval brain (at 60 hours old) (Bodenstein in Demerec (1950)) appeared morphologically similar to the *C. vicina* post-feeding larval brain at ~178 hours (3911 ADH) (Fig. 6.10a). The *Drosophila* pupal brain and compound eyes 3 and 45 hours after puparium formation (Bodenstein in Demerec (1950)) (3 and 45% of time through pupal stage) were similar in morphology to *C. vicina* pupal anatomy at 59 and 71% through the pupal stage (6659 and 8313 ADH) respectively (Fig. 6.11e, h). These observations were expected as despite the close evolutionary relationship between *D. melanogaster* and *C. vicina* (Hennig (1981) in Codd *et al.*, 2007), they have different lifestyles and lifecycle lengths.

Unlike muscle or the salivary glands, the brain and eyes are large organs that undergo continual development from the larval stage through to eclosion, without histolysis, which means these features are well suited for age estimation. Transverse sections generally showed the most development detail, including the laminar ganglionaris migrating towards the lengthening retinal cells (Fig. 6.11h). With further analysis of the head and appropriate section selection, it may be possible to use the brain and eyes to estimate age to within 500-1000 ADH (1-2 days at 22°C); sections observed in this study were taken from pupae aged ~600 ADH apart, and distinct changes are notable at each time point, at this resolution.

6.3.2.2 The thorax

Multiple developmental changes occurred within the thorax however all were complete by 9976 ADH (Figs. 6.12k and 6.13i). The histolysis of intersegmental muscle occurred in a short timeframe, and was completed by 5558 ADH as noted by sagittal sections (Fig 6.12b). In *Drosophila*, all larval muscle is histolysed by 9% through the pupal stage (Bodenstein in Demerec (1950)); much earlier than in *C. vicina* (5558 ADH; 23% though the pupal stage). This feature’s use in age estimation is thus limited to the early pupal stage, but still provides a valuable age marker.

Development of thoracic muscle was most easily followed in *C. vicina* by examining longitudinal sections. Development was first noted just after head eversion (phanerocephalic pupa) at 6106 ADH or 30% (Fig. 6.12e); much later than was noted in *Drosophila* at 11% through the pupal stage. Longitudinal muscles were two-thirds their final length at 7761 ADH or 53% of the *C. vicina* pupal stage (Fig. 6.12h), again later than observed in *Drosophila* at 22% through the pupal stage. Complete muscle development was observed at 83% thought the *C. vicina* pupal stage, much later than 44% as observed in *Drosophila* (Bodenstein in Demerec (1950)). Temporal correlation between these two species for this feature was lower than expected. This may be due to difficulties in muscle density interpretation which varies with section location. In spite of this age could be estimated to within 1000 ADH. Completion of a comprehensive study of muscle cell ultrastructure using transmission electron microscopy (TEM), such as that conducted by Crossley (1972) may yield more information for accurate age estimation. The suitability of TEM for routine forensic work is low however, due to the associated cost and sample preparation time.

Though legs and wings were readily identified in sagittal and transverse sections, their development was difficult to determine due to their small size. This made comparison with *Drosophila* data impossible. Leg muscle develops and wings become more folded, but such subtle changes and inconsistent observation in sections makes these features unreliable for age estimation. To improve reliability of observations, dissection and differential staining of muscle would be useful, possibly enabling age and PMI estimation using these tissues.

Degeneration of the salivary glands, like intersegmental muscle histolysis, was observed using longitudinal sections until 5558 ADH (23%) (Fig. 6.15b). *Drosophila* showed similarly early loss of salivary glands by 13% through the pupal stage (Bodenstein in Demerec (1950)). Therefore, this feature could only indicate the age of a pupa as younger (or older) than 5558 ADH, i.e. with low resolution, in conjunction with other developments. Like the mouthparts, the thoracic ganglion was detected in few slides (Fig. 6.14) and therefore is not useful to monitor development without dissection.

6.3.2.3 The abdomen

The lack of feature development in the abdomen indicates possible low utility in pupal age estimation. Initial changes in the abdomen include the histolysis of the larval fat body, which appears complete by 6106 ADH (Fig. 6.16d); like other larval features, this can be used to estimate age in early pupae up to head eversion. The eosin staining change in the fat body from purple (acidic) to red (basic) is indicative of release of glycogen, lipid and protein into the haemolymph for histogenesis of adult organs (Cohen in Resh & Cardé (2009)). *Drosophila* oenocytes (secretory cells associated with the fat body), in comparison, persist up to half way through the pupal stage (Bodenstein in Demerec (1950)); closer observation and identification of these cells with TEM may increase the utility of this tissue in age estimation.

The small size and convolutions of the digestive system relative to the fat body makes this a complex feature to follow during development. During the pre-pupal stage, the larval crop and oesophagus are everted with the cephalopharyngeal skeleton upon head eversion (Lowne 1895), therefore they were not observed in sections. The degenerating larval midgut ('yellow body' or 'corpus luteum') was observed within the new adult midgut by 5558 ADH (23% through the pupal stage; Fig. 6.17d), similar to ~20% previously noted in *C. vicina* (Lowne 1895; Perez 1910). The migration of the corpus luteum from the thorax to the abdomen is readily distinguished and can be used to estimate age of pupae between 5558 and 6659 ADH. After migration to the abdomen at 6659 ADH (~40% through the pupal stage), the midgut appeared more convoluted, i.e. increased in length, in agreement with Lowne (1895). An increase in diameter of the larval malpighian tubules in the pupal stage in *C. vicina* has been previously reported (Lowne 1895) but was not observed in the present study.

Rectal papillae were observed sporadically in some sections from 8865 ADH (6.17l: hindgut) and so they cannot be used as an age indicator. Malpighian tubules were observed in this study after 53% development, though Lowne detected them at around 81%. This discrepancy may be due to misidentification of the tubules by Lowne. The tracheal network was visible from 9976 ADH (Fig. 6.17m), and the observation of this system would indicate a pupal age of >9976 ADH, i.e. nearing eclosion.

Based on the pre-eclosion size increases observed in *Drosophila* (Bodenstein in Demerec (1950)), the gonads were expected to be a good age indicator. However, both male and female Calliphoridae gonads are round unlike *Drosophila* which has coiled testes Differentiation between sexes is difficult and since the greatest size increase in *C. vicina* occurs after meat-feed in the adult stage, developmental changes were insufficient to allow age estimation. The gonads were first observed 5013 ADH in transverse sections and their form remains unchanged throughout the stage (Fig. 6.18).

6.3.2.4 Overall development summary

Much of the development observed using histology occurred prior to 9976 ADH (~11 days after puparium formation at 22°C) and only minor changes occur during the final ~1000 ADH of pupal development, as is seen for external morphology. This correlates with the observation of initial pupal emergence from around this age (Chapter 3.3.3).

The chronology of morphological developments observed in the present study is similar to those observed in *L. cuprina*, *M. vomitoria*, *D. melanogaster* and existing *C. vicina* studies (Barritt & Birt 1971; Weissman 1874a, b, c; Lowne 1895; Perez 1910; Bodenstein (1950) in Demerec 1950). However, the absence of information about rearing conditions and paucity of morphological observations provided, timings were different and comparison is difficult. The present study provides a controlled comparison with future developmental studies in other species.

The developmental timeline data provided from this study allows age estimation by histological examination of pupae and comparison to the images shown. It may be possible to obtain a more accurate age estimate by a) dissection of organs and tissues prior to examination or b) by examination of more sections from the pupa. Dissection of the organ systems is relatively time consuming (especially if processing multiple organs/systems are to be used) and is destructive, preventing for example RNA analysis should it be required. It also has the potential to damage and reduce information obtainable from other tissues. Dissection would, however, improve observation of a specific organ or tissue and permit more focused sectioning allowing different sectioning planes for multiple organs from the same pupa. This might be particularly useful if the brain (transverse) and thoracic muscle (longitudinal) were examined. Retaining more pupal sections for analysis would limit the amount of tissue loss, but would increase the resources required and time taken for analysis. Clearly improvements in accuracy of PMI would need to be balanced against the extra work involved.

6.3.3 Estimation of age using Optical Coherence Tomography

The pilot study using OCT was to test whether morphology information could be obtained without histology for age estimation. Non-destructive *in vivo* methods are obviously advantageous and would permit further analyses to be performed.

The main limitation of the OCT system used for these studies is the lack of vertical resolution. The tissues absorb the light strongly so that penetration is limited to 1-2mm and resolution is lost. Preserved pupae with puparia removed allowed the most detailed images to be obtained and differentiation between 4d and 10d pupae was possible. The sclerotisation of 10d pupae increased the light scattering, thus improved surface and internal resolution, indicating this method would be most suited to age estimation of older samples. However, the use of OCT on preserved pupae offers no advantage over standard external morphological examination, which provides more accurate age estimates. Age estimation of live pupae using OCT would be advantageous to PMI estimation; estimates may be accurate to within a few days (based on gross morphological changes), providing an initial assessment prior to rearing of the pupa to eclosion, or performing targeted age estimation using other methods such as gene expression.

For OCT to be adopted as a useful method for morphological analysis, the vertical resolution or penetration depth must be improved. This could be achieved by using a laser with a longer wavelength than 1130nm, such that less light is absorbed by the tissue, however this technology is unavailable at present. The injection of contrast agents such as microspheres into living organisms has been shown to improve image quality, by increasing the light-scattering properties of the tissues (Lee *et al.,* 2003; Boppart & Suslick 2006). This method would require the pupa to remain alive for a period of time sufficient for this to occur, reducing the accuracy of age and PMI estimation. Overall, OCT may have some future potential as a tool for examination of internal and external morphology of live pupae, however for it to replace external morphology and/or histological examination, improvements must be made.

6.4 Conclusion

Histological pupal age estimation can be performed using five main features: the brain, compound eyes, intersegmental and thoracic muscle, digestive system and fat body. In addition, the salivary glands indicate whether a pupa is younger or older than 5558 ADH. Observation of these features is facilitated by transverse sectioning of the head and longitudinal sectioning of the thorax and abdomen. Inconsistencies in section selection and resulting tissue loss mean observation of development and detection of small features like appendages is difficult. The use of OCT is limited due to the poor vertical resolution; it is not a substitute for histological analysis at present.

Overall, histological analyses can be used to estimate age from internal morphological development to within +/-600 ADH. This method is most useful when external morphological examination is not possible, but is most reliable when used in collaboration with an estimate obtained from external morphology or gene expression.

Chapter 7 – Developmental gene expression throughout pupal development

7.1 Introduction

The phenotypic changes that occur during metamorphosis have been shown to be useful in pupal age estimation, as described in Chapters 5 and 6. However, assessment of these markers is qualitative and necessarily subjective, limiting the reliability of the age estimate. Underpinning these morphological developments are changes at the molecular level, particularly gene expression. This provides the potential for a more quantitative measurement and a more accurate, reliable and objective age estimate.

7.1.1 Biochemical methods age estimation

Pupal age estimation has been attempted in other Diptera using biochemical changes that occur during metamorphosis. In *Protophormia terraenovae* and *Drosophila melanogaster*, steroidogenesis and pupal cuticle protein production were shown to fluctuate predictably with age (respectively). However, reliable age estimation using these methods was not possible in pupae older than approximately 25% developed; 2-3 days in *P. terraenovae* or 24 hours in *D. melanogaster* (Gaudry *et al.,* 2006; Doctor *et al.,* 1985). Age estimation using these methods has not been pursued, likely due to their apparent limited timeframe of use.

Variation in production and degradation of volatile organic compounds (VOCs), including cuticular hydrocarbons (CHCs), has also been investigated. CHCs are linear molecules with chain lengths ranging from 19 to 70 carbon atoms (Drijfhout 2010) and are measured by gas chromatography-mass spectrometry (GC-MS). Pupal CHC composition was species-specific for *P. terraenovae*, *C. vicina* and *C. vomitoria* and permitted age estimates with a 1-3 days accuracy (Roux *et al.,* 2008). Similarly, *C. vicina* larval and pupal age estimation was possible to within a 3-4 day window based on the abundances of species in the total VOC spectrum (Frederickx *et al.,* 2012). CHC composition has been used as an age indicator of *Aedes aegypti* adults, however it is dependent on environmental conditions and requires multiple regression models to achieve an accuracy of +/- 10 days (Desena *et al.,* 1999; Gerade *et al.,* 2004). Degradation of *C. megacephala* pupal CHCs after adult emergence can estimate PMI up to 90 days after emergence (Zhu *et al.,* 2007), although the environmental effects on pupal CHCs and VOCs has yet to be fully studied, therefore the accuracy of this method is unknown. Recently, *A. aegypti* adult CHC age estimation has been surpassed by that of temporal gene expression with an accuracy of +/- 5 days (Cook *et al.,* 2006).

7.1.2 Age estimation using developmentally-regulated gene expression

Translation of selected subsets of mRNA is required for all developmental processes including larval tissue histolysis, imaginal disc development and remodelling of larval tissue. This is controlled by up- and down-regulation of gene transcription throughout development and measurement of transcript levels can indicate age.

Few studies into Calliphoridae age estimation by gene expression have been published. In the absence of an annotated genome, selection of suitable developmentally expressed genes (DEGs) and housekeeping genes (HKGs) is difficult. As a result many studies have utilised differential-display reverse-transcriptase PCR (ddRT-PCR) to identify candidate DEGs. This method amplifies a fraction of the transcriptome at different timepoints using a specific selection of anchored and arbitrary primers. Genes with the highest expression levels are preferentially amplified, and compared between the timepoints using gel electrophoresis (Bauer *et al.,* 1994).

Three ddRT-PCR studies in Calliphoridae pupae (Table 7.1) have shown pronounced developmental expression changes. In *C. vicina*, expression levels three DEGs (one of which was discovered using ddRT-PCR) were studied by qPCR, normalised to an internal HKG level and revealed the potential to estimate pupal age in ADH (Ames *et al.,* 2006). However, ddRT-PCR band patterns in *Lucilia sericata* appeared to correspond to genetic lineage than differential expression between ages (Zehner *et al.,* 2006). The most recent study examined expression levels of thirteen genes (ten DEGs, nine of which were identified by ddRT-PCR and three HKGs, one of which was identified by ddRT-PCR) in pupae 24, 120 and 216 hours after puparium formation (APF) (Zehner *et al.,* 2009). qPCR data indicated RP49 (Ribosomal protein 49; 60S subunit) was the most consistently expressed HKG and two of the newly discovered (unidentified) DEGs were the most differentially expressed.

However, these data are unsuitable for age estimation as derivation of DEG/HKG ratios was not possible because expression levels were compared to either the post-feeding larval (Ames *et al.,* 2006) or early pupal (Zehner *et al.,* 2009) stages. This is not possible from crime-scene samples for which age must be obtained from (ideally) multiple intrinsic gene expression ratios, after normalisation to a HKG such as actin

Table 7.1 Summary of studies on Calliphoridae pupal gene expression. Three studies have been conducted into pupal age estimation by measurement of temporal gene expression in the Calliphoridae. Each has used a variety of genes identified by ddRT-PCR and developmental expression patterns have been analysed using comparison of band patterns or ratios produced by quantitative PCR.

Authors	Species	Timepoints	Genes	Gene expression level comparison
(Zehner *et al.* 2006)	*Lucilia sericata*	4	Multiple (band patterns)	Visualisation of band patterns produced by one set of ddRT-PCR primers, amplifying both captive bred and wild colonies.
(Ames *et al.* 2006)	*Calliphora vicina*	15	4	3 pupal DEG transcription levels obtained by quantitative PCR were normalised to a HKG level and compared to the post-feeding larval stage.
(Zehner *et al.* 2009)	*Calliphora vicina*	3	13	10 pupal DEG and 3 pupal HKG transcription levels were obtained by quantitative PCR and compared for three pupal stages; early, mid and late.

(Ames *et al.,* 2006). Additionally, in these experiments expression levels were reported over few time-points; testing of multiple DEGs at regular intervals throughout the pupal stage is required to monitor expression level changes and assess suitability for age estimation. Disappointingly for the present study, it was not possible to identify Diptera orthologues of the 11 DEGs identified, perhaps due to divergence time between species, or fragment lengths being too short. These unidentified genes may be sex-linked or under circadian control therefore may not exhibit reliable developmental expression patterns and so evaluation of the suitability of these genes for age estimation is not possible.

Selection of genes from existing Calliphoridae or other Diptera datasets has been used for age estimation of *L. sericata* eggs. Binary (on/off) and fluctuating developmental expression levels of three DEGs of known function in development were measured, normalised to combined (average) RP49 and β Tubulin levels and correlated to age in ADH. Egg age was able to be estimated to within 25% of the stage (2 out of 8 hours) (Tarone *et al.,* 2007). This work was then expanded to include the analysis of nine DEGs over the entire lifecycle (Tarone & Foran 2011). Expression level changes throughout the pupal stage did not exceed 4-fold for any gene and levels of two genes varied with temperature. Nevertheless, the data improved pupal age estimates that were based on size and developmental stage alone (which the authors acknowledged were poor indicators of pupal age).

The use of a combination of HKG expression levels in these studies averages out inherent variation in the individual genes. The number and nature of HKG genes required depends on the organism, stage and tissue types used and should be specifically selected for the study (Vandesompele & Preter 2002; Jian *et al.,* 2008; Lourenço & Mackert 2008). Further, instead of ddRT-PCR, Tarone and Foran selected genes with known sequences in *L. sericata* or *L. cuprina* based on their functions and expression patterns of their orthologues in *D. melanogaster*, and so they were likely to display some variation in expression levels in the Calliphoridae. Unfortunately, the limited sequence data for *C. vicina* currently prevents selection of optimal genes in the same way. In contrast, age estimation models based on developmental gene expression were successfully developed for the *Culicidae* (mosquitoes).

The Culicidae are important vectors of malaria and other pathogens and adult age dictates their ability to transmit disease. Age estimation based on CHC level was unable to predict age after 12 days – the most important age for transmission and so age estimation using developmental gene expression was studied. Eight *Drosophila* orthologues were selected (Table 7.2) which show significant changes in expression level in *D. melanogaster* adults. These were deemed unlikely to be affected be reproductive or digestive status. Three HKGs were tested and Ribosomal Protein S17 was selected as being the most consistently expressed (Table 7.2). qRT-PCR (SYBR green method) was used to measure expression level variation as a function of adult age and regression analysis was used to create age prediction models. The models (R^2 value of ~0.7) were then used for age prediction of blind samples, to within +/- 5 days (Cook *et al.,* 2006). However, Calliphoridae and Culicidae gene expression varies with season and temperature (Tarone & Foran 2011; Gerade *et al.,* 2004) and

Table 7.2 Genes examined for age estimation of *Aedes aegypti* adults. Ae. aegypti genes were selected using known function and expression data in *Drosophila*. One HKG (RpS17) was selected for normalisation of eight DEGs. Accession numbers are given in brackets.

***Drosophila* gene**	**Putative function**	***Ae.aegypti* orthologue**
RpS17 (CG3922)	Structural ribosomal protein	Ae-RpS17 (AY927787)
fizzy (CG4274)	Cell cycle, cell physiology	Ae-4274 (TC6602)
CG4679	-	Ae-4679 (TC66515)
me@31B (CG4916)	Nucleic acid metabolism	Ae-4916 (TC54107)
CG6639	-	Ae-6639 (AY431255)
Rpd3 (CG7471)	Histone methylation	Ae-7471 (TC62395)
CG8505	Structural component of cuticle	Ae-8505 (AY432732)
CG12750	Protein biosynthesis	Ae-12750 (TC63489)
Scp1 (CG15848)	Calcium-binding protein	Ae-15848 (TC59614)

as a result, multiple regression models were developed to correct for these variables and give more accurate age estimates (Hugo & Cook, 2010).

Similar age estimation models were developed for adult *Anopheles gambiae*. Microarray analysis identified the 40S ribosomal protein S7 as the most consistently expressed HKG and 2713 DEGs. Four of these DEGs were selected for age estimation, one of which was also identified in *A. aegypti* (Ae-15848; Table 7.2). The resulting R^2 value for the regression model was 0.82 and validation resulted in consistent age prediction within +/- 4.2 days (Cook & Sinkins 2010) which is more accurate than age estimation of *A. aegypti*. These studies highlight parallels within the Culicidae, such as similarly suitable HKGs and DEGs; this may also be applicable to the Calliphoridae.

7.1.3 C. vicina pupal age estimation using developmental gene expression

To develop a suitable gene expression based estimation methods for *C. vicina* the initial tasks were to identify suitable target genes and choose a method of measurement. Two approaches are possible: microarray analysis of multiple transcript levels or quantitative PCR of selected amplicons.

Microarrays are comprised of a set of immobilised genome-wide or custom selection of DNA probes or cDNA expressed sequence tags (ESTs) of known sequence. Typically, mRNA is extracted from the required stages (or tissues) and the cDNA fluorescently tagged allowing quantification of hybridisation levels in the arrayed sequences (NCBI 2007). This method has been used in Drosophilidae and Culicidae for DEG analysis (Table 7.3) for which there is extensive genomic sequence data. These studies have identified genes with considerable changes in developmental expression, which may be suitable for age estimation, however since *C. vicina* genome or transcriptome data are absent, microarray analysis is not possible. Larval and adult ESTs are available for another calliphorid, *Cochliomyia hominivorax*, but this

Table 7.3 Summary of microarray analysis studies of differential gene expression in Drosophilidae and Culicidae. Much of the work conducted into developmental and differential gene expression has involved *Drosophila* spp. Studies have looked at individual tissues, specific lifecycle stages, species differences and genes under control mechanisms.

Species	Analysis	Authors
Drosophila spp.	Wing development	(Ren *et al.* 2005)
D. melanogaster	Circadian rhythm control	(McDonald & Rosbash 2001)
Aedes aegypti *D. melanogaster*	Ecdysone control	(Margam *et al.* 2006; White *et al.* 1999)
D. melanogaster *D. simulans*	Species and sex differences	(Ranz *et al.* 2003)
D. melanogaster	Pupal somatic and germline tissues	(Lebo *et al.* 2009)
D. melanogaster	Lifecycle expression levels	(Arbeitman *et al.* 2002)

is unsuitable for *C. vicina* age estimation because of a) the lack of pupal ESTs and b) the unknown hybridisation efficiency between species.

The alternative approach is the use of qRT-PCR to measure expression levels of specific genes. Quantification of individual transcripts is carried out during the early exponential phase of PCR using the measurement of fluorescence intensity, either by SYBR green (a DNA intercalating agent) or labelled TaqMan probes (Fig. 7.1). SYBR green binds non-specifically to double stranded DNA hence the level of fluorescence increases as the PCR products are synthesised. This method has been widely used to measure expression levels for age estimation (Tarone *et al.,* 2007; Tarone & Foran 2011; Cook *et al.,* 2006; Cook & Sinkins 2010), however analysis of multiple genes in a single reaction is not possible. TaqMan dual-labelled probes provide greater specificity and enable multiplexing by tagging probes with different fluorophores (Scanlan *et al.,* 2001), ultimately saving time and costs. The probes bind to single-stranded DNA and as polymerisation occurs, the flurophore is separated from the quencher and fluorescence is detected (Fig. 7.1). In both the SYBR green and TaqMan methods the PCR cycle at which the fluorescence rises above the background noise is called the threshold cycle (C_T). Higher C_T values indicate lower levels of gene expression, which is measured relative to an internal loading control by the difference between the C_T values of the DEG and HKG; the ΔC_T method.

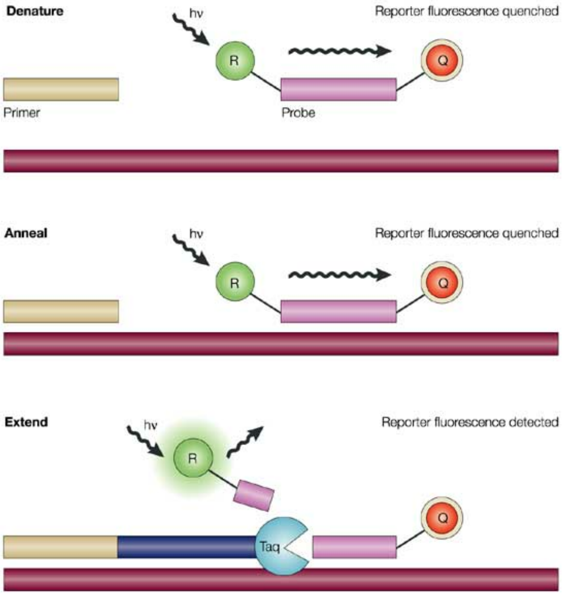

Figure 7.1 Taqman probe principles. Taqman probes comprise a single strand of DNA with a sequence complementary to that of the target gene. Bound to the 5' and 3' ends are a fluorescent reporter (R) and a quencher (Q). After binding to the target gene in the annealing phase, the probe is cleaved by the 5'-3' exonuclease activity of the polymerase in extension phase, releasing the fluorescent reporter from the close proximity to the quencher. Fluorescence is emitted when the free reporter is excited by an external light source. Fluorescence levels increase in the exponential phase with each PCR cycle (Koch 2004).

Developmentally expressed genes suitable for measurement by the ΔC_T method using qRT-PCR can be discovered using ddRT-PCR (Ames *et al.,* 2006; Zehner *et al.,* 2009), but their functions have not been identified. Zehner *et al.,* (2006) suggested there are morphological changes and other dipteran expression data that could be used to predict usefulness of candidate genes for qRT-PCR analysis. For example, examination of larval serum protein 2 (LSP-2) expression in *C. vicina* indicated similar expression levels to those seen in *Drosophila* spp. (Ames *et al.,* 2006). However, only partial sequence data for 52 *C. vicina* genes are available and their developmental expression patterns may not be suitable for pupal stage since they were identified for other purposes. Drosophilidae and Culicidae studies (Lebo *et al.,* 2009; Margam *et al.,* 2006) may provide candidate *C. vicina* genes. However, examination of transcript levels relies on the ability to design appropriate cross-species degenerate primers. This can often be difficult due to the limited homology (~76%) and long divergence time (100 million years) between *D. melanogaster* and *C. vicina* (Simpson 2007). Despite these limitations, this method has the potential for selection of the most differentially expressed genes.

7.1.4 Conclusions and aims

At present there are insufficient data to estimate *C. vicina* pupal age using developmental gene expression. Due to the absence of genome data suitable DEGs and HKGs were sought from alternative species. Changes in transcript levels of these genes will be tested for correlation with age in ADH to provide a model for quantitative age estimation. The aims of this study were therefore:

- Select and design degenerate primers for suitable candidate DEGs and HKGs from other dipteran and insect studies
- Examine the expression levels of these genes by semi-quantitative PCR to test for suitability.
- Upon selection of optimal genes, measure the DEG expression levels relative to an overall HKG expression level by real time PCR using TaqMan probes.
- Use regression analysis to develop a model for age estimation.

7.2 Results

Expression levels of developmental genes were measured in 42 pupae collected throughout metamorphosis in order to develop a method of quantitative age estimation. Pupal ages were calculated as described in Chapter 5.2.1, and were part of the same set collected for histological analysis (Table 6.5).

7.2.1 Verification of RNA quality

Accurate measurement of gene expression levels requires extraction of intact RNA. For initial experiments RNA was extracted from a single pupa every 24 hours throughout the pupal stage using a Macherey Nagel kit adapted to include with additional steps (see Chapter 2 for details). Two groups of seven pupae were processed simultaneously to minimise processing time, contamination and degradation by RNases. RNA integrity was initially assessed by agarose gel analysis using visualization of defined 18S rRNA bands at ~800 bp of a dsDNA ladder and the absence of low molecular-weight smearing as an indicator of quality (Fig. 7.2). The lack of a 28S rRNA band is due to the hidden break in this insect rRNA. Heating the rRNA at 40-60°C for a few minutes denatures the hydrogen bonds holding the two fragments together. This causes the 28S rRNA to separate and comigrate with the 18S band to approximately the 800 bp region, increasing its intensity on agarose gels (Inada & Pleiss, 2009; Winnebeck, 2010). Overall the yield and integrity of rRNA was good (Fig. 7.2). The yield from only one pupa at 10530 ADH (13 days at 22°C) was poor, suggesting the pupa may have died prior to preservation. In total, RNA was extracted from three pupae per time-point (data not shown).

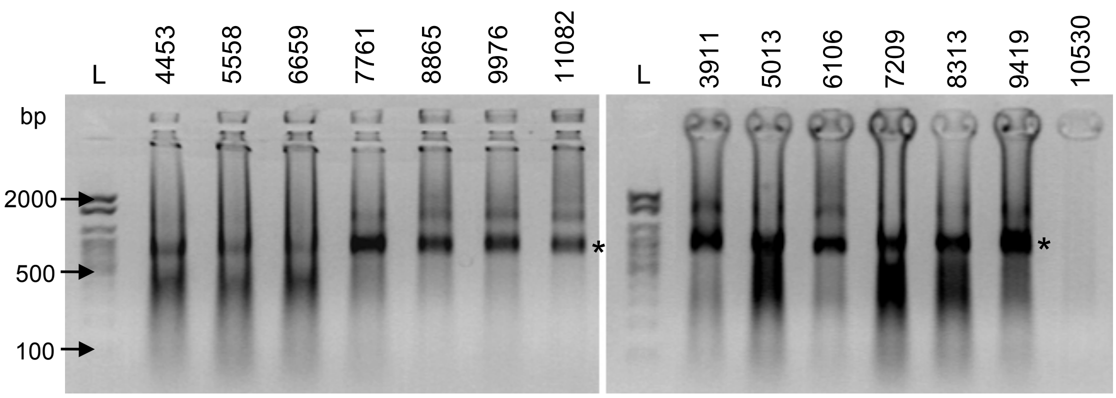

Figure 7.2. Examination of RNA extracts. RNA was extracted from a single pupa (three in total; data not shown) every 24 hours. Extracts were visualised on a 1.5% agarose gel stained with ethidium bromide. L =100bp dsDNA ladder. Lane headings indicate pupal ages in ADH. Ribosomal RNA bands (at ~800bp dsDNA) are indicated by asterisks.

Following RNA extraction an additional DNase I digestion was conducted to ensure removal all traces of gDNA. This was evidenced by failure to detect of the 85bp actin PCR product from amplifications conducted on such extracts prior to reverse transcription (data not shown). After the reverse transcription step amplification of actin (85bp) and arylphorin (133bp) products from fixed amounts of cDNA was used to assess RNA integrity and yield. Although mRNA transcripts degrade at different rates (Sachs, 1993), this gives a crude but better indication of integrity and overall suitability for quantification than visualisation of RNA extract integrity. Amplification products of the expected size were obtained from all pupae, which indicating the suitability of the cDNA for qPCR (Fig. 7.3). It also reduced wastage of qPCR reagents and time: a single cDNA sample (pupa aged 5013 ADH) failed to produce a PCR product initially and was reverse-transcribed and amplified again (Fig 7.3). In pupae aged 4453, 9976 and 10530 ADH it was necessary to repeat PCR amplification of the cDNA to obtain PCR products (Fig 7.3). It was recognised that whilst amplification of the cDNA was successful for these genes, qPCR may not necessarily yield products from other targets due to variation in degradation rates between transcripts.

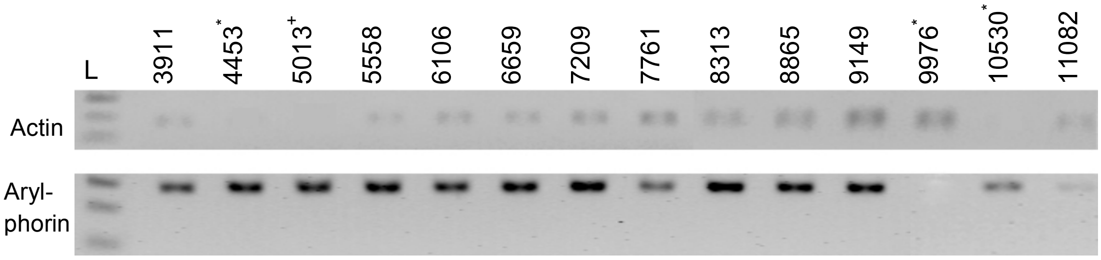

Figure 7.3 Examination of PCR products. RNA extracted from each pupa was reverse transcribed to cDNA, then amplified by PCR (35 cycles) to test the integrity and suitability for qPCR. L = DNA ladder. Lane headings indicate pupal ages in ADH. Actin (85bp) and arylphorin (133bp) PCR products were amplified from all cDNA from the first pupal extracts. Faint bands (asterisks) were reamplified successfully. '+' indicates the pupal RNA which required repeated reverse-transcription and PCR to yield a product.

7.2.2 Semi-quantitative PCR

The selection of HKGs is dependent on which tissue/stage/sex is being analysed (Ling & Salvaterra, 2011; Shen & Jiang, 2010) and so a selection process for each investigation should be conducted. Due to the absence of an annotated *C. vicina* genome or transcriptome, selection and amplification of suitable genes for pupal age estimation using temporal/developmental expression analysis was complex. The expression data available for *Drosophila, Aedes* and *Anopheles* spp. on FlyBase and in other publications (Lebo, Sanders, Sun, & Arbeitman, 2009; Margam, Gelman, & Palli, 2006; Marinotti & Calvo, 2006) was used to select candidate genes. Elongation factor 1a (EF1α), ribosomal protein 49/L32 (RP49 or RpL32) and glyceraldehyde 3-phosphate dehydrogenase (GAPDH) were identified as candidate HKGs, based on existing data from other insects (Appendix IV, Table A4). High levels of conservation between HKGs (Hoy, 2003) allowed degenerate primer design (after Bagnall & Kotze (2010)) and amplification of these genes in *C. vicina*.

Semi-quantitative PCR was used for the initial assessment of expression level by measuring PCR product intensity. Whilst this does not measure expression level as accurately as qRT-PCR (Marone *et al.,* 2001) by ensuring observations were made in the exponential phase of the amplification it enabled candidate gene selection. Equal amounts of pupal cDNA (100 ng) were amplified using appropriate primers for GAPDH, EF1α and RP49. PCR products obtained during the exponential phase were used to compare gene transcript levels throughout development. GAPDH expression showed most variation throughout metamorphosis (Fig. 7.4). Similar variability was also observed for GAPDH in *Lucilia cuprina* (Bagnall & Kotze, 2010). RP49 and EF1α were therefore selected for normalisation of DEG levels, with EF1α showing the most consistent expression level.

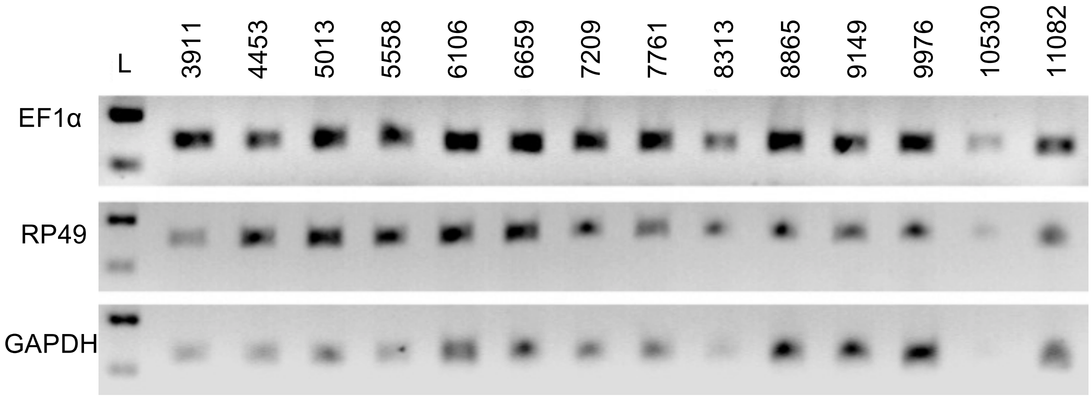

Figure 7.4. Semi-quantitative PCR analysis of HKG expression. Individual pupal cDNA was analysed by semi-quantitative PCR to estimate expression levels throughout the pupal stage. L = DNA ladder. Lane headings indicate pupal ages in ADH. PCR products shown are EF1α (139 bp), Rp49 (143 bp) and GAPDH (155 bp) amplicons, all after 26 cycles of amplification.

Candidate DEGs were identified from Lebo *et al.,* (2009) and Margam, Gelman, & Palli (2006) (Fig. 7.5 and Table 7.4). Despite multiple attempts at degenerate primer design using sequences from *Drosophila* spp., *Aedes* spp., *Lucilia* spp. and *Sarcophaga* spp. where possible, amplification of genes failed repeatedly. This may be due to insufficient conservation between families. For example, *C. vicina* Trp only shares a 76% amino acid identity with Drosophilidae; a result of 100 million years divergence between the two families (Simpson, 2007). Six DEGs (Arrestin, Ecr, LSP-2, Opsin, Shaker and Trp) were selected from existing *C. vicina* data based on morphology (available on NCBI and Ensembl: Appendix IV Table A5). However, the expression levels were not always optimal for age estimation of the pupal stage and the cDNA sequences available lacked introns (incomplete gene sequences).

As before, semi-quantitative PCR was used to assess changes in expression (Fig 7.6). Arrestin and Ecr showed similar expression patterns. However, Ecr has only one known isoform (Table A5), hence it may be a more reliable candidate gene. LSP-2 and Shaker showed similar in expression patterns throughout metamorphosis. Based on *Drosophila* spp. data, LSP-2 has the higher expression level and since Shaker is located on the X chromosome, which could result in sex-specific expression levels, LSP-2 was selected for qPCR analysis. Opsin amplification was poor and produced intense primer dimer bands so this gene was not used. Trp showed distinct changes in expression. Shaker and Trp showed temporal expression patterns similar to that

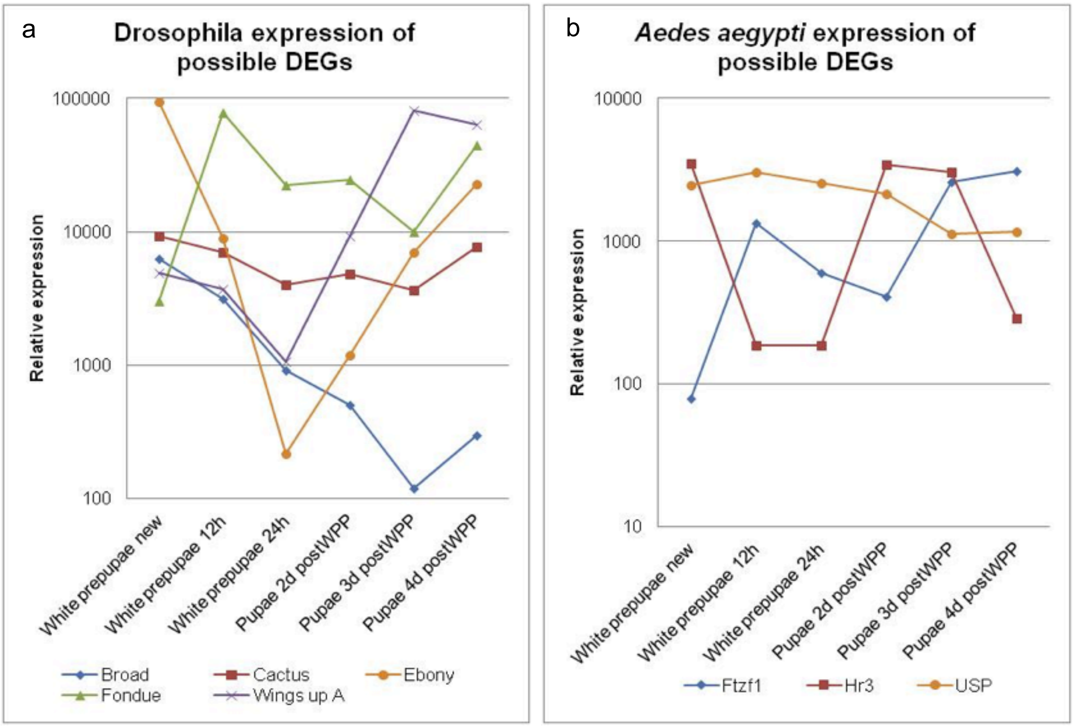

Figure 7.5. *Drosophila* and *Aedes* pupal expression levels of candidate DEGs. Genes were selected from a) Lebo *et al.*, (2009), and b) (Margam *et al.* 2006) based on function and *Drosophila* and *Aedes* expression levels (obtained from www.flybase.org). Prepupae indicates pre-head eversion; postWPP indicates after white pupal stage.

Table 7.4 Functions of possible suitable DEGs. Examples of functions in *Drosophila* of possible DEGs suitable for age estimation of pupal stage (obtained from www.flybase.org).

Gene	Chromosome	Function
Broad	X	Photoreceptor development
		Larval CNS remodelling
		Salivary gland histolysis
Cactus	2L	Dorsal appendage formation
		CNS development
		Oogenesis
Ebony	3R	Pigmentation
		Photoreceptor activity
		Circadian behaviour
Fondue	2L	Hemolymph coagulation
		Metamorphosis
		Puparium formation
Wings up A	X	Muscle development
		Nervous system development
		Heart development
Ftzf1	3L	Leg development
		Olfactory behaviour
		Metamorphosis/pupation
Hr3	2R	Brain development
		Bristle formation
		Wing development
USP	X	Dendrite morphogenesis
		Muscle development
		Imaginal disc development

observed in *D. melanogaster* though Arrestin or Ecr patterns were quite different. LSP-2 expression was constitutively high in *C. vicina*, whereas in *D. melanogaster*, in accordance with function, it appears to decrease with age of pupae. These unusual profiles may be due to non-linearity of semi-quantitative PCR, or may indicate these genes have different or multiple roles in Calliphoridae metamorphosis, in comparison to the Drosophilidae. Therefore, the genes selected for quantitative PCR analysis were Ecr, LSP-2 and Trp.

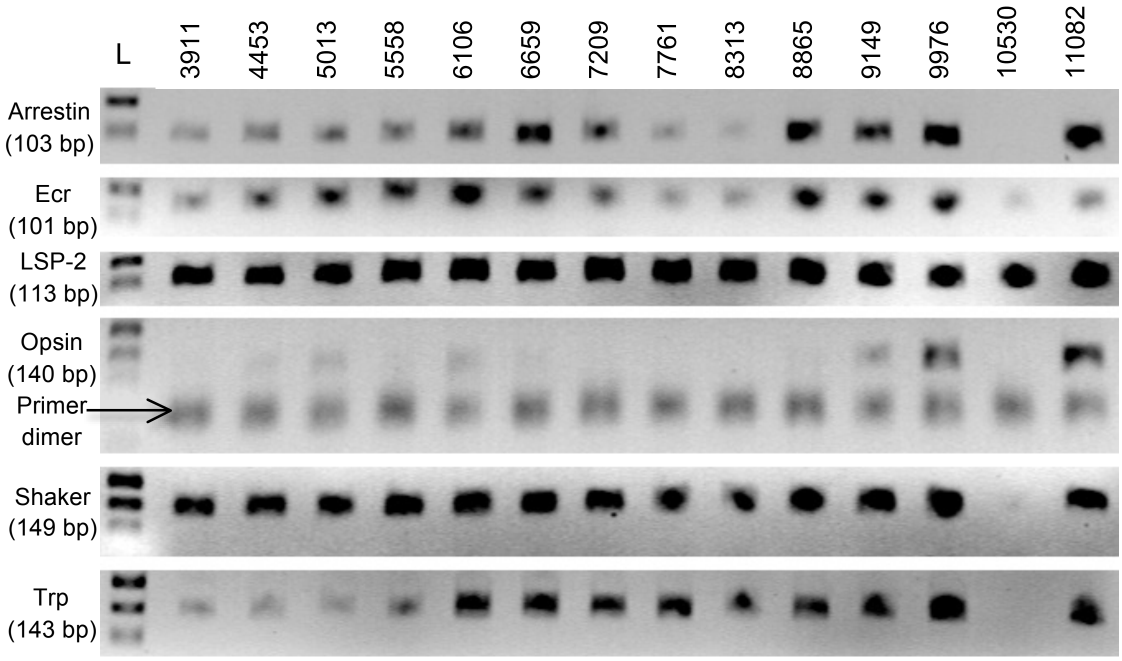

Fig. 7.6. Semi-quantitative PCR analysis of DEG expression. Individual pupal cDNA was analysed by semi-quantitative PCR to estimate expression levels throughout the pupal stage. L = DNA ladder. Lane headings indicate pupal ages in ADH. PCR products are shown from all *C. vicina* DEGs.

7.2.3 Quantitative PCR

qRT-PCR measurement of HKG and DEG transcript levels was conducted on three pupae (biological replicates) sampled at 24-hour intervals making three C_T measurements of each. Anomalous data points that were outside +/- 1 C_T i.e. a maximum of 4-fold difference in expression level of the mean transcript expression for the time-point were removed. This resulted in removal of 15, 3, 7, 3 and 13 C_T values (out of a total 126) for Rp49, EF1α, Ecr, LSP-2 and Trp respectively. All samples had at least 6 individual C_T measurements remaining for all genes other than pupae aged 10530 ADH for RP49, which had 4. The smallest and largest standard deviation values were obtained from pupae at 9976 and 8313 ADH respectively (Table A6 and Fig. 7.7). The differences between housekeeping gene C_T levels were minimal and always between +/- 2 (maximum 8 fold difference) which facilitated combination (by averaging) of expression levels. The geometric mean C_T for both HKGs over the entire pupal stage was 22.72. The use of the geometric instead of the arithmetic mean of 2 – 4 housekeeping genes to give a normalization factor has been previously suggested to reduce inherent variation in HKG expression level in bees, plants and human cells (Jian *et al.,* 2008; Lourenço & Mackert, 2008; Vandesompele & Preter, 2002). As an initial indicator the mean of two commonly used HKGs can be averaged. In larger-scale analyses multiple genes are selected, amplified and their individual stability indicated by analysis of C_T values using software such as GeNorm and Normfinder (Jian *et al.,* 2008; Ponton *et al.,* 2011; Scharlaken *et al.,* 2008; Van Hiel *et al.,* 2009) prior to averaging of the most stable genes. Both methods have been carried out recently in *Lucilia* spp. (Tarone & Foran 2011; Bagnall & Kotze 2010). The HKGs examined in this study displayed similar low C_T levels to LSP-2 and consistently lower C_T values than Ecr and Trp. Trp had an initially high C_T, which decreased with time throughout the pupal stage.

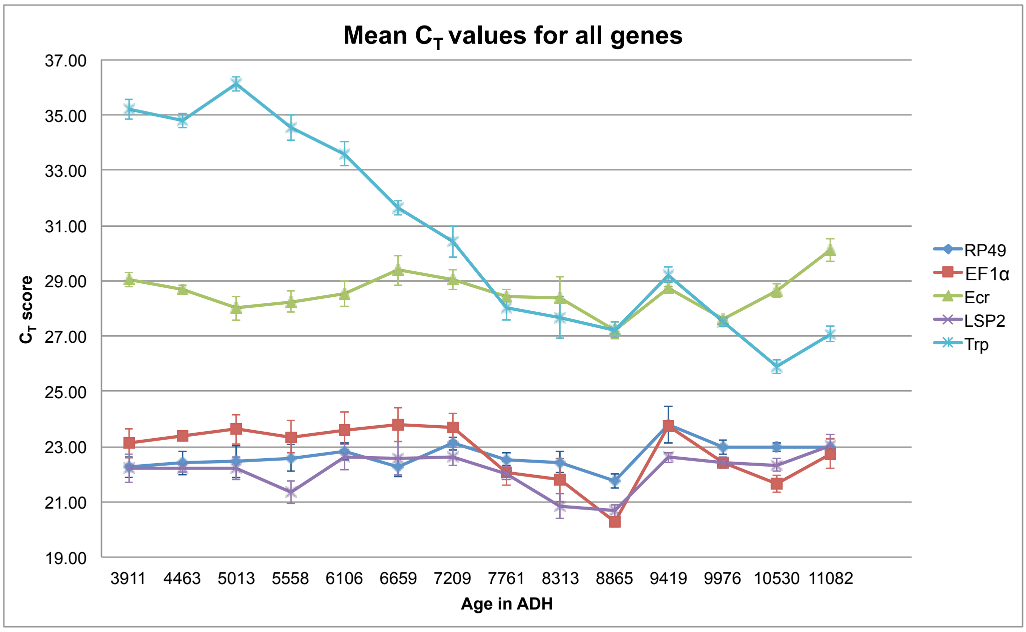

Figure 7.7. C_T variation with pupal age. Changing C_T values with pupal age (mean of three PCR replicates of three pupae) are shown for each gene. Lower C_T value indicates higher expression level (prior to normalisation).

ΔC_T values for all pupae were calculated as relative expression ratios for age estimation (Appendix IV Table A7) using both combined HKG data (Fig. 7.8a). Combining poor HKGs may reduce the accuracy of data and impede reliable age estimation. Therefore, ΔC_T values were also calculated as relative expression ratios to each HKG (Fig. 7.8b), enabling detailed observation of individual variation and HKG averaging effects. Despite similarity in overall trends, differences in relative expression ratios are observable (Fig. 7.8). The data also allow use of the most stable HKG only; RP49 (see Chapter 7.2.4). ΔC_T values were then converted to fold changes in expression relative to the lowest overall expression level; Trp at 5013 ADH, normalised to 1 (Table A7 and Fig. 7.8c-d).

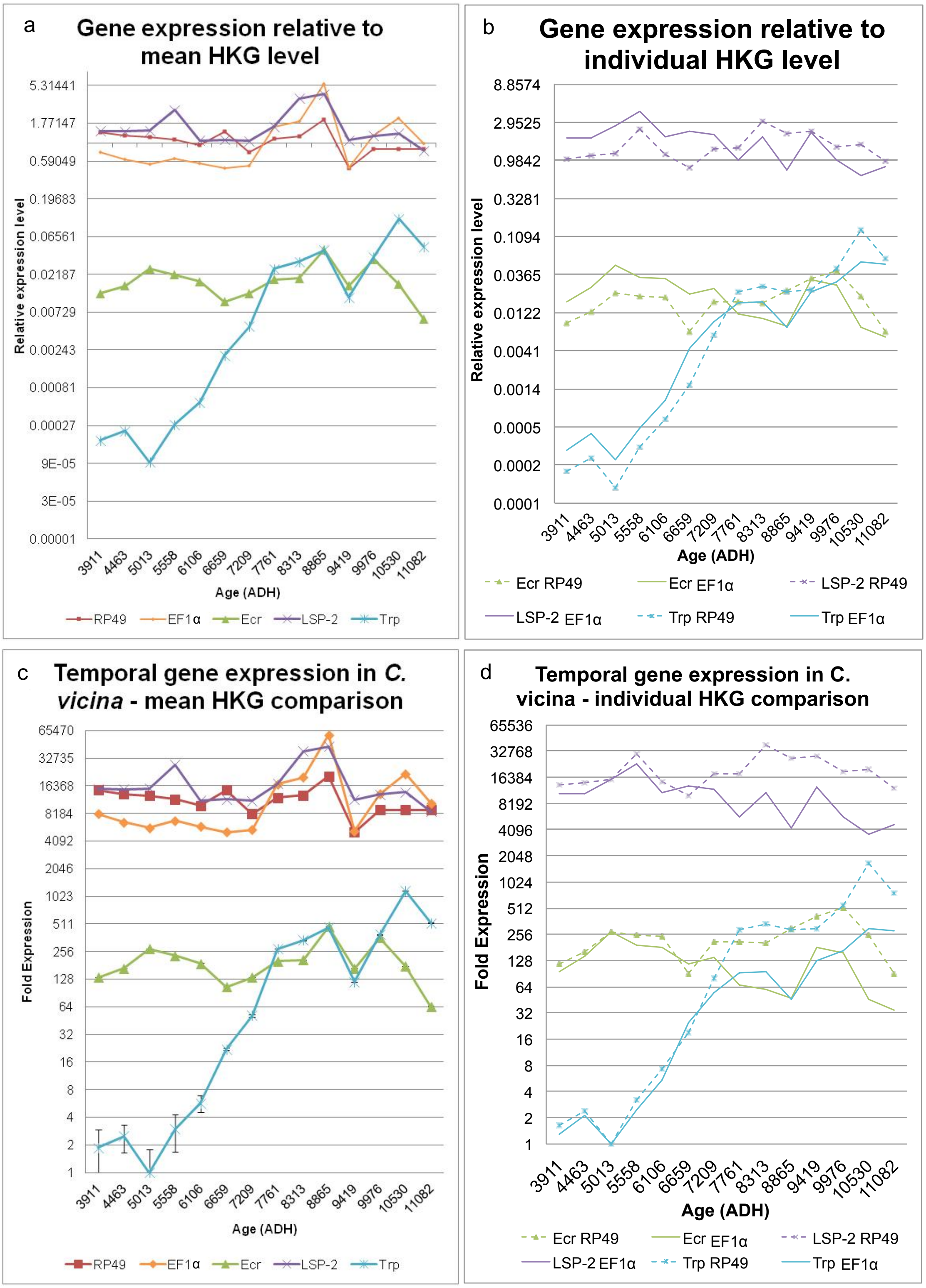

Figure 7.8 Relative temporal gene expression in *C.vicina*. Five genes were amplified from pupal RNA extracted from 24-hourly samples. DEG:HKG expression ratios were calculated and are plotted using a logarithmic scale and displayed relative to the a) mean overall HKG level and b) RP49 (or EF1α) at each age across the pupal stage and normalised to lowest levels and c) relative to the mean overall HKG level or d) relative to RP49 (or EF1α) at each age in ADH. RP49 represented by dashed lines; EF1α by solid lines (in b and d).

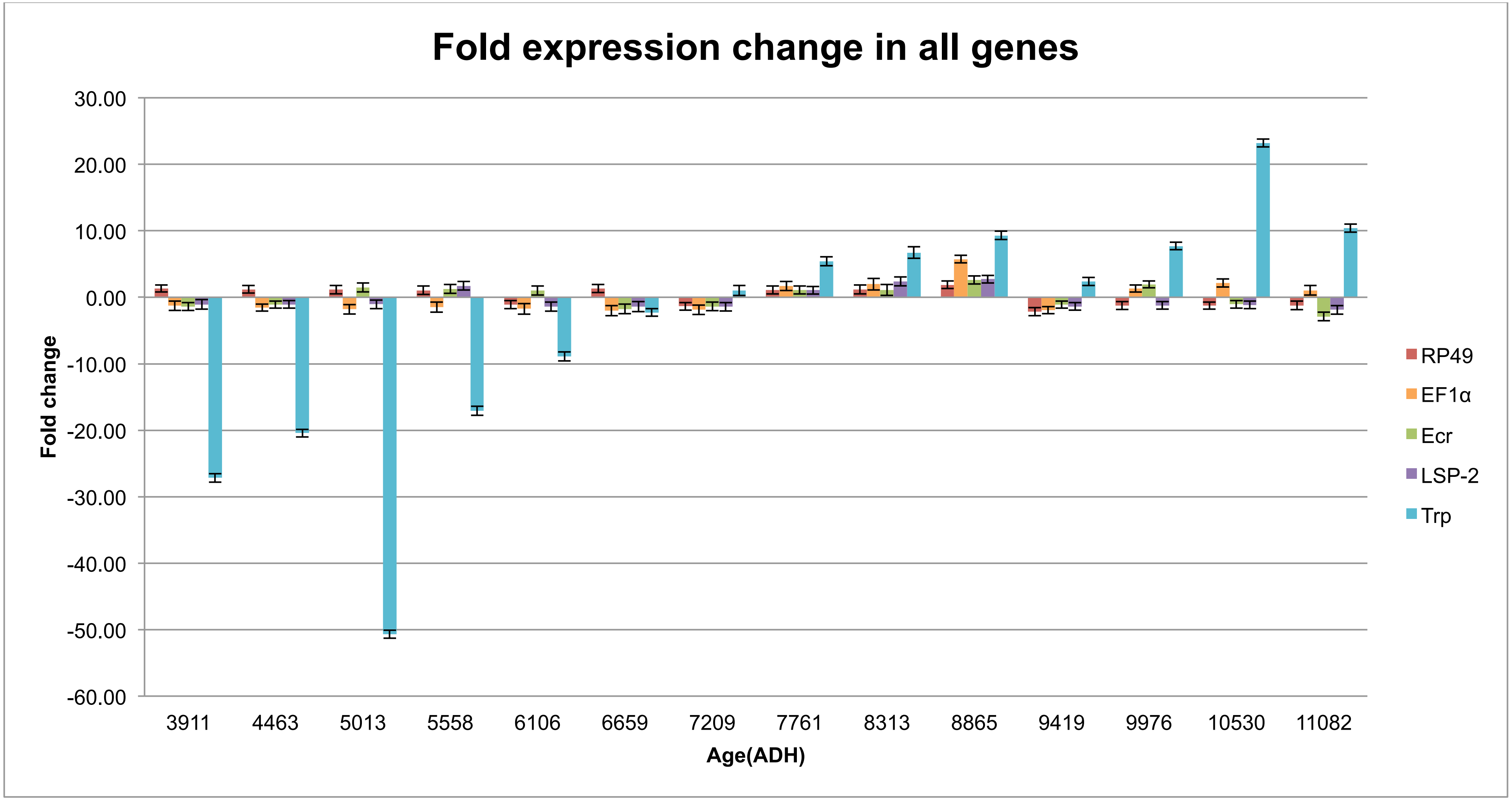

Figure 7.9 Fold expression changes observed in all genes. The change in fold expression relative to the geometric mean pupal stage level (for each gene) is displayed for all genes across the pupal stage.

The overall geometric mean of each gene was used to calculate changes in fold expression over the pupal stage (Fig. 7.9). Transcript levels of Ecr, LSP-2, RP49 and EF1α changed very little during developmental expression, with a fold-expression range from 4 to 7. In contrast, Trp displayed a 74-fold variation in expression range (Fig. 7.9), indicating its utility as an age marker.

7.2.4 Statistical analysis and age estimation

Calculation of the mean and standard deviations of 2^{CT} values for all genes indicated LSP-2 was the most consistently expressed (Mean = $5.0x10^{6}$, S.D. = $1.9x10^{6}$) and Trp was the most variable (Mean = $1.3x10^{10}$, S.D. = $2.2x10^{10}$). RP49 expression was less variable than EF1α (S.D. = $2.6x10^{6}$ and $4.5x10^{6}$ respectively) however a paired T-test indicated EF1α and RP49 were not significantly different from each other (P = 0.16) so were combined to give a mean overall HKG level. Regression analysis was conducted on all relative expression data obtained from all genes (mean HKG and individual HKGs, Table A7). Trp was the only statistically significant predictor of age whether assessed relative to both mean and individual HKG levels (P = 0.014, 0.011 and 0.004 for 'Trp Mean', 'Trp Rp49' and 'Trp EF1α' respectively). The R^2 value for the resulting age estimation equation, which utilised all DEGs normalised to the mean and individual HKG levels (Equation 7.1) was 98.5%. This was tested for accuracy using existing expression levels to create 'age estimates' (Table 7.5). The error range

```
Age (ADH) = 3853 - 521139 Ecr Mean + 2194 LSP-2 Mean + 519500 Trp
            Mean + 510275 Ecr RP49 - 3852 LSP-2 RP49 - 447430 Trp
            RP49 + 42659 Ecr EF1α + 1206 LSP-2 EF1α + 156262 Trp
            EF1α
```

Equation 7.1 Pupal age estimation equation using gene expression data. Regression analysis was carried out on all relative expression data (126 ratios) to produce this equation for pupal age estimation. Each expression value is multiplied by the constant stated. 'Ecr Mean' indicates the value for the relative expression normalised to the geometric mean HKG level obtained for the sample. 'Ecr RP49' and 'Ecr EF1α' indicate the value for the relative expression normalised to the individual Rp49 and EF1α genes.

Table 7.5 Age estimation using the regression equation. Existing data obtained for each age was entered into the regression equation to give a predicted age for 14 pupae. The ADH and lifecycle % error (using a total 11082 ADH) were calculated for each age. Green/red shading indicates estimates within/outside the +/- 360 ADH error calculated from residuals.

Actual age	Predicted age	ADH error	Pupal stage % error	Lifecycle % error
3911	4129	218	2.9	2.0
4463	4273	-190	-2.6	-1.7
5013	5281	268	3.6	2.4
5558	5666	108	1.5	1.0
6106	6126	20	0.3	0.2
6659	6421	-238	-3.2	-2.1
7209	7409	200	2.7	1.8
7761	8040	279	3.7	2.5
8313	8499	186	2.5	1.7
8865	8392	-473	-6.4	-4.3
9419	8866	-553	-7.4	-5.0
9976	10279	303	4.1	2.7
10530	9984	-546	-7.3	-4.9
11082	10773	-309	-4.1	-2.8

obtained from random sample testing was from -553 to +303 ADH (-7.5 to +4.2% of the pupal stage and -5 to +3% of the lifecycle) (Table 7.5). Calculation of the mean residual value and 95% confidence intervals gave an error of +/- 360 ADH; smaller than that observed for 11/14 samples (Table 7.5).

7.3 Discussion

The aim of this work was to develop a gene-expression based age estimation method. This was achieved using regression analysis of the expression ratios of three DEGs (Ecr, LSP-2 and Trp), normalised to two internal housekeeping gene levels (RP49 and EF1α), correlated to age in ADH. The age estimation accuracy of this method was +/-600 ADH; similar to that of external morphological analysis.

7.3.1 RNA extraction and verification quality

Reproducible and reliable extraction, reverse-transcription and PCR amplification of high integrity RNA is essential for accurate pupal age estimation using temporal gene expression. RNA is readily degraded by RNases, therefore rapid extraction was carried out to minimise degradation and maximise yield. Pupae were first completely homogenised using a bead beater for 45 seconds; this was kept as brief as possible to minimise heat generation. The homogenate was then incubated with Proteinase K prior to loading on the spin column to prevent clogging. These adaptations have no effect on gene expression analyses (Egyházi *et al.,* 2004). Pupal RNA was then extracted using a standard kit and protocol, which minimised loss of RNA and prevented degradation by rapid sample processing. In total, RNA was extracted from three pupae per time-point ensuring intra-age variability was measured. As only 24-hourly time-points were analysed, all pupae were selected from a single time-series/sampling period. Validation of intra-sample variation of similar-aged pupae would strengthen this dataset but selection of these individuals is difficult, as temperature data are collected (and ages calculated) after sampling is finished.

7.3.2 Gene selection, primer design and semi-quantitative PCR

Elongation factor 1a (EF1α), Ribosomal protein 49/L32 (RP49 or RPL32) and Glyceraldehyde 3-phosphate dehydrogenase (GAPDH) were initially selected as candidate housekeeping genes. Due to their generally conserved expression levels GAPDH and RP49 have been commonly used as HKGs in *Drosophila* spp. expression studies. In the honey bee (*Apis mellifera*) all three genes were assessed as suitable HKGs for qRT-PCR normalisation (Lourenço & Mackert, 2008; Scharlaken *et al.,* 2008). EF1α and RP49 (or other ribosomal protein genes) were also considered the most consistently expressed housekeeping genes in locust (*Schistocerca gregaria*) (Van Hiel *et al.,* 2009) and flatfish (Infante *et al.,* 2008). Recently, GAPDH expression has been shown to be consistently expressed within most human tissue types, however it varies between them (Barber, *et al.,* 2005). Although, it has been shown to be a poor HKG in blood (Dheda *et al.,* 2004).

Selection of single copy genes minimises the potential for unintended isoform (paralogous gene) amplification, which could complicate measurement of gene expression, hence Ecr was selected in preference to Arrestin. This does assume that no other isoforms for this gene were present in *C. vicina*; actin, for example, has 6 known isoforms in *D. melanogaster* (Fyrberg *et al.,* 1983) but only one (currently known) in *C. vicina* (Ames *et al.,* 2006). Avoiding X-linked genes minimises the potential for sex-linked expression differences. Genes with a variety of known metamorphic functions were selected with the aim of providing markers of age from different morphological locations, facilitating future analysis of spatial gene expression.

7.3.3 Analysis of C_T values using quantitative PCR

Semi-quantitative PCR analysis of transcript levels of the genes selected indicated a temporal changes in their expression occurred. Quantitative PCR provided a more precise measure of relative DEG abundance by analysis of ΔC_T values and expression level ratios. The raw intra-sample range and standard error of C_T values for each gene at each time-point was very low, with only 41 of 630 values (6.5%) showing a greater than 4-fold expression difference compared to the mean. Fifteen of these values (2.4% total) were erroneously high and were obtained from a poor (low yield) extract from a pupa at 10530 ADH, indicating it had likely died prior to preservation. All 41 values were classed as anomalous and excluded from the analysis. The overall range of +/- $1C_T$ for each gene at all time-points indicated very low intra-sample variation and therefore high gene expression stability and a reliable analysis. Both HKGs were expressed at a similar level; the difference in geometric mean C_T across the pupal stage was 0.11 (1.08 fold). This facilitated combination of HKGs into a normalization factor, which was used to standardize DEG level.

7.3.4 Gene expression analysis for age estimation

The ΔC_T method (Tarone & Foran 2011; Antonov *et al.,* 2005) was used to obtain gene expression ratios. It compares expression of two genes for a single sample rather than between samples, which of course is not possible for crime scene samples. The absolute quantification of transcripts was not required for this study, therefore standard curves were not produced.

qRT-PCR analysis indicated the expression of RP49 showed less variation than EF1α yet both displayed greater variation in expression than LSP-2, which is not considered as a HKG. The observed HKG variation may be due to the examination of whole organism HKG expression level; GAPDH has been shown to vary 15-fold between human tissue types (Barber *et al.,* 2005). This highlights the problems with using single or few combined genes to normalise gene expression when multiple tissues or developmental stages are analysed. RP49 and EF1α may more consistent expression levels in a single tissue type or during a shorter developmental stage. In *D. melanogaster*, the expression of RP49 and EF1α was dependent on the investigation variable such as diet, heat shock or bacterial infection (Ponton *et al.,* 2011). GAPDH was previously found to be a poor candidate in Diptera (Shen & Jiang, 2010), and RP49 and EF1α have not been compared to other HKGs in the Calliphoridae. In the most recent study, β tubulin, Acidic ribosomal phosphoprotein PO and 28S rRNA genes were considered the most consistently expressed during the pupal stage (Bagnall & Kotze, 2010). Unfortunately, these data were not available when the HKGs for this study were selected and they also did not consider RP49 and EF1α.

The variation in expression levels of Ecr and LSP-2 were of similar magnitude to the housekeeping genes and showed little variation in level throughout the pupal stage so these genes have limited value as age markers. The main role of Ecr is in the control of ecdysis (Carmichael *et al.,* 2005) however it has additional roles in imaginal disc, neuron and gonad development (Table A5). Its expression was therefore expected to display some variation during metamorphosis, as it does in *D. melanogaster*. LSP-2 functions as a larval storage protein and expression levels were expected to decrease as observed in *D. melanogaster*. Instead, LSP-2 expression levels remained at a similar level throughout metamorphosis. Trp showed similar expression patterns in *C. vicina* and *D. melanogaster*. These differences observed in Drosophilidae and Calliphoridae expression may be explained in part by gene copy number. Single-copy genes (like Trp) have been shown to have greater homology between species than genes with multiple copies (Ecr = six transcript/splice variants, LSP-2 = five similar genes/paralogues), supporting the idea that changes in gene expression lead to speciation (Gu *et al.,* 2004). These issues complicate the process of candidate gene selection using *Drosophila* spp. data and highlight the importance of obtaining full genomic and transcriptome data for forensically important species to allow selection of single copy genes for expression analysis for age estimation purposes.

The data obtained from all five genes analysed was used to create a regression equation with a correlation coefficient of 98.5%. Using this, it was possible to obtain pupal age estimates with an experimentally-derived window of error of +/- 600 ADH (+/- 27 hrs at 22°C) and +/- 5% of the lifecycle. The residual-derived error of +/- 360 ADH (+/- 16 hrs at 22°C) encompassed 11/14 pupae (79%). This is already similar to that achieved using 23 morphological features, yet this method removes the subjectivity associated with qualitative morphological ageing methods.

Developmental gene expression has been used to estimate the age of adult female mosquitoes, with a reported accuracy of +/- 5 days (+/- 12.5% error of a 20-day testing period). Their study used one HKG and eight DEGs, or with reduced accuracy using only three DEGs (Cook *et al.,* 2007). The present study at least shows the potential of this method for age estimation of *C. vicina* pupae, with only three DEGs and two HKGs. Since only one of the tested genes (Trp) showed significant differential expression it is not possible to provide a more precise age estimate from this dataset above. However, this work does indicate the suitability of the method, using genes such as RP49 and Trp, for improving precision of PMI estimation from pupae.

7.4 Conclusion

The data obtained in this study indicate quantitative pupal age estimation is possible, to within +/- 600 ADH (or +/- 360 ADH with approx. 80% reliability), using the regression equation formed from the analysis of three temporally expressed genes, relative to two housekeeping genes. RP49 was most suitable for normalisation though a combined HKG approach was preferred due to the whole-organism gene expression approach. Trp was the most suitable DEG, varying 74-fold over the pupal stage, but all three DEGs varied significantly with age therefore were utilised in the regression equation. More work is required to identify further HKGs that are consistently expressed across the whole organism and DEGs that show significant expression variation across the pupal stage. This requires comparison of the *L. sericata* transcriptome and EST data to existing Diptera data to identify candidates for qPCR testing. Ideally the development of a *C. vicina* genome and transcriptome will enable targeted gene selection for pupal age and PMI estimation.

Chapter 8 – Discussion and Conclusions

8.1 A multidisciplinary approach to pupal age estimation

The aim of this work was to explore and develop methods for pupal age estimation, which would result in improved precision of PMI estimation based on this stage. This has been achieved by the following:

a) Quantification of developmental variation in the egg and pupal stages, allowing both proposition of developmental protocols that minimise sample age variation and application of developmental error windows to age estimates from crime scene samples.
b) Development of new preservation protocols for pupae collected at the crime scene, for both optimal preservation for particular individual age estimation methods, and an overall general preservative suitable for all pupae, regardless of post-crime scene analysis required.
c) Production of an external morphological timeline and accompanying novel qualitative and statistical age estimation methods, based on the development of 23 features, resulting in age estimates accurate to within +/- 500 ADH.
d) Identification of internal morphological features using specialised histological protocols and optical computed tomography, which provide additional approximate age markers.
e) Identification and analysis of suitable housekeeping and developmentally expressed genes by quantitative, reverse-transcriptase PCR and the ΔC_T method, for pupal age estimation using regression analysis.

Accurate and reliable PMI estimation must be based upon robust observation and documentation of development, which in the case of pupal age estimation starts with the collection of samples of accurately known age. Pupae observed in this study were collected from eggs laid within a known time interval (60 minutes; 22 ADH) and with minimised precocious development (<2.55%), resulting in minimal variation and so ages are accurately known. With the natural variation in lifecycle length quantified to +/- 500 ADH, this error was applied to correlation of developmental markers (morphological or gene expression) to age, giving a maximum estimate window of approximately +/- 1 day at 22°C. It has not been tested whether this value varies under fluctuating temperatures or across different populations thus the window applied for PMI estimation (at present) should be as natural variation dictates.

Good preservation of samples is an absolute prerequisite for development of a reference database of pupal age markers, timeline or similar. This is also true for samples collected from a crime scene, where it is important that the protocols developed are applied without delay to maximise the possibilities for all age estimation analyses.

External morphological age estimation is rapid, straightforward and cost-effective. Age estimates are readily obtained using the Pupal Age Estimator, which combines a manual age-range correlation method with regression analysis. A statistically derived error of +/- 320 ADH was applied to age estimates with minimal success. The variation in lifecycle length, especially notable at the end of the pupal stage, is large; hence applying an error of +/- 500 ADH (as observed) gave much more reliable age estimates. This indicates that the methods developed here are able to estimate age with high precision and so predicted age ranges given are only limited by the natural variation in development.

Internal histological markers provide indicators of pupal age, but due to difficulties in tracing their development using histology, their utility is limited compared with external morphology and ages obtained must be regarded as approximate. At present analysis of internal morphology is most valuable when other methods are not possible, such as when pupae are degraded or putrefied due to poor preservation, such as lack of piercing or hot-water-killing. Though of limited utility at present, future developments in OCT may make this method more applicable.

Assuming optimal preservation, quantitative gene expression analysis in principle provides the most reliable estimator of age. Of the genes considered in this study, RP49 and Trp appear the most suitable and the data collected can provide an approximate age estimate. As previously discussed, further suitable age marker genes need to be identified and environmental effects on gene expression must be explored before accurate age estimates can be obtained from pupae.

The most significant outcome of this work is the combination of all methods, giving a multidisciplinary approach to pupal age estimation. Using all available age estimation methods on a batch of pupae collected from a crime scene enables a more robust estimate to be obtained, since each method provides an independent estimate of age.

In the event that only limited samples are available from a crime scene it may, in principle, be possible to use all methods discussed in this paper on a single pupa if fixed by HWK and preserved in 80% ethanol, with storage at -20°C. Age analysis should start with molecular species identification using DNA extracted from the removed puparium (Mazzanti *et al.,* 2010). External morphological analysis followed by histological or OCT examination of internal morphology can then be carried out. Surplus sections (where taken) could be used for gene expression analysis of a specific body tagma, e.g. abdomen; methods for RNA extraction from formalin-fixed tissue sections have been documented (Bohmann *et al.,* 2009).

8.2 Further work

In addition to testing the methods described in this study on a single pupa, there are many aspects of the individual methods that can be improved.

8.2.1 Error estimation

Assessment and application of suitable error margins and age range windows is essential for reliable PMI estimation. Errors are present from sample collection through to eclosion (lifecycle length variation) and finally at age estimation using all methods.

The effects of precocious egg occurrence on *C. vicina* developmental studies can be minimised but its potential effect on PMI estimation is considerable, at rates of about 9% occurrence. With this knowledge, a reasonable interpretation of precocious egg possibility can be made for *C. vicina*, but not for other species. The levels of wild and captive-colony precocious egg occurrence in other forensically important species and their effects on PMI estimation and developmental studies should be examined accordingly.

An age range of +/- 500 ADH is established from observation of lifecycle length variation in *C. vicina* at 22°C. This has been applied throughout the present study as an error or age window, with 95% of age estimates based on external morphology falling within this range. This error must also be examined under different developmental conditions including at different constant and fluctuating temperatures, as well as for multiple *C. vicina* populations. These data would add to the reliability of this error, improving the robustness of PMI estimation.

The statistically-derived error of +/- 320 ADH was obtained using residual analysis of the 244 pupae used in blind-sample tests. This age window was applied to both semi-blind and blind samples with approximately 65% of actual ages falling within this window. This is far lower than the +/- 500 ADH window, suggesting it requires further development. A larger sample set could be used to obtain a more suitable mean and standard error of the residuals. Equally, alternative statistical analyses could be used to obtain goodness of fit data and estimate the error.

Improvements in the calculation of accurate pupal age for developmental research could be made by accurate temperature measurement. This would involve controlling larval mass size to minimise heat generation and iButton movement. Trialling alternative temperature measurement methods such as using infrared thermometers may also improve age calculation, however disturbance (movement of larvae, meat or other rearing materials) must remain at a minimum to prevent possible changes in lifecycle length. The accuracy of PMI estimation is maximised by precise measurement of larval mass and environmental temperatures using infra-red or probe thermometers.

8.2.2 Morphological observation and analysis

Morphological observation is reliant on adequate preservation. Although the present study identifies optimal and universal preservatives, these were not tested beyond 6-8 months storage. The current protocols should ideally be tested after pupae have remained in the preservatives for at least one year. Until this work has been conducted, analysis of entomological specimens must be carried out as soon as possible after collection.

Many improvements could be made to the Pupal Age Estimator including validation of the ADH ranges by increasing the developmental dataset. Morphological development should be documented from multiple *C. vicina* populations reared under a range of constant and fluctuating temperatures. Observation of quantitative changes such as measurement of leg, labellum or labrum length, or that of finer features by SEM may improve the reliability of the age estimates obtained.

Histological age estimation may be made more accurate by examination of cellular change (e.g. oenocyte identification and development) using transmission electron microscopy (TEM). Dissection and sectioning of individual features such as the appendages and mouthparts or those that provide the most accurate age estimate may also prove a time-worthy investment as it would improve consistency in observation. Increasing sampling rates from 24-hourly to 6-hourly intervals would also give additional data. In time, developments in OCT equipment and/or methodologies may allow age estimation of live pupae, reducing the need for histological sectioning.

8.2.3 Developmental gene expression

The gene expression analysis performed here was conducted on optimally preserved pupae, stored without solution at -80°C. Comparisons must be made between expression ratios obtained from these pupae and those preserved using the universal method (pierce, HWK and storage in 80% ethanol at -20°C).

Clearly, further genes like Trp need to be identified alongside extended HKG analysis and selection of an appropriate combination. Further research would be greatly facilitated by the production of an annotated genome, preferably together with transcriptome data from the pupal stage. Comparison between the *C. vicina* and *Drosophila* genome/transcriptome data would enable rapid selection of target DEGs and permit qRT-PCR primer and probe design, as performed for *A. aegypti* (Cook *et al.,* 2007). Transcriptome and EST data has been recently produced for *Lucilia sericata* and *Lucilia cuprina*. 24-61% of *Drosophila* genes were discovered in *Lucilia* spp. sequence data, with identification rates of 70-80% by comparison to the databases using NCBI's BLAST tool. Expression levels throughout the immature stages were analysed, thus providing putative age markers for further gene expression studies (Lee *et al.,* 2011; Sze & Dunham 2012). With suitable genes identified, development of multiplex PCR using different Taqman fluorophores (Bustin, 2000) would reduce the time and cost of the age estimation process. Finally, development of different gene expression models for multiple crime scene environments (developmental temperatures etc.) may improve accuracy and reliability of age estimation.

8.3 Conclusions

Overall, this work provides data, protocols and methods, which significantly improves current *C. vicina* pupal age estimation and ultimately enhances the utility of this stage and its precision in PMI estimation. The Pupal Age Estimator, based on combined age-range correlation and regression methods, can give estimates using external morphology to within +/- 500 ADH with 95% reliability. Histological analysis of six additional key internal morphological features can be used to provide a collaborative approximate age estimate to within +/- 600 ADH. Most reliably, regression analysis of developmental gene expression ratios obtained from five genes using qRT-PCR can give quantitative age estimates also to within +/- 600 ADH. Whilst these methods can be used in isolation to estimate pupal age combination of these methods into a multidisciplinary approach will provide a more reliable age and PMI estimate.

References

Aak, A., Birkemoe, T. & Leinass, H.P., 2011. Phenology and life history of the blowfly *Calliphora vicina* in stockfish production areas. *Entomologia Experimentalis et Applicata*, 139(1), pp.35-46.

Adams, Z. & Hall, M., 2003. Methods used for the killing and preservation of blowfly larvae, and their effect on post-mortem larval length. *Forensic Science International*, 138(1-3), pp.50-61.

Aegerter-Wilmsen, T. *et al.,* 2007. Model for the regulation of size in the wing imaginal disc of *Drosophila*. *Mechanisms of Development*, 124(4), pp.318-326.

Amendt, J. *et al.,* 2007. Best practice in forensic entomology—standards and guidelines. *International Journal of Legal Medicine*, 121(2), pp.90-104.

Amendt, J. *et al.,* 2000. Forensic entomology in Germany. *Forensic Science International*, 113(1-3), pp.309-314.

Amendt, J., Zehner, R. & Reckel, F., 2008. The nocturnal oviposition behaviour of blowflies (Diptera: Calliphoridae) in Central Europe and its forensic implications. *Forensic Science International*, 175(1), pp.61-64.

Ames, C., Turner, B. & Daniel, B., 2006. Estimating the post-mortem interval (II): The use of differential temporal gene expression to determine the age of blowfly pupae. *International Congress Series*, 1288, pp.861-863.

Amorim, J.A. & Ribeiro, O.B., 2001. Distinction among the puparia of three blowfly species (Diptera: calliphoridae) frequently found on unburied corpses. *Memorias Do Instituto Oswaldo Cruz*, 96(6), pp.781-784.

Anderson, G. S, 2000. Minimum and Maximum Development Rates of Some Forensically Important Calliphoridae (Diptera). *Journal of Forensic Sciences*, 45(4), pp.824-832.

Anderson, G S & VanLaerhoven, S.L., 1996. Initial studies on insect succession on carrion in Southwestern British Columbia. *Journal of Forensic Sciences*, 41(4), pp.613-621.

Anderson, G. S, 2004. Determining time of death using blow fly eggs in the early postmortem interval. *International Journal of Legal Medicine*, (118), pp.240-241.

Antonov, J. *et al.,* 2005. Reliable gene expression measurements from degraded RNA by quantitative real-time PCR depend on short amplicons and a proper normalization. *Laboratory investigation; a journal of technical methods and pathology*, 85(8), pp.1040-50.

Arbeitman, M.N. *et al.,* 2002. Gene expression during the life cycle of *Drosophila melanogaster*. *Science*, 297(5590), pp.2270-5.

Archer, M. *et al.,* 2006. Fly pupae and puparia as potential contaminants of forensic entomology samples from sites of body discovery. *International Journal of Legal Medicine*, 120(6), pp.364–368.

Arnott, S. & Turner, B, 2008. Post-feeding larval behaviour in the blowfly, *Calliphora vicina*: Effects on post-mortem interval estimates. *Forensic Science International*, 177(2-3), pp.162-167.

Aschoff, J. & Von Saint Paul, U., 1990. Circadian rhythms in the blowfly, Phormia terraenovae: control of phase within the range of entrainment. *Physiological Entomology*, 15(2), pp.129-135.

Bagnall, N.H. & Kotze, A.C., 2010. Evaluation of reference genes for real-time PCR quantification of gene expression in the Australian sheep blowfly, Lucilia cuprina. *Medical and veterinary entomology*, 24(2), pp.176-81.

Bainbridge, S.P. & Bownes, M., 1981. Staging the Metamorphosis of *Drosophila melanogaster*. *Journal of Embryology and Experimental Morphology*, 66, pp.57-80.

Barber, R.D. *et al.,* 2005. GAPDH as a housekeeping gene: analysis of GAPDH mRNA expression in a panel of 72 human tissues. *Physiological genomics*, pp.00025–2005.

Barritt, L.C. & Birt, L.M., 1971. Development of Lucilia cuprina - Correlation of Biochemical and Morphological Events. *Journal of Insect Physiology*, 17(6), pp.1169-1183.

Barton Browne, L., 1981. Ovarian development and oosorption in autogenous females of the blowfly, Lucilia cuprina. *International Journal of Invertebrate Reproduction*, 3, pp.169-179.

Barton Browne, L., 1958. The choice of communal oviposition sites by the Australian Sheep Blowfly Lucilia cuprina. *Australian Journal of Zoology*, 6(3), pp.241-247.

Barton Browne, L., 1960. The role of olfaction in the stimulation of oviposition in the blowfly, Phormia regina. *Journal of Insect Physiology*, 5, pp.16-22.

Bauer, D. *et al.,* 1994. Detection and differential display of expressed genes by DDRT-PCR. *PCR methods and applications*, 4(2), pp.S97-108.

Benecke, M, 1998. Six forensic entomology cases: description and commentary. *Journal of forensic sciences*, 43(4), pp.797-805.

Benecke, M. & Zweihoff, R., 2004. Neglect of the elderly: forensic entomology cases and considerations. *Forensic science international*, 146 Suppl, pp.S195-9.

Beno, M., Liszekova, D. & Farkas, R., 2007. Processing of soft pupae and uneclosed pharate adults of *Drosophila* for scanning electron microscopy. *Microscopy Research and Technique*, 70(12), pp.1022-1027.

Berridge, M.J. *et al.,* 1976. Salivary gland development in the blowfly, Calliphora erythrocephala. *Journal of Morphology*, 149(4), pp.459-482.

Bodenstein, D., 1950. The postembryonic development of *Drosophila*. In M. Demerec, ed. *Biology of Drosophila*. Hafner Publishing Company, New York-London, pp. 275–367.

Bohmann, K. *et al.,* 2009. RNA extraction from archival formalin-fixed paraffin-embedded tissue: A comparison of manual, semiautomated, and fully automated purification methods. *Clinical chemistry*, 55(9), p.1719.

Bonacci, T. *et al.,* 2009. A case of *Calliphora vicina* Robineau-Desvoidy, 1830 (Diptera, Calliphoridae) breeding in a human corpse in Calabria (southern Italy). *Legal Medicine*, 11(1), pp.30-32.

Boonsriwong, W. *et al.,* 2007. Fine structure of the alimentary canal of the larval blow fly Chrysomya megacephala (Diptera: Calliphoridae). *Parasitology research*, 100(3), pp.561–574.

Boppart, S.A. *et al.,* 1996. Imaging developing neural morphology using optical coherence tomography. *Journal of neuroscience methods*, 70(1), pp.65–72.

Boppart, S.A. *et al.,* 1997. Noninvasive assessment of the developing Xenopus cardiovascular system using optical coherence tomography. *Proceedings of the National Academy of Sciences of the United States of America*, 94(9), p.4256.

Boppart, Stephen A & Suslick, K.S., 2006. Microsphere contrast agents for OCT. In pp. 409-427.

Bourel, B. *et al.,* 1999. Effects of morphine in decomposing bodies on the development of *Lucilia sericata* (Diptera: Calliphoridae). *Journal of forensic sciences*, 44(2), pp.354-8.

Bourel, B. *et al.,* 2003. Flies eggs: a new method for the estimation of short-term post-mortem interval? *Forensic science international*, 135(1), pp.27–34.

Bourel, B. *et al.,* 2001. Immunohistochemical contribution to the study of morphine metabolism in Calliphoridae larvae and implications in forensic entomotoxicology. *Journal of forensic sciences*, 46(3), pp.596-9.

Bownes, M., 1975. Photographic study of development in living embryo of *Drosophila melanogaster*. *Journal of Embryology and Experimental Mophology*, 33(June), pp.789-801.

Bozzola, J.J. & Russell, L.D., 1999. *Electron microscopy: principles and techniques for biologists*, Jones & Bartlett Learning.

Bradu, A. *et al.,* 2009. Dual optical coherence tomography/fluorescence microscopy for monitoring of *Drosophila melanogaster* larval heart. *Journal of Biophotonics*, 2(6-7), pp.380–388.

Brazil, B.G. & Brazil, R.P., 2000. Sexing sand fly pupae (Diptera: Psychodidade: Phlebotominae). *Memorias Do Instituto Oswaldo Cruz*, 95(4), pp.471-472.

Buesa, R., 2008. Histology without formalin? *Annals of diagnostic pathology*, 12(6), pp.387-396.

Bustin, S.A., 2000. Absolute quantification of mRNA using real-time reverse transcription polymerase chain reaction assays. *Journal of Molecular Endocrinology*, 25(2), pp.169-193.

Byrd, J.H. & Castner, J.L. eds., 2009. *Forensic Entomology: The Utility of Arthropods in Legal Investigations* 2nd ed., New York: CRC Press.

Callahan, R.F., 1962. Effects of parental age on the life cycle of the house fly, Musca domestica Linnaeus (Diptera: Muscidae). *Journal of the New York Entomological Society*, pp.150–158.

Campobasso, C P, Di Vella, G. & Introna, F, 2001. Factors affecting decomposition and Diptera colonization. *Forensic Science International*, 120(1-2), pp.18-27.

Catts, E., 1992. Problems in estimating the postmortem interval in death investigations. *Journal of Agricultural Entomology*, 9(4), pp.245-255.

Catts, E.P. & Haskell, N.H., 1990. *Entomology & death: a procedural guide*, Clemson, S.C.: Joyces Print Shop, Inc.

Chen, T.-Y., 1929. On the Development of Imaginal Buds in Normal and Mutant *Drosophila*. *Journal of Morphology*, 47(1), pp.135-199.

Choma, M.A. *et al.,* 2006. In vivo imaging of the adult *Drosophila melanogaster* heart with real-time optical coherence tomography. *Circulation*, 114(2), p.e35.

Codd, V., Dolezel, D. & Stehlik, J., 2007. Circadian rhythm gene regulation in the housefly Musca domestica. *Genetics*, 177(3), pp.1539-1551.

Condic, M.L., Fristrom, D. & Fristrom, J W, 1991. Apical Cell-Shape Changes During *Drosophila* Imaginal Leg Disk Elongation - A Novel Morphogenetic Mechanism. *Development*, 111(1), pp.23-33.

Cook, D.F. & Dadour, I R, 2011. Larviposition in the ovoviviparous blowfly Calliphora dubia. *Medical and veterinary entomology*, 25(1), pp.53-7.

Cook, P E *et al.,* 2007. Predicting the age of mosquitoes using transcriptional profiles. *Nature Protocols*, 2(11), pp.2796-2806.

Cook, P E & Sinkins, S.P., 2010. Transcriptional profiling of Anopheles gambiae mosquitoes for adult age estimation. *Insect molecular biology*, 19(6), pp.745-51.

Cook, P E *et al.,* 2006. The use of transcriptional profiles to predict adult mosquito age under field conditions. *Proceedings of the National Academy of Sciences of the United States of America*, 103(48), pp.18060-5.

Cottrell, C., 1962. The Imaginal Ecdysis of Blowflies. The Control of Cuticuar Hardening and Darkening. *Journal of Experimental Biology*, 39(3), p.395.

Cottrell, C.B., 1962. The imaginal ecdysis of blowflies. Detection of the blood-borne darkening factor and determination of some of its properties. *Journal of Experimental Biology*, 39, pp.413-430.

Cox, M.L. *et al.,* 2006. Assessment of fixatives, fixation, and tissue processing on morphology and RNA integrity. *Experimental and Molecular Pathology*, 80(2), pp.183-191.

Crossley, A.C., 1965. Transformations in the abdominal muscles of the blue blow-fly, Calliphora erythrocephala (Meig), during metamorphosis. *Journal of Embryology and Experimental Morphology*, 14(1), pp.89-110.

Crossley, A.C., 1972. Ultrastructural changes during transition of larval to adult intersegmental muscle at metamorphosis in the blowfly Calliphora erythrocephala. II. The formation of adult muscle. *Journal of Embryology and Experimental Morphology*, 27(1), pp.75-101.

Davies, K. & Harvey, M, 2012. Internal morphological analysis for age estimation of blow fly pupae (Diptera: Calliphoridae) in post-mortem interval estimation. *Journal of Forensic Sciences*. DOI: 10.1111/j.1556-4029.2012.02196.x.

Davies, L, 2006. Lifetime reproductive output of *Calliphora vicina* and *Lucilia sericata* in outdoor caged and field populations; flight vs. egg production? *Medical and veterinary entomology*, 20(4), pp.453-8.

Davies, L, 2002. Seasonal and spatial changes in blowfly production from small and large carcasses at Durham in lowland northeast England. *Medical and veterinary entomology*, 13(3), pp.245–251.

Davies, L, 1990. Species composition and larval habitats of blowfly (Calliphoridae) populations in upland areas in England and Wales. *Medical and Veterinary Entomology*, 4(1), pp.61-8.

Davies, L. & Ratcliffe, G., 1994. Development rates of some pre-adult stages in blowflies with reference to low temperatures. *Medical and Veterinary Entomology*, 8(3), pp.245-254.

Davies, L. 1948. Laboratory studies on the egg of the blowfly, *Lucilia sericata* (MG.). *The Journal of Experimental Biology*, (25), pp.71-85.

Davies, R.L. *et al.,* 1988. A technique for studying the development, metamorphosis and morphology of insects, using projection X-ray microscopy. *Journal of Microscopy*, 149(3), pp.199-205.

Day, D.M. & Wallman, J.E., 2008. Effect of preservative solutions on preservation of Calliphora augur and Lucilia cuprina larvae (Diptera: Calliphoridae) with implications for post-mortem interval estimates. *Forensic Science International*, 179(1), pp.1-10.

Day, D.M. & Wallman, J.F., 2006. Width as an alternative measurement to length for post-mortem interval estimations using Calliphora augur (Diptera : Calliphoridae) larvae. *Forensic Science International*, 159(2-3), pp.158-167.

Dekeirsschieter, J. *et al.,* 2009. Cadaveric volatile organic compounds released by decaying pig carcasses (Sus domesticus L.) in different biotopes. *Forensic Science International*, 189(1-3), pp.46-53.

Delhaes, L. *et al.,* 2001. Case report: Recovery of *Calliphora vicina* first-instar larvae from a human traumatic wound associated with a progressive necrotizing bacterial infection. *American Journal of Tropical Medicine and Hygiene*, 64(3-4), pp.159-161.

Demerec, M., 1950. *Biology of Drosophila* 1st Facsim., New York: Cold Spring Harbor Laboratory Press.

Dennell, R., 1947. A study of an insect cuticle: the formation of the puparium of Sarcophaga falculata Pand. (Diptera). *Proceedings of the Royal Society of London. Series B*, 134(874), pp.79-110.

Desena, M.L. *et al.,* 1999. Aedes aegypti (Diptera: Culicidae) Age Determination by Cuticular Hydrocarbon Analysis of Female Legs. *Journal of Medical Entomology*, 36(6), p.7.

Dheda, K. *et al.,* 2004. Validation of housekeeping genes for normalizing RNA expression in real-time PCR. *Biotechniques*, 37, pp.112–119.

Disney, R. & Manlove, J., 2005. First occurrences of the Phorid, Megaselia abdita, in forensic cases in Britain. *Medical and Veterinary Entomology*, 19(4), pp.489–491.

Dobzhansky, T., 1930. Studies on the intersexes and supersexes in *Drosophila melanogaster*. *Bull. Bur. Genet. Leningrad*, 8, pp.91–158.

Doctor, J., Fristrom, D. & Fristrom, J W, 1985. The pupal cuticle of *Drosophila*: biphasic synthesis of pupal cuticle proteins in vivo and in vitro in response to 20-hydroxyecdysone. *The Journal of Cell Biology*, 101(1), pp.189-200.

Donovan, S.E. *et al.,* 2006. Larval growth rates of the blowfly, *Calliphora vicina*, over a range of temperatures. *Medical and Veterinary Entomology*, 20(1), pp.106-14.

Drijfhout, F.P., 2010. Cuticular Hydrocarbons: A New Tool in Forensic Entomology? In J. Amendt *et al.,* eds. *Current concepts in forensic entomology*. Springer, pp. 179-203.

Duarte, G.T., De Azeredo-Espin, Ana Maria L. & Junqueira, A.C.M., 2008. The Mitochondrial Control Region of Blowflies (Diptera: Calliphoridae): A Hot Spot for Mitochondrial Genome Rearrangements. *Journal of Medical Entomology*, 45(4), pp.667-676.

Easton, C. & Feir, D., 1991. Factors Affecting the Oviposition of Phaenicia sericata (Meigen) (Diptera : Calliphoridae). *Journal of the Kansas Entomological Society*, 64(3), pp.287-294.

Egyházi, S. *et al.,* 2004. Proteinase K added to the extraction procedure markedly increases RNA yield from primary breast tumors for use in microarray studies. *Clinical chemistry*, 50(5), pp.975-6.

Einarsson, Á. *et al.,* 2002. Consumer-resource interactions and cyclic population dynamics of Tanytarsus gracilentus (Diptera: Chironomidae). *Journal of Animal Ecology*, 71(5), pp.832–845.

Erzinclioglu, Z., 1996. *Blowflies (Naturalists Handbook)*, Richmond Publishing Company.

Fagerström, T. & Wiklund, C., 1982. Why do males emerge before females? Protandry as a mating strategy in male and female butterflies. *Oecologia*, 52(2), pp.164 - 166.

Finell, N. & Jarvilehto, M., 1983. Development of the compound eyes of the blowfly Calliphora erythrocephala: changes in morphology and function during metamorphosis. *Annales Zoologici Fennici*, 20, pp.223-234.

Florell, S.R. *et al.,* 2001. Preservation of RNA for functional genomic studies: a multidisciplinary tumor bank protocol. *Modern pathology: an official journal of the United States and Canadian Academy of Pathology, Inc*, 14(2), pp.116-28.

Foran, D., 2007. *Generating More Precise Post Mortem Interval Estimates With Entomological Evidence: Reliable Patterns of Gene Expression Throughout Calliphorid Larval and Pupal Development* U. S. D. of Justice, ed., Michigan.

Fortier, T.M. *et al.,* 2006. how functions in leg development during *Drosophila* metamorphosis. *Developmental Dynamics*, 235(8), pp.2248–2259.

Fraenkel, G. & Bhaskaran, G., 1973. Pupariation and pupation in cyclorrhaphous flies (Diptera): terminology and interpretation. *Annals of the Entomological Society of America*, 66(2), pp.418–422.

Frederickx, C. *et al.,* 2012. Volatile organic compounds released by blowfly larvae and pupae: New perspectives in forensic entomology. *Forensic science international*.

Freeman, W.M. *et al.,* 1999. Quantitative RT-PCR: pitfalls and potential. *Biotechniques*, 26, pp.112–125.

Fristrom, J.W. *et al.,* 1982. The formation of the pupal cuticle by *Drosophila* imaginal discs in vitro. *Developmental Biology*, 91(2), pp.337–350.

Frohlich, A. & Meinertzhagen, I.A., 1982. Synaptogenesis in the 1st Optic Neuropil of the Flys Visual System. *Journal of Neurocytology*, 11(1), pp.159-180.

Fujimoto, J.G., 2003. Optical coherence tomography for ultrahigh resolution in vivo imaging. *Nature biotechnology*, 21(11), pp.1361–1367.

Fyrberg, E.A. *et al.,* 1983. Transcripts of the six *Drosophila* actin genes accumulate in a stage- and tissue-specific manner. *Cell*, 33(1), pp.115-23.

Gagliano-Candela, R. & Aventaggiato, L., 2001. The detection of toxic substances in entomological specimens. *International Journal of Legal Medicine*, 114(4), pp.197–203.

Gaudry, E. *et al.,* 2001. Activity of the forensic entomology department of the French Gendarmerie. *Forensic Science International*, 120(1-2), pp.68-71.

Gaudry, E. *et al.,* 2006. Study of steroidogenesis in pupae of the forensically important blow fly *Protophormia terraenovae* (Robineau-Desvoidy) (Diptera : Calliphoridae). *Forensic Science International*, 160(1), pp.27-34.

Gerade, B.B. *et al.,* 2004. Field Validation of Aedes aegypti (Diptera: Culicidae) Age Estimation by Analysis of Cuticular Hydrocarbons. *Journal of Medical Entomology*, 41(2), pp.231-238.

Gilbert, B.M. & Bass, W.M., 1967. Seasonal Dating of Burials from the Presence of Fly Pupae. *Society for American Archaeology*, 32(4), pp.534-535.

Giulietti, A. *et al.,* 2001. An overview of real-time quantitative PCR: applications to quantify cytokine gene expression. *Methods (San Diego, Calif.)*, 25(4), pp.386-401.

Godfrey, T.E. *et al.,* 2000. Quantitative mRNA expression analysis from formalin-fixed, paraffin-embedded tissues using 5’ nuclease quantitative reverse transcription-polymerase chain reaction. *Journal of Molecular Diagnostics*, 2(2), pp.84-91.

Goff, M.L. & Lord, W.D., 1994. Entomotoxicology. A new area for forensic investigation. *The American journal of forensic medicine and pathology : official publication of the National Association of Medical Examiners*, 15(1), pp.51-7.

Goodman, B.A. *et al.,* 1995. Nuclear-magnetic-resonance microscopy as a non-invasive tool to study the development of lepidopteran pupae. *Journal of Insect Physiology*, 41(5), pp.419-424.

Graham-Smith, G., 1930. Further Observations on the Anatomy and Function of the Proboscis of the Blow-fly, Calliphora erythrocephala L. *Parasitology*, 22(01), pp.47–115.

Graham-Smith, G., 1938. The generative organs of the blow-fly, Calliphora erythrocephala L., with special reference to their musculature and movements. *Parasitology*, 30(04), pp.441–476.

Grassberger, M. & Reiter, C., 2001. Effect of temperature on *Lucilia sericata* (Diptera: Calliphoridae) development with special reference to the isomegalen- and isomorphen-diagram. *Forensic Science International*, 120(1-2), pp.32-36.

Greco, M. *et al.,* 2006. X-ray computerised tomography as a new method for monitoring Amegilla holmesi nest structures, nesting behaviour and adult female activity. *Entomologica Experimentalis et Applicata*, 120, pp.71-76.

Greenberg, B., 1973. *Flies and disease. Vol. II. Biology and disease transmission.*, Princeton University Press.

Greenberg, B., 1991. Flies as Forensic Indicators. *Journal of Medical Entomology*, 28(5), pp.565-577.

Greenberg, B. & Kunich, J.C., 2002. *Entomology and the Law*, Cambridge: Cambridge University Press.

Grodowitz, M., Krchma, J. & Broce, A., 1982. A method for preparing soft bodied larval Diptera for scanning electron microscopy. *Journal of the Kansas Entomological Society*, 55(4), pp.751-753.

Grzeschik, N.A. & Knust, E., 2005. IrreC/rst-mediated cell sorting during *Drosophila* pupal eye development depends on proper localisation of DE-cadherin. *Development*, 132(9), pp.2035-2045.

Gu, Z., Rifkin, S., White, P. & Wen-Hsiung, L., 2004. Duplicate genes increase gene expression diversity within and between species. *Nature genetics*, 36, pp 577-579.

Haddad, D. *et al.,* 2004. NRM Imaging of the honeybee brain. *Journal of Insect Science*, 4(7), p.7.

Hallock, K.J., 2005. Magnetic resonance microscopy of flows and compressions of the circulatory , respiratory , and digestive systems in pupae of the tobacco hornworm , Manduca sexta. *Journal of Insect Science*, 8, pp.1-7.

Hart, A.G. *et al.,* 2003. Magnetic resonance imaging in entomology: a critical review. *Journal of Insect Science*, 3(5), p.9.

Harvey, M L, Mansell, M.W., *et al.,* 2003. Molecular identification of some forensically important blowflies of southern Africa and Australia. *Medical and veterinary entomology*, 17(4), pp.363-9.

Harvey, M L *et al.,* 2008. A global study of forensically significant calliphorids: Implications for identification. *Forensic Science International*, 177(1), pp.66-76.

Harvey, M., 2006. *A Molecular Study of the Forensically Important Calliphoridae (Diptera): Implications and Applications for the future of Forensic Entomology*. University of Western Australia.

Harvey, M L, Dadour, I R & Gaudieri, S., 2003. Mitochondrial DNA cytochrome oxidase I gene: potential for distinction between immature stages of some forensically important fly species (Diptera) in western Australia. *Forensic science international*, 131(2-3), pp.134-9.

Hausman, S.A., 1949. Some morphological and histological studies of the developing compound eye in the vinegar fly *Drosophila melanogaster*. *Trans Am Microsc Soc.*, 68(2), pp.154-162.

He, L. *et al.,* 2007. Identification of necrophagous fly species using ISSR and SCAR markers. *Forensic Science International*, 168(2-3), pp.148-53.

Hewitt, C.G., 1907. The Structure, Development, and Bionomics of the House-fly, Musca domestica, Linn. Part I.— The Anatomy of the Fly. *Quarterly Journal of Microscopical Science*, 2(51), pp.395-448.

Van Hiel, M.B. *et al.,* 2009. Identification and validation of housekeeping genes in brains of the desert locust Schistocerca gregaria under different developmental conditions. *BMC Molecular Biology*, 10 (56)

Hinton, H., 1963. The respiratory system of the egg-shell of the blowfly, Calliphora erythrocephala Meig., as seen with the electron microscope. *Journal of Insect Physiology*, 9(1), pp.121-129.

Hobson, R.P., 1937. Sheep Blow-Fly Investigations VII. Observations on the Development of Eggs and Oviposition in the Sheep Blowfly, *Lucilia sericata* MG. *Annals of Applied Biology*, 25(3), pp.573-582.

Holler, T. *et al.,* 2006. A comparison of yeast hydrolysate and synthetic food attractants for capture of Anastrepha suspensa (Diptera: Tephritidae). *Florida Entomologist*, 89(3), pp.419–420.

Holloway, B.A., 1991. Identification of third-instar larvae of flystrike and carrion-associated blowflies in New Zealand (Diptera: Calliphoridae). *New Zealand Entomologist*, 14, pp.24-28.

Hoy, M.A., 2003. *Insect Molecular Genetics: An Introduction to Principles and Applications*, Academic Press.

Huchet, J.B., 2010. Archaeoentomological study of the insect remains found within the mummy of Namenkhet Amun (San Lazzaro Armenian Monastery, Venice/Italy). *Advances in Egyptology*, 1, pp.59-80.

Hugo, L. & Cook, P., 2010. Field validation of a transcriptional assay for the prediction of age of uncaged Aedes aegypti mosquitoes in Northern Australia. *PLoS Neglected Tropical Diseases*, 4(2), p.e608.

Huntington, T., 2007. Maggot Development During Morgue Storage and Its Effect on Estimating the Post-Mortem Interval. *Journal of forensic sciences*, 52(2), pp.453-458.

Hwang, C. & Turner, B, 2005. Spatial and temporal variability of necrophagous Diptera from urban to rural areas. *Medical and Veterinary Entomology*, 19, pp.379-391.

Inada, M. & Pleiss, J.A., 2009. Genome-Wide Approaches to Monitor Pre-mRNA Splicing. In J. Weissman, C. Guthrie, & G. Fink, eds. *Methods in Enzymology: Guide to Yeast Genetics: Functional Genomics, Proteomics and other Systems Analysis*. Academic Press, pp. 51-75.

Infante, C. *et al.,* 2008. Selection of housekeeping genes for gene expression studies in larvae from flatfish using real-time PCR. *BMC molecular biology*, 9(1), p.28.

Introna, F., Campobasso, C. P., & Goff, M. L., 2001. Entomotoxicology. *Forensic Science International*, *120*(1-2), pp.42–7.

Introna, F., Campobasso, C P. & Di Fazio, A., 1998. Three case studies in forensic entomology from southern Italy. *Journal of forensic sciences*, 43(1), pp.210-214.

Ireland, S. & Turner, B. 2006. The effects of larval crowding and food type on the size and development of the blowfly, Calliphora vomitoria. *Forensic Science International*, 159(2), pp.175-181.

Jarvilehto, M & Finell, N, 1983. Development of the Function of Visual Receptor-Cells dring the Pupal Life of the fly Calliphora. *Journal of Comparative Physiology*, 150(4), pp.529-536.

Jasanoff, A. & Sun, P.Z., 2002. In vivo magnetic resonance microscopy of brain structure in unanesthetized flies. *Journal of magnetic resonance (San Diego, Calif.: 1997)*, 158(1-2), pp.79-85.

Jian, B. *et al.,* 2008. Validation of internal control for gene expression study in soybean by quantitative real-time PCR. *BMC molecular biology*, 9(1), p.59.

Kamal, A., 1958. Comparative study of thirteen species of sarcosaprophagous Calliphoridae and Sarcophagidae (Diptera) I. Bionomics. *Annals of the Entomological Society of America*, 51(3), pp.261-271.

Kambe, M. *et al.,* 2008. In-vivo Imaging of Developing Wings in Butterfly Pupa by Using Optical Coherence Tomography. *Journal of the Korean Physical Society*, 53(2), pp.1290-1294.

Karandikar, K.R. & Ranade, D.R., 1965. Studies on the pupation of Musca domestica nebulo Fabr (Diptera-Cyclorrhapha-Muscidae). *Proceedings: Plant Sciences*, 61(4), pp.204-213.

Kharbouche, H. *et al.,* 2008. Codeine accumulation and elimination in larvae, pupae, and imago of the blowfly *Lucilia sericata* and effects on its development. *Int J Legal Med*, 122(3), pp.205-11.

Kirby, W. & Spence, W., 1828. *An Introduction to Entomology or Elements of the Natural History of Insects*, London: Longman, Rees, Orme, Brown and Green.

Koch, D.A. *et al.,* 1998. Effects of preservation methods, parasites, and gut contents of black flies (Diptera: Simuliidae) on polymerase chain reaction products. *Journal of Medical Entomology*, 35(3), pp.314-318.

Konopka, R. & Benzer, S., 1971. Clock mutants of *Drosophila melanogaster*. *Proceedings of the National Academy of Sciences*, 68(9), pp.2112-2116.

Krafka, J., 1924. Development of the compound eye of *Drosophila melanogaster* and its bar-eyed mutant. *Biol Bull*, 47, pp.143-148.

De Kramer, J.J. & Van Der Molen, L.G., 1984. Development of the labellar taste hairs in the blowfly, *Calliphora vicina* (Insecta, Diptera). *Zoomorphology*, 104, pp.1-10.

Kulshrestha, S.K., 1970. Morpho-histological changes in the ovarioles of Musca domestica nebulo Fabr. (Muscidae: Diptera) during pre-oviposition period. *Journal of Natural History*, 4, pp.137-144.

Laing, J., 1935. On the Ptilinum of the Blow-fly (Calliphora erythrocephala). *Review Literature And Arts Of The Americas*, (308), pp.497-521.

Lakes, R. & Pollack, G.S., 1990. The development of the sensory organs of the legs in the blowfly, Phormia regina. *Cell and tissue research*, 259(1), pp.93-103.

Lebo, M.S. *et al.,* 2009. Somatic, germline and sex hierarchy regulated gene expression during *Drosophila* metamorphosis. *BMC Genomics*, 10(80).

Lee, S.F. *et al.,* 2011. Identification, analysis, and linkage mapping of expressed sequence tags from the Australian sheep blowfly. *BMC genomics*, 12(1), p.406.

Lee, T.M. *et al.,* 2003. Engineered microsphere contrast agents for optical coherence tomography. *Optics letters*, 28(17), pp.1546-8.

Lehmacher, C. *et al.,* 2009. The *Drosophila* wing hearts consist of syncytial muscle cells that resemble adult somatic muscles. *Arthropod structure & development*, 38(2), pp.111-23.

Lessinger, A. & Azeredo-Espin, A., 2000. Evolution and structural organisation of mitochondrial DNA control region of myiasis-causing flies. *Medical and Veterinary Entomology*, 14(1), pp.71-80.

Levy, M. & Bautz, A.M., 1985. Degeneration of Larval Salivary Glands during Metamorphosis of the Blowfly, Calliphora Erythrocephala Meigen (Diptera, Calliphoridae). *International Journal of Insect Morphology and Embryology*, 14(5), pp.281-290.

Lewis, O.L., Farr, C.L. & Kaguni, L.S., 1995. *Drosophila melanogaster* mitochondrial DNA: completion of the nucleotide sequence and evolutionary comparisons. *Insect Molecular Biology*, 4(4), pp.263 - 278.

Ling, D. & Salvaterra, P., 2011. Robust RT-qPCR data normalization: validation and selection of internal reference genes during post-experimental data analysis. *PloS one*, 6(3), p.17762.

Linville, J.G., Hayes, J. & Wells, J D, 2004. Mitochondrial DNA and STIR analyses of maggot crop contents: Effect of specimen preservation technique. *Journal of Forensic Sciences*, 49(2), pp.341-344.

Livak, K.J. & Schmittgen, T.D., 2001. Analysis of relative gene expression data using real-time quantitative PCR and the 2(-Delta Delta C(T)) Method. *Methods (San Diego, Calif.)*, 25(4), pp.402-8.

Lourenço, A. & Mackert, A., 2008. Validation of reference genes for gene expression studies in the honey bee, Apis mellifera, by quantitative real-time RT-PCR. *Apidologie*, 39 (3), pp.372-385

Lowne, B., 1895. *Anatomy, physiology, morphology, and development of the blow-fly (Calliphora erythrocephala): a study in the comparative anatomy and morphology of insects.*, Kessinger Publishing (Nov 2009).

Madhavan, M.M. & Madhavan, K., 1980. Morphogenesis of the epidermis of adult abdomen of *Drosophila*. *Journal of Embryology and Experimental Morphology*, 60, pp.1-31.

Marchenko, M.I., 2001. Medicolegal relevance of cadaver entomofauna for the determination of the time of death. *Forensic Science International*, 120(1-2), pp.89-109.

Margam, V.M., Gelman, D.B. & Palli, S.R., 2006. Ecdysteroid titers and developmental expression of ecdysteroid-regulated genes during metamorphosis of the yellow fever mosquito, Aedes aegypti (Diptera : Culicidae). *Journal of Insect Physiology*, 52(6), pp.558-568.

Marinotti, O. & Calvo, E., 2006. Genome-wide analysis of gene expression in adult Anopheles gambiae. *Insect Molecular Biology*, 15(1), pp.1-12.

Matheny, E.S. *et al.,* 2004. Optical coherence tomography of malignancy in hamster cheek pouches. *Journal of Biomedical Optics*, 9, p.978.

Mazzanti, M. *et al.,* 2010. DNA degradation and genetic analysis of empty puparia: genetic identification limits in forensic entomology. *Forensic science international*, 195(1-3), pp.99-102.

McDonald, M.J. & Rosbash, M., 2001. Microarray analysis and organization of circadian gene expression in *Drosophila*. *Cell*, 107(5), pp.567-78.

Mendonça, P.M. *et al.,* 2008. Identification of fly eggs using scanning electron microscopy for forensic investigations. *Micron*, 39(7), pp.802-807.

Metscher, B.D., 2009. MicroCT for comparative morphology: simple staining methods allow high-contrast 3D imaging of diverse non-mineralized animal tissues. *BMC Physiol*, 9(11).

Michaelis, T. *et al.,* 2005. In vivo 3D MRI of insect brain: cerebral development during metamorphosis of Manduca sexta. *NeuroImage*, 24(2), pp.596-602.

Myskowiak, J.B. & Doums, C., 2002. Effects of refrigeration on the biometry and development of *Protophormia terraenovae* (Robineau-Desvoidy) (Diptera : Calliphoridae) and its consequences in estimating post-mortem interval in forensic investigations. *Forensic Science International*, 125(2-3), pp.254-261.

NCBI, 2007. Microarrays: Chipping away at the mysteries of Science and Medicine. Available at: http://www.ncbi.nlm.nih.gov/About/primer/microarrays.html [Accessed April 15, 2012].

Nabity, P., Higley, L. & Heng-Moss, T., 2006. Effects of temperature on development of Phormia regina (Diptera: Calliphoridae) and use of developmental data in determining time intervals in forensic entomology. *Journal of medical entomology*, 43(6), pp.1276-1286.

Nelson, L.A., Wallman, J.F. & Dowton, M., 2008. Identification of forensically important Chrysomya (Diptera: Calliphoridae) species using the second ribosomal internal transcribed spacer (ITS2). *Forensic Science International*, 177(2-3), pp.238-47.

Noriega, N.C., Kohama, S.G. & Urbanski, H.F., 2009. Gene expression profiling in the rhesus macaque: methodology, annotation and data interpretation. *Methods (San Diego, Calif.)*, 49(1), pp.42-9.

Null, B. *et al.,* 2008. High-resolution, in vivo magnetic resonance imaging of *Drosophila* at 18.8 Tesla. *PLoS One*, 3(7), pp. e2817

Oliveira, M.T., Azeredo-Espin, A.M.L. & Lessinger, A.C., 2007. The mitochondrial DNA control region of Muscidae flies: evolution and structural conservation in a dipteran context. *Journal of molecular evolution*, 64(5), pp.519-27.

O'Brien, C. & Turner, B.D., 2004. Impact of paracetamol on *Calliphora vicina* larval development. *International Journal of Legal Medicine*, 118(4), pp.188-189.

Pai, C. *et al.,* 2007. Application of forensic entomology to postmortem interval determination of a burned human corpse: a homicide case report from southern Taiwan. *Journal of the Formosan Medical Association*, 106(9), pp.792-798.

Papaj, D.R., 2000. Ovarian dynamics and host use. *Annual review of entomology*, 45, pp.423-48.

Pappas, C. & Fraenkel, G., 1977. Nutritional aspects of oogenesis in the flies Phormia regina and Sarcophaga bullata. *Physiological zoology*, pp.237–246.

Park, S.H. *et al.,* 2009. Sequences of the cytochrome C oxidase subunit I (COI) gene are suitable for species identification of Korean Calliphorinae flies of forensic importance (Diptera: Calliphoridae). *Journal of Forensic Science*, 54(5), pp.1131-4.

Payne, J., 1965. A Summer Carrion Study of the Baby Pig Sus Scrofa Linnaeus. *Ecology*, 46(5), pp.592-602.

Perez, C., 1910. Recherches histologiques sur la métamorphose des muscides Calliphora erythrocephala Mg. *Archives of Zoological Experimental Genetics*, 4, pp.1-274.

Peterson, A., 1916. The Head-capsule and Mouthparts of the Diptera. *Illinois Biological Monographs*, 3(2).

Pitts, K.M. & Wall, R., 2004. Adult mortality and oviposition rates in field and captive populations of the blowfly *Lucilia sericata*. *Ecological Entomology*, 29(6), pp.727-734.

Ponton, F. *et al.,* 2011. Evaluation of potential reference genes for reverse transcription-qPCR studies of physiological responses in *Drosophila melanogaster*. *Journal of insect physiology*, 57(6), pp.840-50.

Post, R.J., Flook, P.K. & Millest, A.L., 1993. Methods for the Preservation of Insects for DNA Studies. *Biochemical Systematics and Ecology*, 21(1), pp.85-92.

Price, W.S. *et al.,* 1999. Visualising the postembryonic development of Sarcophaga peregrina (flesh fly) by NMR microscopy. *Physiological Entomology*, 24(4), pp.386-390.

Putman, R., 1977. Dynamics of the blowfly, Calliphora erythrocephala, within carrion. *The Journal of Animal Ecology*, 46(3), pp.853–866.

Quicke, D.L.J., Belshaw, R. & Lopez-Vaamonde, C., 1998. Preservation of hymenopteran specimens for subsequent molecular and morphological study. *Zoologica Scripta*, 28(1-2), pp.261-267.

Ranade, D.R., 1977. Studies on External Metamorphosis of Musca domestica Nebulo Fabr. (Diptera-Cyclorrhapha-Muscidae) Part III. Imaginal Discs and Development of The Thoracic Appendages, The Legs and Wings. *Journal of Animal Morphology and Physiology*, 24(2), pp.277-284.

Ranz, J.M. *et al.,* 2003. Sex-dependent gene expression and evolution of the *Drosophila* transcriptome. *Science*, 300(5626), pp.1742-1745.

Ratcliffe, S. & Webb, D., 2003. PCR-RFLP identification of Diptera (Calliphoridae, Muscidae and Sarcophagidae)--a generally applicable method. *Journal of Forensic Sciences*, 48(4), pp.783-785.

Reed, C.T., Murphy, C. & Fristrom, D., 1975. Ultruastructure of the Differentiating Pupal Leg of *Drosophila melanogaster*. *Wiheim Rouxs Archives of Developmental Biology*, 178(4), pp.285-302.

Reed, H.B., 1958. A study of dog carcass communities in Tennessee, with special reference to the insects. *The American Midland Naturalist*, 59(1), pp.213–245.

Ren, N. *et al.,* 2005. Gene expression during *Drosophila* wing morphogenesis and differentiation. *Genetics*, 171(2), pp.625-38.

Resh, V.H. & Cardé, R.T., 2009. *Encyclopedia of insects (Google eBook)*, Academic Press.

Richards, C.S., Paterson, I.D. & Villet, M.H., 2008. Estimating the age of immature Chrysomya albiceps (Diptera: Calliphoridae), correcting for temperature and geographical latitude. *International journal of legal medicine*, 122(4), pp.271-9.

Richards, C.S., Rowlinson, C.C. & Hall, M.J.R., 2012. Effects of storage temperature on the change in size of *Calliphora vicina* larvae during preservation in 80% ethanol. *International journal of legal medicine*. DOI: 10.1007/s00414-021-0683-9

Ring, R.A., 1973. Changes in dry weight, protein, and nucleic acid content during diapause and normal development of the blowfly, *Lucilia sericata*. *Journal of insect physiology*, 19(3), pp.481-94.

Rivero, A. & West, S.A., 2005. The costs and benefits of host feeding in parasitoids. *Animal Behaviour*, 69(6), pp.1293-1301.

Robertson, C.W., 1936. The metamorphosis of *Drosophila melanogaster*, including an accurately timed account of the principal morphological changes. *Journal of Morphology*, 59(2), pp.351 - 399.

Rotte, C., Walz, B. & Baumann, O.D.A.-S.E.P.2008, 2008. Morphological and functional characterization of the thoracic portion of blowfly salivary glands. *Arthropod strucure and development*, 37(5), pp.372-382.

Roux, O., Gers, C. & Legal, L.D.A.D., 2008. Ontogenetic study of three Calliphoridae of forensic importance through cuticular hydrocarbon analysis. *Medical and Veterinary Entomology*, 22(4), pp.309-17.

Sachs, A.B., 1993. Messenger RNA degradation in eukaryotes. *Cell*, 74(3), pp.413-21.

Sanford, M.R., Pechal, J.L. & Tomberlin, J.K., 2011. Rehydration of forensically important larval Diptera specimens. *Journal of medical entomology*, 48(1), pp.118-25.

Sanna, P.P. *et al.,* 2005. Gene profiling of laser-microdissected brain regions and sub-regions. *Brain research. Brain research protocols*, 15(2), pp.66-74.

Saunders, D., 1979. The circadian eclosion rhythm in Sarcophaga argyrostoma: delineation of the responsive period for entrainment. *Physiological Entomology*, 4(3), pp.263-274.

Saunders, D.S. & Hayward, S., 1998. Geographical and diapause-related cold tolerance in the blow fly, *Calliphora vicina*. *Journal of Insect Physiology*, 44(7-8), pp.541-551.

Saxena, S., 2011. Age estimation of indian adults from orthopantomographs. *Brazilian Oral Research*, 25(3), pp.225-229.

Scanlan, M. *et al.,* 2001. Humoral immunity to human breast cancer: antigen definition and quantitative analysis of mRNA expression. *Cancer Immunity*, 1, p.4.

Scharlaken, B. *et al.,* 2008. Reference Gene Selection for Insect Expression Studies Using Quantitative Real-Time PCR: The Head of the Honeybee, Apis mellifera , After a Bacterial Challenge. *Journal of Insect Science*, 8(33), pp.1-10.

Schmitt, A. *et al.,* 2005. Rhodopsin patterning in central photoreceptor cells of the blowfly *Calliphora vicina*: cloning and characterization of Calliphora rhodopsins Rh3, Rh5 and Rh6. *Journal of Experimental Biology*, 208(7), pp.1247-1256.

Schoenly, K., 1992. A statistical analysis of successional patterns in carrion-arthropod assemblages: implications for forensic entomology and determination of the postmortem interval. *Journal of Forensic Sciences*, 37(6), pp.1489-1513.

Schroeder, H., 2003. Use of PCR–RFLP for differentiation of calliphorid larvae (Diptera, Calliphoridae) on human corpses. *Forensic Science International*, 132(1), pp.76-81.

Sharanowski, B.J., Walker, E.G. & Anderson, Gail. S, 2008. Insect succession and decomposition patterns on shaded and sunlit carrion in Saskatchewan in three different seasons. *Forensic Science International*, 179(2-3), pp.219-40.

Shen, G. & Jiang, H., 2010. Evaluation of endogenous references for gene expression profiling in different tissues of the oriental fruit fly Bactrocera dorsalis (Diptera: Tephritidae). *BMC molecular biology*, 11(76).

Shiga, S., 2003. Anatomy and functions of brain neurosecretory cells in Diptera. *Microscopy Research and Technique*, 62(2), pp.114-131.

Simon, C. *et al.,* 1994. Evolution, weighting, and phylogenetic utility of mitochondrial gene sequences and a compilation of conserved polymerase chain reaction primers. *Annals of the Entomological Society of America*, 87(6), pp.651-701.

Simpson, P., 2007. The stars and stripes of animal bodies: evolution of regulatory elements mediating pigment and bristle patterns in *Drosophila*. *Trends in genetics*, 23(7), pp.350-8.

Siriwattanarungsee, S. *et al.,* 2005. Morphology of the puparia of the housefly, Musca domestica (Diptera: Muscidae) and blowfly, Chrysomya megacephala (Diptera: Calliphoridae). *Parasitology research*, 96(3), pp.166-70.

Sivasubramanian, P. & Biagi, M., 1983. Morphology of the Pupal Stages of the Fleshfly, Sarchophaga-Bullata (Parker) (Diptera, Sarcophagidae). *International Journal of Insect Morphology and Embryology*, 12(5-6), pp.355-359.

Slone, D.H. & Gruner, S.V., 2007. Thermoregulation in larval aggregations of carrion-feeding blow flies (Diptera: Calliphoridae). *Journal of Medical Entomology*, 44(3), pp.516-23.

Smith, K.V., 1986. *A Manual of Forensic Entomology.*, London: The Trustees of the British Museum (Natural History).

Smith, P., 1985. Responsiveness to light of the circadian clock controlling eclosion in the blowfly, Lucilia cuprina. *Physiological entomology*, 10(3), pp.323-336.

Snodgrass, R.E., 1930. *Principles of Insect Morphology*, London ET - 1st: McGraw-Hill.

Soler, C. *et al.,* 2004. Coordinated development of muscles and tendons of the *Drosophila* leg. *Development*, 131(24), pp.6041-6051.

Spradbery, J. & Schweizer, G., 1981. Oosorption during ovarian development in the screw-worm fly, Chrysomya bezziana. *Entomologia Experimentalis et Applicata*, 30(3), pp.209–214.

Sprey, T.H.., 1970. Morphological and histochemical changes during the development of some of the imaginal disks of Calliphora erythrocephala. *Netherlands Journal of Zoology*, 20(2), pp.253-275.

Statheropoulos, M., Spiliopouiou, C. & Agapiou, A., 2005. A study of volatile organic compounds evolved from the decaying human body. *Forensic Science International*, 153(2-3), pp.147-155.

Stevens, J., 2003. The evolution of myiasis in blowflies (Calliphoridae). *International journal for parasitology*, 33(10), pp.1105-1113.

Stevens, J. R., Wall, R. & Wells, J. D., 2002. Paraphyly in Hawaiian hybrid blowfly populations and the evolutionary history of anthropophilic species. *Insect Molecular Biology*, 11(2), pp.141-148.

Su, H. *et al.,* 2008. Use of inter-simple sequence repeat markers to develop strain-specific SCAR markers for Flammulina velutipes. *Journal of Applied Genetics*, 49(3), pp.233-5.

Sukontason, K L, Narongchai, P., *et al.,* 2006. Morphological comparison between Chrysomya rufifacies (Macquart) and Chrysomya villeneuvi Patton (Diptera: Calliphoridae) puparia, forensically important blow flies. *Forensic Science International*, 164(2-3), pp.230-234.

Sukontason, K L, Kanchai, C., *et al.,* 2006. Morphological observation of puparia of Chrysomya nigripes (Diptera: Calliphoridae) from human corpse. *Forensic Science International*, 161(1), pp.15-19.

Sukontason, K., Narongchai, P., Kanchai, C., *et al.,* 2007. Forensic entomology cases in Thailand: a review of cases from 2000 to 2006. *Parasitology research*, 101(5), pp.1417–1423.

Sukontason, K. *et al.,* 2004. Identification of forensically important fly eggs using a potassium permanganate staining technique. *Micron*, 35(5), pp.391-395.

Sukontason, K. *et al.,* 2005. Morphology of second and third instars of Chrysomya villeneuvi Patton (Diptera: Calliphoridae), a fly species of forensic importance. *Forensic Science International*, 154(2-3), pp.195-199.

Sukontason, K L, Ngern-Klun, R., *et al.,* 2007. Identifying fly puparia by clearing technique: application to forensic entomology. *Parasitology Research*, 101(5), pp.1407-16.

Sukontason, K.L. *et al.,* 2008. Morphology of immature stages of Hemipyrellia ligurriens (Wiedemann) (Diptera: Calliphoridae) for use in forensic entomology applications. *Parasitology Research*, 103(4), pp.877-887.

Sukontason, K.L. *et al.,* 2007. Fine Structure of the Eggshell of the Blow Fly, Lucilia cuprina. *Journal of Insect Science*, 7(9), pp.1-8.

Sze, S. & Dunham, J., 2012. A de novo transcriptome assembly of *Lucilia sericata* (Diptera: Calliphoridae) with predicted alternative splices, single nucleotide polymorphisms and transcript. *Insect Molecular Biology*.

Tabor, K.L., Fell, R.D. & Brewster, C.C., 2005. Insect fauna visiting carrion in Southwest Virginia. *Forensic Science International*, 150(1), pp.73-80.

Tamura, K. *et al.,* 2007. MEGA4: Molecular Evolutionary Genetics Analysis (MEGA) software version 4.0. *Molecular Biology and Evolution*, 24(8), pp.1596-9.

Tantawi, T.. & Greenberg, B., 1993. The effect of killing and preservative solutions on estimates of maggot age in forensic cases. *Journal of Forensic Sciences*, 38(3), pp.702-707.

Tarone, A. M. & Foran, D. R., 2011. Gene Expression During Blow Fly Development: Improving the Precision of Age Estimates in Forensic Entomology. *Journal of Forensic Sciences*, 56(S1), p.S112-S122.

Tarone, A.M, Jennings, K.C. & Foran, D.R., 2007. Aging blow fly eggs using gene expression: a feasibility study. *Journal of Forensic Sciences*, 52(6), pp.1350-1354.

Taylor, J. & Adler, P.N., 2008. Cell rearrangement and cell division during the tissue level morphogenesis of evaginating *Drosophila* imaginal discs. *Developmental Biology*, 313(2), pp.739-751.

Thomsen, M., 1969. The neurosecretory system of the adult Calliphora erythrocephala. IV. A histological study of the corpus cardiacum and its connections with the nervous system. *Zeitschrift für Zellforschung und Mikroskopische Anatomie*, 94(2), pp.205-219.

Tissot, M. & Stocker, R.F., 2000. Metamorphosis in *Drosophila* and other insects: the fate of neurons throughout the stages. *Progress in Neurobiology*, 62(1), pp.89-111.

Trabalon, M. *et al.,* 1988. Changes in cuticular hydrocarbon composition in relation to age and sexual behavior in the female Calliphora vomitoria (Diptera). *Behavioural processes*, 17(2), pp.107–115.

Trabalon, M. *et al.,* 1992. Cuticular hydrocarbons of Calliphora vomitoria (Diptera): relation to age and sex. *General and Comparative Endocrinology*, 85(2), pp.208-16.

Truman, J.W. & Riddiford, L.M., 1999. The origins of insect metamorphosis. *Nature*, (401), pp.447–452.

Tsai, C.J., 2006. *Comparing DNA damage caused by formaldehyde, glutaraldehyde, Carnoy's and methacarn in cancer tissue fixations*. Bowling Green State University.

Turchetto, M., Lafisca, S. & Costantini, G., 2001. Postmortem interval (PMI) determined by study sarcophagous biocenoses: three cases from the province of Venice (Italy). *Forensic science international*, 120(1), pp.28-31.

VanLaerhoven, S.L., 2008. Blind validation of postmortem interval estimates using developmental rates of blow flies. *Forensic Science International*, 180(2-3), pp.76-80.

Vandesompele, J. & Preter, K.D., 2002. Accurate normalization of real-time quantitative RT-PCR data by geometric averaging of multiple internal control genes. *Genome Biology*, 3(7).

Villet, M.H., Richards, C.S. & Midgley, J.M., 2010. Contemporary Precision, Bias and Accuracy of Minimum Post-Mortem Intervals Estimated Using Development of Carrion-Feeding Insects. In Jens Amendt *et al.,* eds. *Current Concepts in Forensic Entomology*. Springer, pp. 109-137.

Vink, C. *et al.,* 2005. The effects of preservatives and temperatures on arachnid DNA. *Invertebrate Systematics*, (19), pp.99-104.

Vinogradova, E.B., 2009. Effect of Food and Temperature on the Reproduction of the Blowfly, *Calliphora vicina* R.-D. (Diptera, Calliphoridae), a Popular Model Object in Biological Research. *Entomological Review*, 89(2), pp.137-142.

Vogt, W., Woodburn, T., Ellem, B., *et al.,* 1985. The relationship between fecundity and oocyte resorption in field populations of Lucilia cuprina. *Entomologia experimentalis et applicata*, 39(1), pp.91–99.

Vogt, W., Woodburn, T. & Gerwen, A., 1985. The influence of oocyte resorption on ovarian development rates in the Australian sheep blowfly, Lucilia cuprina. *Entomologia experimentalis et applicata*, 39(1), pp.85–90.

Wallis, D.I., 1962. Olfactory Stimuli and Oviposition in the Blowfly, Phormia Regina Mg. *Journal of Experimental Biology*, 39, pp.603-615.

Watari, Y. & Arai, T., 1997. Effects of photoperiod and aging on locomotor activity rhythms in the onion fly, Delia antiqua. *Journal of insect physiology*, 43(6), pp.567-576.

Wecker, S., Hornschemeyer, T. & Hoehn, M., 2002. Investigation of insect morphology by MRI: Assessment of spatial and temporal resolution. *Magnetic Resonance Imaging*, 20(1), pp.105-111.

Weissman, A., 1874a. The Metamorphosis of Flies. I. *The American Naturalist*, 8(10), pp.603-612.

Weissman, A., 1874b. The Metamorphosis of Flies. II. *The American Naturalist*, 8(11), pp.661-667.

Weissman, A., 1874c. The Metamorphosis of Flies. III. *The American Naturalist*, 8(12), pp.713-721.

Wells, J D & King, J., 2001. Incidence of precocious egg development in flies of forensic importance. *Pan pacific Entomologist*, (77), pp.235-239.

Wells, J D, Wall, R. & Stevens, J R, 2007. Phylogenetic analysis of forensically important Lucilia flies based on cytochrome oxidase I sequence: a cautionary tale for forensic species determination. *International Journal of Legal Medicine*, 121(3), pp.229-233.

White, K.P. *et al.,* 1999. Microarray Analysis of *Drosophila* Development During Metamorphosis. *Science*, 286(5447), pp.2179-2184.

Whitten, J.M., 1957. The Post-embryonic Development of the Tracheal System in *Drosophila melanogaster*. *Quarterly Journal of Microscopical Science*, s3(98), pp.123-150.

Whitworth, T., 2003. A Key to the Puparia of 27 Species of North American Protocalliphora Hough (Diptera: Calliphoridae) from Bird Nests and Two New Puparial Descriptions. *Proceedings of the Entomological Society of Washington*, 105(4), pp.995-1033.

Whitworth, T., 2006. Keys to the Genera and Species of Blowflies (Diptera: Calliphoridae) of America North of Mexico. *Proceedings of the Entomological Society of Washington*, 108(3), pp.689-725.

Wigglesworth, V B, 1954a. *Physiology of Insect Metamorphosis*, Cambridge: The University Press.

Wigglesworth, V., 1965. Insect Hormones. *Endeavour*, 24, p.21.

Wigglesworth, V B, 1954b. *The Principles of Insect Physiology* 7th ed., London: Chapman and Hall.

Wigglesworth, Vincent B, 1968. *The life of insects*, New American Library.

Willems, G., 2001. A review of the most commonly used dental age estimation techniques. *Journal of Forensic Odonto-Stomatology*, 19(1), pp.9-17.

Winnebeck, E., 2010. Why does insect RNA look degraded? *Journal of Insect Science*, 10(159), pp.1-7.

Wunderer, H. & Smola, U., 1982. Morphological Differentiation of the Central Visual Cells R7/8 in Various Regions of the Blowfly Eye. *Tissue & Cell*, 14(2), pp.341-358.

Yocum, G., Zdárek, J. & Joplin, K., 1994. Alteration of the eclosion rhythm and eclosion behavior in the flesh fly, Sarcophaga crassipalpis, by low and high temperature stress. *Journal of Insect Physiology*, 40(1), pp.13-21.

Zdarek, J. & Friedman, S., 1986. Pupal Ecdysis in Flies - Mechanisms of Evagination of the Head and Expansion of the Thoracic Appendages. *Journal of Insect Physiology*, 32(11), pp.917-923.

Zehner, R., Amendt, J & Boehme, P., 2009. Gene expression analysis as a tool for age estimation of blowfly pupae. *Forensic Science International: Genetics Supplement Series*, 2(1), pp.292-293.

Zehner, R., Mösch, S. & Amendt, J, 2006. Estimating the postmortem interval by determining the age of fly pupae: Are there any molecular tools? *International Congress Series*, 1288, p.621.

Zhu, G.H. *et al.,* 2007. Puparial case hydrocarbons of Chrysomya megacephala as an indicator of the postmortem interval. *Forensic Science International*, 169(1), pp.1-5.

Zimmermann, B., 2003. Distribution and serotonin-induced activation of vacuolar-type H+-ATPase in the salivary glands of the blowfly *Calliphora vicina*. *Journal of Experimental Biology*, 206(11), pp.1867-1876.

Zumpt, F., 1965. Myiasis in man and animals in the Old World. A Textbook for Physicians, Veterinarians and Zoologists. London: Butterworths.

Zwaan, B., Zijlstra, W. & Keller, M., 2008. Potential constraints on evolution: sexual dimorphism and the problem of protandry in the butterfly Bicyclus anynana. *Journal of genetics*, 87(4), pp.395-405.

Appendix I – PMI estimation using ADH

This PMI estimation example is based on using lifecycle data and hourly temperatures of the eldest *Calliphora vicina* larvae present on a cadaver.

Multiple 1st instar larvae were collected at 4pm 06/06/09 and measured, giving a geometric mean of 5.5 mm. Using Fig A1 (Donovan, *et al.,* 2006), the age of the larvae was calculated as being ~700 ADH.

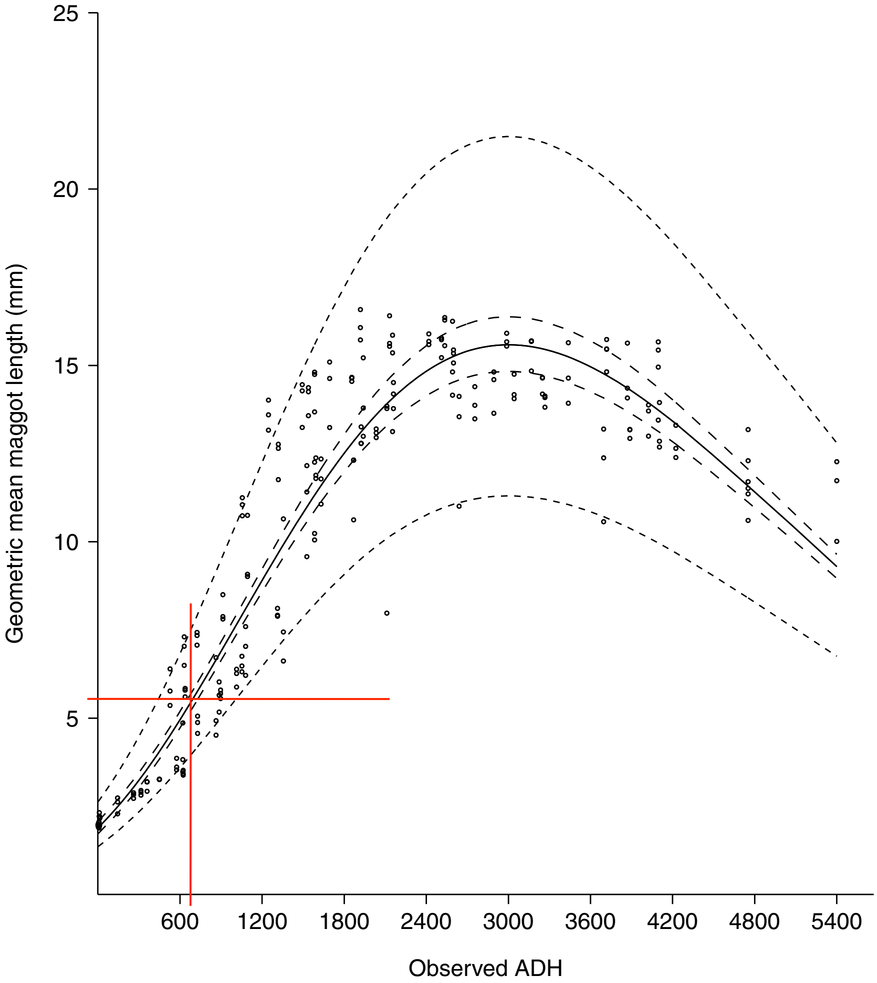

Figure A1 Growth curve for the largest larvae of *Calliphora vicina.* Geometric mean lengths of larvae plotted against age in ADH, with hyperbolic function (solid line) fitted, showing 95% confidence limits (dashed line) and observation limits (dotted line). Red lines indicate ADH estimation of 1st instar larvae

The temperature of the vicinity has been compared to weather station data, and a regression analysis has given R^2 = 0.9, indicating a high correlation between crime scene and weather station data.

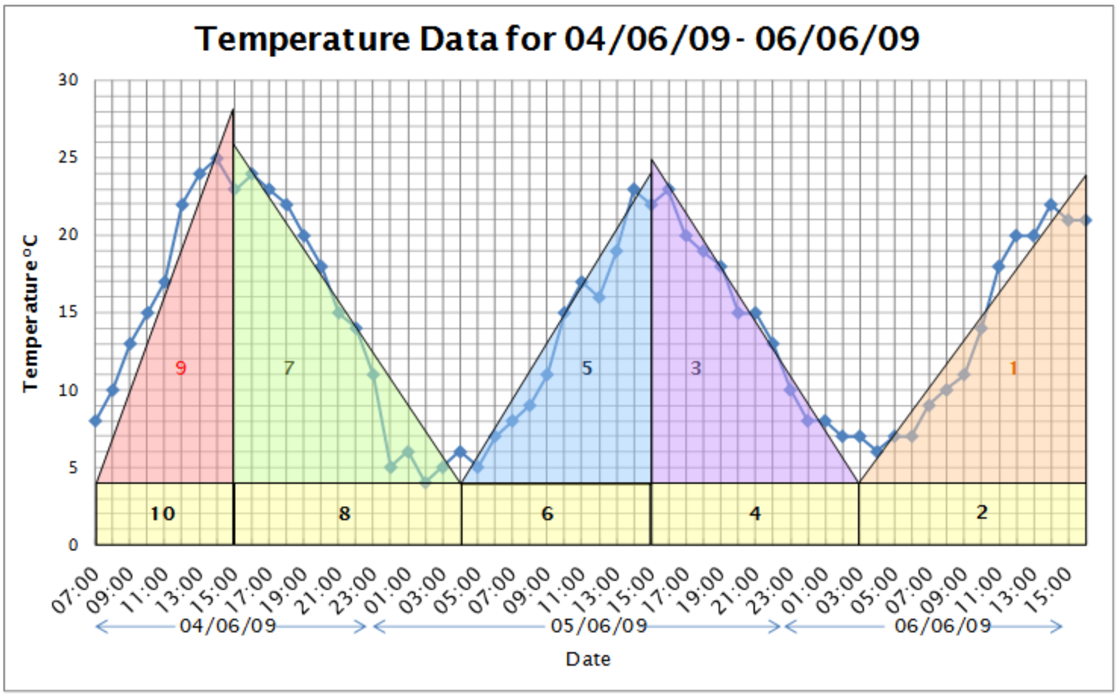

Figure A2 Calculation of ADH using hourly temperatures for the example scene. Temperatures obtained near the scene are plotted against time, with the approximate areas marked out for ADH calculation. Change in temperature is multiplied against time for each area and halved. All areas are totalled for total ADH accumulated.

Using either individual hourly temperatures, or by estimating ADH using areas (Fig. A2), the minimum period of insect activity (PIA) can be estimated. *Calliphora vicina* have a LDT of 1°C, which must be removed from calculations:

General formula: ADH = time (hrs) at temperature x (temperature – LDT)

Area 1 = $\frac{\text{13hrs x (24 °C - 4°C)}}{2}$ = 130 ADH

Area 2 = 13hrs x (4°C - 1°C) = 39 ADH

ADH accumulated from all areas totals 784 ADH (Table A1), greater than that of the age of the larvae. This difference must be subtracted:

784 ADH – 700 ADH = 84 ADH

On 04/06/09 the mean temperature between 07:00 and 12:00 was 14.2°C, which gives an ADH of:

6 hours x (14.2°C – 1°C) = 79.2 ADH.

Between 07:00 and 13:00 the mean temperature was 15.6°C, which gives an ADH of:

7 hours x (15.6°C – 1°C) = 102.2 ADH

This indicates oviposition occurred between 12:00 and 13:00 on 04/06/09. The standard time given for flies arriving at a cadaver is 4 hours, as such the minimum PMI is 56 hours from collection, giving a time since death estimate of 08:00, 04/06/09. The PMI estimate is always given a window of accuracy, usually that of ~6 hours to account for environmental conditions, body placement and natural variation in fly species. Therefore the final time since death estimate is 05:00 – 11:00, 04/06/09. Due to the rarity of oviposition during darkness, insect activity probably commenced at sunrise on 04/06/09

Table A1 ADH calculation for each area of the graph (Fig. A2). The area of each section was calculated as shown in the text, and the accumulated ADH shown in the table. An LDT of 1°C has been taken into account for the growth of *C.vicina* larvae.

Area	**Temperature change**	**Time**	**ADH**	**Running ADH total**
1	20	13	130	130
2	3	13	39	169
3	21	12	126	295
4	3	12	36	331
5	20	11	110	441
6	3	11	33	474
7	22	13	143	617
8	3	13	39	656
9	26	8	104	760
10	3	8	24	**784**

Appendix II – Preservation Solutions

Table A2 indicates the compositions of preservative solutions tested on 4d and 7d pupae. All pupae were pierced prior to placement in all preservatives listed, except 'Dry' storage.

Table A2. Preservation solution compositions. Pupae were preserved in multiple preservatives to test the effects on morphology and integrity of DNA and RNA. The solutions and their components are indicated here. Component solutions are given at stock concentration (without dilution). Volumes are those used for storage, except the hot-water kill (HWK) which is the volume of the petri-dish used to hold pupae before immersion.

Preservative	Component Solution	Volume/mL
HWK	Boiling tap water	110
70% ethanol	Absolute ethanol	14
	Distilled water	6
80% ethanol	Absolute ethanol	16
	Distilled water	4
95% ethanol	Absolute ethanol	19
	Distilled water	1
Kahles	Absolute ethanol	5.6
	Formaldehyde	2.2
	Glacial acetic acid	0.8
	Distilled water	11.4
Bouins	Picric acid (saturated aqueous solution)	14.5
	Formaldehyde	4.5
	Glacial acetic acid	1
Carnoys	Absolute ethanol	12
	Chloroform	6
	Glacial acetic acid	2
Modified methacarn	Methanol	17.8
	Glacial acetic acid	2.2
Propylene glycol	Propylene glycol	20
Isopropanol	Isopropanol	20
RNAlater	RNAlater	20
Dry	Stored without solution	-

Appendix III – Species Identification using the Cytochrome Oxidase I gene

Calliphoridae Cytochrome Oxidase I gene sequences at least 1167bp in length were obtained from NCBI (Table A3). Species identification of preserved pupae was conducted using phylogenetic analysis (Figure A3) and included all sequences identified in Table A3.

Table A3 Calliphoridae 1167bp COI gene sequences. The sequences identified were obtained from the NCBI database, with species names and accession numbers given.

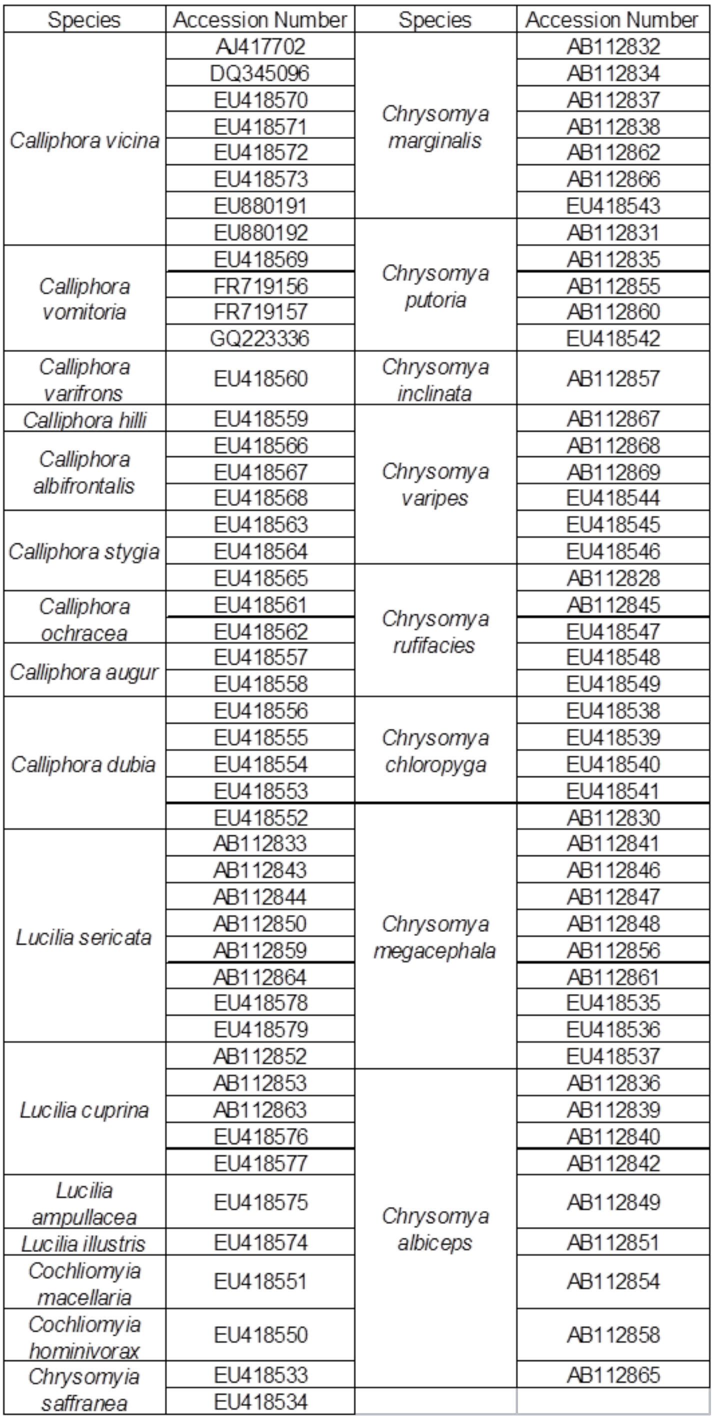

Species	Accession Number	Species	Accession Number
Calliphora vicina	AJ417702	*Chrysomya marginalis*	AB112832
	DQ345096		AB112834
	EU418570		AB112837
	EU418571		AB112838
	EU418572		AB112862
	EU418573		AB112866
	EU880191		EU418543
	EU880192	*Chrysomya putoria*	AB112831
Calliphora vomitoria	EU418569		AB112835
	FR719156		AB112855
	FR719157		AB112860
	GQ223336		EU418542
Calliphora varifrons	EU418560	*Chrysomya inclinata*	AB112857
Calliphora hilli	EU418559	*Chrysomya varipes*	AB112867
Calliphora albifrontalis	EU418566		AB112868
	EU418567		AB112869
	EU418568		EU418544
Calliphora stygia	EU418563		EU418545
	EU418564		EU418546
	EU418565	*Chrysomya rufifacies*	AB112828
Calliphora ochracea	EU418561		AB112845
	EU418562		EU418547
Calliphora augur	EU418557		EU418548
	EU418558		EU418549
Calliphora dubia	EU418556	*Chrysomya chloropyga*	EU418538
	EU418555		EU418539
	EU418554		EU418540
	EU418553		EU418541
	EU418552	*Chrysomya megacephala*	AB112830
Lucilia sericata	AB112833		AB112841
	AB112843		AB112846
	AB112844		AB112847
	AB112850		AB112848
	AB112859		AB112856
	AB112864		AB112861
	EU418578		EU418535
	EU418579		EU418536
Lucilia cuprina	AB112852		EU418537
	AB112853	*Chrysomya albiceps*	AB112836
	AB112863		AB112839
	EU418576		AB112840
	EU418577		AB112842
Lucilia ampullacea	EU418575		AB112849
Lucilia illustris	EU418574		AB112851
Cochliomyia macellaria	EU418551		AB112854
Cochliomyia hominivorax	EU418550		AB112858
Chrysomyia saffranea	EU418533		AB112865
	EU418534		

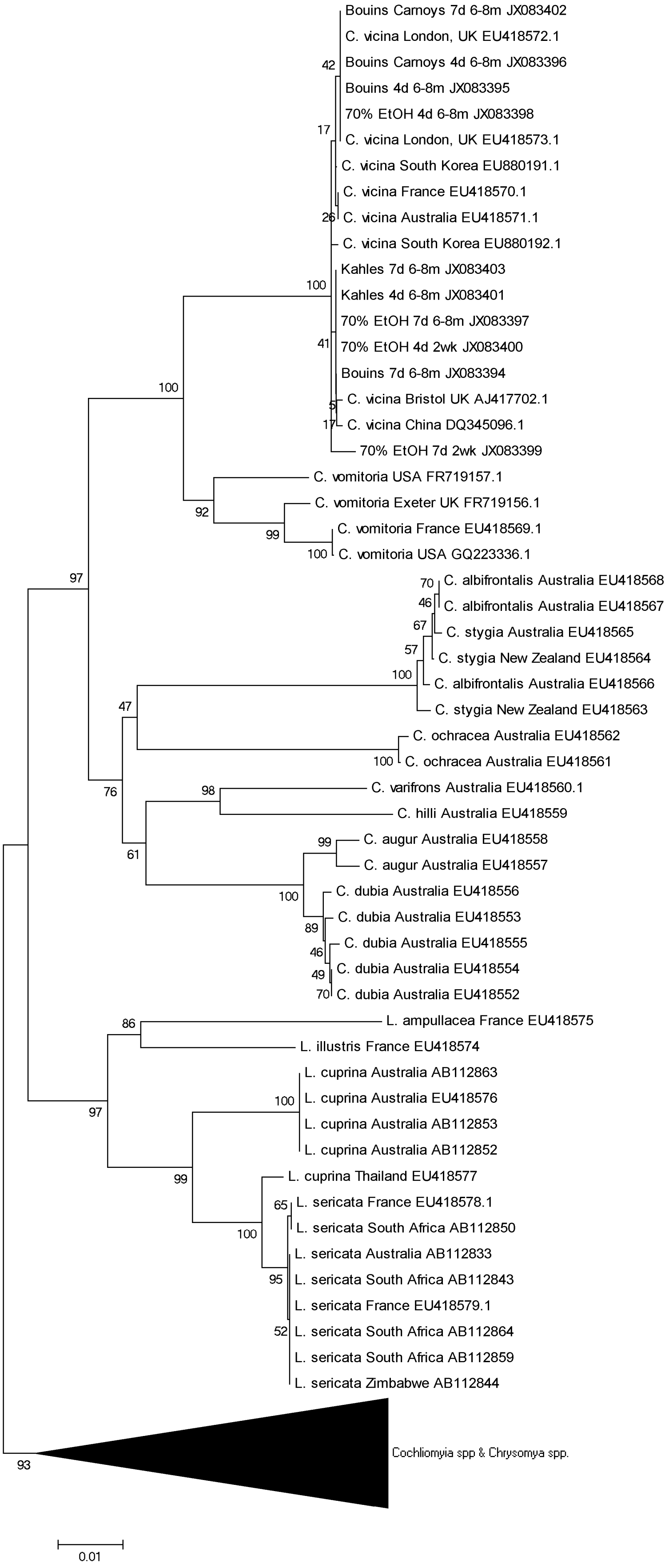

Figure A3 Species identification of preserved pupae by phylogenetic analysis. Sequences obtained from NCBI (Table S2) were compared with those obtained for preserved pupae, using neighbour joining analysis with a bootstrap test of 1000 replicates.

Appendix IV – Developmental Gene Expression for Age Estimation

Differential Gene selection and Primer Design

Candidate genes for pupal age estimation were selected from those identified in previous insect studies. Gene and protein information was obtained for HKGs (Table A4) and degenerate primers were designed based on protein sequences (Table 7.4). DEGs were selected and semi-qPCR primers designed from available *C. vicina* sequence data (Table A5) as degenerate primer design from optimally expressed genes seleted from other organisms failed. Three DEGs were then chosen for qPCR analysis based on their developmental expression levels, functional variety and gene location and structure.

Table A4. Housekeeping genes selected for analysis. Three HKGs were identified from previous research (Chapter 7.4.2.1) as being potentially suitable for normalisation of gene expression in *C. vicina*. General gene structure information obtained from Flybase (www.flybase.org), Interactive fly (www.sdbonline.org) and Ensembl (www.ensembl.org). Sequences were obtained from NCBI (www.ncbi.nlm.nih.gov).

Gene	Isoforms	Chromosome	Transcripts	Exons	Transcript length (bp)	Protein length	Aligned sequences for primer design
EF1α	100E	X	4	3	1158 - 1199	148	*C. vomitoria*, *Protocalliphora azurea*, *Cynomya mortuorum*, *Chrysomya* spp., *Cochliomyia hominivorax*, *Muscina* spp., *Hydrotaea* spp., *Musca domestica*.
	48D	2R	2				
GAPDH	1	2R	2	1-2	1285 - 1483	332	*L. cuprina*, *M. domestica*, *Drosophila* spp., *Lutzomyia longipalpis, Glossina mortisans*.
	2	X	2				
RP49 (RpL32)	1	3R	5	2-3	590 - 830	134 - 147	Drosophilidae, *Anopheles* spp., *Culex spp.*, *Aedes spp.*, *Bombyx mori*, *Apis mellifera*, *Lucilia sericata*

Table A5. Candidate *C. vicina* DEGs. Genes were selected from available *C. vicina* sequences on NCBI and primers designed using Primer-BLAST. Gene structure information obtained from Ensembl (www.ensembl.org) Examples of function in *Drosophila* shown, obtained from www.flybase.org. Genes in bold were selected for qPCR analysis.

Gene	Isoforms	Chromosome	Transcripts	Exons	Transcript length (bp)	Protein length	Accession number	Function
Arrestin 1	1	2L	2	4	1435-2207	364	X79072.1	Photoreceptor maintenance
	2	3L	1	3		401		
Ecdysone receptor (Ecr)	1	2R	6	5-8	4089-5874	669-878	AF325360.1	Neuron development Gonad development Imaginal disc development
Larval serum protein (LSP-2)	1	3L	1	1	2304	701	U89789.1	Nutrient reservoir Nutrient transport
Opsin	1	3R	1	5	1597	373	M58334.1	Adult locomotion Eye morphogenesis Neuron development
Shaker	1	X	11	7-16	1286-4526	297-655	AY428053.1	Circadian rhythm Light detection Axon extension
Transient receptor potential (Trp)	1	3R	1	14	4130	1275	Z80230.1	Light detection Calcium ion transport

Evaluation of CT values

Anomalous CT values greater than +/- $1C_T$ were removed and the resulting data is summarised in Table A6 for all five genes. Minimal differences between EF1α and RP49 demonstrate similarity in expression levels between the two genes. Trp was expressed at a lower level than the other genes. ΔC_T and relative expression levels of genes were then calculated (Table A7).

Table A6. Individual C_T variation with pupal age. Raw gene expression data is produced in the form of CT values. Lower C_T values indicate higher levels of expression. The mean C_T values are displayed for each gene and pupal age, with standard deviation and standard errors calculated. Maximum and minimum standard errors for each gene are in bold. The differences between housekeeping genes Rp49 and EF1α for each age are also shown. Data was used to construct Figure 7.7.

Age	**RP49**			**EF1α**			*EF1α - Rp49 C_T difference*	**Ecr**			**LSP-2**			**Trp**		
	Mean C_T	**Std. Dev.**	**Std. Error**	**Mean C_T**	**Std. Dev.**	**Std. Error**		**Mean C_T**	**Std. Dev.**	**Std. Error**	**Mean C_T**	**Std. Dev.**	**Std. Error**	**Mean C_T**	**Std. Dev.**	**Std. Error**
3911	22.26	1.06	0.38	23.11	1.55	0.52	*-0.85*	29.03	0.81	0.27	22.21	1.58	0.53	35.20	1.06	0.37
4463	22.40	1.10	0.42	23.41	0.21	0.07	*-1.01*	28.71	0.35	0.12	22.23	0.45	**0.15**	34.79	0.72	0.27
5013	22.46	1.54	0.58	23.62	1.58	0.53	*-1.16*	28.00	1.28	0.43	22.20	1.22	0.41	36.10	0.62	0.25
5558	22.59	1.29	0.49	23.36	1.75	0.58	*-0.77*	28.25	1.15	0.38	21.33	1.23	0.41	34.53	1.35	0.45
6106	22.82	0.96	0.32	23.57	2.07	0.69	*-0.75*	28.53	1.38	0.46	22.62	1.42	0.47	33.59	1.23	0.43
6659	22.25	1.00	0.33	23.78	1.84	0.61	*-1.53*	29.38	1.54	0.54	22.59	1.84	**0.61**	31.63	0.75	0.25
7209	23.11	0.73	0.24	23.69	1.46	0.49	*-0.58*	29.03	1.04	0.35	22.64	0.96	0.32	30.41	1.64	0.58
7761	22.53	0.71	0.24	22.04	1.31	0.44	*0.49*	28.45	0.61	0.22	22.03	0.72	0.24	28.00	1.26	0.42
8313	22.44	1.17	0.39	21.80	2.37	**0.79**	*0.64*	28.40	1.98	**0.75**	20.85	1.34	0.45	27.69	2.29	**0.76**
8865	21.75	0.76	0.25	20.26	0.52	0.17	*1.49*	27.19	0.90	0.30	20.67	0.71	0.24	27.22	0.86	0.29
9419	23.78	1.46	**0.65**	23.73	0.37	0.15	*0.05*	28.72	0.21	0.08	22.60	0.42	0.17	29.20	0.69	0.28
9976	22.97	0.75	0.25	22.40	0.17	**0.06**	*0.57*	27.60	0.22	**0.07**	22.41	0.64	0.21	27.49	0.45	**0.15**
10530	22.97	0.42	**0.14**	21.66	0.96	0.32	*1.31*	28.64	0.73	0.24	22.32	0.69	0.23	25.90	0.77	0.26
11082	22.97	1.01	0.34	22.73	1.61	0.54	*0.24*	30.10	1.20	0.40	23.03	1.26	0.42	27.06	0.84	0.28

Table A7 Calculation of gene expression ratios. ΔC_T was calculated using the mean of both HKGs over all ages, and individual genes (Rp49 and EF1α) at each age. ΔC_T was converted to a relative expression value by inversion (1/2^ΔC_T) and calculated relative to the lowest level (Trp at 5013 ADH).

Expression relative to the mean of both HKGs

Age	**ΔC_T (DEG - HKG)**			**1/(2^ΔCT): Relative exp.**			**Relative fold expression**		
	Ecr	**LSP-2**	**Trp**	**Ecr**	**LSP-2**	**Trp**	**Ecr**	**LSP-2**	**Trp**
3911	6.31	-0.51	12.48	0.0126	1.4208	0.0002	134.36	15181.22	1.87
4463	5.99	-0.49	12.07	0.0157	1.4013	0.0002	167.73	14972.21	2.48
5013	5.28	-0.52	13.38	0.0257	1.4307	0.0001	274.37	15286.81	1.00
5558	5.53	-1.39	11.81	0.0216	2.6149	0.0003	230.72	27939.14	2.97
6106	5.81	-0.10	10.87	0.0178	1.0693	0.0005	190.02	11425.74	5.70
6659	6.66	-0.13	8.91	0.0099	1.0918	0.0021	105.42	11665.82	22.16
7209	6.31	-0.08	7.69	0.0126	1.0546	0.0048	134.36	11268.44	51.63
7761	5.73	-0.69	5.28	0.0188	1.6096	0.0257	200.85	17198.56	274.37
8313	5.68	-1.87	4.97	0.0195	3.6471	0.0318	207.94	38967.94	340.14
8865	4.47	-2.05	4.50	0.0450	4.1317	0.0441	481.04	44146.15	471.14
9419	6.00	-0.12	6.48	0.0156	1.0843	0.0112	166.57	11585.24	119.43
9976	4.88	-0.31	4.77	0.0339	1.2369	0.0366	362.04	13216.02	390.72
10530	5.92	-0.40	3.18	0.0165	1.3165	0.1101	176.07	14066.74	1176.27
11082	7.38	0.31	4.34	0.0060	0.8048	0.0493	64.00	8599.28	526.39

Expression relative to Rp49

Age	**ΔC_T (DEG - HKG)**			**1/(2^ΔCT): Relative exp.**			**Relative fold expression**		
	Ecr	**LSP-2**	**Trp**	**Ecr**	**LSP-2**	**Trp**	**Ecr**	**LSP-2**	**Trp**
3911	6.77	-0.05	12.94	0.0092	1.0353	0.0001	116.97	13216.02	1.62
4463	6.31	-0.17	12.39	0.0126	1.1251	0.0002	160.90	14362.31	2.38
5013	5.54	-0.26	13.64	0.0215	1.1975	0.0001	274.37	15286.81	1.00
5558	5.66	-1.26	11.94	0.0198	2.3950	0.0003	252.48	30573.63	3.25
6106	5.71	-0.20	10.77	0.0191	1.1487	0.0006	243.88	14664.09	7.31
6659	7.13	0.34	9.38	0.0071	0.7900	0.0015	91.14	10085.54	19.16
7209	5.92	-0.47	7.30	0.0165	1.3851	0.0063	210.84	17682.08	81.01
7761	5.92	-0.50	5.47	0.0165	1.4142	0.0226	210.84	18053.61	288.01
8313	5.96	-1.59	5.25	0.0161	3.0105	0.0263	205.07	38431.46	335.46
8865	5.44	-1.08	5.47	0.0230	2.1140	0.0226	294.07	26987.43	288.01
9419	4.94	-1.18	5.42	0.0326	2.2658	0.0234	415.87	28924.41	298.17
9976	4.63	-0.56	4.52	0.0404	1.4743	0.0436	515.56	18820.27	556.41
10530	5.67	-0.65	2.93	0.0196	1.5692	0.1312	250.73	20031.74	1675.06
11082	7.13	0.06	4.09	0.0071	0.9593	0.0587	91.14	12245.81	749.61

Expression relative to EF1α

Age	**ΔC_T (DEG - HKG)**			**1/(2^ΔCT): Relative exp.**			**Relative fold expression**		
	Ecr	**LSP-2**	**Trp**	**Ecr**	**LSP-2**	**Trp**	**Ecr**	**LSP-2**	**Trp**
3911	5.92	-0.90	12.09	0.0165	1.8661	0.0002	94.35	10660.59	1.31
4463	5.30	-0.90	11.38	0.0254	1.8661	0.0004	145.01	10660.59	2.14
5013	4.38	-1.42	12.48	0.0480	2.6759	0.0002	274.37	15286.81	1.00
5558	4.89	-2.03	11.17	0.0337	4.0840	0.0004	192.67	23331.64	2.48
6106	4.96	-0.95	10.02	0.0321	1.9319	0.0010	183.55	11036.54	5.50
6659	5.60	-1.19	7.85	0.0206	2.2815	0.0043	117.78	13034.07	24.76
7209	5.34	-1.05	6.72	0.0247	2.0705	0.0095	141.04	11828.67	54.19
7761	6.41	-0.01	5.96	0.0118	1.0070	0.0161	67.18	5752.61	91.77
8313	6.60	-0.95	5.89	0.0103	1.9319	0.0169	58.89	11036.54	96.34
8865	6.93	0.41	6.96	0.0082	0.7526	0.0080	46.85	4299.64	45.89
9419	4.99	-1.13	5.47	0.0315	2.1886	0.0226	179.77	12503.12	128.89
9976	5.20	0.01	5.09	0.0272	0.9931	0.0294	155.42	5673.41	167.73
10530	6.98	0.66	4.24	0.0079	0.6329	0.0529	45.25	3615.55	302.33
11082	7.37	0.30	4.33	0.0060	0.8123	0.0497	34.54	4640.29	284.05